แบบแผนเครื่องรับไฮบริดไมโมสำหรับเครือข่ายรับรู้ทางวิทยุ

นายธนพงศ์ คุ้มญาติ

HYBRID-MIMO RECEIVER SCHEME FOR

COGNITIVE RADIO NETWORKS

Tanapong Khomyat

A Thesis Submitted in Partial Fulfillment of the Requirements for the

Degree of Doctor of Engineering in Telecommunication

Suranaree University of Technology

Academic Year 2014

ธนพงศ์ คุ้มญาติ : แบบแผนเครื่องรับไฮบริดไมโมสำหรับเครือข่ายรับรู้ทางวิทยุ (HYBRID-MIMO RECEIVER SCHEME FOR COGNITIVE RADIO NETWORKS)อาจารย์ที่ปรึกษา : รองศาสตราจารย์ ดร.พีระพงษ์ อุฑารสกุล, 166หน้า.

เครือข่ายรับรู้ทางวิทยุ (Cognitive radio network: CRN) ถูกสร้างขึ้นเพื่อแก้ปัญหาความไม่เพียงพอของแถบความถี่วิทยุ เนื่องจากความต้องการสื่อสารแบบไร้สายที่เพิ่มขึ้นอย่างรวดเร็ว เพื่อแก้ปัญหานี้ เครือข่ายรับรู้ทางวิทยุได้รับอนุญาตให้เข้าถึงช่องสัญญาณใดๆของเครือข่ายปฐมภูมิ (Primary network: PN) ที่ไม่ใช้งานบนพื้นที่ร่วมกันภายใต้การควบคุมพลังงาน เพื่อจำกัดสัญญาณแทรกสอดในเครือข่ายปฐมภูมิ การตรวจจับแถบความถี่ (Spectrum sensing) และการแบ่งแถบความถี่ (Spectrum sharing) ถูกใช้งานในเครือข่ายรับรู้ทางวิทยุ เพื่อตรวจสอบช่องสัญญาณที่ใช้งานอยู่ และช่องสัญญาณที่ไม่ใช้งานเพื่อหาช่วงเวลาที่สามารถเข้าใช้งานได้ ยิ่งไปกว่านั้นเครือข่ายรับรู้ทางวิทยุสามารถใช้เทคนิคไมโม (Multiple-input multiple-output: MIMO) ที่แตกต่างกันเพื่อให้ได้สมรรถนะที่ดีที่สุด เนื่องจากผู้ใช้งานแต่ละคนมีช่องสัญญาณที่แตกต่างกันเสมอ โดยทั่วไปมีเทคนิคไมโมสองแบบคือ เทคนิคการสลับเชิงตำแหน่งและเวลา (Space-time block coding: STBC) และเทคนิคการสลับเชิงตำแหน่ง (Spatial multiplexing: SM) ระบบไมโมหลายโมดที่เรียกว่าแบบแผนเครื่องรับไฮบริดไมโม (Hybrid MIMO receiver scheme: HMRS)ถูกเสนอและถูกใช้สำหรับเครือข่ายรับรู้ทางวิทยุ เทคนิคการตัดสัญญาณแทรกสอดแบบต่อเนื่อง (Successive interference cancellation: SIC) และเทคนิคการตรวจจับไมโม ถูกใช้งานร่วมกันสำหรับแบบแผนเครื่องรับไฮบริดไมโมเพื่อแยกและตรวจจับสัญญาณทุกชั้นที่เครื่องรับ จากผลการจำลอง สมรรถนะอัตราผิดพลาดสัญลักษณ์ (Symbol error rate: SER) ของแบบแผนเครื่องรับไฮบริดไมโมมีค่าดีกว่าระบบไฮบริดไมโมแบบเดิมที่ใช้เทคนิคการแยกเมตริกย่อย ยิ่งไปกว่านั้นเครื่องส่งของระบบที่เสนอมีความซับซ้อนน้อยในงานวิจัยนี้สมรรถนะอัตราผิดพลาดสัญลักษณ์ของแบบแผนเครื่องรับไฮบริดไมโมและระบบไฮบริดไมโมเดิมถูกเปรียบเทียบเพื่อแสดงถึงประโยชน์ของเทคนิคที่เสนอ และวิเคราะห์อัตราผิดพลาดบิตของระบบที่เสนอเมื่อมีการประมาณช่องสัญญาณผิดพลาดนอกจากนี้ผลการวัดจากชุดทดสอบที่สร้างขึ้นรับรองว่าระบบที่เสนอมีประสิทธิภาพดีกว่าระบบไมโมแบบเดิมจากอัตราผิดพลาดบิต

สาขาวิชา <u>วิศวกรรมโทรคมนาคม</u>ลายมือชื่อนักศึกษา_____
ปีการศึกษา 2557ลายมือชื่ออาจารย์ที่ปรึกษา_____

TANAPONG KHOMYAT : HYBRID-MIMO RECEIVER SCHEME FOR COGNITIVE RADIO NETWORKS. THESIS ADVISOR : ASSOC. PROF. PEERAPONG UTHANSAKUL, Ph.D., 166 PP.

MIMO/SPATIAL MULTIPLEXING/SPACE-TIME BLOCK CODING/ SUCCESSIVE INTERFERENCE CANCELLATION/COGNITIVE RADIO NETWORK

Cognitive radio network (CRN) has been established to fix the problem of lacking radio spectrum in the future because the wireless communication demands are rapidly increased. In order to solve this problem, CRN is permitted to access any unused channel of the primary network (PN) in the common area under the power control criteria to restrict the interference on PN. The spectrum sensing and spectrum sharing technique are applied by CRN to aware the active and unused channel of PN and make opportunity to access any unused channel. Moreover, each user of CRN can applies different multiple-input multiple-output (MIMO) scheme to obtain the optimum performance because each user always faces the different channel. Generally, there are two such MIMO schemes, namely, the space-time block coding (STBC) and the spatial multiplexing (SM). The multi-mode MIMO systems, called hybrid MIMO receiver scheme (HMRS) is proposed and applied for CRN. The simple techniques, successive interference cancellation (SIC) and SM detection are jointly applied for HMRS to separate and detect all layers at the receiver. From the simulation results, symbol error rate (SER) performance of HMRS outperforms the

existing hybrid MIMO techniques that apply sub-matrix decomposition technique. In addition, the HMRS transmitter can detect all layers with low complexity. In this research, the SER performance of HMRS and the existing hybrid MIMO are compared to validate the advantage of the proposed technique. The analytical bit error rate (BER) is derived with channel estimation error (CEE).Besides the measured results from hardware implementation confirm that the HMRS outperforms the conventional MIMO systems in term of BER.

School of Telecommunication Engineering   Student's Signature_____
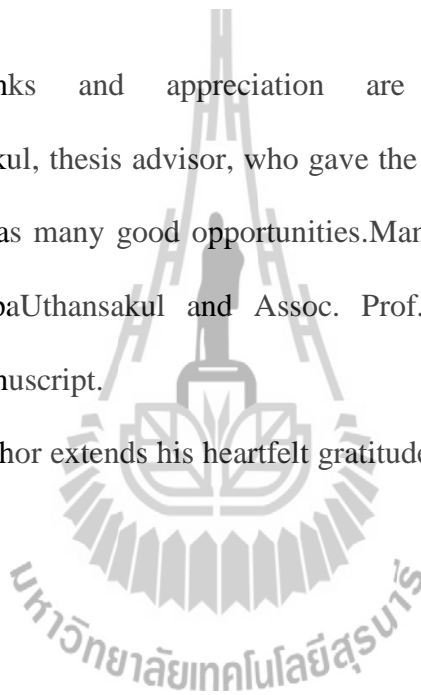
Academic Year 2014   Advisor's Signature_____

ACKNOWLEDGMENTS

TanapongKhomyat

TABLE OF CONTENTS

TABLE OF CONTENTS (Continued)

TABLE OF CONTENTS (Continued)

TABLE OF CONTENTS (Continued)

TABLE OF CONTENTS (Continued)

TABLE OF CONTENTS (Continued)

LIST OF TABLES

LIST OF FIGURES

LIST OF FIGURES (Continued)

LIST OF FIGURES (Continued)

SYMBOLS AND ABBREVIATIONS

σ_z^2	=	Noise variance
$\boldsymbol{\beta}_{Na}$	=	Coefficient vector
$p_{\gamma_n}(\gamma_n)$	=	Probability density function
$\boldsymbol{\psi}_{N_a}$	=	Pattern vector for appearance of error propagation
$\bar{\gamma}$	=	Signal to noise ratio (SNR)
BER	=	Bit error rate
BPSK	=	Binary phase shift keying
C	=	Number of possible symbols in constellation
CEE	=	Channel estimation error
CRN	=	Cognitive radio networks
C_P	=	Channel capacity
d_{EP}	=	Symbol distance
E_r	=	Average power for each receive antenna
E_s	=	Symbol energy
EP	=	Error propagation
FC	=	Fusion centre
$\boldsymbol{H}$	=	Channel matrix
HMRS	=	Hybrid MIMO receiver scheme
IC	=	Interference cancellation

SYMBOLS AND ABBREVIATIONS (Continued)

J	=	Number of SM user
LD	=	Linear detection
M	=	Number of receive antenna in multiuser systems
MIMO	=	Multiple-input Multiple-output
MMSE	=	Minimum mean square error
N	=	Number of user
N_r	=	Number of receive antenna
N_t	=	Number of transmit antenna
N_a	=	Number of other layers
OSIC	=	Ordered successive interference cancellation
$\boldsymbol{P_{b,N_a}}$	=	Bit error rate vector
$P_{e,Hb}$	=	Probability of bit error for hybrid MIMO systems
PN	=	Primary networks
PU	=	Primary user
QAM	=	Quadrature amplitude modulation
QPSK	=	Quadrature phase shift keying
SER	=	Symbol error rate
SIC	=	Successive interference cancellation
SM	=	Spatial multiplexing
STBC	=	Space-Time block coding
SU	=	Secondary user

SYMBOLS AND ABBREVIATIONS (Continued)

W	=	Weight matrix
w_{ep}	=	Error propagation matrix
WRAN	=	Wireless regional area networks
$\mathbf{x}$	=	Transmitted symbol matrix
$\hat{x}_{ML}$	=	Detected symbol of maximum likelihood detection
$\hat{x}_{MMSE}$	=	Detected symbol of minimum mean square error
$\hat{x}_{ZF}$	=	Detected symbol of zero forcing
y	=	Received signal matrix
z	=	White Gaussian noise vector

CHAPTER I

INTRODUCTION

1.1   Rationale and Background

At the present, telecommunication systems arethe important factor for worldwide communications. Several communication standards have been established by the Institute of Electrical and Electronics Engineer (IEEE). These standards are defined for producing any systems and equipment that can be commonly used.Telecommunication technologies and wireless applications have been continuously developed to support the unlimited demand of worldwide communication. Unfortunately, the radio spectrum is the limited resources. It will not be enough to consume in the nearly future.In contrast, from the operated frequency survey report of the Federal Communication Commission (FCC),they found that many radio channels in several standards are occupied by a few users or no user during any time. From the research of McHenry (2005) and Honglian (2011), the idea for reusing the unused radio channels was established to solve the lacking spectrum problem in the future. From this reason, the IEEE 802.22 standard was developed for the Cognitive Wireless Regional Area Network (WRAN) or the Cognitive Radio Network (CRN) that any users can access the vacant channel at any time without interference in the primary network (Mitora, 2000 and Haykin, 2005). From Figure 1.1, some Secondary Users (SU) occupy the unused channel with the limited power that may interfere with
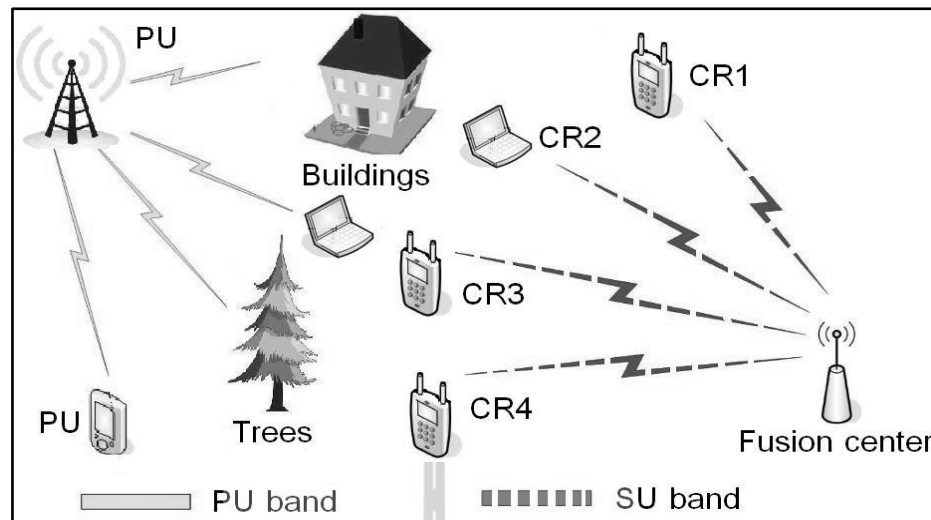
Figure 1.1 Cognitive radio networks.

Primary Network (PN) or Primary User (PU). Therefore CRN should aware spectrum utilizationaround by using spectrum sensing as well as power control criteria. From this reason, hybrid MIMO systems is the favour option for CRN because this technique obtain an advantages from both spatial multiplexing (SM) and space-time block coding (STBC) scheme that can improve channel capacity (Foschini, 1996) and increase diversity order (Alamouti, 1998 and Tarokh, 1999), respectively. Moreover hybrid MIMO systems can take higher advantage than the conventional MIMO in limited power scenario. From literature review,several hybrid MIMO schemes were proposed (Tan, 2009; Song, 2010; Freitas, 2005;Cortez, 2008; Ming, 2007 andMohd, 2004). The efficient techniques such as Interference Cancellation (IC) (Steffen, 2006) and Linear Detection (LD) (Yong, 2012) have been proposed as well as the sub-matrix calculation method. However all conventional hybrid MIMO techniques do not cancel interference before detect the first stream that can cause remaining a high interference in the received signals. Therefore this research proposes the novel hybrid

MIMO technique that can mitigate interference before detect the first stream, namely, Hybrid MIMO Receiver Scheme (HMRS). This technique applies Successive Interference Cancellation (SIC), SM detection and STBC jointly to obtain the higher performance than the conventional works in literature review when considering the simulation results and analysis.In this thesis, Symbol Error Rate (SER), Bit Error Rate (BER) and Cost-index performance are utilized toreveal the advantage of the proposed technique. The Cost-index performance is the SER to channel capacity ratio that can be used to indicate the efficiency of communication networks. The relationship between communication efficiency and the Cost-index performance is thoroughly explained in Section 4.6. Additionally the hardware implementation of HMRS is also carried out to verify the benefit of this work.

1.2   Research Objective

The objective of this thesis is to propose the HMRS that improve the efficiency of CRN. The detail of research objective can be explained as follows.

1.2.1   Studyprinciples and basic theory of SIC and multi-layer detection of hybrid MIMO systems.

1.2.2   Develop HMRS systems for applying in CRN.

1.2.3   Design and implement HMRS testbed for studying performance of the proposed technique.

1.3   ThesisHypotheses

1.3.1   To cancel interference in the received signals before detecting the first

layer can improve SER performance by considering from the computer simulation. Thereforethis criterion should take the benefit when applying in practice.

1.3.2 The higher SER performance of SM users can be offered when the receiver detect SM layer after STBC layer because STBC technique can mitigate the effect of error propagation.

1.4 Basic Agreement

1.4.1 For simulation and hardware, two users equipped with two antennas per user transmit data streams to the receiver equipped with four antennas.

1.4.2 Computer programing is used to simulate SER performance of the proposed technique and conventional hybrid MIMO.

1.4.3 Time synchronization is assumed to be a perfect case at the receiver.

1.4.4 The equally transmitted powers are allocated for all users.

1.5 Scope and Limitation of the study

1.5.1 The transmitted signals are propagated over slow fading channels. QPSK modulation is applied for data streams. Either SM or STBC technique is chosen for each user.

1.5.2 The receiver equipped with four antennas applies SIC and MIMO detection in simulation and hardware implementation.

1.5.3 Testbed implementation is established on the basis of a device that can be found in practice.

1.6   Methods

1.6.1   Methodology

1) Literature review will be carried out to study and search the related works.

2) Computer programing is used to simulate the performances of hybrid MIMO systems.

3) Mathematical analysis is used to verify the accuracy of simulation.

1.6.2   Research Location

Communications laboratory, Telecommunication engineering, F4 building, Suranaree University of Technology, 111 University Avenue, T. Suranaree, A. Maung, NakhornRachasima 30000, Thailand.

1.6.3   InstrumentsforHardware Implementation

1) Computer notebook

2) Matlab program

3) Power amplifier

4) RF signal generator

5) Oscilloscope

6) Power supply

1.7   Thesis Contents

This thesis is divided into seven chapters. The first chapter includes problem and rationale, research objective, hypotheses, basic agreement, scope and limitation of the study and methods. Chapter II presents results of literature review and the related works. The principle and theory of MIMO and hybrid MIMO systems are discussed in

Chapter III. Chapter IV describes principle of the proposed technique and BER derivation. Chapter V presents the simulation results compared with analytical results. The implementation of HMRS testbed is illustrated in Chapter VI. Chapter VII provides discussions and conclusions.

Covariance of the effective post-processing noise for ZF detection and STBC decoding in the presence of channel estimation error and error propagation, and the effective SNR per symbol after STBC decoding are derived in Appendix A. The publications of HMRS technique are presented in Appendix B.

CHAPTER II

LITERATURE REVIEW

2.1   Introduction

In wireless communication, message or data from transmitter is delivered to the receiver by facing the different radio channel. The mobility of users, environment, carrier frequency and co-channel interference have been directly affected to the signal quality at the receiver. From these reasons, many research and experiment have been continuously implemented to solve these problems and supported the new communication standard. CRN was established to solve the inadequacy of radio channel in the future (Mitora, 2000). Any users in CRN are permitted to access any used channel in the common area with PN by applying power limitation criteria. Each user should equip a spectrum sensing circuit either analog or digital type (Honglian, 2011)to protect users in PN. Moreover, by the restriction of radio channel and transmitted power, each user may apply the different MIMO scheme (Tan, 2009; Song, 2010; Freitas, 2005; Cortez, 2008; Ming, 2007 and Mohd, 2004) called hybrid MIMO systems. Hybrid MIMO system is the interesting option to be adopted in CRN because it can control power in different channel better than the conventional MIMO techniques (Foschini, 1996). Hybrid MIMO technique can improve both channel capacity gain and diversity gain without spreading code and the expanded channels.

Table 2.1 Detected sensitivity for CRN devices.

Specification	Applications		
	Analog TV	Digital TV	Wireless Mics
Sensitivity	-94 dBm	-116 dBm	-107 dBm
SNR	1 dB	-21 dB	-12 dB

Each stream can be separated and detected by using interference cancellation (IC) technique (Steffen Reinhardt, 2006; Zijain, 2008;Y. Chun, 2008 and K.Kim, 2009) with MIMO detection. This research designs the novel efficient hybrid MIMO technique to improve efficiency of conventional hybrid MIMO systems.For achieving this goal, the literature review and related work should be surveyed and studied in order to deeply understand principle and criteria of the conventional hybrid MIMO. The database IEEE and textbook are used for reference in this thesis.

The content in this chapter is to discuss the principle of CRN, literature review and related work. The principle, decoding and detection of the conventional MIMO and the existing hybrid MIMO are described.

2.2 Cognitive Radio Network (CRN)

In the near future, the radio channels will notbe enoughusedfor worldwide communication. FCC in United States surveysthe spectrum occupancy during 30-2900 MHz in several states(McHenry, 2005). The results show that somechannels are slightly used or unused but any users of other standard cannot access those vacant channels according to the government law. From this reason, the IEEE 802.22 standard has been established and used for CRN to mitigate this problem. From Figure 1.1, any CR userscan access the same channels with PN such as NTSC, DVB
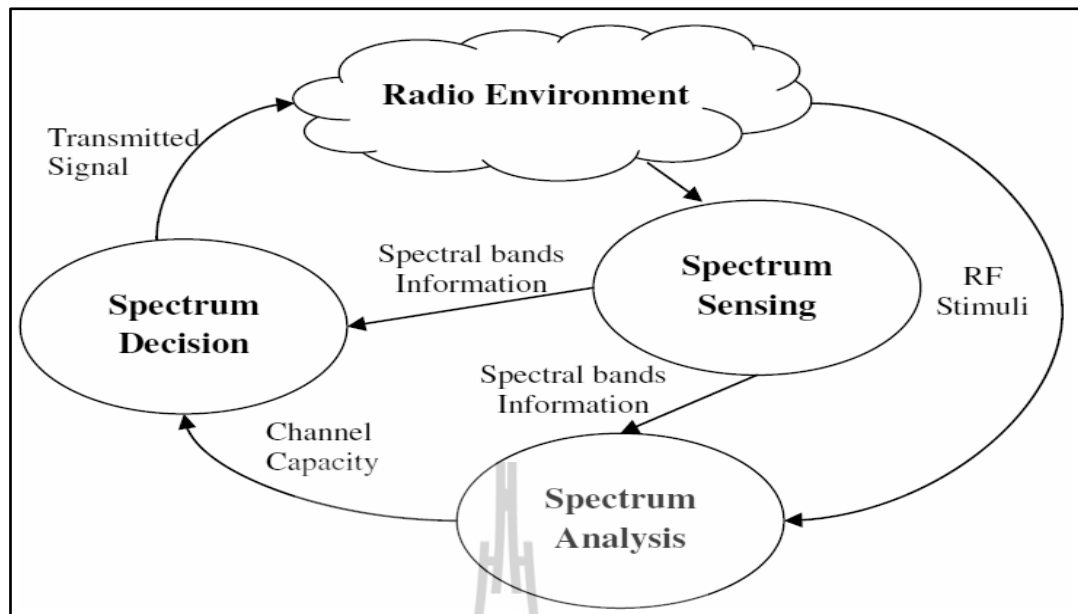
Figure 2.1 The basic recognition loop in CRN (Honglian, 2011).

and wireless microphone under the power control criteria to protect PN from interference. CRN should be equipped by spectrum sensing devices with probability of fault detection 0.1 and enough sensitivity as shown in Table 2.1.

2.2.1 Basic Recognition Loop in CRN

CRN devices should have the ability to sense spectrum, analyse and make decision for applying the optimum transmission method such as modulation channel coding MIMO scheme and transmitted power as shown in Figure 2.1; the CRN systems can be divided into three parts as follows.

1) Spectrum sensing is used to sense the active PN channel and search any unused channel. The spectrum sensing method can be divided into two types that the first is cyclostationary detector for OFDM signals and the second is energy detection for analog signals. The example of digital signal is shown in Figure 2.2.
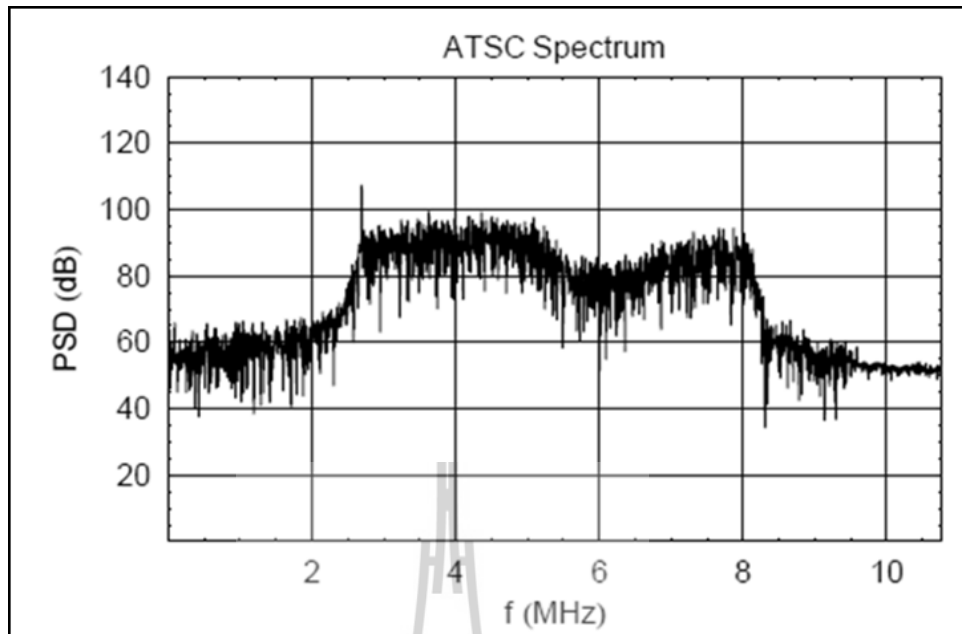
Figure 2.2 Example of the detected ATSC signals (Honglian, 2011).

2) Spectrum analysis is used to receive data from spectrum sensing part as shown in Figure 2.1. The block diagram of digital signal detection isshown in Figure 2.3.The FFT processing can be applied to sense the active sub-channels of OFDM signal. Figure 2.4 presents the block diagram of energy detection. This technique can be used to sense the active channel of analog signals. The collected data is used to analyse the channel capacity and forward the results to the spectrum decision part.
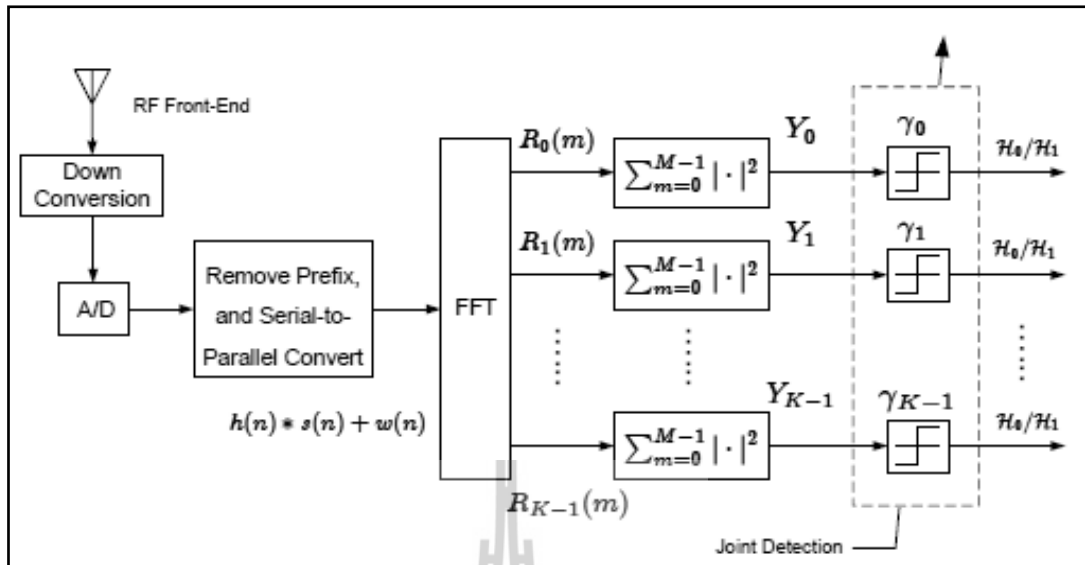
Figure 2.3 Digital signal detection block diagram (Honglian, 2011).
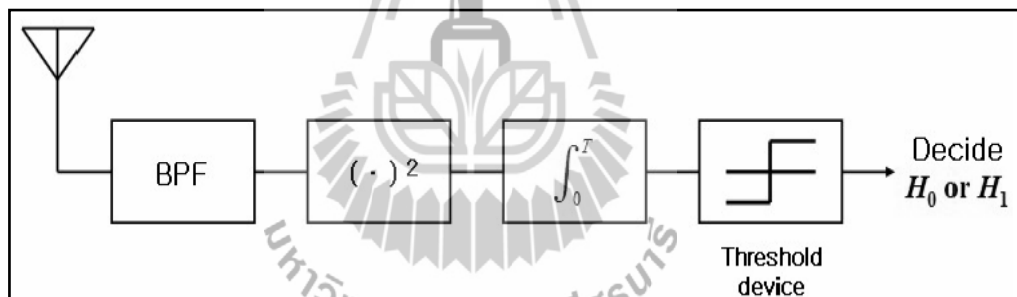
Figure 2.4 Energy detection block diagram (Honglian, 2011).
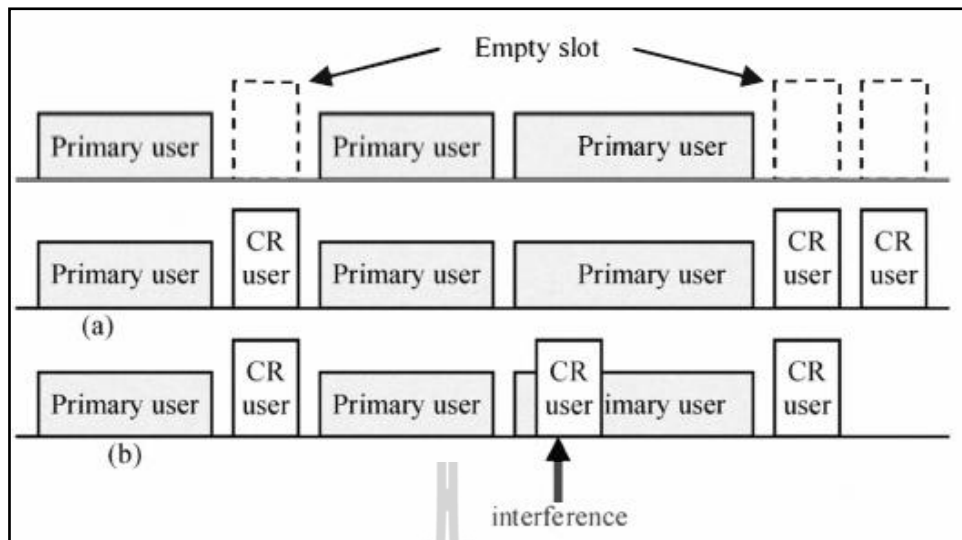
Figure 2.5 Problem during occupy the vacant channel in CRN (Honglian, 2011).

3) Spectrum decision is used to choose the optimum transmission scheme by considering the analysis results from the spectrum analysis part.

The detected devices should have enough sensitivity for rapid change of carrier frequency as well as the probability of corrected detection should be higher than 0.9. After the Fusion Centre (FC) chooses the optimum transmission schemes forall users, FC will command all users to transmit according to the decision by feedback channels.
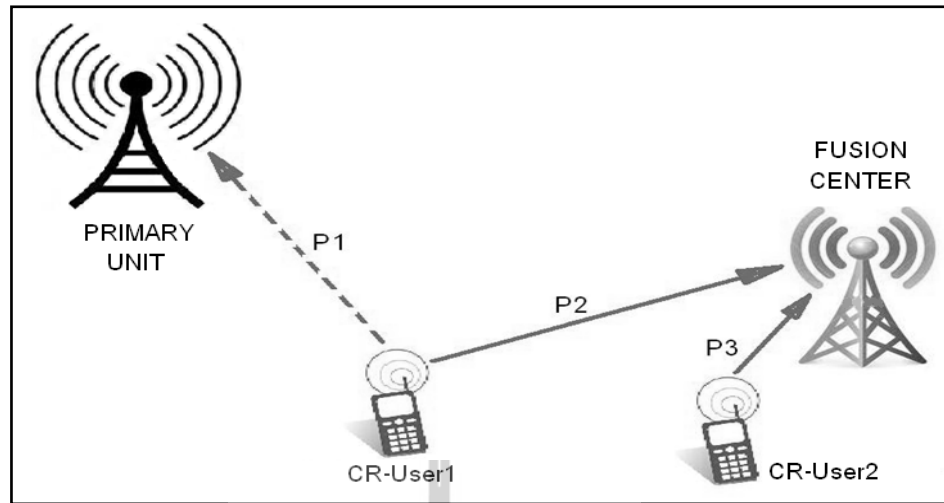
Figure 2.6 Each user adopts different MIMO scheme to control interference at PU.
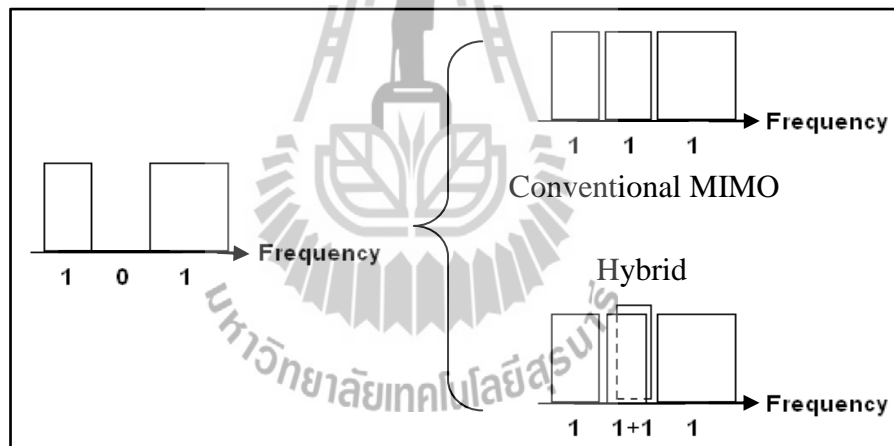
Figure 2.7 Efficiency of hybrid MIMO when occupies vacant channel in CRN.

2.3 The Need of Hybrid-MIMO to CRN

Because of the limitation of spectrum band (as shown in Figure 2.5) and transmitted power in CRN, all users should have ability to change the transmission

scheme as well as MIMO scheme to protect PN from the over limit of interference. The advantage of hybrid MIMO to CRN can be described as follow.

2.3.1 Advantage of Hybrid-MIMO

For the CRN scenario, each user can be independently travelled around network. Thus each user will face the different channel as well as the different distance from FC under the power control to protect PU. From Figure 2.6, CR-User1 locates closely to PU. Therefore this user should adopt the low transmitted power scheme to protect PU by using STBC MIMO instead of SM MIMO that use higher transmitted power. On the other hand, CR-User2 locates far away from PU, thus this user can adopt SM MIMO to get the higher spectral efficiency although this scheme use the high transmitted power. From above reasons, if each user in CRN can adopt different MIMO scheme, the CRN can increase the spectral efficiency instead of using the conventional MIMO that may occupy channel for only one user.

2.3.2 The Spectrum Efficiency of Hybrid-MIMO

For a single vacant channel case, by considering the need in the sub section 2.3.1, two users of hybrid MIMO or more can occupy the vacant channel simultaneously. Therefore CRN will achieve double capacity gain instead of using the conventional MIMO that may take lower capacity gain as shown in Figure 2.7.

2.4 Literature Review and Related Work

2.4.1 MIMO Systems

MIMO communication is the advanced technology for recent and future platform. Both transmitting and receiving side are equipped with multiple antennas to expand the opportunity for receiving the higher receive signal. Both

diversity gain and channel capacity can be increased corresponding to the number of antennas. The Spatial Multiplexing (SM) MIMO (Foschini, 1996) applies multiple antennas at transmitter and receiver to increase capacity gain as well as the Space-Time Block Coding (STBC) MIMO (Alamouti, 1998 and Tarokh, 1999) applies two time slots and two antennas to transmit block coding message to the receiver. The combination signal and orthogonal symbols at the receiver can increase the signal reliability and diversity gain.

2.4.2 Hybrid-MIMO Systems

Hybrid-MIMO system has been developed for applying in flexible work. Both channel capacity and diversity gain can be improved when each user can adopt different MIMO scheme to increase spectrum efficiency. The first hybrid-MIMO system (Mohd, 2004) can switch MIMO scheme automatically according to channel condition by using feedback signal from the receiver. However this scheme offers a quite low data rate. Then Successive Interference Cancellation (SIC) and Linear Detection (LD) are adopted into hybrid-MIMO system (Freitas, 2005). The multi-layer STBC system was proposed (Ming, 2007)by trade-off between the higher diversity gain and complexity. Thenthe special hybrid-MIMO code was proposed (Cortez, 2008) while matric decomposition and inverse matrix are applied at the receiver. Next, the two STBC layers scheme was proposed (Tan, 2009) by applying SIC and LD but the system offer quite low data rate that cause by two STBC layers. Finally, the computational method was proposed (Song, 2010) by applying matrix decomposition and inverse matrix to separate and detect all streams. However this method offers the high complexity and quite low diversity gain. From above reasons, this thesis proposes the method to apply SIC and LD to separate all layers and cancel

the interference from other users before detect the first stream. By this technique, the receiver can cancel more interference than the existing hybrid-MIMO.

2.4.3 Interference Cancellation Technique

This technique can be divided into two types (Reinhardt, 2006;Bai, 2008; Chun, 2008 and Kim, 2009). The first is SIC. The interference of other users can be cancelled according to the special order without considering the noise level in each layer. The second type is the Ordered Successive Interference Cancellation (OSIC). The interferences in all layers are compared and sorted according to the noise level. The first layer for detection should have the lowest interference. This technique offers higher complexity than the first technique while both techniques offer the approximate diversity gain.

2.4.4 MIMO Technique in CRN

The MIMO technique can be efficiently applied in CRN to improve the channel capacity and diversity gain (Mao, 2012; Alian, 2012 and Driouch, 2012). Moreover the MIMO OFDM systems can be used to increase the spectrum efficiency of CRN, because several users can apply a single vacant channel simultaneously.

2.5 Summary

This chapter explains the meaning and principle of CRN, literature review, principle of encoding and decoding of both MIMO and hybrid MIMO systems while the benefits of each technique are also described. Moreover the interference cancellation and MIMO system used in CRN are briefly explained.

CHAPTER III

PRINCIPLE OF MIMO ANDHYBRID-MIMO SYSTEMS

3.1   Introduction

This chapter discusses about the principle and theory of MIMO systems. The steps of IC that are jointly applied with MIMO detection are described. Moreover noise power in SM detection and SM-SIC systems is presented. The principle of hybrid MIMO and the channel capacity calculation are discussed. Finally SER analysis of hybrid MIMO systems is briefly discussed.

3.2   MIMO Detection

MIMO transmitter and receiver are equipped with multiple antennas. The transmit signal are sent through MIMO channel to the receiver at the same time. The received signal at the receiver can be written as

$$\boldsymbol{y} = \boldsymbol{Hx} + \boldsymbol{z} \quad (3\text{-}1)$$

$$\begin{bmatrix} \boldsymbol{y}_1 \\ \vdots \\ \boldsymbol{y}_{N_r} \end{bmatrix} = \begin{bmatrix} h_{11} & \cdots & h_{1N_t} \\ \vdots & \ddots & \vdots \\ h_{N_r 1} & \cdots & h_{N_r N_t} \end{bmatrix} \begin{bmatrix} \boldsymbol{x}_1 \\ \vdots \\ \boldsymbol{x}_{N_t} \end{bmatrix} + \begin{bmatrix} z_1 \\ \vdots \\ z_{N_r} \end{bmatrix} \quad (3\text{-}2)$$

where **y** denotes the received signal vector, **H** denotes the channel matrix, **x** denotes the transmitted symbol vector and **z** denotes the white Gaussian noise vector with zeromean and variance σ_z^2. Assign N_r and N_t represent the number of receive antenna and the number of transmit antenna, respectively.

3.2.1 Linear Signal Detection

When the transmitted signals arrive to the receiver, the received signal will be detected by applying weight matrix **W** by

$$\tilde{\mathbf{x}} = [\tilde{x}_1 \ \tilde{x}_2 \ \tilde{x}_3 ... \tilde{x}_{N_t}]^T = \mathbf{W}\mathbf{y} \tag{3-3}$$

where (3-3) represents the detected symbol. The linear signal detection can be generally divided into two methods. One is Zero-Forcing (ZF) technique and another is Minimum Mean Square Error (MMSE).

1) Zero-Forcing (ZF)

The interference of other streams can be cancelled by weight matrix as follows.

$$\mathbf{W}_{ZF} = (\mathbf{H}^H \mathbf{H})^{-1} \mathbf{H}^H \tag{3-4}$$

where $(\cdot)^H$ represents conjugate transpose operation and the dimension of **H** is $N_r x N_t$. The detected symbols can be detected by

$$\tilde{\mathbf{x}}_{ZF} = \mathbf{W}_{ZF} \mathbf{y} = \mathbf{x} + (\mathbf{H}^H \mathbf{H})^{-1} \mathbf{H}^H \mathbf{z} = \mathbf{x} + \mathbf{z}_a \tag{3-5}$$

where $\mathbf{z}_a = [z_{a1} \ z_{a2} \ z_{a3} ... z_{aNr}]^T$ denotes the noise vector due to ZF process.

2) Minimum Mean Square Error (MMSE)

The interference of other streams can be cancelled by weight matrix as follows.

$$W_{MMSE} = \left(H^H H + \sigma_z^2 I \right)^{-1} H^H \tag{3-6}$$

where I denotes the identity matrix with dimension $N_r x N_t$. The detected symbols can be detected by

$$\hat{x}_{MMSE} = W_{MMSE} y = (H^H H + \sigma_z^2 I)^{-1} H^H y = \hat{x} + (H^H H + \sigma_z^2 I)^{-1} H^H z \tag{3-7}$$

3.3.2 Maximum Likelihood Detection

For detection, the minimum Euclidean distance is used to choose the optimum signal. This distance can be calculated from the difference between the received signal and the multiply product of channel matrix and all possible symbols in constellation. The detected symbols can be obtained by

$$\hat{x}_{ML} = \arg\min_{x \in C^{Nt}} \left\| y - Hx \right\|_F^2 \tag{3-8}$$

where C denotes all possible symbols in constellation and $\left\| \cdot \right\|_F^2$ represents Frobenius norm operation that the meaning is $\left\| A \right\|_F \square \sqrt{\sum_{i=1}^{a} \sum_{j=1}^{b} \left| A_{ij} \right|^2}$, where a and b denote the number of row and the number of column of matrix A, respectively.
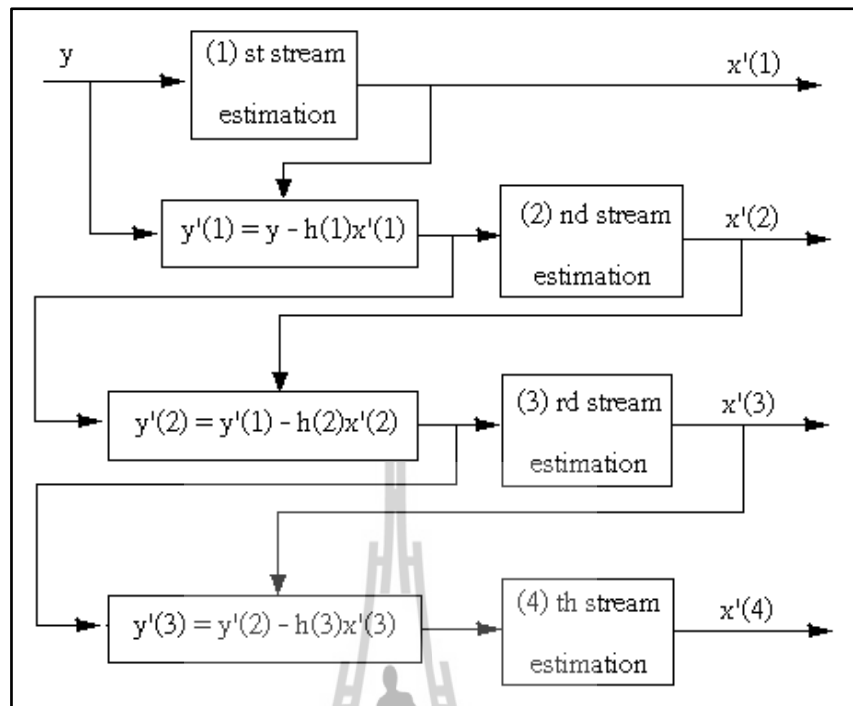
Figure 3.1 Principle of multi-layer detection (Cho, 2012).

3.3 Interference Cancellation in MIMO Systems

Generally, the MIMO received signal consist of multilayer signal from each transmit antenna. The receiver should cancel all signals of other users and detect only signal of the desired user. After that, the second layer can be detected by cancelling symbols of the first layer and other users. Then other layers can be detected by repeating above instructions until detecting the last layer. This process can be explained in Figure 3.1 where the four layers from four transmit antennas are transmitted to the single receive antenna. This method applies SM detection jointly with SIC. The interference cancellation can be divided into two methods as follows.

3.3.1 SIC

For this method, the interference of other users can be cancelled according to the special order without considering the noise level in each layer. As shown in Figure 3.1, parameter *n* of *x'(n)* is not selected by considering its noise power level.

3.3.2 OSIC

For this technique, the interference in all layers are compared and sorted according to the noise level. The first layer for detection should have the lowest interference. Considering Figure 3.1, parameter *n* of *x'(n)* is selected by considering noise power level in all layers. Thus the layer at *x'(4)* has the highest noise power level because this is the last layer for detection.

3.4 Noise Power in Interference Cancellation Process

For this part, the noise power of linear detection is calculated and compared to the noise power in the linear detection joining with SIC technique as follows.

3.4.1 Noise Power in ZF Detection

From (3-5), the detected symbol vector is $\check{x}_{ZF} = x + (H^{H}H)^{-1}H^{H}z$. Thus noise signal after detection is $\tilde{z}_{ZF} = (H^{H}H)^{-1}H^{H}z$. The power of noise can be calculated by using SVD decomposition as follows, where $H = U\Sigma V^{H}$.

$$\left\|\tilde{z}_{ZF}\right\|_{F}^{2} = \left\|(H^{H}H)^{-1}H^{H}z\right\|_{F}^{2}$$

$$= \left\|\left(\left(U\Sigma V^{H}\right)^{H}\left(U\Sigma V^{H}\right)\right)^{-1}V\Sigma U^{H}z\right\|_{F}^{2}$$

$$= \left\| \left(\boldsymbol{V\Sigma U}^{\mathrm{H}} \boldsymbol{U\Sigma V}^{\mathrm{H}} \right)^{-1} \boldsymbol{V\Sigma U}^{\mathrm{H}} \boldsymbol{z} \right\|_{\mathrm{F}}^{2}$$

$$= \left\| \left(\boldsymbol{V\Sigma}^{2} \boldsymbol{V}^{\mathrm{H}} \right)^{-1} \boldsymbol{V\Sigma U}^{\mathrm{H}} \boldsymbol{z} \right\|_{\mathrm{F}}^{2}$$

$$= \left\| \boldsymbol{V\Sigma}^{-2} \boldsymbol{V}^{\mathrm{H}} \boldsymbol{V\Sigma U}^{\mathrm{H}} \boldsymbol{z} \right\|_{\mathrm{F}}^{2}$$

$$\left\| \tilde{z}_{\mathrm{ZF}} \right\|_{\mathrm{F}}^{2} = \left\| \boldsymbol{V\Sigma}^{-1} \boldsymbol{U}^{\mathrm{H}} \boldsymbol{z} \right\|_{\mathrm{F}}^{2} \quad (3\text{-}9)$$

By using the unitary matrix property in Frobenius norm operation that can be presented as $\left\| \boldsymbol{VA} \right\|_{F}^{2} = \left\| \boldsymbol{A} \right\|_{F}^{2}$, (3-9) can be reformed to be

$$\left\| \tilde{z}_{\mathrm{ZF}} \right\|_{\mathrm{F}}^{2} = \left\| \boldsymbol{\Sigma}^{-1} \boldsymbol{U}^{\mathrm{H}} \boldsymbol{z} \right\|_{\mathrm{F}}^{2}. \qquad (3\text{-}10)$$

Then the average noise power for ZF detection can be described as

$$\mathrm{E} \left\{ \left\| \tilde{\mathbf{z}}_{\mathrm{ZF}} \right\|_{\mathrm{F}}^{2} \right\} = \mathrm{E} \left\{ \left\| \boldsymbol{\Sigma}^{-1} \mathbf{U}^{\mathrm{H}} \mathbf{z} \right\|_{\mathrm{F}}^{2} \right\}$$

$$= \mathrm{E} \left\{ \mathrm{tr} \left(\boldsymbol{\Sigma}^{-1} \mathbf{U}^{\mathrm{H}} \mathbf{z} \mathbf{z}^{\mathrm{H}} \mathbf{U} \boldsymbol{\Sigma}^{-1} \right) \right\}$$

$$= \mathrm{tr} \left(\boldsymbol{\Sigma}^{-2} \mathrm{E} \left\{ \mathbf{z} \mathbf{z}^{\mathrm{H}} \right\} \right)$$

$$= \sigma_{\mathrm{z}}^{2} \mathrm{tr} \left(1 / \boldsymbol{\Sigma}^{2} \right)$$

$$= \sigma_{\mathrm{z}}^{2} / \sum_{\mathrm{i=1}}^{\min(\mathrm{Nr,Nt})} \sigma_{\mathrm{i}}^{2} \quad (3\text{-}11)$$

3.4.2 Noise Power in ZF Detection Joining with SIC

For this technique, the noise power in the first layer equals to part 3.4.1 but noise signal in the next layer is cancelled. Then the first detected symbol x1 is used to regenerate the received signals (where the transmitted symbols is $x = [x_1 \ x_2 \ x_3 ... x_{Nt}]^T$) for the first layer as $y_1 = H_{L1} \tilde{x}_{ZF1} = H_{L1}(x_1 + za_1)$, where $H_{L1} = [h_{11} \ h_{21} \ h_{31} ... h_{Nr1}]^T$ denotes the sub-channel for x1. Next, the regenerated signals are removed from the received signal and then the received signal of the second layer can be taken by $y_{L2} = y - y_1$. The weight matrix of ZF in the second layer can be written by

$$W'_{ZF} = (H_{L2}^H H_{L2})^{-1} H_{L2}^H \tag{3-12}$$

where H_{L2} denotes channel matrix that cancel H_{L1} away from H, where $H_{L2} = U_{L2} \Sigma_{L2} V_{L2}^H$ with dimension $N_r x N_t - 1$. Then the detected symbol of the second layer can be obtained by

$$\tilde{x}_{ZF2} = W'_{ZF} y_{L2} = W'_{ZF}\left(y - H_{L1}(x_1 + z_{a1})\right)$$

$$= W'_{ZF}\left(H_{L1}x_1 + H_{L2}x_{L2} + z - H_{L1}x_1 - H_{L1}z_{a1}\right)$$

$$= W'_{ZF}\left(H_{L2}x_{L2} + z - H_{L1}z_{a1}\right)$$

$$= x_{L2} + W'_{ZF}\left(z - H_{L1}z_{a1}\right)$$

$$= x_{L2} + W'_{ZF}\left(z - z_d\right) \tag{3-13}$$

where$x_{L2}=[x_2\ x_3\ x_4 ... x_{Nt}]^{\mathrm{T}}$ denotes all symbols in the second layer and $z_d = H_{L1}z_{a1}$. From (3-12) and (3-13), the noise power in the second layer can be carried out by

$$\left\| \tilde{z}_{ZFL2} \right\|_F^2 = \left\| (H_{L2}^H H_{L2})^{-1} H_{L2}^H (z - z_d) \right\|_F^2$$

$$= \left\| \left((U_{L2}\Sigma_{L2}V_{L2}^H)^H (U_{L2}\Sigma_{L2}V_{L2}^H) \right)^{-1} V_{L2}\Sigma_{L2}U_{L2}^H (z - z_d) \right\|_F^2$$

$$= \left\| \left(V_{L2}\Sigma_{L2}U_{L2}^H U_{L2}\Sigma_{L2}V_{L2}^H \right)^{-1} V_{L2}\Sigma_{L2}U_{L2}^H (z - z_d) \right\|_F^2$$

$$= \left\| \left(V_{L2}\Sigma_{L2}^2 V_{L2}^H \right)^{-1} V_{L2}\Sigma_{L2}U_{L2}^H (z - z_d) \right\|_F^2$$

$$= \left\| V_{L2}\Sigma_{L2}^{-2}V_{L2}^H V_{L2}\Sigma_{L2}U_{L2}^H (z - z_d) \right\|_F^2$$

$$= \left\| V_{L2}\Sigma_{L2}^{-1}U_{L2}^H (z - z_d) \right\|_F^2 \quad (3\text{-}14)$$

By the same reason to (3-9) and (3-10), V_{L2} can be cancelled without any effect to (3-14). Thus the signal power in ZF detection joining with SIC for the second layer is

$$E\left\{ \left\| \tilde{z}_{ZFL2} \right\|_F^2 \right\} = E\left\{ \left\| \Sigma_{L2}^{-1}U_{L2}^H (z - z_d) \right\|_F^2 \right\}$$

$$= E\left\{ tr\left(\Sigma_{L2}^{-1}U_{L2}^H (z - z_d)(z - z_d)^H U_{L2}\Sigma_{L2}^{-1} \right) \right\}$$

$$= tr\left(\Sigma_{L2}^{-2} E\left\{ (z - z_d)(z - z_d)^H \right\} \right)$$

$$= \sigma_{z2}^2 tr\left(1/\Sigma_{L2}^2 \right)$$

$$= \sigma_{z2}^2 / \sum_{i=1}^{\min(Nr,Nt-1)} \widehat{\sigma}_i^2 \quad (3\text{-}15)$$
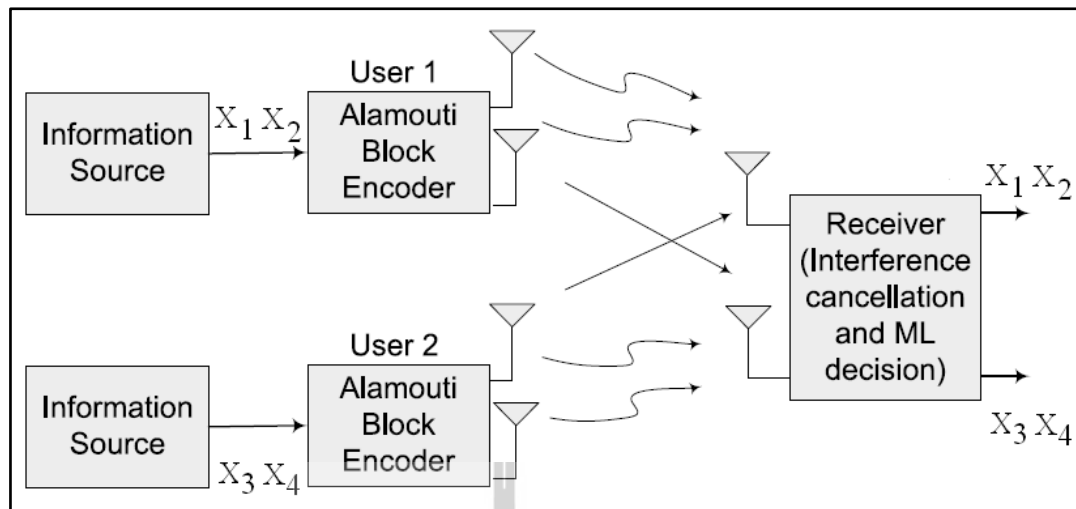
Figure 3.2 Multiuser detection of Alamouti signal (Tan, 2009).

From (3-11) and (3-15), these equations show that the average noise power in the second layer for SIC technique is reduced when compared to detection in the first layer due to σ_{z2}^2 less than σ_z^2. Because some interference is removed as presented in (3-13) while the summation of $\widehat{\sigma}_i^2$ approximate to the summation of σ_i^2. Moreover σ_{z2}^2 and σ_z^2 offer very small noise power and they arethe dividend in equation. Besides,if they are compared with the summation of σ_i^2 and $\widehat{\sigma}_i^2$ that have the higher power and they are the denominator in equation, this mean that the performance of ZF detection joining with SIC technique outperforms the general ZF detection.

3.5   Principle of Hybrid-MIMO Systems

This section explains basic principle of the conventional hybrid-MIMO according to literature review. They can be divided into four techniques as follows.

3.5.1   MU Detection of Alamouti Signal (A-BLAST)

Two users at transmitting side transmit their data streams simultaneously during two time slots over MIMO channel. From Figure 3.2, the receiver applies SM detection (ZF, MMSE, or ML) joining with SIC. Anyway this scheme offer quite low data rate because Alamouti code is adopted for both users. Its encoding process and decoding can be described as follows.

$$x_a = \begin{bmatrix} x_1 & -x_2^* \\ x_2 & x_1^* \end{bmatrix}, \quad x_b = \begin{bmatrix} x_3 & -x_4^* \\ x_4 & x_3^* \end{bmatrix} \quad (3\text{-}16)$$

$$x = \begin{bmatrix} x_a \\ x_b \end{bmatrix} \quad (3.17)$$

$$H = \begin{bmatrix} h_{11} & h_{21} & h_{31} & h_{41} \\ h_{12} & h_{22} & h_{32} & h_{42} \\ h_{13} & h_{23} & h_{33} & h_{43} \\ h_{14} & h_{24} & h_{34} & h_{44} \end{bmatrix} \quad (3\text{-}18)$$

$$y = Hx = \begin{bmatrix} y_1 & y_5 \\ y_2 & y_6 \\ y_3 & y_7 \\ y_4 & y_8 \end{bmatrix} \quad (3\text{-}19)$$

where x_a denotes the transmitted power of the first user, x_b denotes the transmitted power of the second user, H denotes MIMO channel with dimension $N_r \times N_t$ and

y denotes the received signal during two time slots. Then ML is used to detect the

desired symbols from the first user as

$$\check{x} = \arg\min_{\check{x}_k \in C^{Nt}} \left\| y - H\check{x}_k \right\|_F^2 \quad (3\text{-}20)$$

$$H_a = \begin{bmatrix} h_{11} & h_{21} \\ h_{12} & h_{12} \\ h_{13} & h_{13} \\ h_{14} & h_{14} \end{bmatrix} \quad (3\text{-}21)$$

Then the received signal of the first user can be regenerated by (3-22) and cancel this

signal from the received signal in (3-19) to achieve the received signal for the second

user as shown in (3-23).

$$\hat{y}_a = H_a \begin{bmatrix} \hat{x}_1 & -\hat{x}_2^* \\ \hat{x}_2 & \hat{x}_1^* \end{bmatrix} \quad (3\text{-}22)$$

where $\hat{x}_1$ and $\hat{x}_2$ denote the detected symbols of the first user that can be obtained by

(3-20).

$$\hat{y}_b = y - \hat{y}_a = \begin{bmatrix} y_{b1} & y_{b2} \\ y_{b3} & y_{b4} \\ y_{b5} & y_{b6} \\ y_{b7} & y_{b8} \end{bmatrix} \quad (3\text{-}23)$$

$$\hat{y}_b^\nabla = \begin{bmatrix} y_{b1} & y_{b2}^* & y_{b3} & y_{b4}^* & y_{b5} & y_{b6}^* & y_{b7} & y_{b8}^* \end{bmatrix}^T \quad (3\text{-}24)$$

$$\boldsymbol{H}_b = \begin{bmatrix} h_{31} & h_{41} \\ h_{32} & h_{42} \\ h_{33} & h_{43} \\ h_{34} & h_{44} \end{bmatrix} \tag{3-25}$$

$$\check{\boldsymbol{H}}_b = \begin{bmatrix} h_{31} & h_{41}^* & h_{32} & h_{42}^* & h_{33} & h_{43}^* & h_{34} & h_{44}^* \\ h_{41} & -h_{31}^* & h_{42} & -h_{32}^* & h_{43} & -h_{33}^* & h_{44} & -h_{34}^* \end{bmatrix}^T \tag{3-26}$$

$$\boldsymbol{H}_b^\dagger = (\check{\boldsymbol{H}}_b^H \check{\boldsymbol{H}}_b)^{-1} \check{\boldsymbol{H}}_b^H \tag{3-27}$$

Then the detected symbols for the second user can be decoded by

$$\check{\boldsymbol{x}}_b = \boldsymbol{H}_b^\dagger \hat{\boldsymbol{y}}_b^\nabla \tag{3-28}$$

3.5.2 Transmit Diversity and Combining Scheme for SM (TDCSM)

At the receiver, the received signal matrix and MIMO channel matrix are decomposed into sub-matrix that has the specific form. Then these matrixes are used to cancel the interference and used to detect data streams for all users as shown in Figure 3.3. The TDCSM process can be started by dividing the channel matrix $\boldsymbol{H}$ into several sub-matrixes as follows.

$$\boldsymbol{A} = \begin{bmatrix} h_{11} & h_{21} \\ h_{12} & h_{22} \end{bmatrix} \qquad , \qquad \boldsymbol{B} = \begin{bmatrix} h_{31} & h_{41} \\ h_{32} & h_{42} \end{bmatrix} \tag{3-29}$$

$$\boldsymbol{C} = \begin{bmatrix} h_{13} & h_{23} \\ h_{14} & h_{24} \end{bmatrix} \qquad , \qquad \boldsymbol{D} = \begin{bmatrix} h_{33} & h_{43} \\ h_{34} & h_{44} \end{bmatrix} \tag{3-30}$$

$$\boldsymbol{x} = \begin{bmatrix} x_1 & x_5 \\ x_2 & x_6 \\ x_3 & -x_4^* \\ x_4 & x_3^* \end{bmatrix} \tag{3-31}$$

$$\boldsymbol{x}_a = \begin{bmatrix} x_1 & x_5 \\ x_2 & x_6 \end{bmatrix} \quad , \quad \boldsymbol{x}_b = \begin{bmatrix} x_3 & -x_4^* \\ x_4 & x_3^* \end{bmatrix} \tag{3-32}$$

$$\boldsymbol{y} = \boldsymbol{Hx} + \boldsymbol{z} = \begin{bmatrix} y_1 & y_5 \\ y_2 & y_6 \\ y_3 & y_7 \\ y_4 & y_8 \end{bmatrix} = \begin{bmatrix} \boldsymbol{y}_a \\ \boldsymbol{y}_b \end{bmatrix} \tag{3-33}$$

The received signals are decomposed into two sub-matrixes as

$$\boldsymbol{y}_a = \begin{bmatrix} y_1 & y_5 \\ y_2 & y_6 \end{bmatrix} \quad , \quad \boldsymbol{y}_b = \begin{bmatrix} y_3 & y_7 \\ y_4 & y_8 \end{bmatrix} \tag{3-34}$$

$$\boldsymbol{y}_a = \boldsymbol{Ax}_a + \boldsymbol{Bx}_b + \boldsymbol{z}_1 \tag{3-35}$$

$$\boldsymbol{y}_b = \boldsymbol{Cx}_a + \boldsymbol{Dx}_b + \boldsymbol{z}_2 \tag{3-36}$$

These sub-matrixes are used to decoded the STBC symbols by

$$\hat{\boldsymbol{x}}_b = [\hat{s}_3 \ \hat{s}_4]^T = \boldsymbol{A}^{-1}\boldsymbol{y}_a - \boldsymbol{C}^{-1}\boldsymbol{y}_b$$

$$= (\boldsymbol{A}^{-1}\boldsymbol{B} - \boldsymbol{C}^{-1}\boldsymbol{D})\boldsymbol{x}_b + \boldsymbol{A}^{-1}\boldsymbol{z}_1 - \boldsymbol{C}^{-1}\boldsymbol{z}_2 \tag{3-37}$$
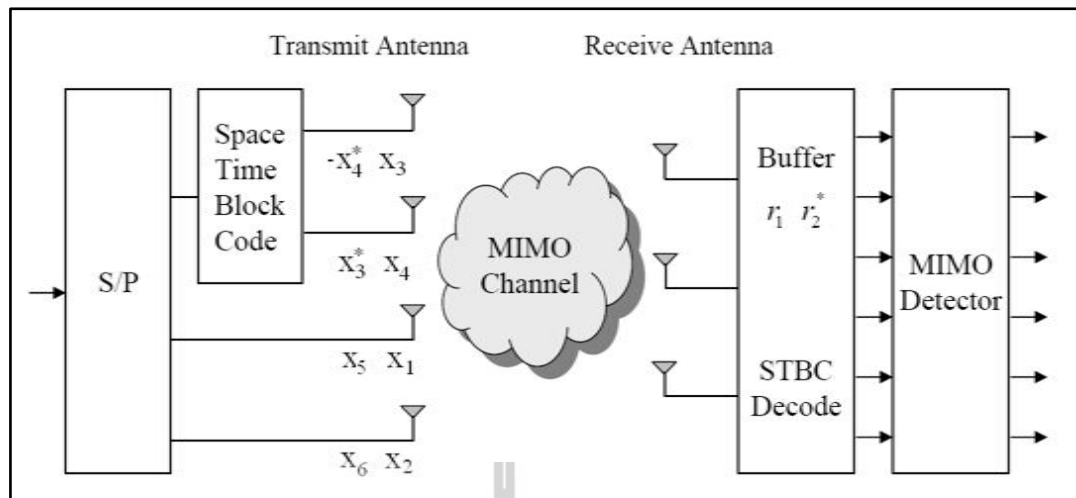
Figure 3.3 TDCSM block diagram (Song, 2010).

The signal from (3-37) is used to regenerate received signal for the SBTC user and cancels with the received signals by

$$\hat{y}_a = y - \begin{bmatrix} h_{11} & h_{21} \\ h_{12} & h_{22} \\ h_{13} & h_{23} \\ h_{14} & h_{24} \end{bmatrix} \begin{bmatrix} \hat{x}_3 & -\hat{x}_4^* \\ \hat{x}_4 & \hat{x}_3^* \end{bmatrix} \quad (3-38)$$

The received signals of the SM user from (3-38) are used for ML detection as

$$\hat{\mathbf{x}}_a = \arg\min_{\mathbf{x}_k \in C^{N_t-2}} \left\| \hat{\mathbf{y}}_a - \begin{bmatrix} \mathbf{A} \\ \mathbf{C} \end{bmatrix} \mathbf{x}_k \right\|_F^2 \quad (3-39)$$
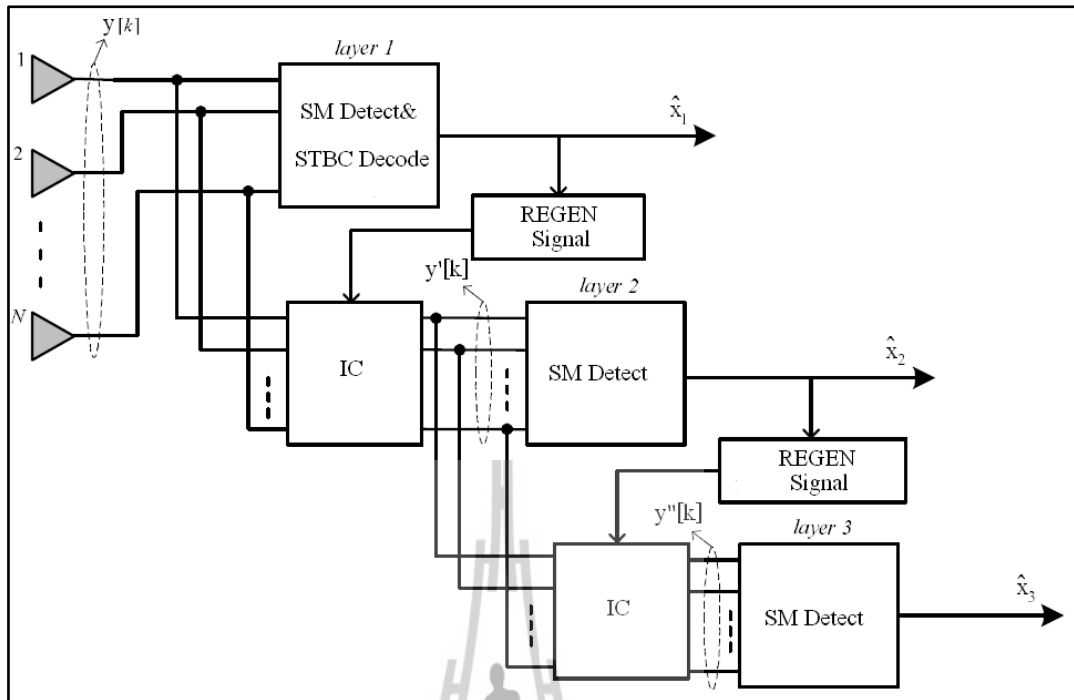
Figure 3.4 HMTS block diagram (Freitas, 2005)

3.5.3 Hybrid MIMO Transceiver Scheme (HMTS)

The transmitted signals are decoded by SM code and STBC code and transmit pass through MIMO channel. The receiver applies MMSE detection jointly with SIC to separate and detect the transmitted symbols for each user. The process of encoding and decoding for HMTS are described as follows.

$$x = \begin{bmatrix} x_1 & x_2 & x_3 & x_4 \\ x_5 & x_6 & -x_4^* & x_3^* \end{bmatrix}^T \tag{3-40}$$

$$y = Hx + z = \begin{bmatrix} y_1 & y_5 \\ y_2 & y_6 \\ y_3 & y_7 \\ y_4 & y_8 \end{bmatrix} \tag{3-41}$$

The received signals from (3-41) are detected by ML detection by

$$\widehat{x} = \arg\min_{x_k \in C^{Nt}} \|y - Hx_k\|_F^2 \tag{3-42}$$

The detected symbols from (3-42) do not employed because they combine with a rich interference. Anyway, these symbols are used for STBC decoding process as shown

$$\widehat{x}_{STBC} = [\widehat{x}_3 \; \widehat{x}_4]^T \tag{3-43}$$

$$H_{STBC} = \begin{bmatrix} h_{31} & h_{41} \\ h_{32} & h_{42} \\ h_{33} & h_{43} \\ h_{34} & h_{44} \end{bmatrix} \tag{3-44}$$

$$H_{ASTBC} = \begin{bmatrix} h_{31} & h_{41}^* & h_{32} & h_{42}^* & h_{33} & h_{43}^* & h_{34} & h_{44}^* \\ h_{41} & -h_{31}^* & h_{42} & -h_{32}^* & h_{43} & -h_{33}^* & h_{44} & -h_{34}^* \end{bmatrix}^T \tag{3-45}$$

$$H_{ASTBC}^\dagger = (H_{ASTBC}^H H_{ASTBC})^{-1} H_{ASTBC}^H \tag{3-46}$$

The receiver applies the decoding symbols of STBC user from (3-44) to regenerate the new received signal for STBC user that have lower interference. This process can be described as

$$\hat{y}_{STBC} = H_{STBC} \widehat{x}_{STBC} = \begin{bmatrix} y_a & y_b \\ y_c & y_d \\ y_e & y_f \\ y_g & y_h \end{bmatrix} \tag{3-47}$$

$$\hat{y}_{STBC}^\nabla = \begin{bmatrix} y_a & y_b^* & y_c & y_d^* & y_e & y_f^* & y_g & y_h^* \end{bmatrix}^T \tag{3-48}$$

Then the signals in (3-45) and (3-48) are jointly applied to decode the transmitted symbols of STBC user.

$$\check{\boldsymbol{x}}_{STBC} = \boldsymbol{H}^{\dagger}_{ASTBC}\hat{\boldsymbol{y}}^{\nabla}_{STBC} \tag{3-49}$$

The decoded STBC symbols from (3-49) are used to calculate the received signals for SM user as

$$\hat{\boldsymbol{y}}_{SM} = \boldsymbol{y} - \boldsymbol{H}_{STBC}\check{\boldsymbol{x}}_{STBC} \tag{3-50}$$

Apply the signals from (3-50) into ML detection process to get the transmitted symbols for SM user as shown

$$\check{\boldsymbol{x}}_{SM} = \arg\min_{\boldsymbol{x}_k \in C^{Nt-2}} \left\| \hat{\boldsymbol{y}}_{SM} - \boldsymbol{H}_{SM}\boldsymbol{x}_k \right\|^2_F \tag{3-51}$$

3.5.4 ABBA-VBLAST Hybrid Space-Time Code

The transmitted symbols are encoded by SM code and the special code ABBA and transmit these symbols over MIMO channel. The receiver applies QR decomposition and inverse matrix operation to detect all transmitted symbols from transmitting side. All ABBA process can be explained as

$$\boldsymbol{x}_{spa} = \begin{bmatrix} x_1 & -x_2^* \\ x_3 & -x_4^* \end{bmatrix} \tag{3-52}$$

$$\boldsymbol{x}_{abba} = \begin{bmatrix} x_5 & -x_6^* \\ x_6 & x_5^* \end{bmatrix} \tag{3-53}$$
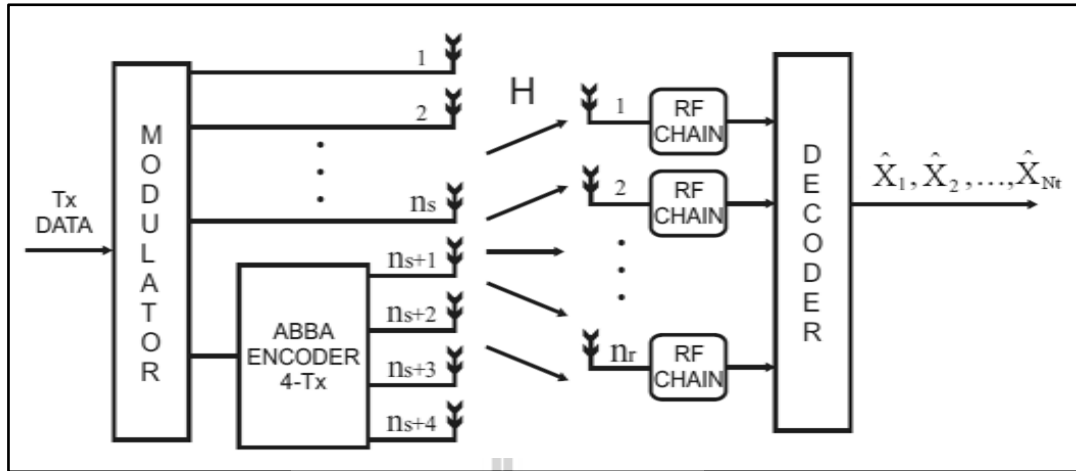
Figure 3.5 ABBA-VBLAST block diagram (Cortez, 2008).

$$y = H \begin{bmatrix} x_{spa} \\ x_{abba} \end{bmatrix} + z \qquad (3\text{-}54)$$

$$y = \begin{bmatrix} y_1^{t1} & y_1^{t2} \\ y_2^{t1} & y_2^{t2} \\ y_3^{t1} & y_3^{t2} \\ y_4^{t1} & y_4^{t2} \end{bmatrix} \qquad (3\text{-}55)$$

The received signal from (3-55) can be rearranged for the next step as

$$y_{LD} = \begin{bmatrix} y_1^{t1} & y_1^{t2*} & y_2^{t1} & y_2^{t2*} & y_3^{t1} & y_3^{t2*} & y_4^{t1} & y_4^{t2*} \end{bmatrix}^T$$

$$y_{LD} = H_{LD} x_{LD} + z_{LD} \qquad (3\text{-}56)$$

QR decomposition can be used to decompose the channel matrix by

$$H_{LD} = \begin{bmatrix} H_{spa} & H_{abba} \end{bmatrix} = Q_{LD} R_{LD} \qquad (3\text{-}57)$$

$$H_{spa} = \begin{bmatrix} H_{1,1}^{spa} & H_{1,2}^{spa} \\ H_{2,1}^{spa} & H_{2,2}^{spa} \\ H_{3,1}^{spa} & H_{3,2}^{spa} \\ H_{4,1}^{spa} & H_{4,2}^{spa} \end{bmatrix} \tag{3-58}$$

$$H_{i,j}^{spa} = \begin{bmatrix} h_{ij} & 0 \\ 0 & -h_{ij}^{*} \end{bmatrix} \tag{3-59}$$

$$H_{abba} = \begin{bmatrix} h_{13} & h_{14}^{*} & h_{23} & h_{24}^{*} & h_{33} & h_{34}^{*} & h_{43} & h_{44}^{*} \\ h_{14} & -h_{13}^{*} & h_{24} & -h_{23}^{*} & h_{34} & -h_{33}^{*} & h_{44} & -h_{43}^{*} \end{bmatrix}^{T} \tag{3-60}$$

$$\breve{y}_{LD} = Q_{LD}^{H} y_{LD} = R_{LD} x_{LD} + \tilde{z}_{LD} \tag{3-61}$$

From (3-61), this equation shows the relationship between the received signals and the transmitted symbols. Apply this relation to decide all decoding symbols by

$$\hat{x}_j = D\left[\frac{\tilde{y}_j - \sum\limits_{i=j+1}^{N_s} r_{j,i} \cdot \hat{x}_i}{r_{j,j}} \right] \tag{3-62}$$

where N_i denotes the number of transmitted symbols, $\hat{x}_i$ denotes element in symbol vector $\hat{x}$ that should detect from element i to N_i and $D[\cdot]$ represents the symbol selection operation for $\hat{x}_j$ that can be chosen when the multiply product between $\hat{x}_i$ and the element of matrix R is approximation to $\tilde{y}_j$, where

$$\tilde{y}_j = r_{j,i} x_j + \sum\limits_{i=j+1}^{N_s} r_{j,i} \cdot x_i + \tilde{z}_j \tag{3-63}$$

From discussion about all hybrid-MIMO techniques show that they apply the complex algorithm to detect and separate message data. Thus this research will modify the conventional hybrid-MIMO schemes to improve diversity gain.Namely, the interference in the received signals are cancelled before detect the first stream. By this criterion, the performance of hybrid-MIMO can be simply improved. The proposed technique will be presented in the next chapter.

3.6   Channel Capacity of Hybrid-MIMO Systems

Channel capacity in communication systems can be indicated that how fastest for data rate can be transmitted over the limit bandwidth without error from radio channels. From this parameter, the limit of wireless transmission can be demonstrated. This section describes the channel capacity of the conventional MIMO and hybrid-MIMO as follows.

3.6.1   Channel Capacity of MIMO Systems

The channel capacities of MIMO signals depend on the information power to noise power ratio, number of transmit and receive antennas, and channel gain. Thus the channel capacity can be increased by increasing transmitted power or number of antenna. This relation can be expressed as

$$C_{MIMO} = E\left\{\log_2 \det(\boldsymbol{I}_{N_r} + \frac{\bar{\gamma}}{N_t}\boldsymbol{H}^H\boldsymbol{H})\right\}$$

(3-64)

where $E\{\cdot\}$ represents expectation operation and $\bar{\gamma}$ denotes signal to noise ratio.

3.6.2 Channel Capacity of Hybrid-MIMO Systems

The encoded matrix at the transmitting side applies both SM MIMO and STBC code by

$$
x_{Hybrid\text{-}MIMO}[k, k+1] = \begin{bmatrix} x_1 & -x_2^* \\ x_2 & x_1^* \\ x_3 & x_5 \\ x_4 & x_6 \end{bmatrix}
\tag{3-65}
$$

where k and $k+1$ denote the first and the second time slot, respectively. All symbols in the first column represent all transmitted symbol in the first time slot as well as the transmitted symbol in the second column represent all transmitted symbol in the second time slot. This equation shows that x_1 and x_2 are encoded by STBC code and they are transmitted during two time slot. Therefore the channel capacity should be multiplied by data symbol rate during two time slot (Thompson, 2004) as

$$
C_{Hybrid\text{-}MIMO} = \delta E \left\{ \log_2 \det(\boldsymbol{I}_{N_r} + \frac{\gamma}{N_t} \boldsymbol{H}_{Hb}^H \boldsymbol{H}_{Hb}) \right\}
\tag{3-66}
$$

where $\boldsymbol{H}_{Hb}$ denotes the MIMO channel during two time slots and $\delta = 3/4$.

$$
\mathbf{H}_{Hb} = \begin{bmatrix} \mathbf{H}_{A,1} & \mathbf{H}_{B,1} \\ \mathbf{H}_{A,2} & \mathbf{H}_{B,2} \\ \mathbf{H}_{A,3} & \mathbf{H}_{B,3} \\ \mathbf{H}_{A,4} & \mathbf{H}_{B,4} \end{bmatrix}
\tag{3-67}
$$

$$
\mathbf{H}_{A,n} = \begin{bmatrix} h_{n1} & h_{n2} \\ -h_{n2}^* & h_{n1}^* \end{bmatrix}
\tag{3-68}
$$

$$\mathbf{H}_{B,n} = \begin{bmatrix} h_{n1} & h_{n2} \\ h_{n1} & h_{n2} \end{bmatrix} \tag{3-69}$$

where the first column and the second column in (3-67) represent MIMO channel for STBC user and SM user, respectively.

3.7 Bit Error Rate of Hybrid-MIMO Systems

For any wireless communication services, the signal quality has been used to indicate the efficiency of wireless networks. The bit error rate (BER) is also the important parameter to demonstrate the quality of service. Several factors can affect to the BER such as environment, mobility, transmitted power and temperature. From this reason, BER of the hybrid-MIMO systems should be derived to demonstrate the performance of the proposed systems. Initially, the effective SNR γ_n can be obtained by combining signal in all layers. Where $\boldsymbol{\gamma}=[\gamma_1 \ \gamma_2 \ \gamma_3 \dots \gamma_L]$, $\gamma_a= \overline{\gamma}c_n$ and define the constant vector $\boldsymbol{c} = [c_1 \ c_2 \ c_3 \ \dots \ c_L]$, where L denotes the number of layersin the received signals. Then γ_n is used to calculate BER of hybrid-MIMO over complex white Gaussian noise channel (Proakis, 2001 and Wang, 2007) by

$$P_{e,Hb}\left(\bar{\gamma};\{c_n\}\right)=\frac{a}{Llog_2C}\sum_{n=1}^{L}Q\left(\sqrt{G\bar{\gamma}c_n}\right) \tag{3-70}$$

where a and G denote the modulation constant for each modulation scheme and $Q(x)=\frac{1}{\pi}\int_0^{\pi}\exp\left(-x^2/2\sin^2\theta\right)d\theta$. Anyway this thesis considers signal over MIMO fading channels. Therefore BER of the hybrid-MIMO system should be derived on fading channels (Ahn, 2008) as follows.

$$P_{e,Hb} = \int\limits_{0}^{\infty} P_{e,Hb}\left(\bar{\gamma};\{c_n\}\right) p_{\gamma_n}(\gamma_n)\, d\gamma_n \qquad (3\text{-}71)$$

where $p_{\gamma_n}(\gamma_n)$ denotes the probability density function (pdf) of the effective SNR that can be described as

$$p_{\gamma_n}(\gamma_n) = \frac{\gamma_n^{Z-1}}{\Gamma(Z)\bar{\gamma}_s^{-(Z)}} e^{-\gamma_n/\bar{\gamma}_s} \qquad (3\text{-}72)$$

where $\bar{\gamma}_s = \gamma_n / \|H_n\|_F^2$, $Z = N_r(N_t/2)$ and $\Gamma(a) = \int_{0}^{\infty} x^{a-1} e^{-a}\, da$. Thus from (3-70) and (3-71), the average BER of hybrid-MIMO systems over fading channel can be expressed as

$$P_{e,Hb} = \frac{a}{L\log_2 C}\left[\int_{0}^{\infty} Q\left(\sqrt{G\gamma_1}\right) p_{\gamma_1}(\gamma_1)\, d\gamma_1 + \int_{0}^{\infty} Q\left(\sqrt{G\gamma_2}\right) p_{\gamma_2}(\gamma_2)\, d\gamma_2 + \ldots + \int_{0}^{\infty} Q\left(\sqrt{G\gamma_L}\right) p_{\gamma_L}(\gamma_L)\, d\gamma_L\right]. \quad (3\text{-}73)$$

However (3-73) is represented in term of Gaussian function integration, it is difficult to calculate the answer. Thus this equation should be reformed to be a low complexity equation before derivingBER. The details of derivation will be explained in Chapter IV.

3.8   Summary

In this chapter, the principle of multi layers MIMO detections are explained including ZF, MMSE and MLD. The criterion of MIMO detection joining with SIC is also discussed. Moreover the principles of several hybrid MIMO systems are demonstrated while the channel capacity and the BER derivation over fading channel are also briefly described.

CHAPTER IV

HYBRID-MIMO RECEIVER SCHEME ANALYSIS

4.1 Introduction

This thesis improves performance of the conventional hybrid-MIMO described in Chapter III by cancelling the interference of other layers before detecting the first layer. The improved hybrid-MIMO systems, namely, the hybrid-MIMO receiver scheme (HMRS) is proposed to adopt in CRN because this technique offers the simple structure andmore flexibility for power limitation in CRN. Moreover the multi-mode HMRS is also proposed that is compatible to CRN environment.

4.2 Structure and Process of Hybrid-MIMO Receiver Scheme

4.2.1 Structure of Hybrid-MIMO receiver scheme

The HMRS technique can be efficiently applied for multiuser systems as well as CRN. Each user can be independently applied the different MIMO scheme while each user equipped with two transmit antennas as shown in Figure 4.1. Then all data streams are transmitted over MIMO fading channels to the receiver.Each part of HMRS receiver can be explained as follows.

1) ML detection is used to detect SM MIMO signals. Anyway this part may be equipped by other SM detection such as ZF and MMSE detection.
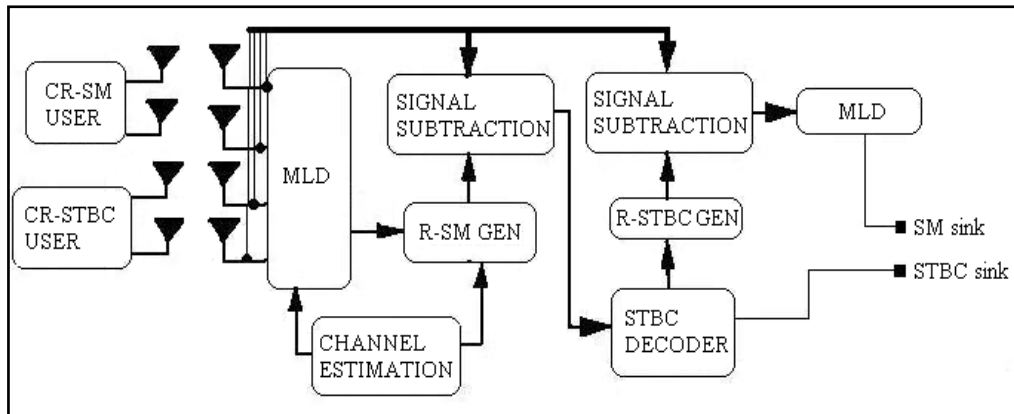
Figure 4.1 HMRS block diagram.

2) SIC or signal subtraction is used to cancel the interference of other users. The cancellations are repeatedly done with SM detection for each layer until completing all layers.

3) Channel estimation is used to measure and estimate MIMO channel for detecting all transmitted symbols.

4) Regenerate received signal (R-SM GEN and R-STBC GEN) is used to regenerate the received signals for SM and STBC user. These signals are generated by estimating channels and detecting symbols.

5) STBC decoder is used to decode STBC signals.

4.2.2 Hybrid-MIMO receiver scheme process

The transmitted signal for SM and STBC users are arranged into two time slot for each transmission block that can be written as

$$\boldsymbol{x}_{SM} = \begin{bmatrix} x_1 & x_5 \\ x_2 & x_6 \end{bmatrix} \tag{4-1}$$

$$\boldsymbol{x}_{STBC} = \begin{bmatrix} x_3 & -x_4^* \\ x_4 & x_3^* \end{bmatrix} \tag{4-2}$$

The symbols in the first and second columns in (4-1) and (4-2) represent the transmitted symbols during the first time slot and the second time slot, respectively. The transmitted symbols of two users can also be represented in the first and the second time slots as shown in (4-3) and (4-4).

$$\boldsymbol{x}^{T1} = \begin{bmatrix} x_1 \\ x_2 \\ x_3 \\ x_4 \end{bmatrix} \tag{4-3}$$

$$\boldsymbol{x}^{T2} = \begin{bmatrix} x_5 \\ x_6 \\ -x_4^* \\ x_3^* \end{bmatrix} \tag{4-4}$$

All transmitted symbols are transmitted over the flat fading channels that have static channel coefficient during two time slots. The MIMO channel can be described by

$$\boldsymbol{H} = \begin{bmatrix} h_{11} & h_{21} & h_{31} & h_{41} \\ h_{12} & h_{22} & h_{32} & h_{42} \\ h_{13} & h_{23} & h_{33} & h_{43} \\ h_{14} & h_{24} & h_{34} & h_{44} \end{bmatrix} \tag{4-5}$$

where h_{ij} denotes the sub-channel between the transmit antenna j and the receive antenna i. The received signals during two time slots are presented by

$$y = \begin{bmatrix} \boldsymbol{y}^{T1} \\ \boldsymbol{y}^{T2} \end{bmatrix} = \begin{bmatrix} \boldsymbol{Hx}^{T1} \\ \boldsymbol{Hx}^{T2} \end{bmatrix} + \begin{bmatrix} \boldsymbol{z}^{T1} \\ \boldsymbol{z}^{T2} \end{bmatrix} = \begin{bmatrix} y_1 & y_5 \\ y_2 & y_6 \\ y_3 & y_7 \\ y_4 & y_8 \end{bmatrix} \tag{4-6}$$

where $\boldsymbol{z}_{Tn}$ denotes a noise at time slot Tn. Then ML detection are applied to detect all

transmitted symbols at time slot Tn by

$$\hat{\boldsymbol{x}}^{Tn} = \arg\min_{\boldsymbol{x}_k \in C^{Nt}} \left\| \boldsymbol{y}^{Tn} - \boldsymbol{H}\hat{\boldsymbol{x}}_k \right\|_F^2 \tag{4-7}$$

The detected signals from (4-7) are used to regenerate the received signal for SM user

that given by

$$\boldsymbol{y}_{SM1} = \begin{bmatrix} \hat{\boldsymbol{H}}_{SM} \hat{\boldsymbol{x}}_{SM}^{T1} \\ \hat{\boldsymbol{H}}_{SM} \hat{\boldsymbol{x}}_{SM}^{T2} \end{bmatrix} \tag{4-8}$$

where $\boldsymbol{y}_{SM1}$ denotes the received signal for SM user (order 1), $\widehat{H}_{SM}$ denotes MIMO

channels for transmitting SM symbols that is located in the first two column of MIMO

channel $\boldsymbol{H}$ and $\hat{\boldsymbol{x}}_{SM}^{Tn}$ denotes the detected symbol for SM user at time slot Tn. Then

SIC is used to cancel signal $\boldsymbol{y}_{SM1}$ from the received signal $\boldsymbol{y}$ that given by

$$\boldsymbol{y}_{STBC1} = \boldsymbol{y} - \boldsymbol{y}_{SM1} = \begin{bmatrix} y_q & y_r \\ y_s & y_t \\ y_u & y_v \\ y_w & y_x \end{bmatrix} \tag{4-9}$$

wherey_{STBC1} denote the received signal of STBC user (order 1), then reform this signals by

$$\mathbf{y}_{STBC}^{\diamond} = \begin{bmatrix} y_q & y_r^* & y_s & y_t^* & y_u & y_v^* & y_w & y_x^* \end{bmatrix}^T \tag{4-10}$$

The signals in (4-10) are used to decode the transmitted symbol for STBC user as given by

$$\hat{\mathbf{x}}_{STBC} = \mathbf{H}_{ASTBC}^{\dagger} \mathbf{y}_{STBC}^{\diamond} \tag{4-11}$$

where

$$\mathbf{H}_{STBC} = \begin{bmatrix} h_{31} & h_{41} \\ h_{32} & h_{42} \\ h_{33} & h_{43} \\ h_{34} & h_{44} \end{bmatrix} \tag{4-12}$$

$$\mathbf{H}_{ASTBC} = \begin{bmatrix} h_{31} & h_{41}^* & h_{32} & h_{42}^* & h_{33} & h_{43}^* & h_{34} & h_{44}^* \\ h_{41} & -h_{31}^* & h_{42} & -h_{32}^* & h_{43} & -h_{33}^* & h_{44} & -h_{34}^* \end{bmatrix}^T \tag{4-13}$$

$$\mathbf{H}_{ASTBC}^{\dagger} = (\mathbf{H}_{ASTBC}^H \mathbf{H}_{ASTBC})^{-1} \mathbf{H}_{ASTBC}^H \tag{4-14}$$

Then the detected symbols in (4-11) are used to regenerate the received signal for STBC user (order 2). These signals are employed in SIC process and can be written as

$$\mathbf{y}_{STBC2} = \begin{bmatrix} \hat{\mathbf{H}}_{STBC} \hat{\mathbf{x}}_{STBC}^{T1} \\ \hat{\mathbf{H}}_{STBC} \hat{\mathbf{x}}_{STBC}^{T2} \end{bmatrix} \tag{4-15}$$

where $\hat{x}_{STBC}^{Tn}$ denotes the detected symbol of STBC user at time slot Tn. Then the signal in (4-15) are cancelled from the received signals by

$$y_{SM2} = y - y_{STBC2} = \begin{bmatrix} y_{SM2}^{T1} \\ y_{SM2}^{T2} \end{bmatrix} \tag{4-16}$$

The signals in from (4-16) are used to detect the transmitted symbols of SM user by ML detection as given by

$$\hat{x}_{SM}^{Tn} = \arg\min_{\hat{x}_k \in C^{Nt-2}} \left\| y_{SM2}^{Tn} - H_{SM} \hat{x}_k \right\|^2 \tag{4-17}$$

4.3   Bit Error Rate of Hybrid-MIMO Receiver Scheme

In wireless networks, BER has been used to demonstrate the efficiency of the systems. The BER for multi-layer detection as well as HMRS should be derived many times for each layer and the average BER for each user should be averaged by the BER of each layer with the effect of error propagation. In this part, the practical problems in multiuser MIMO detection are discussed that these problems are error propagation (EP) and channel estimation error (CEE). These problemsshould be also taken into account for the average BERderivation of each user.

4.3.1   Hybrid-MIMO receiver scheme signals

This research considers the HMRS system with N synchronous co-channel users (e.g. uplink cellular), where each user equipped with N_t-element antenna array (N_t=2 for this work); we assume that J users are in SM mode and the remaining N-J users are in STBC mode. All 2N MIMO streams are simultaneously

transmitted over the same frequency band without additional spreading to a common receiver equipped with M-element antenna array. All users are synchronous in the sense that each user transmits its symbol vector in the synchronization with others. The transmitted signals are assumed to propagate through the $M \times 2N$ random channel matrix $\boldsymbol{H}$ in the uplink communication channel. The MIMO channel is assumed to be a rich-scattering and flat-fading, all sub-channels between all users and receiver are assumed to be independence. This thesis assumes that the mode of operation of each user is known at the receiver, which can be indicated in the packet header. The received signal is then given by

$$Y = \sum_{i=1}^{N} H_i s_i + w \, , \qquad (4\text{-}18)$$

where the received signal Y is an $M \times 1$ vector, the signals of user i are sent through the $M \times N_t$ random channel matrix $\boldsymbol{H}_i$, $\boldsymbol{s}_i$ represents $N_t \times 1$ transmit data symbol vector of user i consisting of N_t symbols each with a constellation size C and $\boldsymbol{w}$ denotes $M \times 1$ vector i.i.d. complex circular Gaussian random variable; each element distributed as $CN(0, N_0)$. The average energy of the transmitted symbol is assumed to be $E_s = E[|s_i|^2]$, where s_i denotes the element of $\boldsymbol{s}_i$. The overall channel matrix is denoted by $\boldsymbol{H} = [\boldsymbol{H}_z \boldsymbol{H}_s]$ that assumed to have unit variance such that $E[\|\boldsymbol{H}\|_F^2] = N_t N M$, where the overall channel for all SM users and all STBC users are denoted by $\boldsymbol{H}_z = [\boldsymbol{H}_1 \boldsymbol{H}_2 \dots \boldsymbol{H}_J]$ and $\boldsymbol{H}_s = [\boldsymbol{H}_{J+1} \boldsymbol{H}_{J+2} \dots \boldsymbol{H}_N]$, respectively, $\|\boldsymbol{A}\|_F$ denotes the Frobenius norm of $a \times b$ matrix $\boldsymbol{A}$, it can be defined as $\|\boldsymbol{A}\|_F \triangleq \sqrt{\sum_{i=1}^{a} \sum_{j=1}^{b} |A_{ij}|^2}$ and $E[\cdot]$ is the expectation operator.

4.3.2 Error Propagation in SIC process

In MIMO uplink channel, we normally use SIC to cancel the early streams of the other users in order to detect the symbols for the desired user. The previous detected symbols $\hat{s}_m$ of other users in (4-19) are used to subtract with real symbols s_m in the received signal Y, where $m = 1, 2, 3,\ldots, N$; then the received signal for user k (desired user) can be described as

$$Y_k = Y - \sum_{m=1}^{N} \widehat{H}_m \hat{s}_m ,\qquad (4\text{-}19)$$

where $k \neq m$. However the previous detected symbols always have the probability of symbol error during detection $(s_m \neq \hat{s}_m)$; thus the cancellation of SIC cannot be completed without error. The error due to SIC process is known as error propagation (EP). The EP has been described in form of distance between two symbols (Prasad and Varanasi, 2001); the average distance can be represented by different value depending on the type of modulation. The symbol distance d_{EP} for C-PSK case can be calculated (Zanella et al., 2005)by $4sin^2(\pi/C)$, where $d_{\text{EP}} = |s_m - \hat{s}_m|^2$. For C-QAM case, the symbol energy should be normalized by the average energy (Foschini, 1996)$E_v = 2(C - 1)/3$. Thus the symbol distance d_{EP} for C-QAM case can be obtained by averaging the distance of all symbol pairs in constellation that,as $d_{\text{EP}} = \left(1/\big(C(C - 1)\big)\right)\sum_i^C \sum_j^C |s_i - s_j|^2$, where s_i and s_j denote the symbol inconstellation of C-QAM signal that are normalized by $\sqrt{E_v}$, and $i \neq j$. The pattern for appearance of EP has 2^{N_a} possible patterns. However the pattern for appearanceof EP can be reduced to be $N_a + 1$possible patterns by using thecoefficient vector

Table 4.1 The detection process of HMRS

Step	Process
1	**Begin:** *The 2N transmitted streams are sent to the receiver at the same time.* Y^{t_n} *represents the received signal vector Y at time slot t_n, where n =1, 2.*
2	*At the first detection, all detected symbol $\hat{s}^{t_n} = [\hat{s}_1^{t_n}, \hat{s}_2^{t_n}, ..., \hat{s}_{2N}^{t_n}]$ are obtained by $2N \times M$ ZF detection. All detected symbols $\hat{s}^{t_n}$ are regenerated to be the estimated receive signal $Y_{SM}^{t_n}$ for all SM users and $Y_{STC}^{t_n}$ for all STBC users at time slot t_n, where $Y_{STC}^{t_n} = [Y_{STC,1}^{t_n} Y_{STC,2}^{t_n} ... Y_{STC,N-J}^{t_n}]$*
3	*At STBC decoding, define $Y_{ST}^{t_n} = Y^{t_n} - Y_{SM}^{t_n}$. The detected symbols $\hat{s}_{STC,i}$ for all STBC users can be obtained by:* for $i = 1$ to N - J $\quad Y_{S,i}^{t_1} = Y_{ST}^{t_1} - \sum_{j=1}^{N-J} Y_{STC,j}^{t_1}$, where $j \neq i$ $$Y_{S,i}^{t_2} = Y_{ST}^{t_2} - \sum_{j=1}^{N-J} Y_{STC,j}^{t_2}$$ $$\hat{s}_{STC,i} = \text{dec}(Y_{S,i}^{t_1}, Y_{S,i}^{t_2})$$ $\quad Y_{STC,i}^{t_1} = Y_{S,i}^{t_1}$ and $Y_{STC,i}^{t_2} = Y_{S,i}^{t_2}$ end *where $\hat{s}_{STC,i}$ is 2x1 detected symbol vector for the ith STBC user and* dec( ) *denotes $N_t \times M$ STBC decoding operation. Define $\hat{s}_c = [\hat{s}_{STC,1}^T \hat{s}_{STC,2}^T \hat{s}_{STC,3}^T ... \hat{s}_{STC,N-J}^T]$, where ^{T} denotes the matrix transpose operation.*
4	*At SM detection, the new received signals $Y_z^{t_n}$ of SM users can be obtained by SIC that, as $Y_z^{t_n} = Y^{t_n} - \ddot{Y}_{STC}^{t_n}$, where $\ddot{Y}_{STC}^{t_n}$ denotes the regenerated receive signal for all STBC users that is generated by the elements of $\hat{s}_c$ according to the STBC structure. Then $Y_z^{t_n}$ is used to detect the transmitted symbols for all SM users by applying $JN_t \times M$ ZF detection.* **End process**.

β_{N_a} that is addressed in the next section, because some patterns of 2^{N_a} possible patterns have the same value with others. The detection process of HMRS that applies ZF detection can be explained in Table 4.1.

4.3.3 Channel Estimation Error Model

The receiver needs to estimate the channels for decoding the symbols from the transmitter, but the perfect channel estimation cannot be done in practice. Thus the model of CEE is described in this part. The good model to explain the

characteristic of estimated channel $\widehat{H}$ at the receiver is (Zanella et al., 2005; Marzetta, 1999 and Hassibi and Hochwald, 2003)

$$\widehat{H} = H + \tau\boldsymbol{\varphi} \qquad (4\text{-}20)$$

where all elements in $\boldsymbol{\varphi}$ are i.i.d zero-mean complex Gaussian having zero-mean and unit variance, and τ is used to measure an accuracy of channel estimation. The value $\tau = 0$ is presented in case of no estimation error. The normalized mean square error (NMSE) between h_{ij} and $\hat{h}_{ij}$ can be written as

$$\text{NMSE} = \frac{E\left[\left|h_{ij} - \hat{h}_{ij}\right|^2\right]}{E\left[\left|h_{ij}\right|^2\right]} = \tau^2, \qquad (4\text{-}21)$$

where h_{ij}, $\hat{h}_{ij}$ represent the $(i,j)^{th}$ element of H and $\widehat{H}$, respectively. The correlation coefficient between the true channel coefficients and their estimates can be defined as

$$\rho = \frac{E\left[h_{ij}\,\hat{h}_{ij}^*\right]}{\sqrt{E\left[\left|h_{ij}\right|^2\right] \cdot E\left[\left|\hat{h}_{ij}\right|^2\right]}} = \frac{1}{\sqrt{1 + \tau^2}}, \qquad (4\text{-}22)$$

where * denotes the complex conjugate operation. The relation between NMSE and ρ in (4-21) and (4-22), can be shown as

$$\rho = 1/\sqrt{1 + \text{NMSE}} \qquad (4\text{-}23)$$

4.3.4 The Closed-Form BER for ZF Receiver

In this section, we derive the effective SNR and the closed-form BER with CEE and EP for ZF detection. At the 4th step in Table 4.1, the transmitted symbol with CEE (Wang et al., 2007) and EP can be written as

$$\hat{\mathbf{s}}_z = \hat{\mathbf{H}}_z^\dagger \mathbf{Y}_z = (\mathbf{H}_z + \tau\boldsymbol{\varphi})^\dagger (\mathbf{H}_z \mathbf{s}_z + \mathbf{w} + N_a \Delta \mathbf{H}_p) \qquad (4\text{-}24)$$

where $\mathbf{H}_z$ represents $M \times JN_t$ channel matrix for all SM users, $\mathbf{s}_z$ denotes the $JN_t \times 1$ symbol vector for the all SM users, † denotes the pseudo-inverse operation, $N_a \Delta \mathbf{H}_p$ term denotes the total EP due to SIC process, $\Delta = \sqrt{d_{EP} E_s}$, $\mathbf{H}_p$ represents $M \times 1$ channel vector for one other user, and the $M \times 1$ received signal vector $\mathbf{Y}_z$ represents $\mathbf{Y}_z^{t_n}$ in Table I, regardless of time slot. However, $\tau \ll 1$ in practice, then the pseudo-inverse of the estimated channel matrix can be approximated by the linear part of the Taylor expansion as

$$\hat{\mathbf{H}}_z^{\ \dagger} \cong \mathbf{H}_z^\dagger (I_M - \tau\boldsymbol{\varphi}\mathbf{H}_z^\dagger) \qquad (4\text{-}25)$$

thus (4-19) can be reformed as

$$\hat{\mathbf{Y}}_z = \mathbf{H}_z^\dagger (I_M - \tau\boldsymbol{\varphi}\mathbf{H}_z^\dagger)(\mathbf{H}_z \mathbf{s}_z + \mathbf{w} + N_a \Delta \mathbf{H}_p)$$

$$= \mathbf{s}_z + \mathbf{H}_z^\dagger \mathbf{w} - \tau\mathbf{H}_z^\dagger \boldsymbol{\varphi}\mathbf{s}_z - \tau\mathbf{H}_z^\dagger \boldsymbol{\varphi}\mathbf{H}_z^\dagger \mathbf{w} + N_a \Delta \mathbf{H}_z^\dagger \mathbf{H}_p - \tau N_a \Delta \mathbf{H}_z^\dagger \boldsymbol{\varphi}\mathbf{H}_z^\dagger \mathbf{H}_p.$$

$$(4\text{-}26)$$

From (4-26), the effective post-processing noise can be written as

$$\widehat{\boldsymbol{w}} = \boldsymbol{H}_z^\dagger \boldsymbol{w} - \tau \boldsymbol{H}_z^\dagger \boldsymbol{\varphi} \boldsymbol{s}_z - \tau \boldsymbol{H}_z^\dagger \boldsymbol{\varphi} \boldsymbol{H}_z^\dagger \boldsymbol{w} + N_a \Delta \boldsymbol{H}_z^\dagger \boldsymbol{H}_p - \tau N_a \Delta \boldsymbol{H}_z^\dagger \boldsymbol{\varphi} \boldsymbol{H}_z^\dagger \boldsymbol{H}_p.$$

$$(4\text{-}27)$$

In Appendix A-I, we derive the covariance matrix of $\widehat{\boldsymbol{w}}$ that can be shown as

$$E[\widehat{\boldsymbol{w}}\widehat{\boldsymbol{w}}^H] =$$

$$\left(N_0 + \tau^2 N_t E_s + \tau^2 N_0 t_r((\boldsymbol{H}_z^H \boldsymbol{H}_z)^{-1}) + \tau^2 N_a \Delta \boldsymbol{s}_z^\dagger t_r((\boldsymbol{H}_z^H \boldsymbol{H}_z)^{-1}) \boldsymbol{H}_p^H (\boldsymbol{H}_z^\dagger)^{-1}\right.$$

$$+ N_a^2 \Delta^2 M + \tau^2 N_a \Delta \boldsymbol{s}_z^H t_r((\boldsymbol{H}_z^H \boldsymbol{H}_z)^{-1}) \boldsymbol{H}_p \left((\boldsymbol{H}_z^\dagger)^H\right)^{-1}$$

$$+ \tau^2 N_a^2 \Delta^2 M t_r((\boldsymbol{H}_z^H \boldsymbol{H}_z)^{-1}))(\boldsymbol{H}_z^H \boldsymbol{H}_z)^{-1} \qquad (4\text{-}28)$$

where $tr(\cdot)$ is the matrix trace operation. The mean of $t_r((\boldsymbol{H}_z^H \boldsymbol{H}_z)^{-1})$ is quite small for practical numbers (Wang et al., 2007) of transmit and receive antennas ($M > JN_t$). Moreover after $t_r((\boldsymbol{H}_z^H \boldsymbol{H}_z)^{-1})$ is scaled by τ^2 where $\tau \ll 1$, the term $\tau^2 t_r((\boldsymbol{H}_z^H \boldsymbol{H}_z)^{-1})$ in (4-28) can be ignored. Therefore (4-28) can be besides presented as

$$E[\widehat{\boldsymbol{w}}\widehat{\boldsymbol{w}}^H] = (N_0 + \tau^2 N_t E_s + N_a^2 \Delta^2 M)(\boldsymbol{H}_z^H \boldsymbol{H}_z)^{-1}. \qquad (4\text{-}29)$$

From (4-26) and (4-28), the effective SNR per symbol of the kth stream can be described as

$$\gamma_k = \frac{E_s/N_0}{(1 + \tau^2 N_t E_s/N_0 + N_a^2 \Delta^2 M/N_0)[(\boldsymbol{H}_z^H \boldsymbol{H}_z)^{-1}]_{kk}},$$

$$k = 1, 2, \ldots, N_t. \qquad (4\text{-}30)$$

Where $[(\boldsymbol{H}_z^H \boldsymbol{H}_z)^{-1}]_{kk}$ denotes the $(k,k)^{th}$ elements of $(\boldsymbol{H}_z^H \boldsymbol{H}_z)^{-1}$ while the value of $1/[(\boldsymbol{H}_z^H \boldsymbol{H}_z)^{-1}]_{kk}$ is a chi-square distributed random variable with $2(M - JN_t + 1)$ degrees of freedom (Winters, 1992 and 1994). Because the SNR distribution of each stream is the same, the subscript k in (4-30) can be dropped. Thus we denote the average SNR per symbol of each stream as $\gamma_z = \bar{\gamma}_s g$, where

$$\bar{\gamma}_s = \frac{E_s/N_0}{(1 + \tau^2 N_t E_s/N_0 + M d_{EP} N_a^2 E_s/N_0)}, \tag{4-31}$$

and g denotes a chi-square distributed random variable with $2(M - JN_t + 1)$ degrees of freedom. However N_a in (4-31) can be defined by 0 for the first detection, because the EP is not presented before SIC process. The approximate BER expression for ZF detection with CEE and EP (Wang et al., 2007) can be written as follows:

$$P_{b,C-QAM}^{ZF} \cong \frac{2}{\sqrt{C} \log_2 \sqrt{C}} \sum_{k=1}^{\log_2 \sqrt{C}} \sum_{i=0}^{(1-2^{-k})\sqrt{C}-1} \left\{ (-1)^{\left\lfloor \frac{i \cdot 2^{k-1}}{\sqrt{C}} \right\rfloor} \left(2^{k-1} - \left\lfloor \frac{i \cdot 2^{k-1}}{\sqrt{C}} + \frac{1}{2} \right\rfloor \right) \right.$$

$$\times \left[\frac{1}{2}(1 - \mu_i) \right]^{G+1} \sum_{j=0}^{G} \binom{G+j}{j} \left[\frac{1}{2}(1 + \mu_i) \right]^j \right\} \tag{4-32}$$

where $\mu_i = \sqrt{(3(2i+1)^2 \bar{\gamma}_s)/(2(C-1) + 3(2i+1)^2 \bar{\gamma}_s)}$, $G = M - JN_t$ and $\lfloor b \rfloor$ represents the largest integer that is no larger than b.

$$P_{b,C-\text{PSK}}^{ZF} \cong \frac{2}{max(log_2 C, 2)} \sum_{i=1}^{min\left(2,\left\lceil\frac{C}{4}\right\rceil\right)} \left\{ \left[\frac{1}{2}(1-\mu_i)\right]^{G+1} \sum_{j=0}^{G} \binom{G+j}{j} \left[\frac{1}{2}(1+\mu_i)\right]^{j} \right\},$$

$$(4\text{-}33)$$

where $\mu_i = \sqrt{\bar{\gamma}_s sin^2((2i-1)\pi/C)/\left(1+\bar{\gamma}_s sin^2((2i-1)\pi/C)\right)}$, $\lceil b \rceil$ represents the

smallest integer that is no smaller than b. If consider only the dominant terms ($i = 0$,

1) in (4-32), the equation can be reformed as (Cho and Yoon, 2002)

$$P_{b,C-\text{QAM}}^{ZF} \cong \frac{2(\sqrt{C}-1)}{\sqrt{C}log_2\sqrt{C}} \left[\frac{1}{2}(1-\mu_0)\right]^{G+1} \sum_{j=0}^{G} \binom{G+j}{j} \left[\frac{1}{2}(1+\mu_0)\right]^{j}$$

$$+\frac{2(\sqrt{C}-1)}{\sqrt{C}log_2\sqrt{C}} \left[\frac{1}{2}(1-\mu_1)\right]^{G+1} \sum_{j=0}^{G} \binom{G+j}{j} \left[\frac{1}{2}(1+\mu_1)\right]^{j}$$

$$(4\text{-}34)$$

4.3.5   The Closed-Form BER for STBC systems

At the 3rd step in Table 4.1, each STBC user applies $2 \times M$ STBC

scheme. The code rate of STBC is 1, there are L symbols transmitted over T time

slots, where L and T are defined to be 2 for this work. The received signal for the ith

STBC user can be obtained by using SIC to cancel data streams of all SM users and

other STBC users from the received signal, it can be described as

$$\boldsymbol{Y}_{s,i} = \boldsymbol{H}_{s,i}\boldsymbol{x}_i + \boldsymbol{w}' + \boldsymbol{w}_{ep} \qquad (4\text{-}35)$$

where $\boldsymbol{Y}_{s,i}$ represents the $M \times 2$ receive signal matrix $\left[\boldsymbol{Y}_{s,i}^{t_1} \boldsymbol{Y}_{s,i}^{t_2}\right]$ during two successive

time slot for the ith STBC user addressed in Table I, $\boldsymbol{H}_{s,i}$ represents $M \times 2$ channel

matrix, $\boldsymbol{x}_i$ is an 2×2 transmission matrix of STBC, $\boldsymbol{w}'$ denotes the $M \times 2$ noise matrix with i.i.d. complex circular Gaussian random variables, each element distributed as $CN(0, N_0)$ and $\boldsymbol{w}_{ep}$ denotes the $M \times 2$ error propagation matrix, each element of $\boldsymbol{w}_{ep}$ can be represented by $w_{ep} = N_a h_{kl} \Delta$. Where h_{kl} denotes the channel gain describing the channel of the EP of 2(N-1) other users from the lth transmit antenna to the kth receive antenna, where h_{ij} denotes the sub-channel of $\boldsymbol{H}_{s,i}$ describing the channel from the jth transmit antenna to the ith receive antenna. The channel matrix $\boldsymbol{H}_{s,i}$ is normalized such that $E\left[\left\|\boldsymbol{H}_{s,i}\right\|_F^2\right] = 2M$.

The average energy of the transmitted symbols per each antenna are assumed to be $E_r/2$, thus the average power of the received signal for each receive antenna is E_r and the average SNR per receive antenna is E_r/N_0. The total average energy of a symbol duration can be written as $E_T = TE_r = 2LE_s$. Thus the average energy of the constellation can be calculated as $E_s = TE_r/2L = E_r/2$. At the receiver, the received signals in the presence of EP are combined for decoding by Maximum Likelihood (ML) decoder. The combined signal at the receiver can be expressed as

$$\tilde{r}_c = \left\|\boldsymbol{H}_{s,i}\right\|_F^2 x + \widehat{w}_p \tag{4-36}$$

where x denotes the element of matrix $\boldsymbol{x}_i$, $\widehat{w}_p$ is the noise plus EP term after combining that can be expressed as

$$\widehat{w}_p = w' \sum_{j=1}^{2} \sum_{i=1}^{M} h_{ij} \tag{4-37}$$

where $w' = \sum_l^{N_a} h_{kl}|x - \hat{x}| + w = \sum_l^{N_a} h_{kl}\Delta + w$, $\hat{x}$ denotes the detected symbol from the previous detection and w is the element of vector $\boldsymbol{w}'$. In Appendix A-II, we derive the covariance of $\hat{w}_p$ that can be described as

$$E[\hat{w}_p \hat{w}_p^*] \cong \|\boldsymbol{H}_{s,i}\|_F^2 (N_0 + N_a\Delta^2). \qquad (4\text{-}38)$$

The transmitted symbol can be determined by $\hat{x}_c = \mathrm{argmin}_{\bar{x} \in C} \left| \tilde{r}_c - \right.$ $\left\| \boldsymbol{H}_{s,i} \right\|_F^2 \bar{x} \right|^2$. Thus from (4-36) and (4-37), the effective SNR per symbol after STBC decoding (Ahn et al., 2008) is derived in Appendix A-III that can be expressed as

$$\gamma_a = \frac{\|\boldsymbol{H}_{s,i}\|_F^2}{2(1/\bar{\gamma} + N_a d_{EP}/2)}, \qquad (4\text{-}39)$$

where $\bar{\gamma} = E_r/N_0 = 2E_s/N_0$. The probability density function (pdf) of the effective SNR (γ_a) under imperfect channel estimation and EP can be described as a function of the correlation coefficient. The similar pdf of the γ_a with CEE have been proposed (Ahn et al., 2008; Gans, 1971 and Roy and Fortier, 2004), the pdf of the received instantaneous SNR is described as

$$p_{\gamma_a}(\gamma_a) = \frac{e^{-q\gamma_a}}{(1 - \rho^2)^{1-D}} \cdot q \sum_{k=0}^{D-1} \left(\frac{1}{k!}\right) \binom{D-1}{k} \left(\frac{\rho^2 \gamma_a}{1 - \rho^2} \cdot q\right)^k$$

$$(4\text{-}40)$$

where $D = 2M$, $q = \|\boldsymbol{H}_{s,i}\|_F^2/\gamma_a = 2(1/\bar{\gamma} + N_a d_{EP}/2)$, and $\binom{n}{k}$ denotes the binomial coefficient given by $\binom{n}{k} = n!/(n-k)! \, k!$. The Bernstein polynomials can be applied

to regroup term (Maaref and Aissa, 2005 and Tomiuk et al., 1999) in (4-40) as follows:

$$p_{\gamma_a}(\gamma_a) = \sum_{k=1}^{D} \frac{B_{k-1}^{D-1}(\rho^2)}{\Gamma(k)} q^k \gamma_a^{k-1} e^{-q\gamma_a} \qquad (4\text{-}41)$$

where $\Gamma(\cdot)$ denotes the Gamma function and the Bernstein polynomials is defined as $B_i^n(t) \triangleq \binom{n}{i} t^i (1-t)^{n-i}$. The exact closed-form SER for STBC systems have been proposed in (Ahn et al., 2008). The SER of C-PSK and rectangular C-QAM for the effective SNR γ_a over an AWGN channel are $P_{e,PSK}(\gamma_a) = a_p Q\left(\sqrt{G_{PSK}\gamma_a}\right)$ and $P_{e,QAM}(\gamma_a) = \left[1 - a_q Q\left(\sqrt{G_{QAM}\gamma_a}\right)\right]^2$, respectively, where $a_p = 2$, $G_{PSK} = 2sin^2(\pi/C)$, $a_q = 2\left(1 - 1/\sqrt{C}\right)$ and $G_{QAM} = 3/(C-1)$ (Prasad and Varanasi, 2001 and Goldsmith, 2005). The SER over fading channel can be often described by

$$\mathcal{V}(b,q,m) = \frac{q^m}{\Gamma(m)} \int_0^\infty Q(\sqrt{bn}) e^{-qn} n^{m-1} dn$$

$$= \frac{1}{2}\left[1 - \varepsilon \sum_{k=0}^{m-1} \binom{2k}{k} \left(\frac{1-\varepsilon^2}{4}\right)^k\right] \qquad (4\text{-}42)$$

where $\varepsilon = \sqrt{b/(b+2q)}$, $b = G_{PSK}$ or G_{QAM} depending on modulation scheme. By applying (4-39), (4-41), (4-42) and the instantaneous SER over AWGN channel, the BERs for C-PSK and C-QAM signalling with CEE and EP can be expressed as

$$P_{b,CPSK}^{STBC} = \frac{a_p}{log_2 C} \sum_{i=1}^{D} B_{i-1}^{D-1}(\rho^2) \; \mathcal{V}(G_{PSK}, q, i) \tag{4-43}$$

$$P_{b,CQAM}^{STBC} = \frac{1}{log_2 C} \left[1 - \left(1 - aq \sum_{i=1}^{D} B_{i-1}^{D-1}(\rho^2) \; \mathcal{V}(G_{QAM}, q, i) \right)^2 \right]$$

$$\tag{4-44}$$

4.3.6 Average BER for STBC Users

From 4.3.1, HMRS MIMO system is operated by STBC and SM users. The receiver detects the transmitted symbols successively by ZF detection and STBC decoding for each user. The BER performances of each user are difference depending on the modulation scheme, number of antennas, and number of users. In this part, we explain the procedure to evaluate the average BER for STBC user in ZF-STBC MIMO systems. By considering the presence of EP in multi-layers detection, the presence of EP can be appeared by N_a+1 different patterns that represented by vector $\boldsymbol{\psi}_{N_a}$ in Table 4.2, each pattern has different frequency for appearance that can be described by the elements of vector $\boldsymbol{\beta}_{N_a}$. The different pattern also gives the different bit error probability according to the element in vector $\boldsymbol{P}_{b,N_a}$ from Table 4.3. Finally, vector $\boldsymbol{\beta}_{N_a}$, $\boldsymbol{\psi}_{N_a}$ and $\boldsymbol{P}_{b,N_a}$ are jointly employed to calculate the average BER for the desired user (Shen et al., 2004 and Zanella et al., 2005). From the first step in Table 4.1, all transmitted symbols are detected by applying $2N \times M$ ZF-detection; the bit error probability at this step named P_z can be evaluated by replacing (4-31) into (4-33) or (4-34) depending on modulation scheme, where N_a in (4-31) is defined by 0 because of no EP in the first detection. Then define $P_z = P_{b0}$ for vector $\boldsymbol{\psi}_{N_a}$ inTable4.2, select the coefficient vector β_(N_a) by determining N_a=2(N-

1)andcomputeBER vector $\boldsymbol{P}_{b,N_a}$ in Table 4.3, where each element in vector $\boldsymbol{P}_{b,N_a}$ can be calculated as follows.

$$\breve{\gamma}_c(\chi) = \frac{\left\|\boldsymbol{H}_{s,i}\right\|_F^2}{2(1/\bar{\gamma} + \chi d_{EP}/2)} \tag{4-45}$$

$$\breve{P}_b(\breve{\gamma}_c(\chi)) = \frac{a_p}{\log_2 C} \sum_{i=1}^{D} B_{i-1}^{D-1}(\rho^2)\ \mathcal{V}\left(G_{PSK}, \frac{\left\|\boldsymbol{H}_{s,i}\right\|_F^2}{\breve{\gamma}_c(\chi)}, i\right) \tag{4-46}$$

Table 4.2 The pattern vector for presence of EP

N_a	Coefficient vector $(\boldsymbol{\beta}_{N_a})$ $\boldsymbol{\beta}_{N_a} = \left[\binom{N_a}{0}, \binom{N_a}{1}, \dots, \binom{N_a}{N_a}\right]$	The pattern vector forappearance of EP $(\boldsymbol{\psi}_{N_a})$
1	[1, 1]	$[P_{b0}, (1 - P_{b0})]$
2	[1, 2, 1]	$[P_{b0}^2, P_{b0}(1 - P_{b0}), (1 - P_{b0})^2]$
3	[1, 3, 3, 1]	$[P_{b0}^3, P_{b0}^2(1 - P_{b0}), P_{b0}(1 - P_{b0})^2, (1 - P_{b0})^3]$
4	[1, 4, 6, 4, 1]	$[P_{b0}^4, P_{b0}^3(1 - P_{b0}), P_{b0}^2(1 - P_{b0})^2, P_{b0}(1 - P_{b0})^3, (1 - P_{b0})^4]$
5	[1, 5, 10, 10, 5, 1]	$[P_{b0}^5, P_{b0}^4(1 - P_{b0}), P_{b0}^3(1 - P_{b0})^2, P_{b0}^2(1 - P_{b0})^3, P_{b0}(1 - P_{b0})^4, (1 - P_{b0})^5]$
6	[1, 6, 15, 20, 15, 6, 1]	$[P_{b0}^6, P_{b0}^5(1 - P_{b0}), P_{b0}^4(1 - P_{b0})^2, P_{b0}^3(1 - P_{b0})^3, P_{b0}^2(1 - P_{b0})^4, P_{b0}(1 - P_{b0})^5, (1 - P_{b0})^6]$
$\vdots$	$\vdots$	$\vdots$
n	$\left[\binom{n}{0}, \binom{n}{1}, \dots, \binom{n}{n-1}, \binom{n}{n}\right]$	$[P_{b0}^n, P_{b0}^{n-1}(1 - P_{b0}), P_{b0}^{n-2}(1 - P_{b0})^2, P_{b0}^{n-3}(1 - P_{b0})^3, \dots, P_{b0}(1 - P_{b0})^{n-1}, (1 - P_{b0})^n]$

Table 4.3 The BER vector

N_a	BER vector $(\boldsymbol{P}_{b,N_a})$
1	$\boldsymbol{P}_{b,1} = \left[\breve{P}_b(\breve{\gamma}(1)), \breve{P}_b(\breve{\gamma}(0))\right]$
2	$\boldsymbol{P}_{b,2} = \left[\breve{P}_b(\breve{\gamma}(2)), \breve{P}_b(\breve{\gamma}(1)), \breve{P}_b(\breve{\gamma}(0))\right]$
3	$\boldsymbol{P}_{b,3} = \left[\breve{P}_b(\breve{\gamma}(3)), \breve{P}_b(\breve{\gamma}(2)), \breve{P}_b(\breve{\gamma}(1)), \breve{P}_b(\breve{\gamma}(0))\right]$
4	$\boldsymbol{P}_{b,4} = \left[\breve{P}_b(\breve{\gamma}(4)), \breve{P}_b(\breve{\gamma}(3)), \breve{P}_b(\breve{\gamma}(2)), \breve{P}_b(\breve{\gamma}(1)), \breve{P}_b(\breve{\gamma}(0))\right]$
5	$\boldsymbol{P}_{b,5} = \left[\breve{P}_b(\breve{\gamma}(5)), \breve{P}_b(\breve{\gamma}(4)), \breve{P}_b(\breve{\gamma}(3)), \breve{P}_b(\breve{\gamma}(2)), \breve{P}_b(\breve{\gamma}(1)), \breve{P}_b(\breve{\gamma}(0))\right]$
6	$\boldsymbol{P}_{b,6} = \left[\breve{P}_b(\breve{\gamma}(6)), \breve{P}_b(\breve{\gamma}(5)), \breve{P}_b(\breve{\gamma}(4)), \breve{P}_b(\breve{\gamma}(3)), \breve{P}_b(\breve{\gamma}(2)), \breve{P}_b(\breve{\gamma}(1)), \breve{P}_b(\breve{\gamma}(0))\right]$
$\vdots$	$\vdots$
n	$\boldsymbol{P}_{b,n} = \left[\breve{P}_b(\breve{\gamma}(n)), \breve{P}_b(\breve{\gamma}(n-1)), \breve{P}_b(\breve{\gamma}(n-2)), \breve{P}_b(\breve{\gamma}(n-3)), \dots, \breve{P}_b(\breve{\gamma}(1)), \breve{P}_b(\breve{\gamma}(0))\right]$

or

$$\breve{P}_b\big(\breve{\gamma}_c(\chi)\big) = \frac{\left[1 - \left(1 - aq \sum_{i=1}^{D} B_{i-1}^{D-1}(\rho^2) \; \mathcal{V}\left(G_{QAM}, \frac{\|H_{s,i}\|_F^2}{\breve{\gamma}_c(\chi)}, i\right)\right)^2\right]}{log_2 C}$$

(4-47)

where $\breve{\gamma}_c(n) = \breve{\gamma}(n)$ in Table 4.3, (4-45), (4-46) and (4-47) are modified from (4-39), (4-43) and (4-44), respectively. (4-46) and (4-47) can be chosen for C-PSK and C-QAM modulation, respectively. All elements of P_{b,N_a} in Table 4.3 can be calculated by (4-45), (4-46) or (4-47). Here, we show a simple method to estimate the probability of bit error $\bar{P}_{b,k}$ of user k take in to account the effects of EP. By using the total probability theorem, we can describe

$$\bar{P}_{b,k} \cong \sum_{n=1}^{N_a+1} \boldsymbol{\beta}_{N_a}(n) \, Pr\big\{EP_n^{(k)}\big\} Pr\big\{e_k | EP_n^{(k)}\big\}$$

(4-48)

where the $N_a + 1$ mutually exclusive events $EP_n^{(k)}$, with $\sum_{n=1}^{N_a+1} \boldsymbol{\beta}_{N_a}(n) Pr\big\{EP_n^{(k)}\big\} = 1$, regarding the $(k-1)$ previous symbols decisions, $Pr\big\{EP_n^{(k)}\big\}$ is the probability of event $EP_n^{(k)}$ and $Pr\big\{e_k | EP_n^{(k)}\big\}$ is the probability of making an error in the detection of the symbols of kth user conditional on the event $EP_n^{(k)}$. For convenient calculation, we write the probability terms in (4-48) into vector form. All elements in $\boldsymbol{\beta}_{N_a}$, $\boldsymbol{\psi}_{N_a}$ and P_{b,N_a} are employed to calculate the average BER for STBC and SM user of ZF-STBC MIMO system by modifying (4-48) as follows.

$$\bar{P}_b \cong \sum_{i=1}^{N_a+1} \boldsymbol{\beta}_{N_a}(i)\,\boldsymbol{\psi}_{N_a}(i)\boldsymbol{P}_{b,N_a}(i). \qquad (4\text{-}49)$$

For calculating the average BER of STBC user $(\bar{P}_{b,STBC})$, the bit error probability P_z of the first detection is initially calculated by replacing (4-31) into (4-33), where $N_a = 0$ and $G = M - N_t N$. Next, we evaluate $\bar{P}_{b,STBC}$ by (4-49), where $N_a = 2(N-1)$, $P_{b0} = P_z$ for vector $\boldsymbol{\psi}_{N_a}$ in Table 4.2 and the elements of $\boldsymbol{P}_{b,N_a}$ in Table 4.3 can be calculated by (4-45), and (4-46) or (4-47).

4.3.7 Average BER for SM users

In order to mitigate the effect of EP from other layers, the transmitted symbols for SM user are detected after STBC decoding and SIC process according to the 4th step in Table 4.1, thus the $\bar{P}_{b,STBC}$ in 4.3.6 is applied for evaluating the average BER for SM user $(\bar{P}_{b,SM})$. $\bar{P}_{b,SM}$ can also be evaluated by (4-49), where $P_{b0} = \bar{P}_{b,STBC}$ for vector $\boldsymbol{\psi}_{N_a}$ in Table 4.2, $N_a = 2(N-J)$, $G = M - JN_t$, and the elements of $\boldsymbol{P}_{b,N_a}$ in Table 4.3 can be calculated by (4-50), and (4-51) or (4-52) as follows.

$$\breve{\gamma}_z(\alpha) = \frac{E_s/N_0}{(1 + \tau^2 N_t E_s/N_0 + M d_{\mathrm{EP}} \alpha^2 E_s/N_0)}, \qquad (4\text{-}50)$$

$$\breve{P}_b\big(\breve{\gamma}_z(\alpha)\big) \cong \frac{2}{max(log_2 C, 2)} \sum_{i=1}^{min\,(2,[C/4])} \left\{ \left[\frac{1}{2}(1 - \mu_i')\right]^{G+1} \sum_{j=0}^{G} \binom{G+j}{j} \left[\frac{1}{2}(1 + \mu_i')\right]^{j} \right\}$$

$$(4\text{-}51)$$

where $\mu_i' = \sqrt{\breve{\gamma}_z(\alpha)sin^2((2i-1)\pi/C)\big/\big(1 + \breve{\gamma}_z(\alpha)sin^2((2i-1)\pi/C)\big)}$,

$$\check{P}_b\big(\check{\gamma}_z(\alpha)\big) \cong \frac{2(\sqrt{C}-1)}{\sqrt{C}\log_2\sqrt{C}}\left[\frac{1}{2}(1-\mu_0')\right]^{G+1}\sum_{j=0}^{G}\binom{G+j}{j}\left[\frac{1}{2}(1+\mu_0')\right]^{j}$$

$$+\frac{2(\sqrt{C}-1)}{\sqrt{C}\log_2\sqrt{C}}\left[\frac{1}{2}(1-\mu_1')\right]^{G+1}\sum_{j=0}^{G}\binom{G+j}{j}\left[\frac{1}{2}(1+\mu_1')\right]^{j}$$

(4-52)

where $\mu_i' = \sqrt{\big(3(2i+1)^2\check{\gamma}_z(\alpha)\big)/\big(2(C-1)+3(2i+1)^2\check{\gamma}_z(\alpha)\big)}$, $\check{\gamma}_z(n) = \check{\gamma}(n)$ in

Table 4.3, (4-50), (4-51) and (4-52) are modified from (4-31), (4-33) and (4-34),

respectively. (4-51) and (4-52) can be selected for C-PSK and C-QAM modulation,

respectively. Finally, all elements of $\boldsymbol{\beta}_{N_a}, \boldsymbol{\psi}_{N_a}$ and $\boldsymbol{P}_{b,N_a}$ in this section are employed

to calculate the average BER for SM user of HMRS systems.

By averaging $\bar{P}_{b,STBC}$ and $\bar{P}_{b,SM}$, the average BER of ZF-STBC MIMO receiver

in the presence of CEE and EP can be obtained. For the general number for N, J and

M, the BER of each user can easily be evaluated by assigning $N_a = 2(N-1)$ for

STBC decoding and $N_a = 2(N-J)$ for SM detection. Moreover, (4-49), Table 4.2

and 4.3 can be used to evaluate the BER for both STBC and SM users.

4.4　Multi-Mode Hybrid-MIMO Receiver Scheme Systems

In CRN scenario, the system operates under the limited resources condition.

Especially, the limited unused channels and power control criteria that any users

should take into account. Moreover each user usually faces the different MIMO

channels, thus the flexible system is the interested option to apply in CRN. From this

reason, this part proposes the multi-mode HMRS system that each user can be applied
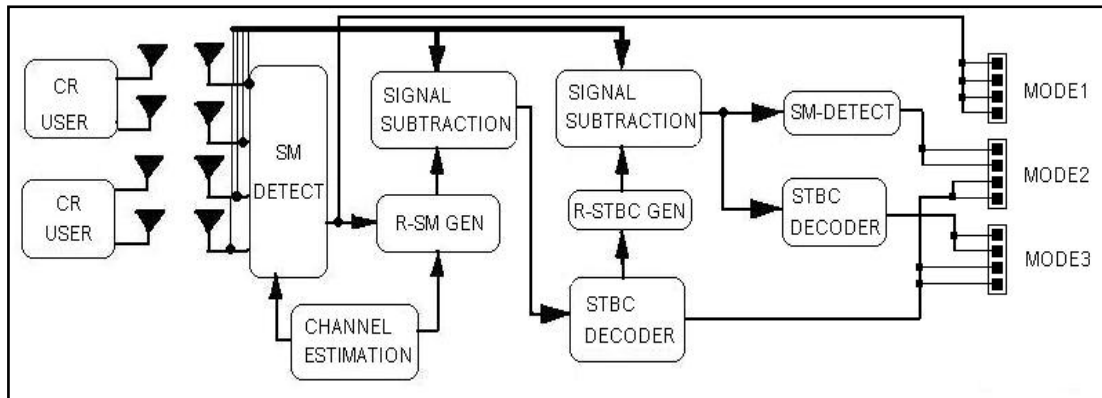
Figure 4.2 Multi-mode HMRS block diagram.

by SM or STBC code while the appropriate transmission mode can be decided by the

receiver or FC. From Figure 4.2, the receiver first estimates MIMO channels for each

user, check the available vacant channel and measure SNR. Then the receiver decides

to apply the optimum transmission scheme such as modulation order,

transmittedpower level (protect PN) and MIMO mode. From Figure 4.2, the three

modes for detection are available at the receiver that can be explained as

    1) Mode 1 is selected for two SM users when overall MIMO channel

is good. This mode can be operated when both users locate far from the PN. Thusa

few interferences from CRN are affected to PN, and both users can be applied SM

MIMO although this technique applies higher transmitted power than STBC code.

    2) Mode 2 is selected when two users apply different MIMO

technique. This case can be occurred when one usercloses to PN while this usershould

apply low transmitted power to protect PN by using STBC code.

Table 4.4 The numbers of flop for various hybrid-MIMO systems.

Systems	Numbers of flop	
	Transmitter	Receiver
A-BLAST	24	2,478
TDCSM	12	548
HMTS	12	2,242
ABBA	24	1,212
Multi-layer STBC	9,216	11,362
Adaptive-MIMO	12	3,168
HMRS (Proposed)	12	2,592

3) Mode 3 is selected when both users apply STBC code. This case can be occurred when both users near PN. Thus STBC code should be applied to protect PN similar to the reason at mode 2.

4.5   Efficiency Comparison for Various Hybrid MIMO techniques

The literature reviews demonstrate that each hybrid MIMO scheme offers different structure, performance, encoding and decoding. These differences are also affected to the cost for establishing the real networks. Thus this part presents the efficiency comparison between several hybrid-MIMO systems based on the differences of the system complexities and system performances. To obtain the criteria of comparison fairly, the number of flop for all systems are computed to represent the system complexity. Each system applies the different algorithms to transmit and detect data as well as the mathematical function. Generally, the complex addition and complex multiplication apply 2 flops and 6 flops, respectively. Table 4.4 presents the numbers of flop for all hybrid-MIMO systems at both transmitter and receiver with N=2 and M=4. The results show that the different numbers of flop are

Table 4.5 The efficiency comparison of various hybrid-MIMO systems.

Systems	Transmitter Complexity			Receiver Complexity			Data Rate			BER			Score
	L	M	H	L	M	H	H	M	L	L	M	H	
	3	2	1	3	2	1	3	2	1	3	2	1	
A-BLAST	O				O				O		O		8
TDCSM	O			O				O				O	9
HMTS	O				O			O			O		9
ABBA	O				O			O				O	8
Multi-layer STBC			O			O	O				O		7
Adaptive-MIMO	O				O			O			O		9
HMRS (Proposed)	O				O			O		O			10

(where H, M and L represent high, medium and low, respectively.)

applied by each scheme. However, only the system complexity cannot be used to reflectenough forrepresenting the overall efficiency of each system.Therefore the efficiency comparisons of various hybrid-MIMO systems are established in the Table 4.5 by utilizing the system complexity from the Table 4.4, data rate and BER performances.From the results, the proposed systemachieves highest score than other techniques. Anyway, the BER performances of several hybrid-MIMO systems and the conventional MIMO systemare presented in the next chapter.

4.6 The Relationship between the Cost-Index and Efficiency of Wireless Systems

From literature review, all hybrid-MIMO techniques offer medium data rate when compared to SM MIMO. However hybrid-MIMO achieve higher data rate thanSTBC code. As well as SER, each technique also offers different performances.Besides,the throughput performance has been also used toindicate the

datatransferefficiency.Generally, the lower difference between the target bit rateand

the though-

Figure 4.3 The relationship between the Cost-index and efficiency of wireless

systems.

put indicate that the systems is the efficient networks.This research defines the SER to

channel capacity ratio to be the Cost-index performance. This part will demonstrate

the relationship between the Cost-index and efficiency of wireless systems as follows.

$$Tp = R(1 - BER) = R(1 - SER / \log_2 M) \qquad (4\text{-}53)$$

$$\frac{Tp}{C_P} = \frac{R(1 - SER / b)}{C_P} \qquad (4\text{-}54)$$

$$\frac{R \cdot SER}{bC_P} = \frac{R - Tp}{C_P} \qquad (4\text{-}55)$$

$$\frac{SER}{C_P} = \frac{b(R-Tp)}{R \cdot C_P} \qquad (4\text{-}56)$$

$$Cost - Index = \frac{C_P}{SER} = \frac{R \cdot C_P}{b(R-Tp)} \quad (4\text{-}57)$$

where M and b denote the number of symbol in constellation and the number of bit per symbol, respectively. From (4-54), Tp and R are normalized by the maximum possible rate C_P to achieve the normalized value. By the relation that the lower difference between the target bit rate and the throughput indicate to the efficient networks and (4-57), demonstrate that the high Cost-index is presented in the efficient network.

4.7   Summary

This chapter discusses about the principle and BER derivation of HMRS. The multi-mode HMRS is also proposed to achieve the optimum advantage. Moreover the efficiency comparisons of the several hybrid-MIMO systems are presented. The relationship between the Cost-index and the efficiency of wireless networks is finally discussed.

CHAPTER V

PERFORMANCE OF HYBRID-MIMO

RECEIVER SCHEME

5.1 Introduction

The previous chapters discuss the principle of several existing hybrid-MIMO, conventional MIMO and the proposed hybrid-MIMO, namely, HMRS systems. Each scheme applies a different technique to encode and decoding data. From these differences, each scheme also offers the different performance. Therefore this chapter demonstrates the performance of HMRS compared with other schemes. The simulation results and analytical results are jointly demonstrated for verifying the validity of this work. In this chapter, the HMRS performances can be demonstrated and divided into three parts. The first part presents the simulated SER comparison between HMRS and other hybrid-MIMO schemes. The second part reveals the analytical BER performance of HMRS in the presence of EP and CEE while the accuracy of channel estimation and the number of user are varied.

5.2 Simulation Performance of Hybrid-MIMO Receiver Scheme

This part presents the SER comparison between HMRS, V-BLAST and the existing hybrid-MIMO. The Monte Carlo simulation is applied to calculate the average SER for each scheme. The transmitter consists of 2 users equipped with 2
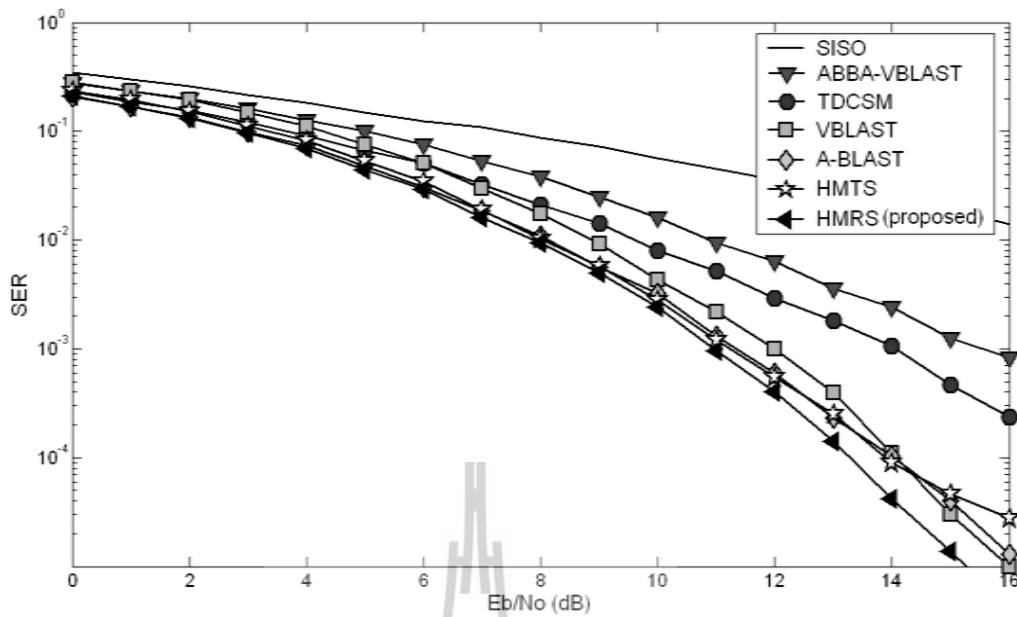
Figure 5.1 SER comparisons between HMRS and other techniques.

antennasper user. The bit streams of both users are mapped by QPSK signals and transmitted over the MIMO flat Rayleigh fading channel. The receiver is equipped with 4 antennas. ML detection and SIC are applied for HMRS systems.This part presents the SER comparisons between HMRS and other schemes in case of the average SER of two users and in case of separated user as follows.

Figure 5.1 presents the SER comparison between HMRS and other. The results show that the ABBA and TDCSM schemes offer worseperformances. Because both schemes apply the matrix calculation method without SIC technique that can efficiently decrease the interference of other users. The other existing schemes, VBLAST, A-BLAST and HMTS offer the better performance because the MIMO detection and SIC arejointly used to cancel interference and detect the transmitted symbols. Besides, the proposed method HMRSoffers the best performance because
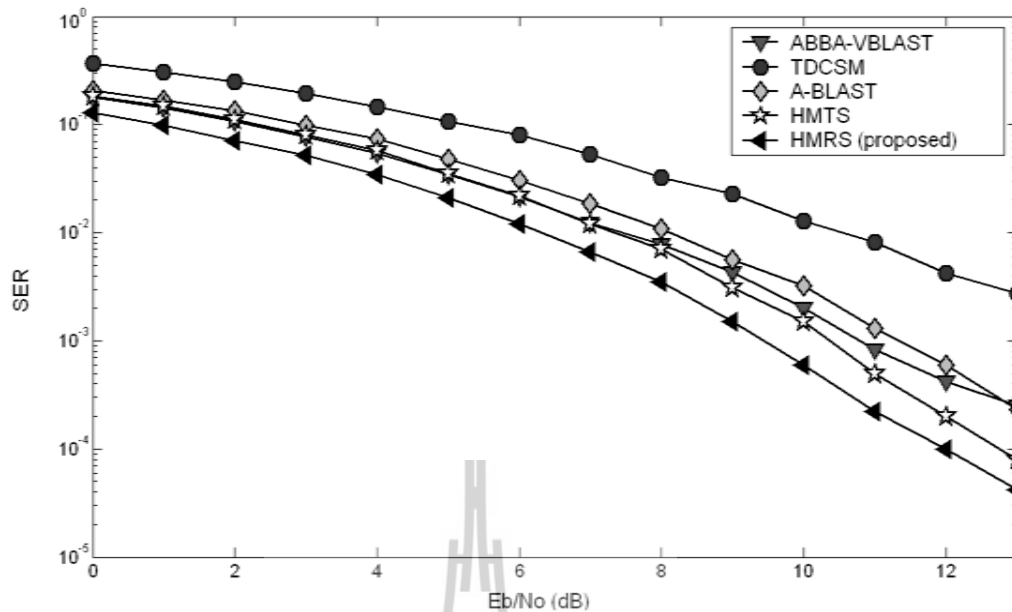
Figure 5.2 SER comparisons between HMRS and other techniques for STBC user.

this technique cancels interference in the received signal before detecting the first layer. At 10-4 SER, HMRS offers higher performance than VBLAST about 1dB.

Figure 5.2 shows the SER comparison for STBC user between HMRS and others. By the same reason to Figure 5.1, HMRS still offers best performance. Besides, the performance of ABBA outperforms TDCSM that is different from Figure 5.1. This isbecause the orthogonal code of ABBA can offer a higher diversity gain.At 10^{-4} SER, HMRS offers higher performance than HMTS about 1dB.

Figure 5.3 shows the advantage of HMRS over VBLAST because the code structure of VBLAST has no orthogonal property of STBCcode. Moreover the data streams of SM user in HMRS are detected after STBC streams that the effect of EP isalready mitigated.Thus the SM user of HMRS can achieve higher performance than VBLAST technique about 0.3dB at 10^{-4} SER.
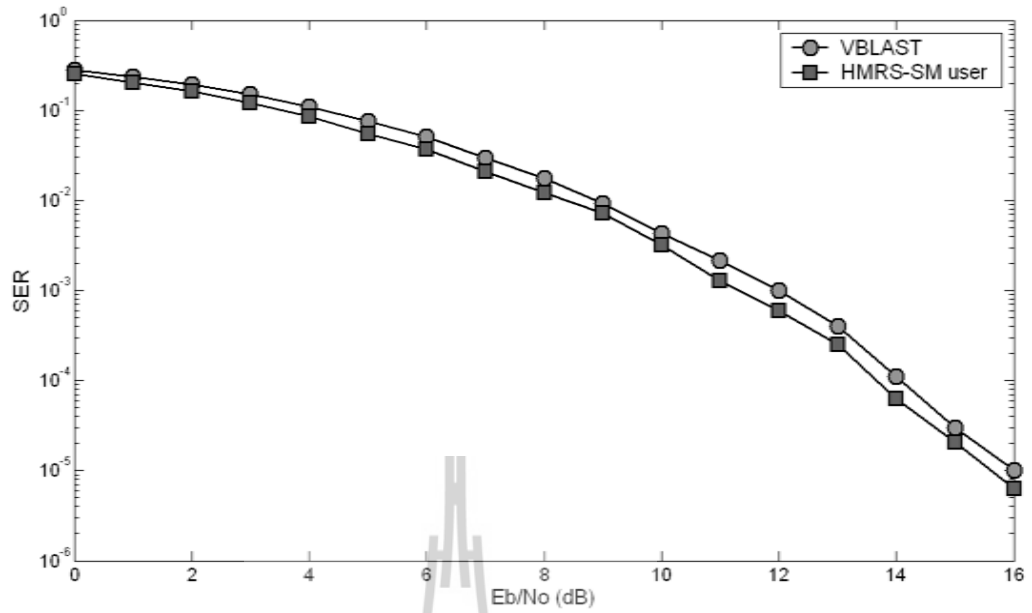
Figure 5.3 SER comparisons between SM user of HMRS and VBLAST.
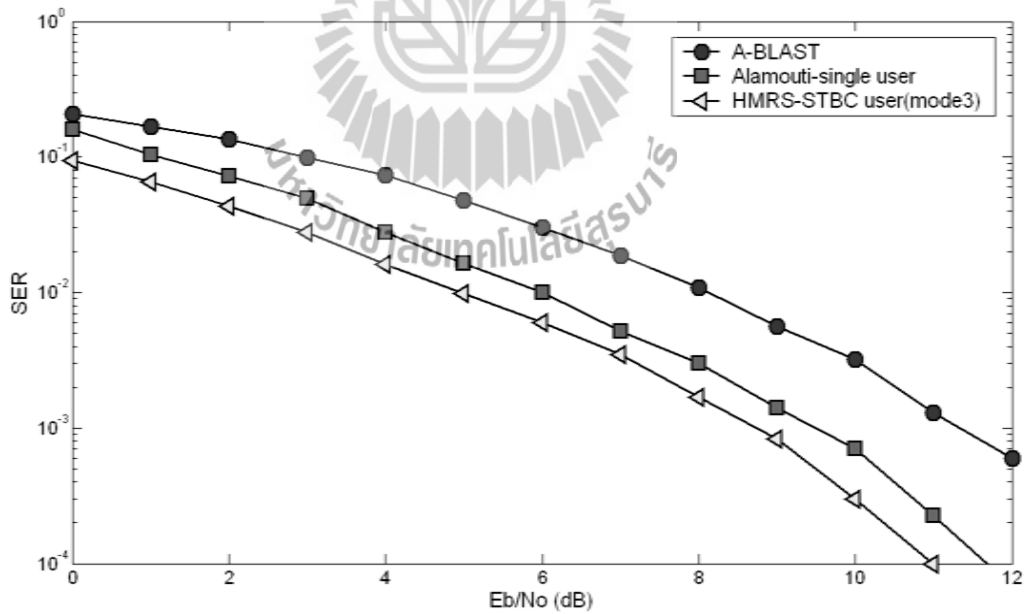
Figure 5.4 The performances of multi-mode HMRS (mode 3), A-BLAST and

Alamoutisingleuser.

Figure 5.4 presents the advantage of multi-mode HMRS. By comparing the SER between mode 3 of multi-mode HMRS (equipped with 2 STBC users) and Alamouti single user (apply 2 antennas at transmitting and receiving side), the resultsshow that the performance ofmulti-user systems (HMRS) outperforms the performance of single user systems (Alamouti) because HMRS cancel the interferencebefore detecting the first stream as well as the orthogonal property in mode 3 of multi-mode HMRS. At 10-4 SER, mode 3 of multi-mode HMRS offers higher performance than Alamouti scheme about 0.65dB.

Figure 5.5 separately presents the performances of each mode in the multi-mode HMRS system. The results show that the best SER performance is offered by mode 3 because of the dual orthogonal code in its transmitted symbol block while this mode offers worse data rate. Mode 2 offers the fair performance due to the orthogonal code of one user. Anyway this mode offers higher data rate than mode 1. Mode 1 offers the worse performance because the 2 SM users have no orthogonal code but this mode can achieve the highest data rate. At 10-4 SER, STBC user of mode 3 offers higher performance than STBC user of mode 2 about 1dB.

Figure 5.6 shows the compromised channel capacity of hybrid MIMO system when compared to V-BLAST and A-BLAST. Because hybrid MIMO is equipped by one SM user and one STBC user, therefore hybrid MIMO offers fair performanceAt 30dB SNR, Hybrid-MIMO system offers higher channel capacity about 13bps/Hz than A-BLAST scheme.
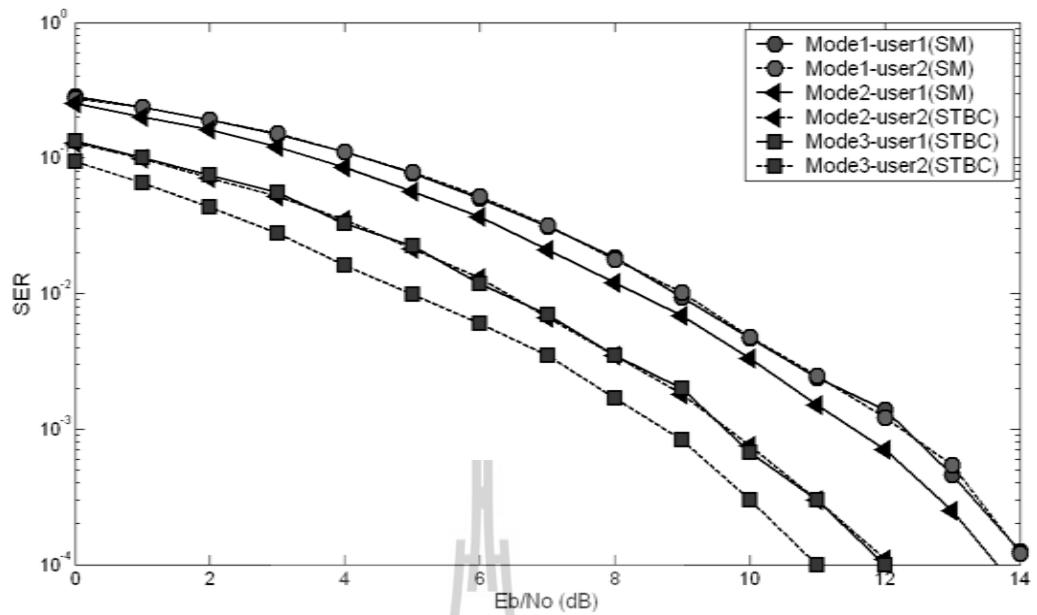
Figure 5.5 Performances of the multi-mode HMRS.
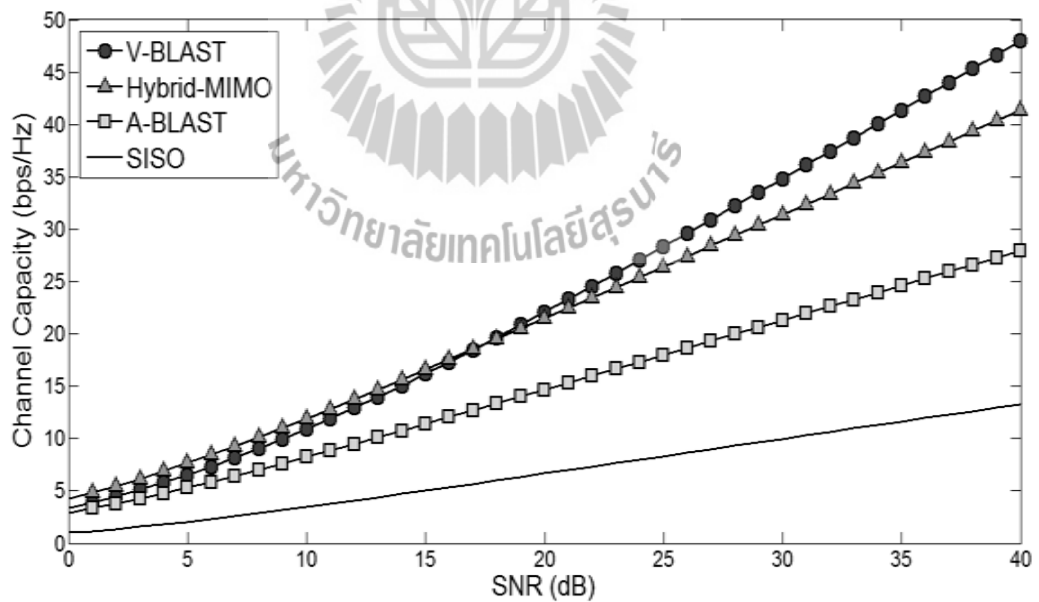
Figure 5.6 Channel capacity comparisons.
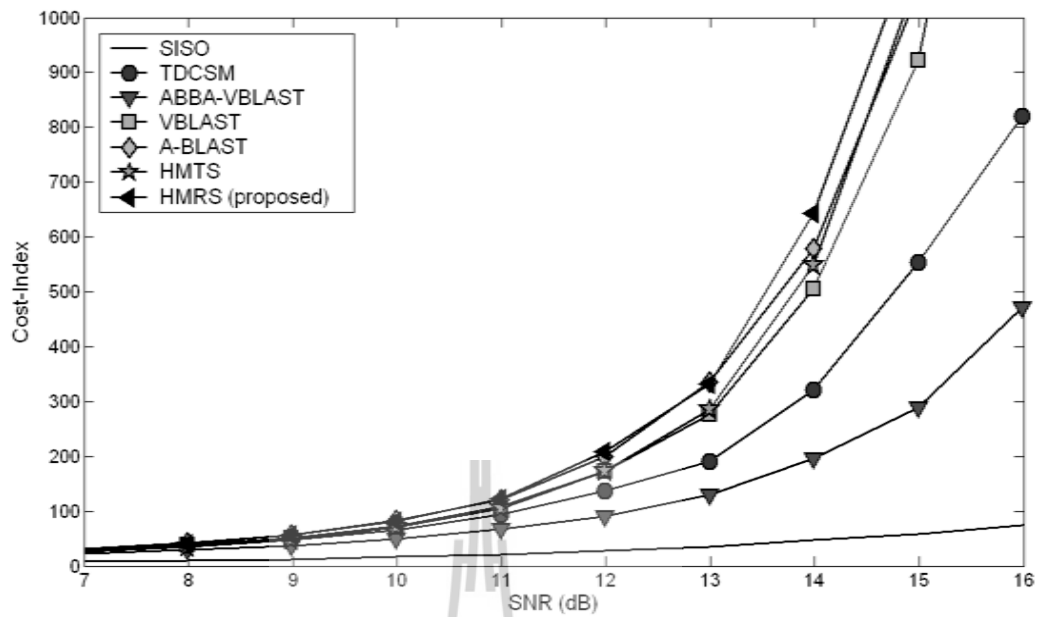
Figure 5.7 Cost-index performances of HMRS and other techniques.
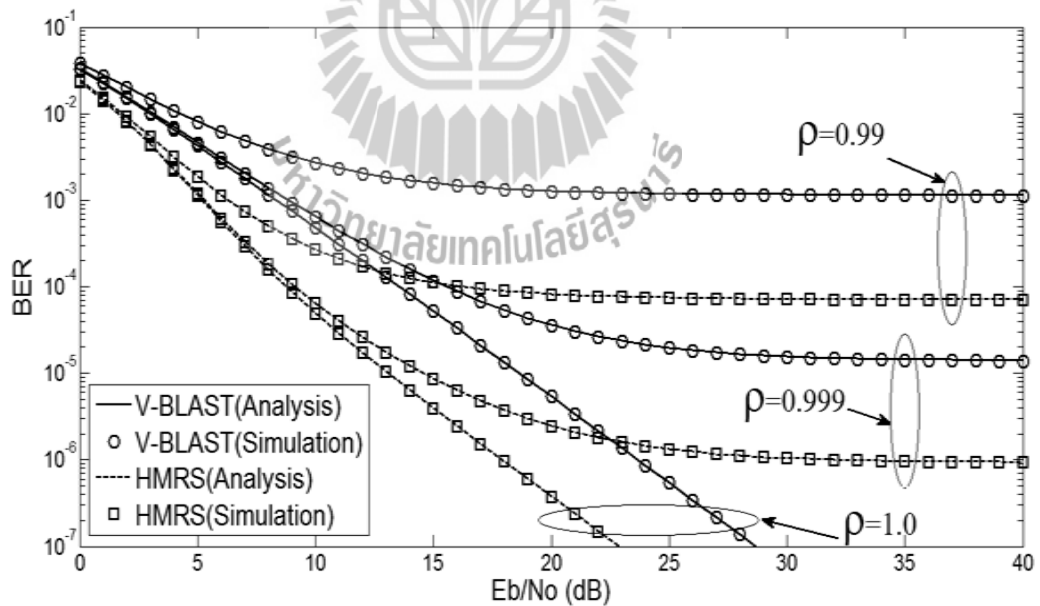
Figure 5.8 BER comparisons between HMRS and V-BLAST.

Figure 5.7 shows the advantage of HMRS when consider the Cost-index performance that can indicate the compromised performance between SER and channel capacity. HMRS offers highest benefit because this scheme achieves the best SER performance and also offers a good channel capacity while A-BLAST offersalmost similar performance to HMRS.

5.3 Analytical SER Performance in the Presence of EP and CEE

This part presents the analytical SER performance of HMRS compared to the VBLAST systems in the presence of EP and CEEthat are similar topractical channels. While the ZF detection and SIC are applied in HMRS receiver. Moreover the number of user and the accuracy of channel estimation are also varied to reveal the performance of HMRS. The analytical SER expression in Section 4.3.6 and Section 4.3.7 are adopted to calculate the average SER for HMRS systems.

Figure 5.8 shows the BER of the QPSK V-BLAST systems (the 2nd layer) and the proposed systems (SM user of QPSK HMRS systems) with CEE and EP when the accuracy of channel estimation are 0.99, 0.999 and 1 (perfect case) for $N=2$ users,M=5 receive antennas. It should be noted that the performance of V-BLAST is worse than that of HMRS for all case of ρ. This means that the EP problem in V-BLAST orZF-SIC receiver can be solved by STBC technique. According to analysis in (4-49) and (4-51), these results agree very well with simulation results that are shown inFigure 5.8. At 10-4 BER, HMRS offers higher performance than V-BLAST about 3dB for perfect channel estimation case.
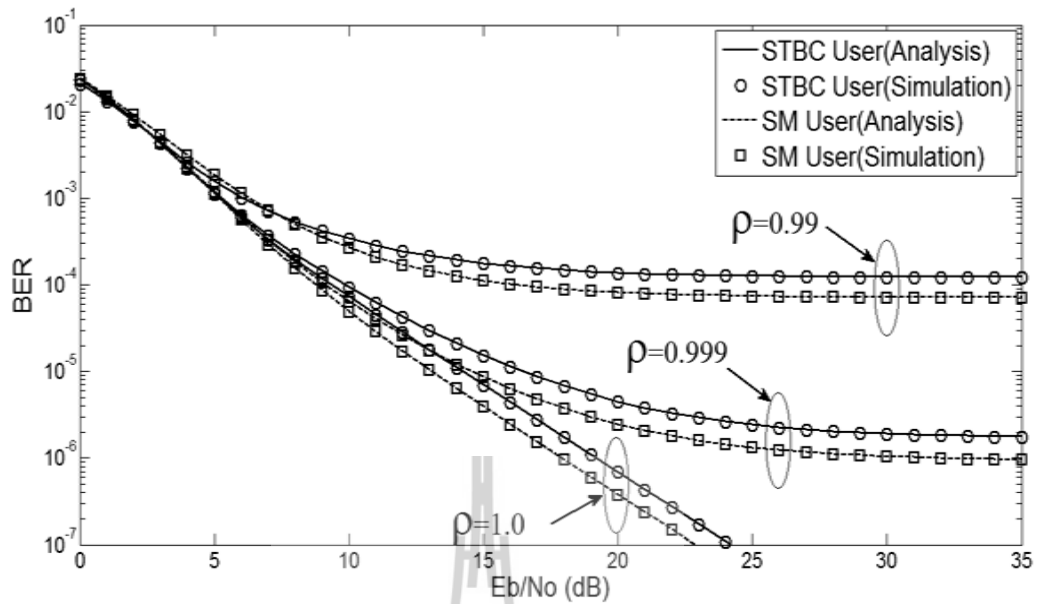
Figure 5.9 BER performance of QPSK HMRS systems with *N*=2, *M*=5.

Figure 5.9 shows the BER performance of QPSK HMRS systems, where the BER expression of STBC user is shown in (4-46) and (4-49). The BER expression of SM user is given by (4-49) and (4-51) when the accuracy of channel estimation are 0.99, 0.999 and 1 for *N*=2 users and *M*=5 receive antennas. From Figure 5.9, we can see that the average BERs of SM user offer a higher reliability than average BERs ofSTBC user because the transmitted streams of SM user are detected after the previous STBC decoding that can mitigate the EP problem. The analytical results correspond closely to the simulation results. At 10-6 BER, SM user offers higher performance than STBC user about 1dB.
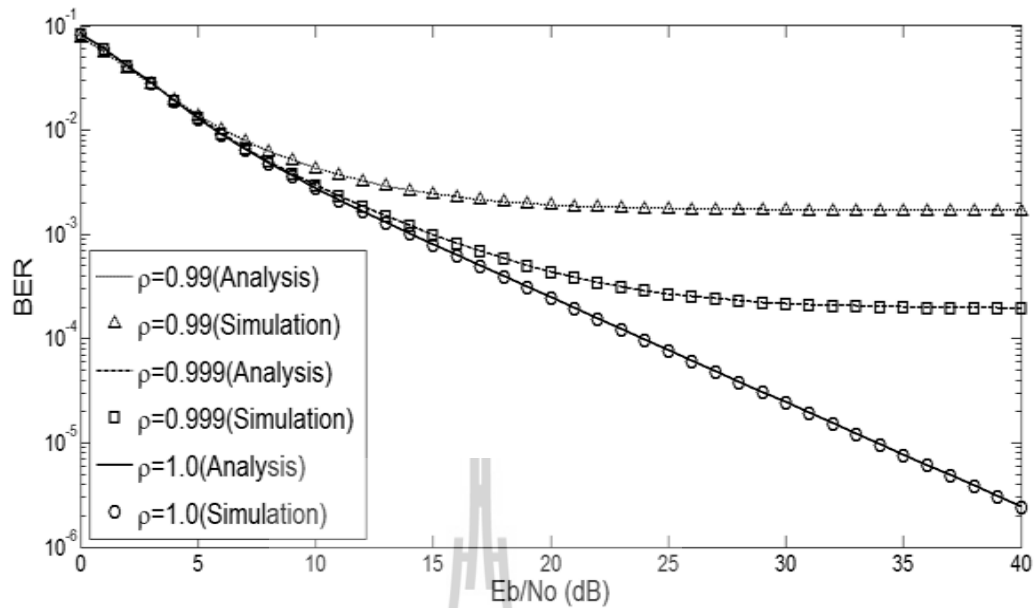
Figure 5.10 BER performance of BPSK HMRS systems with N=2, M=4.

Figure 5.10 demonstrates the average BER performance of BPSK HMRS systems, where the BER performance of both STBC user and SM user are averaged in the presence of CEE and EP. The accuracy of channel estimation is varied by 0.99, 0.999 and 1 (perfect case) for N=2 users and M=4 receive antennas. From Figure 5.10, it is found that the average BER performances are rapidly changed by varying the accuracy of channel estimation, and these agree with simulation results.

Figure 5.11 illustrates the BER performance of 16QAM HMRS systems, where the BER of STBC user is shown in (4-47) and (4-49), and BER of SM user is given by (4-49) and (4-52) with EP. The accuracy of channel estimation is varied by 0.99, 0.999 and 1 (perfect case) for N=2 users and M=6 receive antennas. From Figure 5.11, the results show that the average BERs of SM user correspond closely to
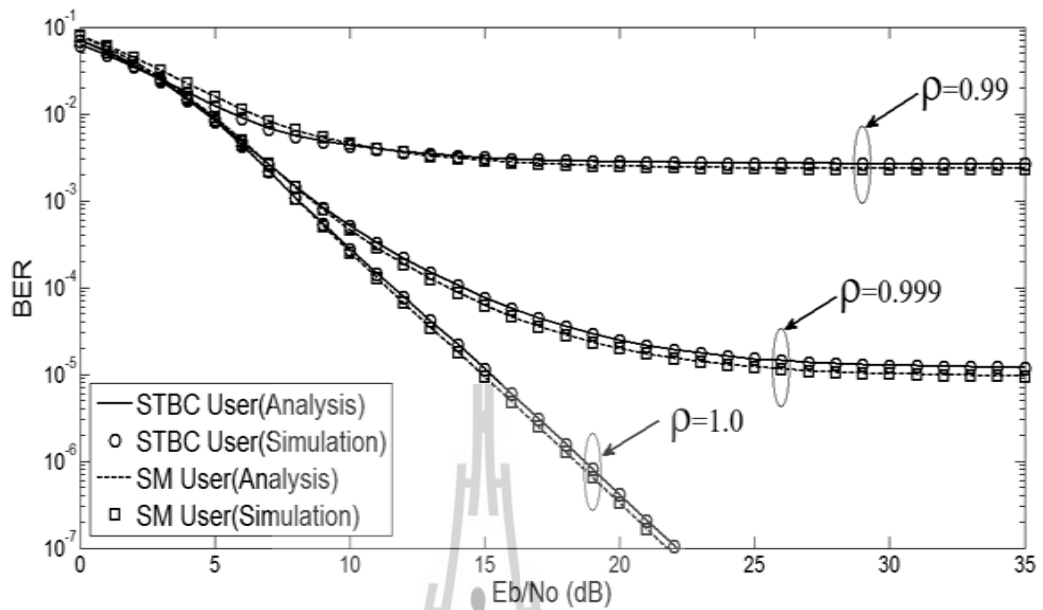
Figure 5.11 BER performance of 16QAM HMRS systems with *N*=2, *M*=6.
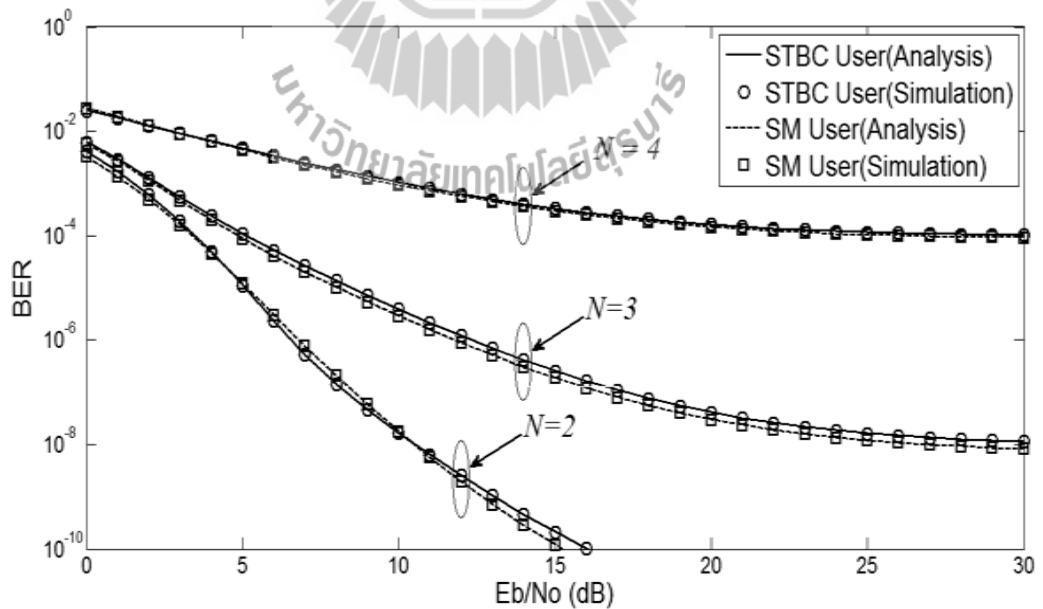
Figure 5.12BER performance of QPSK HMRS systems for different number of users,

ρ=0.999, M=8.
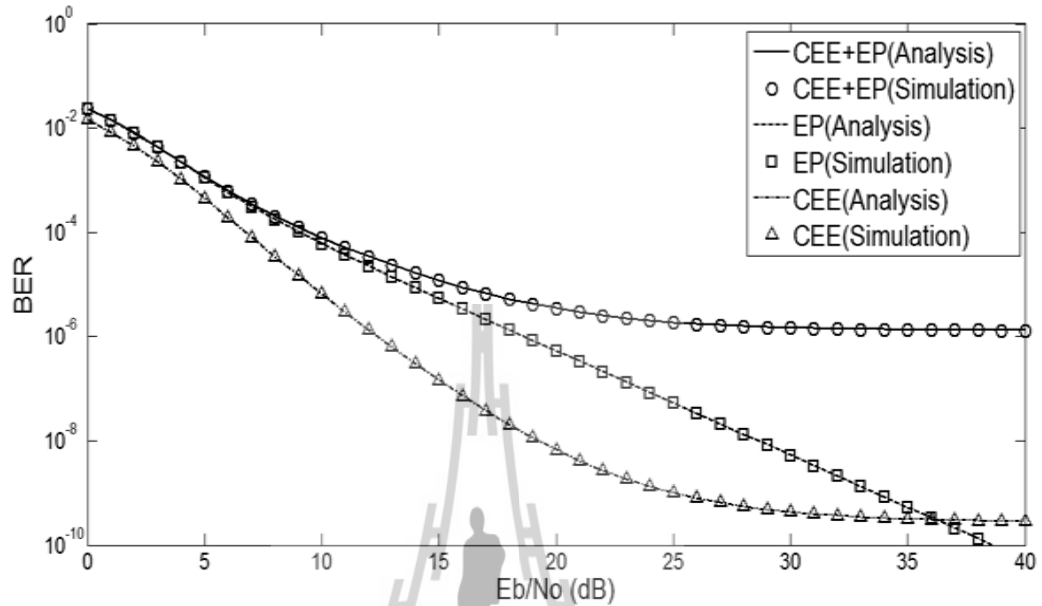
Figure 5.13 BER performance of QPSK HMRS systems fordifferent case of error,

ρ=0.999, N=2, M=5.

the average BERs of STBC user. According to our analytical performances, these

results agree very well with simulation results.

Figure 5.12 demonstrates the BER of QPSK HMRS systems with CEE and EP

when the accuracy of channel estimation is 0.999 for $N = 2$ ($J = 1$), $N = 3$ ($J = 1$) and

$N = 4$ ($J = 2$) with $M = 8$ receive antennas. From Figure 5.12, the simulationresults

agree with analysis that, as the number of user increases, the sensitivity of the

HMRSsystem to the CEE and the EP increases. Because the number of sub-channel is

increased according to N, thus cumulative error due to channel estimation from all

sub-channels is also increased.At 10^{-4} BER, N=2 case offers higher performance than N=3 case about 2dB.

Figure 5.13 presents the BER performance comparison of QPSK HMRS systems between only CEE case, only EP case, and both CEE and EP case. From the first and the second cases, it should be noted that EP degrades BER performance more than CEE. Significantly, the last case offers most impactto the system performance and it is most similar to real scenario. These mean that the problem of CEE and EP should be carefully considered for designing wireless network in practice.

5.4   Summary

This chapter presents the advantage of HMRS system by comparing to other hybrid MIMO schemes in simulation. The results show that the SER performance of HMRS outperforms other hybrid-MIMO. For analytical performance, the accuracy of channel estimation and the number of user are varied. The results show that the performance of HMRS is most affected by the effect of EP and CEE that are alwaysoccurred in practice. Moreover, this part presents the advantage of HMRS in practice and confirms the validity of HMRS principle by the measurement results. The trends of the experimental BER performances are corresponded to the analytical BER performances.

CHAPTER VI

IMPLEMENTATION OFHYBRID-MIMO

RECEIVER SCHEMETESTBED

6.1   Introduction

This chapter presents the implementation of HMRS testbed in order to validate the concept of this thesis.The method to setup HMRS hardware, program software for signal processing and how to import data from hardware into computer are explained. The limitations of experiment and devices are described. Moreover theexperimental scenario for this experiment is also discussed.

6.2   Devices and Components

This part presents the detail and specification of the important devices and components used in HMRS testbed. The function of each devices and components are also explained to understand the overall HMRS implementation.

6.2.1   Radio Frequency Devices

In HMRS testbed, the baseband signals are modulated by intermediate frequencies (IF) signals in field programmable gate array (FPGA) chip. Then these signals are modulated by radio frequency signals to propagate over radio channels. Thus this part presents the specification and function of RF devices that are applied in this experiment as shown in Figure 6.1.
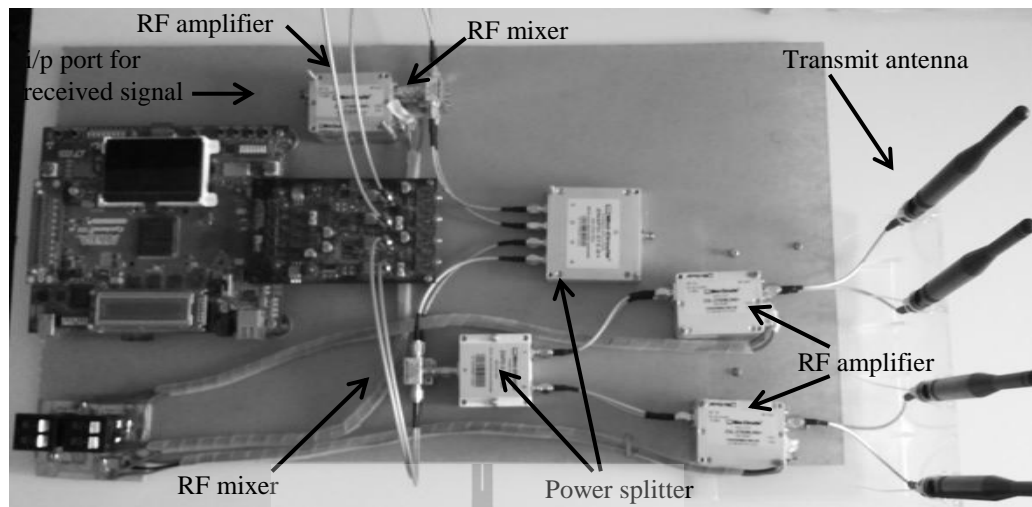
Figure 6.1 HMRS transceiver.

1) RF mixer is used to up convert frequency at the transmitter by mixing the IF signals with carrier frequency from RF generator. This device is also applied at the receiver to convert RF frequency down to IF signalsby mixing with carrier frequency. In this thesis, the model ZX05-73L from Mini circuit brand is selected. It can be operated in the 2400-7000 MHz band with 6.2dB conversion loss and 33dB LO-RF isolation.

2) RF amplifier is used to amplify the power of RF signalat both transmitter and receiver for mitigating the effect from noise and radio channels. In this work, the model ZQL-2700MLNW+ from Mini circuit brand is chosen which can be operated in the 2200-2700 MHz band with 25dB gain.

3) Power splitter is used to split the power of carrier frequency from RF generator for each signal stream at transmit and receive antennas. The model ZN4PD-272+ from Mini circuit brand is applied in this thesis that can be operated
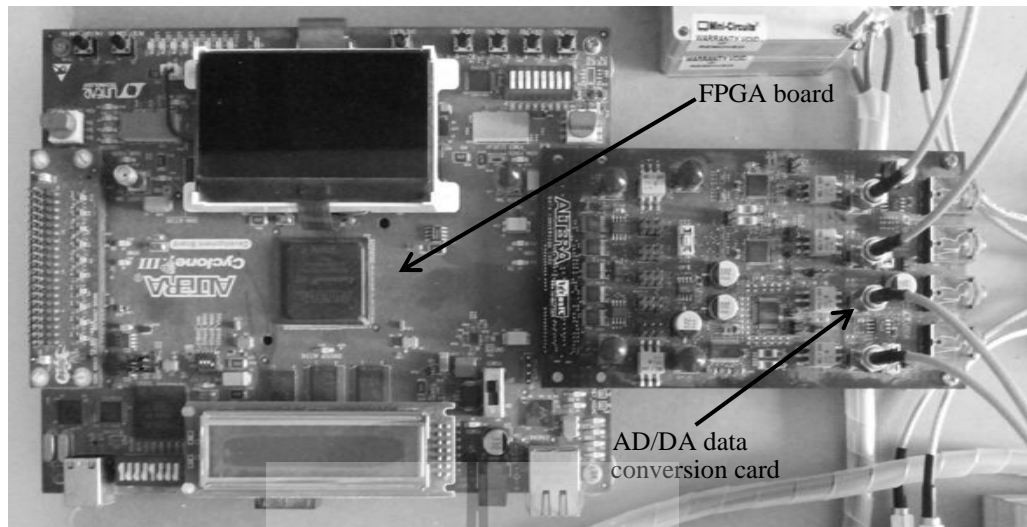
Figure 6.2 FPGA board and AD/DA data conversion card.

the 500-2700 MHz band with 0.9dB insertion loss and 19dB isolation.

4) RF dummy load is used to absorb the power of RF signal when measuring the sub-channel MIMO. In this thesis, the model ANNE-50L+ from Mini circuit brand is used. This product can be operated in the 0-12000 MHz band with 50 ohm impedance.

5) Omni-directional antenna is used to transmit and receive RF signal at both transmitter and receiver in the 2400-2500 MHz band and provides 8dBi omni-directional operation.

6.2.2 FPGA Board

In this research, the signal processing for baseband and IF signal can be implemented on FPGA chip such as QPSK mapping, STBC coding, IF modulation, and low pass filter.The cyclone III 3C120 development board from Altera brand is used in this research. The specification of FPGA chip can be shown in Table 6.1.

Table 6.1 Specification of FPGA board.

ITEM	Detail
FPGA chip model	780-pin Altera Cyclone III EP3C120 FPGA
Logic elements	119,000 LEs
Memory	3,888 kilobits
18x18 bits Multiplier blocks	288
Phase locked loops	4
Clock	50MHz
DAC interface	HSMC port

6.2.3 AD/DA Data Conversion Card

At the transmitter, the digital transmitted signals in FPGA board should be converted to the analog signal for mixing with the carrier frequency at RF part. This thesis applies AD/DA data conversion card from Terasic brand that is equippedwith one HSMC connector for interfacing with FPGA board, two 14-bit A/D converterchannels with 150Msps, two 14-bit D/A converter channels with250Msps.

6.3 Interfacing between Hardware and Software

This thesis implements HMRS testbed on FPGA board that can be interfaced with Quartus II version 11.1sp2 and Matlab. The interfacing between hardware and software can be fully demonstrated in Figure 6.3.
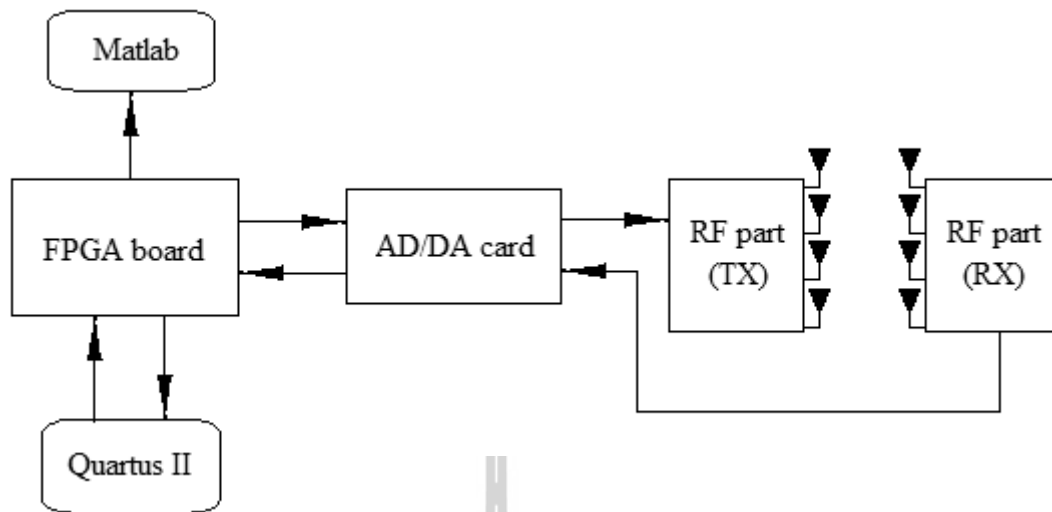
Figure 6.3 Interfacing between hardware and software.

6.3.1 FPGA board and AD/DA card

Figure 6.1 shows that the FPGA board is interfaced with AD/DA card to send and receive the digital data streams. HSMC port is equipped on both FPGA board and AD/DA card to transfer the high speed digital data streams in the transceiver.

6.3.2 AD/DA Card and RF Part

The function of AD/DA card can be divided into two sections. The firstsection is the digital to analog (DA) conversion. DA section sends the analog signal to RF part (TX) for up-converter, amplifier and RF signals propagation. The second section is analog to digital (AD) conversion. AD section receives the IF received signals from RF part (RX) to convert the analog signals to be digital signals. SMA connector can be used to connect all IF signals between AD/DA card and RF part.

6.3.3 Quartus II and FPGA Board

Quartus II is the important tools that can be used to create and connect the sub-function block in HMRS systems by writing VHDL language or applying the ready-made block in Quartus II program.USB port or JTAG is used to program FPGA chip according to the developed diagram in Quartus II.Moreover the signalTap II logic analyzer in Quartus II can be used to illustratethe desired signals that flow inside the FPGA board.

6.3.4 Matlab and FPGA Board

In this thesis, Matlab programing is used to capture all signals from FPGA board and used to make channel estimation and HMRS decoding by employing the captured signals from FPGA board. The captured signals from FPGA board can be transferred to the matrix in Matlab by USB port. Each column in the captured datamatrix is represented to the desired signal on FPGA board that should be used to estimate MIMO channel, validate the desired signals and decoding the HMRS signals.

6.4 Limitations of experiment

In this part, the limitations of experiment are described by considering the physical characteristic of devices and the link budget in experiment. These limitations can be divided into five portions as follows.
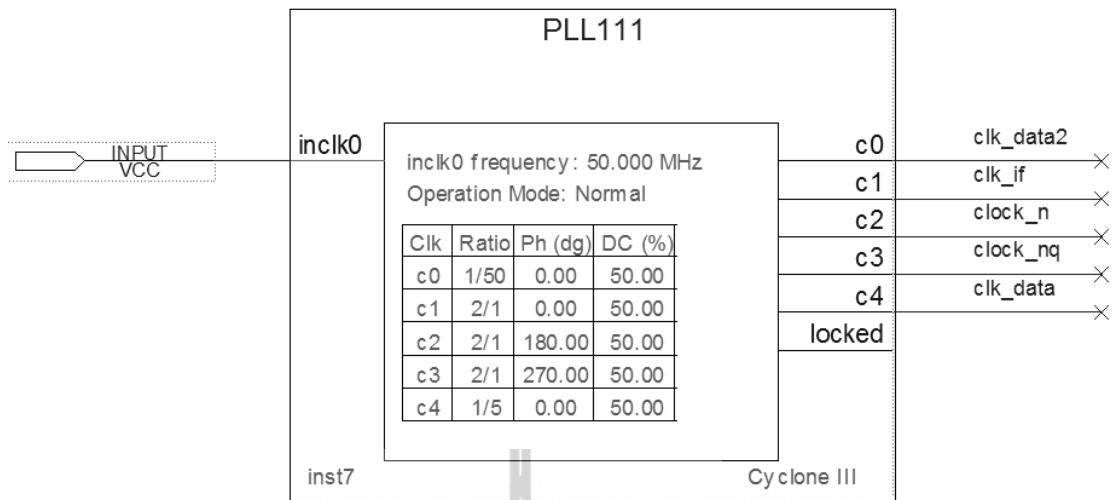
Figure 6.4 Clock generators.

6.4.1 Number of port of AD/DA data conversion card

The AD/DA conversion card applied in the experiment is the product of Terasiccompany. It is equipped with two input SubMiniature version A (SMA) ports and two output SMA ports. Thus the two data streams of the first user need to be copied for the second user by using two ways power splitter. Meanwhile, the four received signals at the receiver need to be measured during two time slots bycapturing the received signals into computer. From this reason, this experiment cannot be implemented as real time systems.

6.4.2 Link Distance

In this experiment, the link distance between the transmitter and the receiver is assigned about 5 meters. This is because the RF power in the experiment is limited by the transmitted power, gain and loss of RF devices, loss in radio channels,

and the interference fromother radio sources. Therefore the gain and loss of power in the systems are briefly described in Table 6.2 as follows.

Table 6.2 Limitations in experiment.

Source	Limitation
Transmitted power	<=18dBm
Amplifier gain/channel	25dB
Cable loss at transmitter	0.8dB
Cable loss at receiver	3.86dB
Loss in splitter	6dB
Loss in mixer	6.2dB
Antenna gain	6dBi
Free space path loss (FSPL)	54.4dB

The Table show that the link distance is limited by many factors from RF devices and radio channels. In fact, the far field generally starts at a distance of $2D^2/\lambda$, where D denotes a length of antenna and λ denotes a wavelength of carrier frequency. Meanwhile, the wavelength and the length of antenna in the experiment are determined as0.12 meter and 0.10meter, respectively. Thus the started pointof far-field region for this work is0.167meter that is shorterthan the link distance of 5 meter in the experiment. This means that the experimental results can be correctly applied to validate an advantage of the proposed system although the link distant of 5 meter is quite short.

6.4.3 Channel estimation error

Channel estimation for 16 sub-channels need to be carried out during two time slots because the AD/DA conversion card has only two output channels. Thus this operation cannot be implemented as real time.As a result, a high error level

is presented in the channel estimation process and high detected efficiency cannot be obtained at the receiver.

6.4.4 Determination of power unit

In simulations and analysis, Eb/No unit is defined as the horizontal axis for BER performances. Meanwhile the transmitted power (P_T) is defined for the experiment in this thesis. For theory, the P_T unit can be converted to be Eb/No unit by scaling with channel gain, bit rate and signal bandwidth. While the theoretical channel gain can be generatedby using a random coefficient function that has specific pattern in statistic. In contrast, the practical channel gain can be rapidly varied in the different locations and durations. Therefore the P_T unit at the horizontal axis of BER performances is not converted to be Eb/No unit. However, for checking a validity of the experimental results, the trend of BER performances of the experiment and the theory are used to compare and validate the advantage of the HMRS system.

6.4.5 MIMO configuration

As the reason in the Section 6.4.1, the AD/DA data conversion card equipped with only two input and two output channels. Thus the minimum number of user and the minimum number of received antennas are determined as two users and four antennas, respectively. Moreover this specification is also corresponded to the theoretical specification in simulation and analysis.
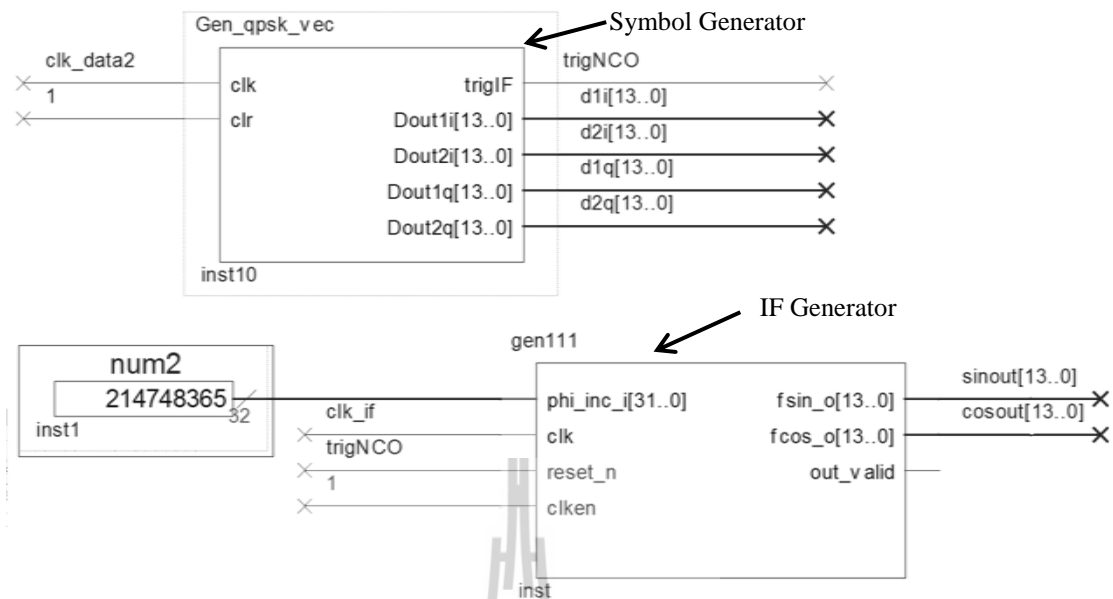
Figure 6.5 Symbol and IF generator.

6.5 The developed systems in Quartus II

For designing and creating HMRS systems on FPGA chip, all sub-function block of the HMRS systems can be developed by Quartus II program that support FPGA chip from Altera's products. This thesis divides the HMRS systems into two parts. The first is transmitter and the remaining is receiver. Each part of the transceiver can be separately explained as follows.

6.5.1 Hybrid-MIMO Receiver Scheme Transmitter

At the HMRS transmitter, the ready-made block and the developed block are connected to generate the HMRS signals for each user. The transmitter can be divided into four parts as follows.
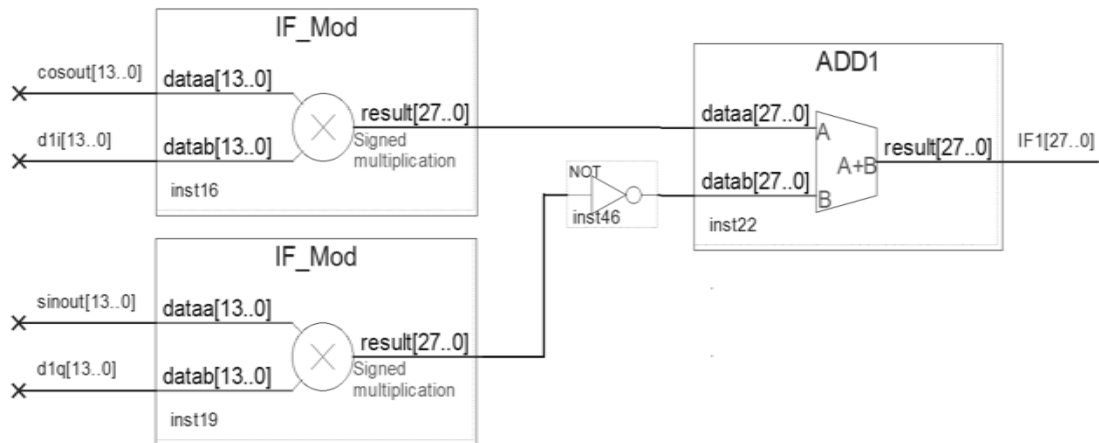
Figure 6.6 QPSK wave form generator.

1) Clock generator is used to generate a group of clock signals that are individually applied for different sub-systems such as symbol generator, IF generator and signal capturing. To succeed this goal, the phase-locked loop (PLL) is used to independently generate the different clock rate for several sub-systems. The frequency and phase of each clock signal can be independently assigned by inserting the favourite frequency into the regulative blank in PLL properties window as shown in Figure 6.4.

2) QPSK symbols and STBC generator is used to generate bit streams for mapping into QPSK format. Then these QPSK streams are ranged into the STBC structure as shown in Figure 6.5.

3) IF generator in Figure 6.5 is used to generate two IF frequencies including sine wave and cosine wave. The favourite values of IF frequency and sampling frequency can be easily assigned in NCO properties window of Quartus II program.

4) QPSK signal generator is used to generate QPSK wave form by multiplying STBC streams with IF signals from IF generator. Then thetwo orthogonal signals are added to form the QPSK wave form as shown in Figure 6.6.

6.5.2 Hybrid-MIMO Receiver Scheme Receiver

This thesis implements the receiver and transmitter into the single FPGA chip. The receiver can be divided into two parts as follows.

1) IF demodulator is used to remove IF frequencies from the received signals. The received IF signals are multiplied with sine and cosine wave from the NCO block as shown in Figure 6.7.

2) Low pass filter (LPF) is used to filter the output signals of IF demodulator to get the envelope of the received signals. This LPF can be created by using FIR filter block in Quartus II program as shown in Figure 6.8. The cut-off frequency and other parameters of LPF can be assigned in the FIR property windows.

6.6 Channel Estimation and Hybrid-MIMO Receiver Scheme Detection in Matlab

This thesis uses Matlab programing to make channel estimation and HMRS detection by using the captured signals that import from FPGA board and transfer data by JTAG cable. These tasks can be explained in this part as follows.
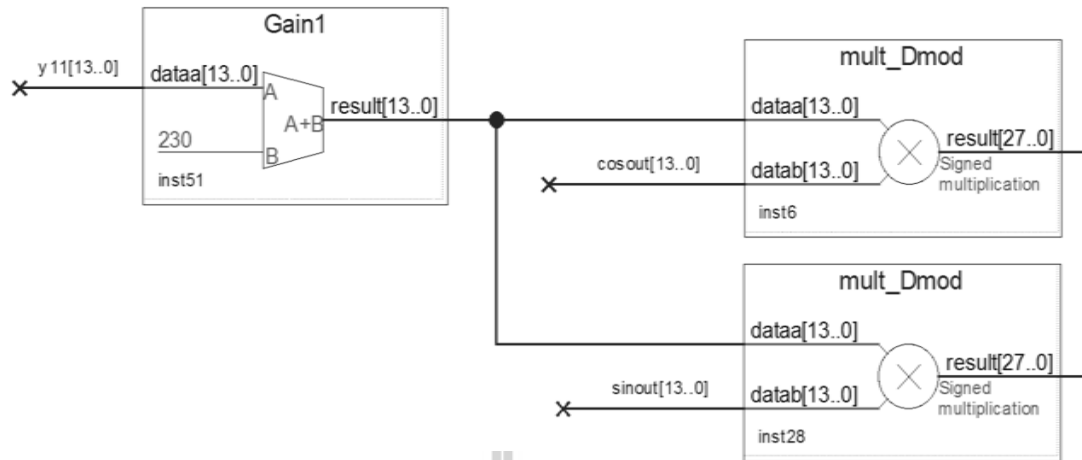
Figure 6.7 IF demodulator.

Figure 6.8 Low pass filter.

6.6.1 Channel Estimation

Initially, the pilot signals are generated by the symbol generator at the transmitter. The symbol patterns of pilot signals are already known at the receiver as well as the received signals.Therefore all sub-channels of MIMO channel can be

estimated by calculating from the pilot signals and the received signals by $\hat{h}_{ij} = y_i x_j^{-1}$, where $\hat{h}_{ij}$ denotes the estimated channel between transmit antenna i and receive antenna j, y_i denotes the received signal at receive antenna i and x_j denotes the pilot signal at transmit antenna j.

6.6.2 Hybrid-MIMO Receiver Scheme Detection

The estimated MIMO channel from 6.5.1 can be used to detect the transmitted symbols for all users in HMRS systems. After the channel estimation period, all streams from all users are transmitted to the receiver in the same time. The transmitted symbol from the transmitting side can be detected according to the processes in Table 4.1. Then the detected symbols of all users and the original transmitted symbols at transmitting side are compared to calculate the BER performances.
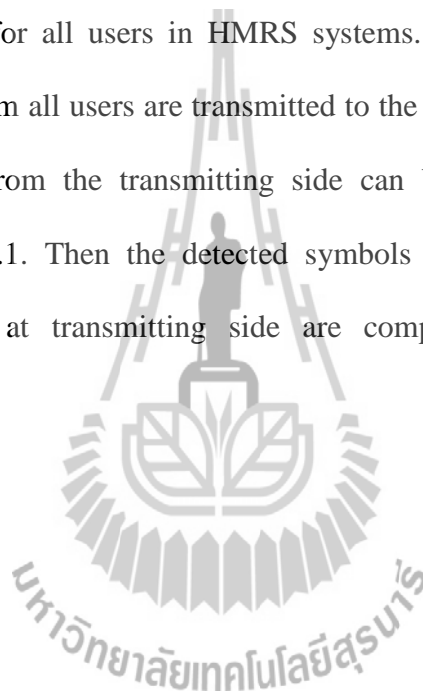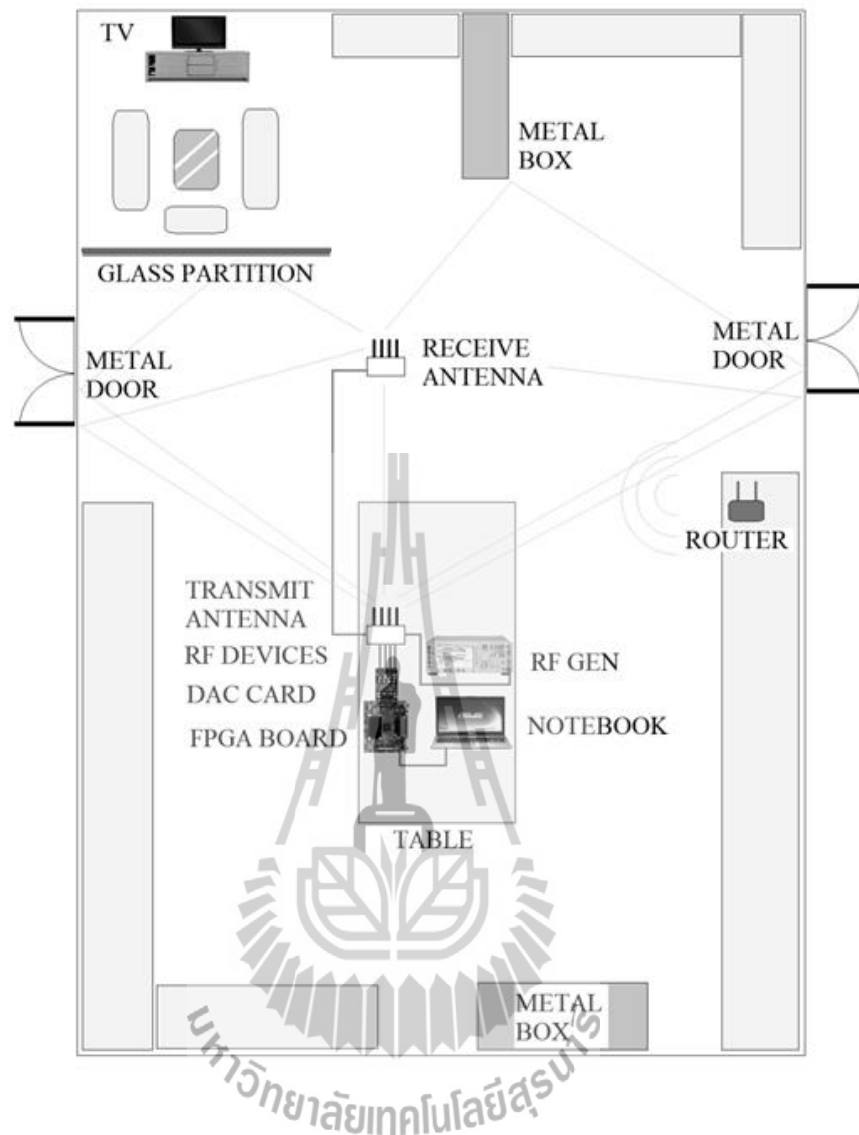
Figure 6.9 Experimental scenarios in F4 building.

6.7   Experimental Scenarios

This experiment operates in the rich scattering environment at F4 building in Suranaree University of Technology.The performances of HMRS and V-BLAST scheme are measured in the three locations to validate and average the practical

(6.10-a) The first location for experiment.

(6.10-b) The second location for experiment.

(6.10-c) The third location for experiment.

Figure 6.10 Photograph of the experiment areas in F4 building.
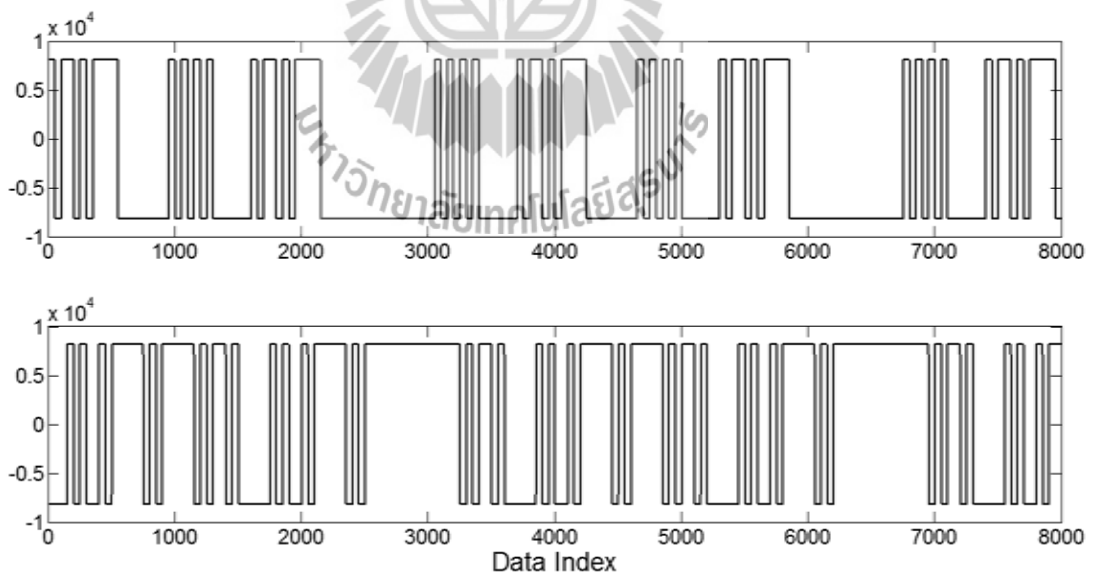
Figure 6.11 Transmitted data at the first transmit antenna.

performances of both schemes. All parameters in experiment are similarly specified for three locations in Figure 6.10 to validate the HMRS performances under the different scenarios. The signal streams from four transmit antennas are transmittedwith the effect of scattering as shown in Figure 6.9 and 6.10. This work applies 2.5 GHz carrier signal for up and down converter to mitigate the effect of interference signals from WLAN networks while the parameters in experiment are assigned asin Table 6.3.

6.8   Experimental Signals

The transmitted bit streams are randomly generated by mathematical function in FPGA chip as shown in Figure 6.11 and 6.12. Each orthogonal bit stream is modulated with IF signals and mixed with the RF signal. The transmitted signal at the transmit antenna can be demonstrated in Figure 6.13. This figure shows that the transmitted signal is repeatedly generated by the same pattern in every period.

In this thesis, the estimated MIMO channel is estimated according to the method in Section 6.5.1. The static channel gain in the experiment area is usually offered thus the average channel gains can be used as shown in Figure 6.14. The figure shows that the different channel gain is offered due to the different scenario of each path.

Table 6.3 The experimental parameters.

Item	Detail
FPGA	Altera/Cyclone III EP3C120F7807N
DAC card	2 SMA input port/2 SMA output port
RF Generator	2.5 GHz/Transmitted power 0-18 dBm
Data rate	1Mbps
IF frequency	5MHz
Sampling frequency	100MHz
Channels	Rich scattering environment
Modulation	QPSK
Link distance	5 meters
Number of user	2
Number of transmit antenna/user	2
Number of receive antenna	4

To prove the benefit of HMRS system, the experimental BER performances and the analytical BER performances are compared to verify the advantage of HMRS systems in real practical channel. Figure 6.16 to Figure 6.19 present the experimentalBER performance when varying the transmitted power. The BER performances between analytical results and practical results are not agreed when considering the horizontal and vertical axis. Because the different properties between real channel and analysed channel such as signal reflection, the scattered object and the interference sources. Moreover, from the reasons in Section 6.4.4, the trend of BER curves of the experiment and the theory are used to validate the advantage of the HMRS system.
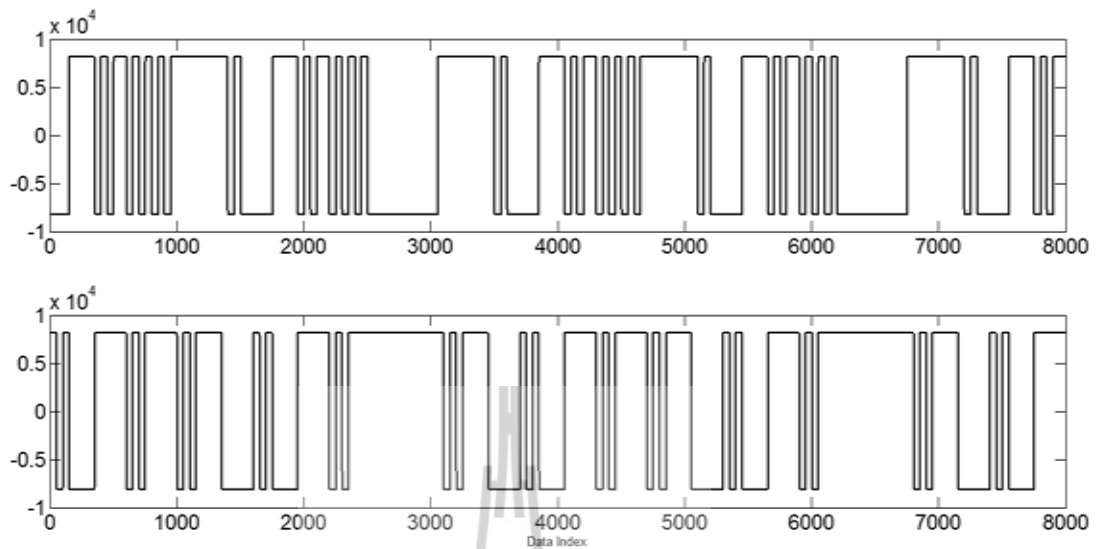
Figure 6.12 Transmitted data at the second transmit antenna.
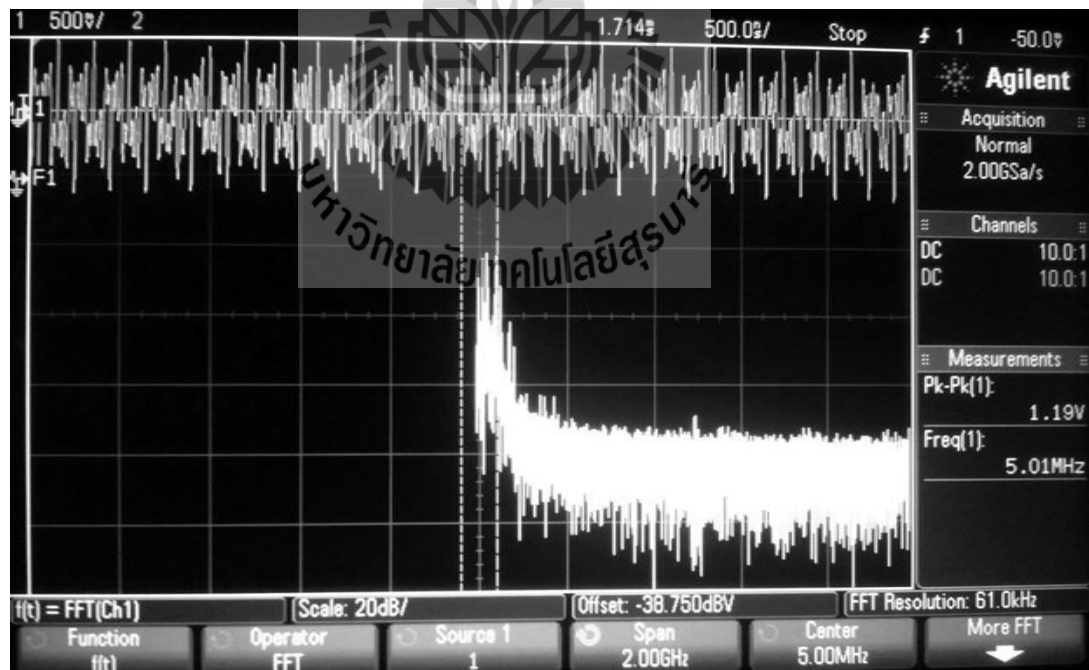
Figure 6.13 Transmitted signal at the AD/DA conversion card.
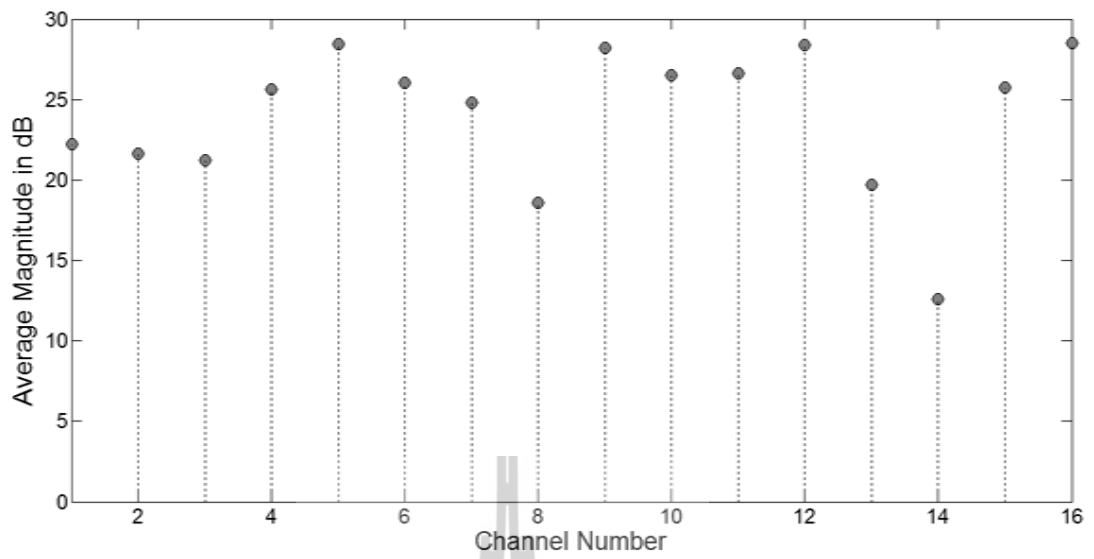
Figure 6.14 Average channels gain.
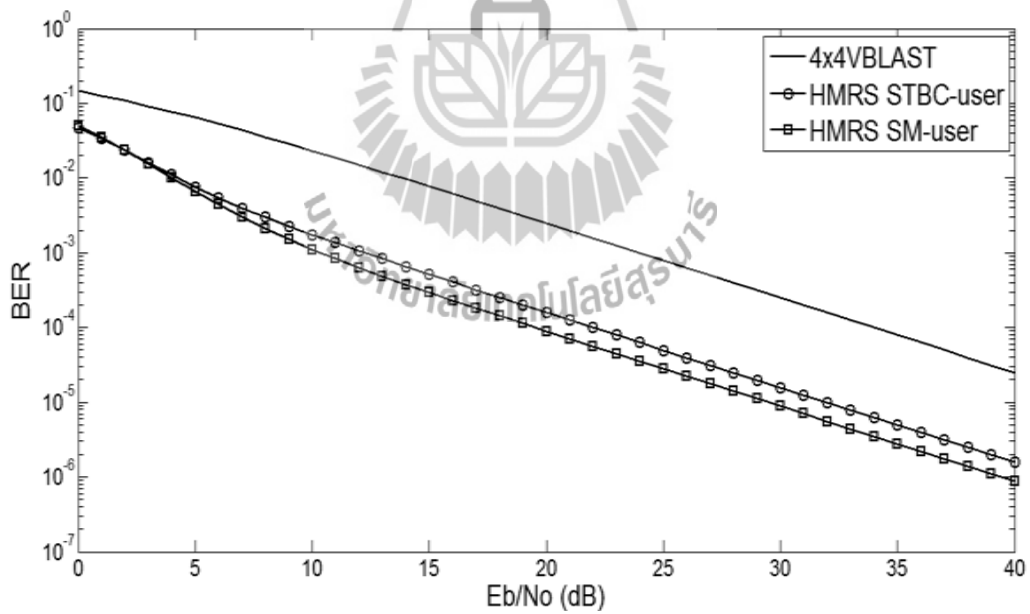
Figure 6.15 The analytical BER performances.
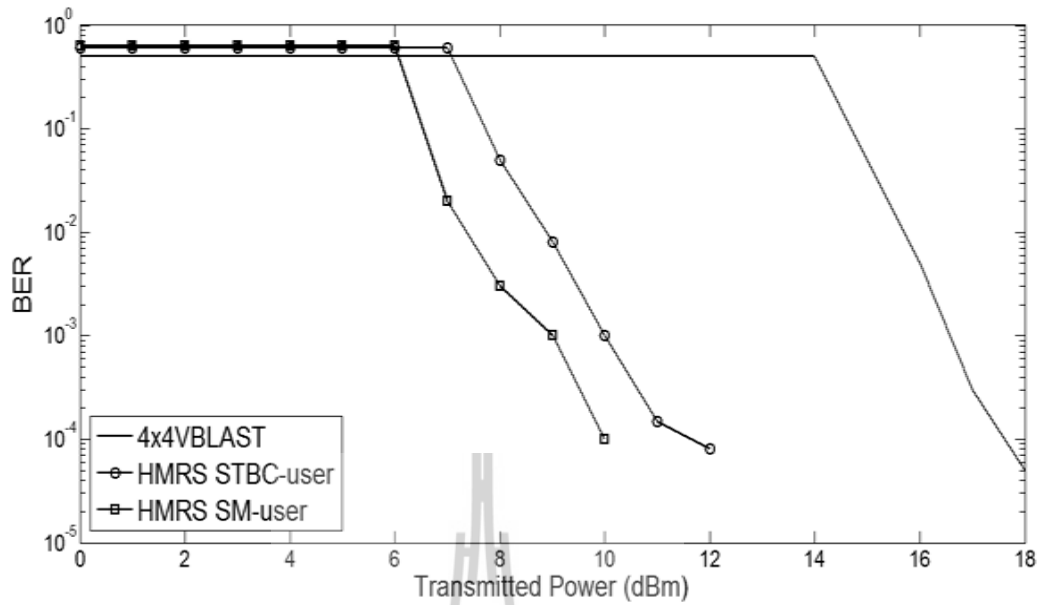
Figure 6.16 The experimental BER performances at the first location with 5 meters
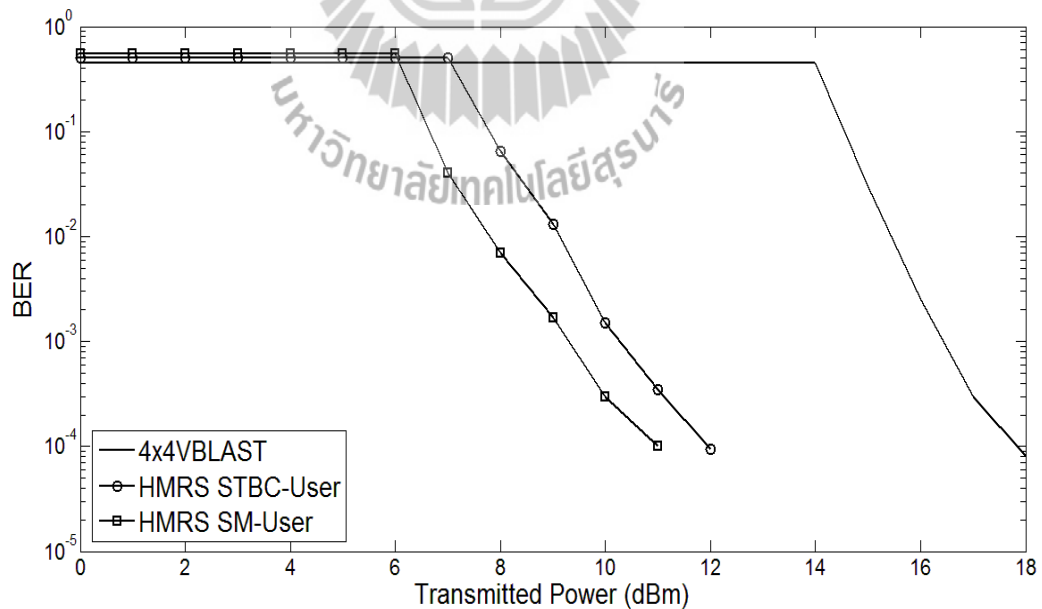
link distance.

Figure 6.17 The experimental BER performances at the second location with 5 meters
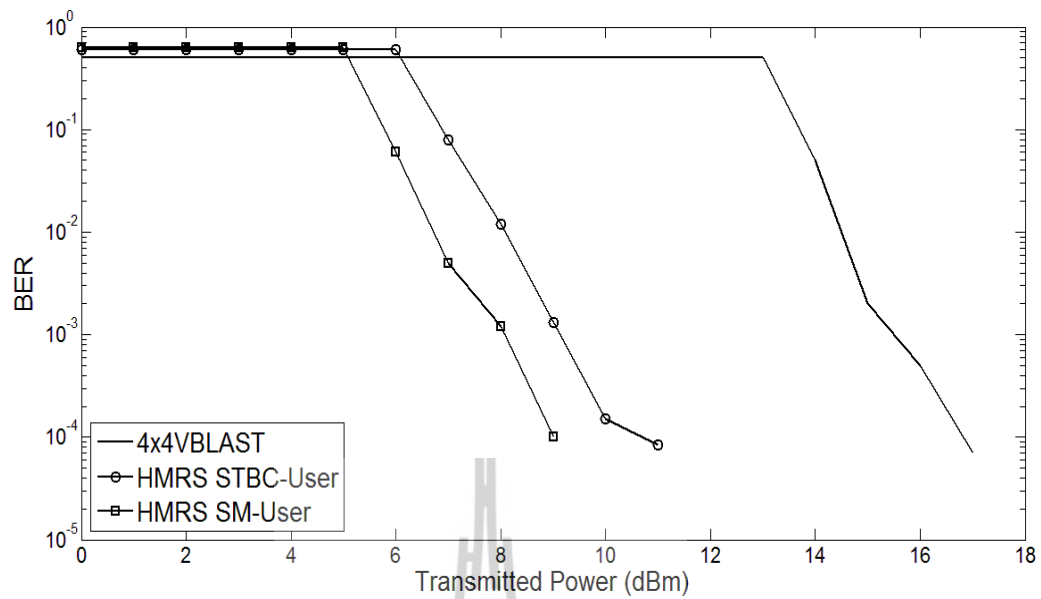
link distance.

Figure 6.18 The experimental BER performances at the third location with 5 meters
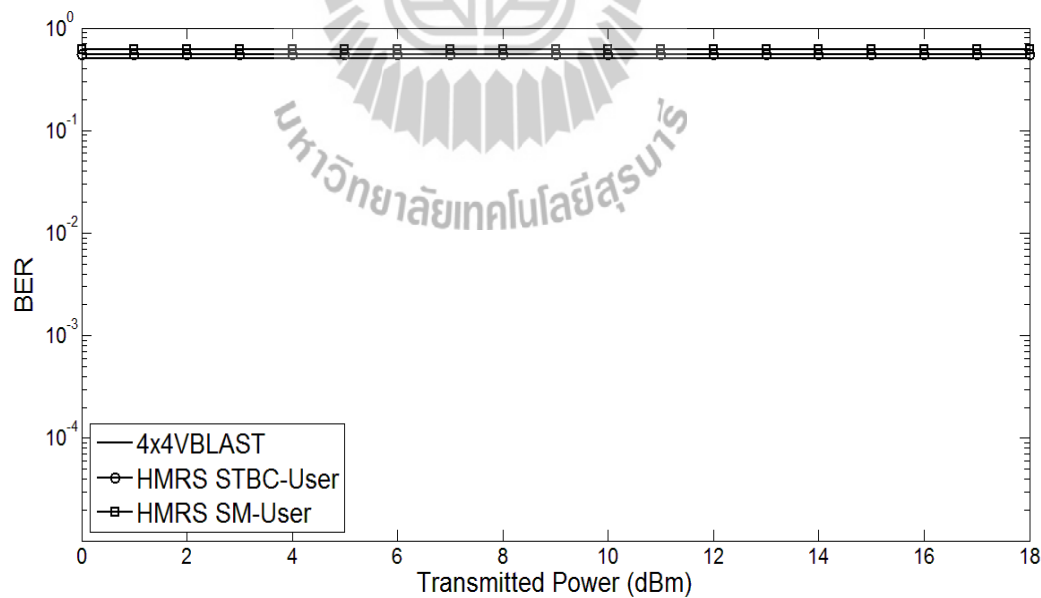
link distance.

Figure 6.19 The experimental BER performances at the first location with 7 meters

link distance.

Figure 6.15 shows the analytical BER performances of V-BLAST and each user of the proposed method. The results show that the SM user of HMRS offers best performance than STBC user of HMRS and V-BLAST system.

Figure 6.16, 6.17 and 6.18 present the experimental BER performances of V-BLAST and each user of the proposed method with 5 meters link distance. The results show that the almost similar BER performances of three locations in Figure 6.10 are offered. This means that the proposed technique still offers the higher advantage than V-BLAST scheme in different locations. Meanwhile SM user of HMRS always offers higher performance than V-BLAST about 7dB at 10^{-4}BER.

Figure 6.19 demonstrates the experimental BER performances of V-BLAST and each user of the proposed method with 7 meters link distance. The results show that all BER curves do not vary at any transmitted power. This means that this HMRS testbed cannot detect data streams by 7 meters link distance but up to 5 meters.

From Figure 6.15 and 6.16, the different powerbetween SM user of HMRS and V-BLAST in analysis and simulation at 10^{-4}BER is 7dB and 12dB, respectively.

By considering the BER performances of analysis and experiment in three locations, the trends of all curves from the experiment in Figure 6.16 to 6.18 arecorresponded to the analytical BER performances in Figure 6.15. From the results, this comparison can confirm the advantage of HMRS in practice.

CHAPTER VII

DISCUSSIONS AND CONCLUSIONS

This thesis proposes the improved hybrid MIMO system, namely, hybrid MIMO Receiver Scheme (HMRS) to efficiently apply in Cognitive Radio Network (CRN). This technique adopts SM detection, STBC code and SIC to cancel interference of other users before detecting the transmitted symbols of SM users and STBC users. The interference in the received signals of HMRS are cancelled before detecting the first data stream to improve the performance of hybrid MIMO while this criteria is not presented by the existing hybrid MIMO systems.

The simulation results from Monte Carlo simulation are demonstrated to reveal the advantage of HMRS against the existing hybrid MIMO systems and the conventional MIMO scheme. Besides, the analytical BER performances are derived in the presence of EP and CEE to verify the validity of simulation results and confirmed the benefits of the proposed technique in the practical scenarios.

The simulation results show that the SER performances of HMRS outperform the existing hybrid MIMO systems as well as the conventional MIMO technique. The channel capacity of the proposed scheme can be offered higher than double user STBC code and slightly approximated to VBLAST receiver. Moreover the Cost-index performance that compromise between SER and channel capacity is proposed to alternatively demonstrates the advantage of HMRS against other techniques.

As the derivation of analytical BER performances, the number of user and the accuracy of channel estimation are varied in the presence of EP and CEE to reveal the HMRS performances in the practical environment. The results show that the effect of EP and CEE can be violently affected to the performance of HMRS. Thus it should be carefully considered these parameters to design the real networks.

This thesis also implements HMRS testbed to confirm the advantage of the proposed technique. The transmitted symbols are generated by FPGA board and AD/DA data conversion card. The transmitted streams are sent over the rich scattering MIMO channels while the received signals from FPGA board can be decoded by transferring data into Matlab program to determine the HMRS performances. The results show that the trends of all BER curves between analysis and the experimental results are well corresponded.

REFERENCES

Ahn, K. S., Heath, R.W. andBaik, H.K. (2008).Shannon capacity and symbol error rate of space-time block codes in MIMO Rayleigh channels with channel estimation error.**IEEE Transaction on Wireless Communications**.**7**(1): 324-333.

Alamouti, S.M. (1998). A simple transmit diversity technique for wireless communication. **IEEE Journal on Selected Areas in Communications**.16(8): 1451-1458.

Alian, E.H. M. and Mitran, P. (2012).Interference mitigation in MIMO-OFDM cognitive radio systems using phase rotation.**In Proceedings of the Wireless Communications and Networking Conference** (pp. 652-657).Paris, France: IEEE.

Bai, Z., Berkmann, J., Spiegel, C., Scholand, T., Bruck, G.H., Drewes, C., Gunzelmann, B. and Jung, P. (2008).OnMIMOwithsuccessiveinterferencecancellationappliedtoUTRALTE. **In Proceedings of the 3rd International Symposium on Communications, Control and Signal Processing** (pp. 1009-1013). Malta: IEEE.

Biglieri, E., Taricco, G. and Tulino, A. (2002).Decoding space-time codes with BLAST architechtures.**IEEE Transaction on Signal Processing**.50(10): 2547-2552.

Cho, K. and Yoon, D. (2002).On the general BER expression of one- and two-dimensional amplitude modulations.**IEEE Transaction on Communication**.50(7): 1074-1080.

Chun, Y. and Kim, S. (2008). Log-likelihood-ratioorderedsuccessive interferencecancellationinmulti-user, multi-modeMIMOsystems.**IEEECommunications Letters**.12(11): 837-839.

Cortez,J., Bazdresch,M., Torres D.and Parra-MichelR. (2008). ABBA- VBLAST hybrid space-time code for MIMO wireless communications. **In Proceedings of the 5th International Conference on Electrical Engineering, Computing Science and Automatic Control** (pp. 257-262). Mexico: IEEE.

Driouch, E. and Ajib, W. (2012).Greedy spectrum sharing for cognitive MIMO network.**In Proceedings of International Conference on Communications and Information Technology**(pp. 139-143). Tunisia: IEEE.

Foschini, G. J. (1996). Layered space-time architecture for wireless communications in a fading environment when using multiple antennas.**Bell Labs Technical Journal**. 1(2): 41-59.

Freitas, W. C.,Francisco, R. P. and Renato, R. L. (2005). Hybrid transceiver schemes for spatial multiplexing and diversity in MIMO systems.**Journal of Communication and Information systems**. 20(3): 63-76.

Gans, M.J. (1971). The effect of Gaussian error in maximal ratio combiners.**IEEE Transaction on Communication Technology**. 19(4): 492-500.

Goldsmith, A. (2005). **Wireless Communications**.Cambridge: CUP.

Hassibi, B. andHochwald, B.M. (2003).How much training is needed in multiple-antenna wireless links?.**IEEE Transaction on Information Theory**. 49(4): 951-963.

Haykin, S. (2005).Cognitive radio: brain-empowered wireless communications.**IEEE Journal on Selected Areas in Communications**. 23: 201-220.

Honglian S. (2011).**Collaborative Spectrum Sensing in Cognitive Radio Networks**.Ph.D. Thesis, University of Edinburgh, Scotland.

Kim, K. and HyuncheolP. (2009).Modifiedsuccessiveinterference cancellationforMIMOOFDMondoublyselectivechannels.**In Proceedings of the Vehicular Technology Conference** (pp. 1-5). Barcelona, Spain: IEEE.

Maaref, A. andAïssa, S. (2005). Capacity of space-time block codes in MIMO Rayleigh fading channels with adaptive transmission and estimation errors. **IEEE Transaction on Wireless Communications**. 4(5): 2568-2578.

Mao, J.,GaoJ., Liu Y.,Xie,G. and Xiuwen L. (2012). Power allocation over fading cognitive MIMO channels: an ergodic capacity perspective.**IEEE Transactions on Vehicular Technology**.61(3): 1162-1173.

Marzetta, T.L. (1999). BLAST training: estimating channel characteristics for high-capacity space-time wireless. **In Proceedings of the 37th Annual Allerton Conference Communications, Control, and Computing**(pp. 958-966). USA: IEEE.

McHenry, M. A. (2005). NSF spectrum occupancy measurements project summary.Technical Report. USA: Shared spectrum company.

Ming. L., Ryuhei, F., Hiroshi, H. and Shuzo, K. (2007). High data-rate DPC-OF/TDMA based on multi-layer STBC coded MIMO OFDM. **In Proceedings**

of the Wireless Communications and Networking Conference (pp. 938-942). Hong Kong, China: IEEE.

Mitola, J. (2000), **Cognitive Radio: An Integrated Agent Architecture for Software Defined Radio**. Ph.D. thesis, Royal Institute of Technology Stockholm, Sweden.

Mohd, H., Bin,H., David,C. andHeng,T. (2004). Adaptive MIMO-OFDM combining space-time block codes and spatial multiplexing**. In Proceedings ofthe International Symposium on Spread Spectrum Techniques and Applications** (pp. 444-448). Sydney, Australia: IEEE.

Prasad, N. and Varanasi, M. (2001).Optimum efficiently decodable layered space-time block codes. **In Proceedings of the 35[th]AsilomarConference on Signals, Systems and Computers**(pp. 227-231). USA: IEEE.

Proakis, J. G. (2001), **Digital Communications**, New York: McGraw-Hill.

Roy, S. and Fortier, P. (2004). Maximal-ratio combining architectures and performance with channel estimation based on a training sequence. **IEEE Transaction on Wireless Communication**. 3(4): 1154-1164.

Shen, C., Zhu, Y. and Jiang, J. (2004).On the performance of V-BLAST with zero-forcing successive interference cancellation receiver.**In Proceedings of the Global Telecommunication Conference**(pp. 2818-2822), USA: IEEE.

Song,Y.,Seong, K., Hyun, P., Hun, L. and Hyoung, S. (2010). A novel efficient detection scheme for hybrid STBC in MIMO-OFDM systems.**In Proceedings of the 12th IEEE International Conference on Communication and Technology**(pp. 701-704). Nanjing, China: IEEE.

Steffen, R., Tufik, B. and Mario H. (2006).Successive interference cancellation for SC/FDE-MIMO system. **In Proceedings of the IEEE International Symposium on Personal, Indoor & Mobile Radio Communications**(pp. 1-5). Helsinki, Finland: IEEE.

Tan,C. W. and Calderbank,A. R. (2009). Multiuser detection of Alamouti signals. **IEEE Transactions on Communications**, 57(7): 2080-2089.

Tarokh, V.,Jafarkhani,H. and Calderbank,A. R. (1999).Space-time block codes from orthogonal designs.**IEEE Transactions on Information Theory**. 5: 1456–1467.

Tomiuk, B.R., Beaulieu, N. C. and Abu-Dayya, A.A. (1999).General forms for maximal ratio diversity with weighting error. **IEEE Transactions on Communications**. 47(4): 488-492.

Wang, C., Edward, K.S., Murch, R.D., Mow, W.H., Cheng, R. S. and Lau, V. (2007).On the performance of the MIMO zero-forcing receiver in the presence of channel estimation error.**IEEE Transactions on Wireless Communications**. 6(3): 805-810.

Winters, J. H., Salz, J. andGitlin, R.D. (1992).The capacity increase of wireless communication systems with antenna diversity.**In Proceedings of the Conference Information Sciences Systems** (pp. 1-5). USA: IEEE.

Winters, J. H., Salz, J. andGitlin, R.D. (1994).The impact of antenna diversity on the capacity of wireless communication systems.**IEEE Transactions on Communication**. 42(2/3/4): 1740-1751.

Yong, S. C., Jaekwon, K. and Won, Y. Y. (2012).**MIMO-OFDM Wireless Communications with Matlab**.John Wiley & Sons (Asia) Pte Ltd.

Zanella, A., Chiani, M. and Win, M.Z. (2005).MMSE reception and successive interference cancellation for MIMO systems with high spectral efficiency.**IEEE Transactions on Wireless Communications**. 4(3): 1244-1253.

Zijian, B., Berkmann, J., Spiegel, C., Scholand, T., Bruck, G.H., Drewes, C., Gunzelmann, B. and Jung, P. (2008).OnMIMOwithsuccessiveinterferencecancellationappliedtoUTRALTE. **In Proceedings of the 3ʳᵈ International Symposium on Communication, Control and Signal Processing**(pp. 1009-1013). Malta: IEEE.
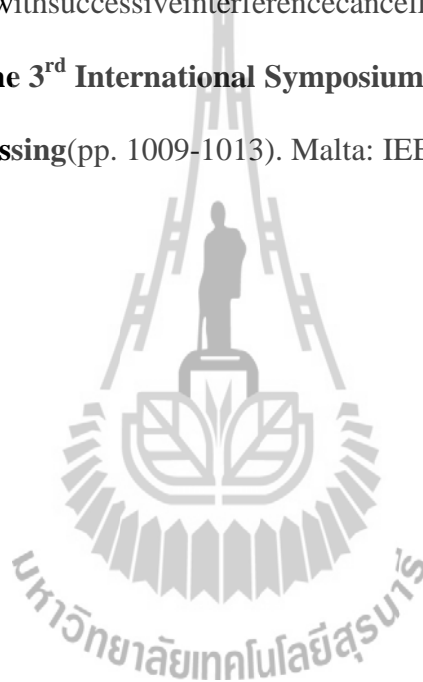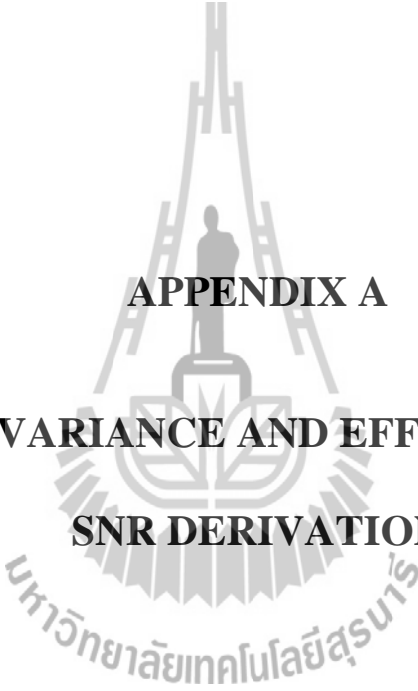
APPENDIX A

COVARIANCE AND EFFECTIVE

SNR DERIVATION

In this appendix, the author derives the covariance of the effective post-processing noise for ZF detection and STBC decoding in the presence of CEE and EP, and derive the effective SNR per symbol after STBC decoding.

A-I Covariance of the effective post-processing noise for ZF detection

$$E[\widehat{\boldsymbol{w}}\widehat{\boldsymbol{w}}^H] = E\big[\big(\boldsymbol{H}_z^{\dagger}\boldsymbol{w} - \tau\boldsymbol{H}_z^{\dagger}\boldsymbol{\varphi s_z} - \tau\boldsymbol{H}_z^{\dagger}\boldsymbol{\varphi H}_z^{\dagger}\boldsymbol{w} + N_a\Delta\boldsymbol{H}_z^{\dagger}\boldsymbol{H}_p - \tau N_a\Delta\boldsymbol{H}_z^{\dagger}\boldsymbol{\varphi H}_z^{\dagger}\boldsymbol{H}_p\big)$$

$$\big(\boldsymbol{H}_z^{\dagger}\boldsymbol{w} - \tau\boldsymbol{H}_z^{\dagger}\boldsymbol{\varphi s_z} - \tau\boldsymbol{H}_z^{\dagger}\boldsymbol{\varphi H}_z^{\dagger}\boldsymbol{w} + N_a\Delta\boldsymbol{H}_z^{\dagger}\boldsymbol{H}_p - \tau N_a\Delta\boldsymbol{H}_z^{\dagger}\boldsymbol{\varphi H}_z^{\dagger}\boldsymbol{H}_p\big)^H\big]$$

$$= E\big[N_0\boldsymbol{H}_z^{\dagger}\big(\boldsymbol{H}_z^{\dagger}\big)^H + \tau^2\boldsymbol{H}_z^{\dagger}\big(\boldsymbol{H}_z^{\dagger}\big)^H\boldsymbol{\varphi\varphi}^H E_s + \tau^2 N_0\boldsymbol{H}_z^{\dagger}\big(\boldsymbol{H}_z^{\dagger}\big)^H\boldsymbol{\varphi\varphi}^H\boldsymbol{H}_z^{\dagger}\big(\boldsymbol{H}_z^{\dagger}\big)^H$$

$$+ \tau^2 N_a\Delta\boldsymbol{H}_z^{\dagger}\big(\boldsymbol{H}_z^{\dagger}\big)^H\boldsymbol{s}_z\boldsymbol{\varphi\varphi}^H\big(\boldsymbol{H}_z^{\dagger}\big)^H\boldsymbol{H}_p^H + N_a^2\Delta^2\boldsymbol{H}_z^{\dagger}\big(\boldsymbol{H}_z^{\dagger}\big)^H\boldsymbol{H}_p^H\boldsymbol{H}_p$$

$$+ \tau^2 N_a\Delta\boldsymbol{H}_z^{\dagger}\big(\boldsymbol{H}_z^{\dagger}\big)^H\boldsymbol{\varphi\varphi}^H\boldsymbol{H}_z^{\dagger}\boldsymbol{H}_p\boldsymbol{s}_z^H + \tau^2 N_a^2\Delta^2\boldsymbol{H}_z^{\dagger}\big(\boldsymbol{H}_z^{\dagger}\big)^H\boldsymbol{\varphi\varphi}^H\boldsymbol{H}_z^{\dagger}\big(\boldsymbol{H}_z^{\dagger}\big)^H\boldsymbol{H}_p^H\boldsymbol{H}_p\big]$$

$$= (N_0 + \tau^2 N_t E_s + \tau^2 N_0 t_r((\boldsymbol{H}_z^H\boldsymbol{H}_z)^{-1})$$

$$+ \tau^2 N_a\Delta\boldsymbol{s}_z t_r((\boldsymbol{H}_z^H\boldsymbol{H}_z)^{-1})\boldsymbol{H}_p^H\big(\boldsymbol{H}_z^{\dagger}\big)^{-1} + N_a^2\Delta^2 M$$

$$+ \tau^2 N_a\Delta\boldsymbol{s}_z^H t_r((\boldsymbol{H}_z^H\boldsymbol{H}_z)^{-1})\boldsymbol{H}_p\big(\big(\boldsymbol{H}_z^{\dagger}\big)^H\big)^{-1}$$

$$+ \tau^2 N_a^2\Delta^2 M t_r((\boldsymbol{H}_z^H\boldsymbol{H}_z)^{-1}))(\boldsymbol{H}_z^H\boldsymbol{H}_z)^{-1}$$

where we permute the matrixes by various relations as follows: $\boldsymbol{H}_z^{\dagger}\big(\boldsymbol{H}_z^{\dagger}\big)^H = (\boldsymbol{H}_z^H\boldsymbol{H}_z)^{-1}$, $E[\boldsymbol{s}_z\boldsymbol{s}_z^H] = E_s\boldsymbol{I}_{N_t}$, $E[\boldsymbol{w}\boldsymbol{w}^H] = N_0\boldsymbol{I}_{N_r}$, $E[\boldsymbol{\varphi\varphi}^H] = N_t\boldsymbol{I}_{N_r}$

and $E[\boldsymbol{\varphi}(\boldsymbol{H}_z^H\boldsymbol{H}_z)^{-1}\boldsymbol{\varphi}^H] = t_r((\boldsymbol{H}_z^H\boldsymbol{H}_z)^{-1})\boldsymbol{I}_{N_r}$.

A-IICovariance of the effective post-processing noise for STBC decoding

$$E[\widehat{w}_p \widehat{w}_p{}^*] = E\left[\left(\sum_{j=1}^{2}\sum_{i=1}^{M} h_{ij}\right)\left(\sum_{j=1}^{2}\sum_{i=1}^{M} h_{ij}\right)^*\right]E[w'w'^*]$$

$$\cong \left\|\boldsymbol{H}_{s,i}\right\|_F^2 E[w'w'^*]$$

$$\cong \left\|\boldsymbol{H}_{s,i}\right\|_F^2 E\left[\left(\left(\sum_{l=1}^{N_a} h_{kl}|x-\hat{x}|\right)+w\right)\left(\left(\sum_{l=1}^{N_a} h_{kl}|x-\hat{x}|\right)+w\right)^*\right]$$

$$\cong \left\|\boldsymbol{H}_{s,i}\right\|_F^2 \left\{E\left[|x-\hat{x}|^2 \sum_{l=1}^{N_a}|h_{kl}|^2\right]+E[ww^*]\right\}$$

$$\cong \left\|\boldsymbol{H}_{s,i}\right\|_F^2 (N_0 + N_a\Delta^2)$$

A-III Effective SNR per symbol after STBC decoding

$$\gamma_a = \frac{E\left[\left(\left\|\boldsymbol{H}_{s,i}\right\|_F^2 x\right)\left(\left\|\boldsymbol{H}_{s,i}\right\|_F^2 x\right)^*\right]}{E[\widehat{w}_p \widehat{w}_p^*]} = \frac{\left\|\boldsymbol{H}_{s,i}\right\|_F^4 E_s}{\left\|\boldsymbol{H}_{s,i}\right\|_F^2 (N_0 + N_a\Delta^2)}$$

$$= \frac{\left\|\boldsymbol{H}_{s,i}\right\|_F^2}{2(1/\bar{\gamma} + N_a d_{EP}/2)}$$

APPENDIX B

PUBLICATIONS

List of Publications

International Journal Paper

Khomyat, T., Uthansakul, P. and Uthansakul, M. (2014).Performance Analysis of MU-MIMO Systems Using HMRS Technique for Various Transmission Modes.**ECTI Transactions on Electrical Engineering, Electronics, and Communication (ECTI-EEC Trans)**.12(1): 53-62. (Scopus Indexing)

Khomyat, T., Uthansakul, P., Uthansakul, M. and Soong, B.H. (2014).On the Performance of the ZF_STBC MIMO Receiver with Channel Estimation Error and Error Propagation.**The Institution of Engineering and Technology (IET) Communication**. 8(18): 3381-3392. (ISI Impact factor 0.72)

International Conference Paper

Khomyat, T., Uthansakul, P. and Uthansakul, M. (2011).Hybrid-MIMO Receiver with Both Space-Time Coding and Spatial Multiplexing Detections for Cognitive Radio Networks.**International Symposium on Intelligent Signal Processing and Communication Systems (ISPACS)**.

Khomyat, T., Uthansakul, P. and Uthansakul, M. (2012).Performance of Hybrid-MIMO Receiver Scheme in Cognitive Radio Network.**International Conference on Mobile, Ubiquitous and Pervasive Computing (ICMUPC)**.

Khomyat, T., Uthansakul, P. and Uthansakul, M. (2013).Performance of MU-MIMO Systems Using HMRS Technique for Various Transmission Modes.**International Conference on Electrical Engineering/Electronics, Computer, Telecommunications and Information Technology (ECTI-CON)**.

Khomyat, T., Uthansakul, P., Uthansakul, M. and Soong, B. H. (2014).Switching Transmission Mode in Multiuser-MIMO Systems.**Asia-Pacific Conference on Communications (APCC)**.

National Conference Paper

Khomyat, T., Uthansakul, P. and Uthansakul, M. (2013).Effect of User Mobility in Hybrid MIMO System on Number of Users of Cognitive Radio Networks.**Conference on Application Research and Development (ECTI-CARD)**.

Performance Analysis of MU-MIMO Systems Using HMRS Technique for Various Transmission Modes

Tanapong Khomyat[*1],

Peerapong Uthansakul[*2], and **Monthippa Uthansakul**[*3], Non-members

ABSTRACT

It is the fact that the bandwidth of wireless communication system is such a limited resource that several techniques are selectively applied to increase the bandwidth efficiency. The highest bandwidth efficiency can be taken by applying Multi-User Multiple-Input Multiple-Output (MU-MIMO) technique. For this technique, the complexity of detection is rapidly increased by increasing the number of users. Thus the lower complex detection is necessarily required for MU-MIMO system. Recently, the simple detection technique called hybrid-MIMO receiver scheme (HMRS) has been proposed by the authors. However, that study neglected the demands of multiple users for transmitting MIMO modes which are crucially unpredictable in practice. In this paper, the performance analysis of MU-MIMO system using HMRS technique to support various types of user transmission modes is presented. Moreover, the nearly exact symbol error rate (SER) analysis of HMRS with the nonlinear error propagation effect over Rayleigh channels is originally presented. The recursive procedure is adopted to derive the nearly closed-form expressions of the error probability of each user. The results indicate that HMRS technique can improve the error rate more than the existing hybrid-MIMO about 8 dB at 10^{-4} SER, increasing the total number of user and number of SM user introduce the diversity gain loss. The simulation results illustrate the performance accuracy of the proposed analysis.

Keywords: Multiple-Input Multiple-Output (MIMO), Maximum Likelihood Detection (MLD), Successive Interference Cancellation (SIC), Space-time Block Code (STBC), Symbol Error Rate (SER).

1. INTRODUCTION

Wireless communications are widely used around the world. The new applications have been frequently established such as WLAN, 3GB, LTE, etc. Many customers need to access the limited spectrum in the same time. Therefore the available bandwidth cannot be enough for every user [1]. The saving bandwidth techniques for wireless communication have been researched and already applied such as TDMA, CDMA, MIMO [2-4], hybrid-MIMO [5-7], MU-MIMO [8], etc. Fig. 1 illustrates the basic structure of MU-MIMO system. The transmitted signals from N users are sent through MIMO channel and reached to the receiver in the same time and frequency to achieve a high bandwidth efficiency, to increase a capacity gain and to keep a benefit of diversity gain. The receiver must have capability to suppress interference and detect all symbols from all users by using multi-user detections such as QR decomposition [9], ZF detection, MMSE detection [10], ML detection [11], Sphere detection [12], IC [13], etc. In 2005, the simple hybrid-MIMO technique called Hybrid-MIMO Transceiver Scheme (HMTS) [14] has been proposed. The two users at transmitting side can select either Space-Time Block Code (STBC) or Spatial Multiplexing (SM) to encode the transmitted signals. It has a simple structure when a few users are operated in the system because MMSE detection and Successive Interference Cancellation (SIC) [15] are jointly applied. However, the complexity of detection at receiver is increased when a lot of users are operated because the MMSE detection and SIC are operated every time of detecting SM layer. Recently, the authors proposed the novel hybrid-MIMO technique called Hybrid-MIMO Receiver Scheme (HMRS) [16] that the system applies ML detection and SIC jointly to detect all symbols in entire layers. The ML detection is operated only one time for every case of N users, thus this scheme has the number of detecting procedures less than HMTS. The comparison of SER performance between HMRS and HMTS is presented in Section IV. However, the work in [16] did not study on the various types of user demand on MIMO transmission modes. In fact, the user demand cannot be predicted and this deviate the system performance from results presented in [16]. Hence, this paper has concerned this issue and proposes the performance analysis to investigate the effect of various MU-MIMO transmission modes.

In literature, the performance analysis of MLD over fading channel is presented in [17-21]. In [22-26],
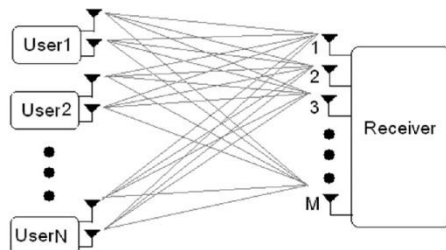
Fig.1: *MU-MIMO system.*

the closed-form expression of symbol error probability is derived for orthogonal space-time block coded (OSTBC) MIMO Rayleigh fading channels with arbitrary number of transmit and receive antennas. The successive procedure of error rate analysis for zero-forcing successive interference cancellation (ZF-SIC) is obviously described in [27] and [28]. However, so far in literature the performance analysis of hybrid-MIMO scheme has never been proposed.

In this paper, the authors investigate the SER performances of HMRS in case of N users, where N can be assigned as 2, 3 and 4, in order to study the effect of the various transmission modes. Because the several users may be randomly operated in practice, thus the evaluation of SER performance under this situation is an important task. The performance analysis of symbol error rate for HMRS hybrid-MIMO systems is also derived. From the above analyzing results, the readers can utilize it on the design of the proper transmitting parameters keenly including the transmitting power, antenna gain, modulation scheme, channel coding scheme and the number of antennas. Moreover, the transmitted signal, the received signal and the structure of N users using HMRS are presented in this work in order to reveal the procedure of the HMRS system.

The remainder of this paper is structured as follows. In section 2, the authors present the system model. Then the analysis of symbol error rate for MLD and STBC systems is described in section 3. The performance analysis of HMRS is explained in section 4. The numerical results and discussion are presented in section 5 and followed by the conclusions in section 6.

2. SYSTEM MODEL

The structure of MU-MIMO system is shown in Fig. 1. All MIMO streams are simultaneously transmitted by N users. Each user equipped with a 2-element antenna array and applies either 2×M STBC or 2×M SM system. The receiver equipped with an M-element antenna array. The transmitted signal vector s is sent through a random channel matrix $\mathbf{H}$ in uplink channel. Flat and slow Rayleigh fading is

assumed to evaluate the SER performance. The receiver can detect all symbols from all users by using MU detection. The received signals can be expressed as

$$\mathbf{y}=\mathbf{H}\mathbf{s}+\mathbf{w} \tag{1}$$

where $\mathbf{y}$ is the vector of received signals, $\mathbf{H}$ is $M \times 2N$ MIMO channel matrix, s represents the $2N \times 1$ transmitted signal vector consisted of $2N$ BPSK symbols with a constellation size of C and average symbol energy E_0 ($E_0 = E_s/2N$) and the M elements of vector $\mathbf{w}$ are samples of independent complex additive white Gaussian noise (AWGN) processes with single-sided power spectral density σ_ω^2. The channel matrix $\mathbf{H}$ is assumed to have a unit variance that can be described as

$$E[\|\mathbf{H}\|_F^2] = 2NM \tag{2}$$

where $\|\mathbf{A}\|_F$ denotes the Frobenius norm of matrix $\mathbf{A}$, it can be expressed as $\|\mathbf{A}\|_F = \sqrt{\sum_{i=1}^a \sum_{j=1}^b |A_{ij}|^2}$ and $E[\cdot]$ represents the expectation operator.

3. SYMBOL ERROR RATE ANALYSIS OF MLD AND STBC DETECTION

The transmitted signals of HMRS can be simultaneously sent by multi-user including SM users and STBC users. The detection of each scheme can be done by using the different algorithm. Therefore, SER of each technique can be derived by applying the different methods and various factors. In this section, the SER analysis of both SM and STBC techniques are separately explained. Then in section 4, the SER expression of both techniques are jointly combined to get the average SER of each user by considering the error propagation effect in SIC process.

3.1 Union Bound on SER for MLD Systems

At the transmitting side of HMRS, any users can apply MLD technique to meet the high speed data rate. The tight union bound on the SER of the nth ($n = 1,,2N$) transmitted signal stream can be derived by applying the expression in [17] and [18]. It is assumed that all the possible symbols in constellation are equally probable. The authors define sc as the set of all C possible symbols transmitted at an especial antenna, and s represents the set of C^{2N} possible symbol vectors form the $2N$ transmit antennas. The authors define the C^{2N-1} vectors s_j as the subset of s for comparing with s_i that differs in their nth position form s_j. The number of s_j vectors can be defined by $C^{2N} - (C^{2N-1})$. The distance metrics of s_i and s_j are denoted by d_i and d_j, respectively. A pairwise error occurs when $D_{ij} = d_i - d_j < 0$. Thus, the union bound on the SER of the signal stream

transmitted by the nth antenna is given by

$$P_{ML} \leq C^{-2N} \sum_{j} \sum_{i, i \neq j} P_{s_c, ij} \qquad (3)$$

where $P_{sc, ij} = P(D_{ij} < 0 | s_c, s_j = \int_{-\infty}^{0} p(D_{ij}) dD_{ij}$ represents the pairwise error probability (PEP) between s_i and s_j and $p(D_{ij})$ is the pdf of D_{ij}. The closed-form expression of $P_{s_c, ij}$ has been presented as

$$P_{s_c, ij} = \frac{1}{(1 + r_{c, ij})^{2M-1}} \sum_{a}^{M-1} \binom{2M-1}{a} r_{c, ij}^a \qquad (4)$$

where

$$r_{c, ij} = A_{c, ij} \Gamma_{c, j} + \sqrt{(A_{c, ij} \Gamma_{c, j})^2 + 2(A_{c, ij} \Gamma_{c, j})} + 1 \qquad (5)$$

and

$$\Gamma_{c, j} = \gamma_c = E_s / \sigma_\omega^2 = \bar{\gamma} \qquad (6)$$

and

$$A_{c, ij} = \|\mathbf{s}_i - \mathbf{s}_j\|^2 / 2E_0 \quad , i \neq j \qquad (7)$$

The BPSK codebook of each transmitting antenna is $\left\{ +\sqrt{E_s/2N}, -\sqrt{E_s/2N} \right\}$. Therefore, $s_i - s_j$ in (7) can only be chosen from $\left\{ +2\sqrt{E_s/2N}, -2\sqrt{E_s/2N} \right\}$.

3.2 SER Analysis of STBC Systems

After STBC streams pass through the MIMO channel, the received signals are combined according to the STBC decoding algorithm. The combined signal y_c at the receiver can be written as

$$y_c = \left[\sum_{i=1}^{2N} \sum_{j=1}^{M} |h_{ij}|^2 \right] s + \widetilde{w} \qquad (8)$$
$$= \|\mathbf{H}\|_F^2 s_l + \widetilde{w}_l, \qquad l = 1, 2, ..., L$$

where L denotes the symbols transmitted over T time slots, the code rate of OSTBC is R=L/T, $\widetilde{w}_l$ is the noise term after combining with a distribution $CN(0, \|\mathbf{H}\|_F^2 \sigma_\omega^2)$. The transmitted symbol can be decoded by $\hat{s}_c = argmin_{s \in C} |y_c - \|\mathbf{H}\|_F^2 s|^2$. Thus, the effective signal-to-noise ratio (SNR) per symbol after STBC decoding can be determined by

$$\gamma_{STBC} = \frac{\|\mathbf{H}\|_F^4 E_0}{\|\mathbf{H}\|_F^2 \sigma_\omega^2} = \frac{E_s}{\sigma_\omega^2} \frac{1}{2N} \|\mathbf{H}\|_F^2 \qquad (9)$$
$$= \frac{\bar{\gamma}}{2N} \|\mathbf{H}\|_F^2$$

where $\bar{\gamma} = \frac{E_s}{\sigma_\omega^2}$ is the average SNR per receiving antenna, $E_0 = E[|s_l|^2] = E_s / 2N$. For the case of perfect CSI in [25], the authors can get the following SER

for BPSK modulation case.

$$P_{STBC} = 2\Im \left(gPSK, \frac{2N}{\bar{\gamma}}, G \right)$$
$$= \frac{1}{\sqrt{\pi}(1+b)^G} \frac{\Gamma(G + \frac{1}{2})}{\Gamma(G+1)} {}_2F_1 \left(G, \frac{1}{2}; G + \frac{1}{2}; \frac{1}{1+b} \right)$$
$$= 1 - \zeta \sum_{k=0}^{G-1} \binom{2k}{k} \left(\frac{1-\zeta^2}{4} \right)^k$$
$$(10)$$

where $\Im(p, q, m) = \frac{q^m}{\Gamma(m)} \int_0^\infty Q(px) e^{-qx} x^{m-1} dx$, $Q(x) = \frac{1}{\pi} \int_0^{\pi/2} exp \left(-\frac{x^2}{2 sin^2 \theta} \right) d\theta$, the Gaussian hypergeometric function defined as ${}_2F_1(e, f; g; r) = \sum_{k=0}^{\infty} \frac{(e)_k (f)_k}{(g)_k} \frac{r_k}{k!}$, $gPSK = 2\sin^2(\pi/C)$, $G = 2NM$, $\zeta = \sqrt{\frac{gPSK}{2q + gPSK}}$, $q = 2N/\bar{\gamma} = \|\mathbf{H}\|_F^2 / \gamma_{STBC}$ and $b = gPSK/2(2N/\bar{\gamma})$.

4. PERFORMANCE ANALYSIS OF HMRS

In this section, the expression of symbol error rate for HMRS systems is derived by considering both SM and STBC users. By considering section 3, the expression of SER analysis of MLD and STBC are clearly explained and it is ready to be applied in this section. In order to understand the method to derive the SER expression of HMRS, the HMRS algorithm has to be firstly discussed in section 4.1. Then, the encoding process at transmitting side and the detection at receiving side for 2 users are explained later.

4.1 HMRS Systems

The hybrid-MIMO system applies both SM and STBC to encode the transmitted signals for each user at the transmitting side. The structure of multi-user HMRS is illustrated in Fig. 2. The N users at transmitting side are encoded by using SM and STBC code where J users and $N - J$ users are applied by encoding SM and STBC code, respectively. The transmitted signals are sent through the MIMO channel. At the receiver, the ML detection is used to get all symbols of SM users. All symbols of STBC users can be successively taken by operating the $N - J$ modules of the sub-received signals generator (GEN Sub-RX), SIC and STBC decoding. In this section, the signals and detecting procedure of the HMRS are demonstrated (where $N=3$, $J=2$ and $M=4$). The equivalent Space-Time Coding matrix for three users HMRS can be given by

$$\mathbf{s} = \begin{bmatrix} s_1 & s_2 & s_3 & s_4 & s_5 & s_6 \\ s_7 & s_8 & s_9 & s_{10} & -s_6^* & s_5^* \end{bmatrix}^T \qquad (11)$$

the $M \times 2N$ MIMO channel can be described as

$$\mathbf{H} = \begin{bmatrix} h_{11} & h_{21} & h_{31} & h_{41} & h_{51} & h_{61} \\ h_{12} & h_{22} & h_{32} & h_{42} & h_{52} & h_{62} \\ h_{13} & h_{23} & h_{33} & h_{43} & h_{53} & h_{63} \\ h_{14} & h_{24} & h_{34} & h_{44} & h_{54} & h_{64} \end{bmatrix} \qquad (12)$$
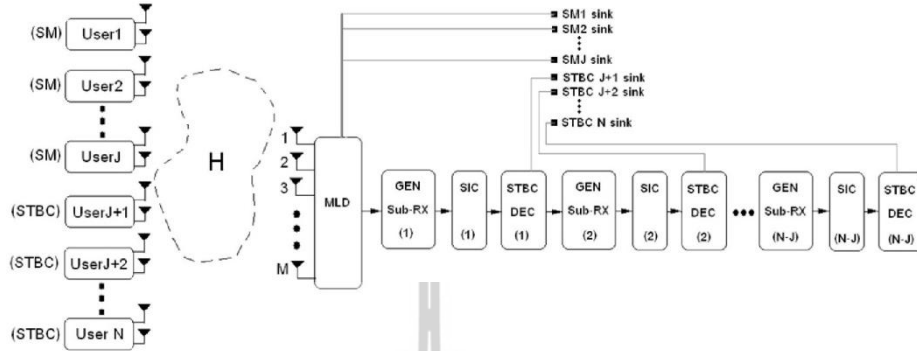
Fig.2: HMRS technique for MU-MIMO system.

where h_{mn} is the complex channel coefficient of the mth transmitting antenna to the nth receiving antenna. The corresponding received signals can be expressed as

$$\mathbf{y} = \mathbf{Hs} + \mathbf{w} = \begin{bmatrix} y_1 & y_5 \\ y_2 & y_6 \\ y_3 & y_7 \\ y_4 & y_8 \end{bmatrix} \qquad (13)$$

then, all symbols of SM user can be calculated by

$$\hat{\mathbf{s}} = \frac{arg\ min}{\tilde{s} \in C^{2N}} \|\mathbf{y} - \mathbf{H\tilde{s}}\|_F^2 \qquad (14)$$

$$\hat{\mathbf{s}}_{SM} = \begin{bmatrix} \hat{s}_1 & \hat{s}_2 & \hat{s}_3 & \hat{s}_4 \\ \hat{s}_7 & \hat{s}_8 & \hat{s}_9 & \hat{s}_{10} \end{bmatrix}^T \qquad (15)$$

where $\hat{\mathbf{s}}_{SM}$ denotes the 1st row to the 4th row in (14). The equivalent received signals of SM users can be generated as

$$\hat{\mathbf{y}}_{SM} = \mathbf{H}_{SM}\hat{\mathbf{s}}_{SM} \qquad (16)$$

where $\mathbf{H}_{SM}$ is the 1st column to the 4th column of MIMO channel $\mathbf{H}$. The equivalent received signals of STBC users can be calculated as

$$\hat{\mathbf{y}}_{STBC} = \mathbf{y} - \hat{\mathbf{y}}_{SM} = \begin{bmatrix} y_a & y_b \\ y_c & y_d \\ y_e & y_f \\ y_g & y_h \end{bmatrix} \qquad (17)$$

$$\mathbf{y}^{\nabla}_{STBC} = [y_a\ y_b^*\ y_c\ y_d^*\ y_e\ y_f^*\ y_g\ y_h^*]^T \qquad (18)$$

where $\mathbf{H}_{STBC}$ is the 5th column to the 6th column of MIMO channel $\mathbf{H}$. The modified $\mathbf{H}_{STBC}$ can be reformed by

$$\mathbf{H}^{\nabla}_{STBC}$$
$$= \begin{bmatrix} h_{51} & h_{61}^* & h_{52} & h_{62}^* & h_{53} & h_{63}^* & h_{54} & h_{64}^* \\ h_{61} & -h_{51}^* & h_{62} & -h_{52}^* & h_{63} & -h_{53}^* & h_{64} & -h_{54}^* \end{bmatrix} \qquad (19)$$

$$\hat{s}_{STBC} = \mathbf{H}^{\nabla}_{STBC}\mathbf{y}^{\nabla}_{STBC} = \begin{bmatrix} \hat{s}_5 \\ \hat{s}_6 \end{bmatrix} \qquad (20)$$

Finally, the decoding symbols of SM and STBC users can be taken from (15) and (20), respectively. As indicated in the HMRS procedure, all symbols of SM users can easily be obtained by using ML detection in only one time but HMTS technique in [14] applies MMSE filter many times to take all symbols of SM users. Hence it can be indicated that the HMRS can offer the benefit of simplification more than the HMTS.

4.2 Performance Analysis of 1SM+1STBC HMRS Systems

In this mode, each user applies MLD and STBC, respectively. The transmitted symbol can be detected by using MLD, SIC and STBC decoding. By considering from (14), the SER expression after MLD detecting as well as SER of SM user ($P_{e,SM}$) can be determined by (3) where the authors define $N=2$ and $M=4$. P_{ML} represents the probability of symbol error equally for each transmitted stream from all transmitting antennas. In order to decode the STBC streams, the interference of SM user needs to be cancelled from the received signals according to (17). Then the error propagation P_{en} (where the subscript $n=1,2,3,4$) after SIC process is presented (*if* $\hat{s}_n - s_n \neq 0$) according to Table 1. where $P_r\{\hat{s}_1 \neq s_1 \bigcap \hat{s}_2 \neq s_2\}$ represents the probability of the event that both s_1 and s_2 are incorrectly detected by MLD. The error propagation from possible 4 cases are used to calculate the average symbol error rate of STBC user of HMRS system. Because the system has two SM detecting symbols ($\hat{s}_1$ *and* $\hat{s}_2$), each case has a different value of error propagation depending on the detectable results of s_1 and s_2. By considering 4 cases of the error propagations in Table 1, the different effective SNRs of STBC user are generated by the error propagations that the effective SNRs are presented in Table 2. From Table 2, the 4 different effective SNRs are used to determine symbol error probability (P_{stcn}) of each

Table 1: *Error propagation of 1SM+1STBC HMRS.*

Case	Error propagation
1)$P_r\{\hat{s}_1 \neq s_1 \bigcap \hat{s}_2 \neq s_2\}$	$P_{e1} = P_{ML}^2$
2)$P_r\{\hat{s}_1 \neq s_1 \bigcap \hat{s}_2 = s_2\}$	$P_{e2} = P_{ML}(1 - P_{ML})$
3)$P_r\{\hat{s}_1 = s_1 \bigcap \hat{s}_2 \neq s_2\}$	$P_{e3} = P_{e2}$
4)$P_r\{\hat{s}_1 = s_1 \bigcap \hat{s}_2 = s_2\}$	$P_{e4} = (1 - P_{ML})^2$

Table 2: *Effective SNRs of 1SM+1STBC HMRS.*

Case	Effective SNR	SER of each case
1	$\gamma_{c1} = \dfrac{\|\mathbf{H}'\|_F^2}{\left(\frac{2N}{\bar{\gamma}}+4^2\right)}$	$P_{stc1} = P_r\{\hat{s}_{STBC} \neq s_{STBC}|P_{e1}\}$
2	$\gamma_{c2} = \dfrac{\|\mathbf{H}'\|_F^2}{\left(\frac{2N}{\bar{\gamma}}+2^2\right)}$	$P_{stc2} = P_r\{\hat{s}_{STBC} \neq s_{STBC}|P_{e2}\}$
3	$\gamma_{c3} = \gamma_{c2}$	$P_{stc3} = P_r\{\hat{s}_{STBC} \neq s_{STBC}|P_{e3}\}$
4	$\gamma_{c4} = \gamma \dfrac{-\|\mathbf{H}'\|_F^2}{2N}$	$P_{stc4} = P_r\{\hat{s}_{STBC} \neq s_{STBC}|P_{e4}\}$

case by applying γ_{cn} in (10), where $N=1$ (because 2 streams of SM user are cancelled from the received signals), s_{STBC} denotes the transmitted symbol of STBC user (s_3 or s_4) and $\mathbf{H}'$ represents the $M \times 2$ MIMO channel of STBC user. Finally, the error propagation and probability of symbol error (P_{stcn}) of all cases from Table 1 and Table 2 are jointly combined to calculate the average SER of STBC user-HMRS, is given by

$$P_{e,STBC(1SM+1STBC\ HMRS)} \leq P_{e1}P_{stc1} + P_{e2}P_{stc2}$$
$$+ P_{e3}P_{stc3} + P_{e4}P_{stc4}$$
$$P_{e,STBC(1SM+1STBC\ HMRS)} \leq$$
$$\left\{ C^{-4} \sum_j \sum_{i,i\neq j} \frac{1}{(1+r_{c,ij})^7} \sum_a^3 \binom{7}{a} r_{c,ij}^a \right\}^2$$
$$x \left\{ 1 - \sqrt{\frac{2}{2q_{c1}+2}} \sum_{k=0}^7 \binom{2k}{k} \left(\frac{\left(1 - \left(\sqrt{\frac{2}{2q_{c1}+2}}\right)^2\right)}{4} \right)^k \right\}$$
$$+ 2C^{-4} \sum_j \sum_{i,i\neq j} \frac{1}{(1+r_{c,ij})^7} \sum_a^3 \binom{7}{a} r_{c,ij}^a$$
$$x \left\{ 1 - \left\{ C^{-4} \sum_j \sum_{i,i\neq j} \frac{1}{(1+r_{c,ij})^7} \sum_a^3 \binom{7}{a} r_{c,ij}^a \right\} \right\}$$
$$x \left\{ 1 - \sqrt{\frac{2}{2q_{c2}+2}} \sum_{k=0}^7 \binom{2k}{k} \left(\frac{\left(1 - \left(\sqrt{\frac{2}{2q_{c2}+2}}\right)^2\right)}{4} \right)^k \right\}$$
$$+ \left\{ 1 - \left\{ C^{-4} \sum_j \sum_{i,i\neq j} \frac{1}{(1+r_{c,ij})^7} \sum_a^3 \binom{7}{a} r_{c,ij}^a \right\} \right\}^2$$
$$x \left\{ 1 - \sqrt{\frac{2}{2q_{c4}+2}} \sum_{k=0}^7 \binom{2k}{k} \left(\frac{\left(1 - \left(\sqrt{\frac{2}{2q_{c4}+2}}\right)^2\right)}{4} \right)^k \right\} \tag{21}$$

where $q_{cn} = \|\mathbf{H}'\|_F^2/\gamma_{cn}$, n=1,2,3,4. The average SER of SM user-HMRS is already determined by (3), then it can be written as $P_{e,SM(1SM+1STBC\ HMRS)} = P_{ML_{N=2,M=4}}$.

Table 3: *error propagation of 2SM+1STBC HMRS*

Error propagation	The number of occurrences of the event
$P_{c1} = P_{ML}^4$	1
$P_{c2} = P_{ML}^3(1 - P_{ML})$	4
$P_{c3} = P_{ML}^2(1 - P_{ML})^2$	6
$P_{c4} = P_{ML}(1 - P_{ML})^3$	4
$P_{c5} = (1 - P_{ML})^4$	1

Table 4: *Effective SNRs of 2SM+1STBC HMRS*

Case	Effective SNR	SER of each case
1	$\gamma_{d1} = \dfrac{\|\mathbf{H}'\|_F^2}{\left(\frac{2N}{\bar{\gamma}}+8^2\right)}$	$P_{s1} = P_r\{\hat{s}_{STBC} \neq s_{STBC}|P_{c1}\}$
2	$\gamma_{d2} = \dfrac{\|\mathbf{H}'\|_F^2}{\left(\frac{2N}{\bar{\gamma}}+6^2\right)}$	$P_{s2} = P_r\{\hat{s}_{STBC} \neq s_{STBC}|P_{c2}\}$
3	$\gamma_{d3} = \dfrac{\|\mathbf{H}'\|_F^2}{\left(\frac{2N}{\bar{\gamma}}+4^2\right)}$	$P_{s3} = P_r\{\hat{s}_{STBC} \neq s_{STBC}|P_{c3}\}$
4	$\gamma_{d4} = \dfrac{\|\mathbf{H}'\|_F^2}{\left(\frac{2N}{\bar{\gamma}}+2^2\right)}$	$P_{s4} = P_r\{\hat{s}_{STBC} \neq s_{STBC}|P_{c4}\}$
5	$\gamma_{d5} = \gamma \dfrac{-\|\mathbf{H}'\|_F^2}{2N}$	$P_{s5} = P_r\{\hat{s}_{STBC} \neq s_{STBC}|P_{c5}\}$

4.3 Performance Analysis of 2SM+1STBC HMRS System

In this mode, MLD and STBC are applied by 2 SM users and 1 STBC user, respectively. All transmitted streams can be detected according HMRS algorithm. By considering from (14), the SER expression after MLD detecting as well as SER of SM user ($P_{e,SM}$) can be determined by (3) where the authors define $N=3$ and $M=4$. P_{ML} represents the probability of symbol error equally for each transmitted stream from all transmitting antennas. In order to decoding the STBC streams (s_5 and s_6), the interference of 2 SM users (s_1, s_2, s_3 and s_4) needs to be cancelled from the received signals by (17). Then the error propagation after SIC process is presented according to Table 3.

where P_{c1} represents event that 4 symbols are wrong detected, P_{c2} represents event that 3 symbols are wrong detected, P_{c3} represents event that 2 symbols are wrong detected, P_{c4} represents event that 1 symbols are wrong detected and P_{c5} represents event that 4 symbols are correctly detected. From Table 4,
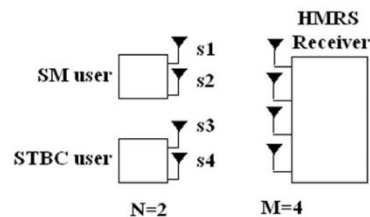
Fig.3: *1SM+1STBC HMRS system.*

the 5 different effective SNRs are used to determine SER (P_{sn}) of each case by applying γ_{dn} in (10), where $N = 1$ (because 4 streams of SM users are cancelled from the received signals). Finally, the error propagation and probability of symbol error (P_{sn}) of all cases from Table 3 and Table 4 are jointly combined to calculate the average SER of STBC user which is given by

$$P_{e,STBC(2SM+1STBC\ HMRS)} \le P_{c1}P_{s1} + 4P_{c2}P_{s2}$$
$$+ 6P_{c3}P_{s3} + P_{c4}P_{s4} + P_{c5}P_{s5}$$
$$P_{e,STBC(2SM+1STBC\ HMRS)} \le$$

$$\left\{ C^{-6} \sum_j \sum_{i,i\neq j} \frac{1}{(1+r_{c,ij})^7} \sum_a^3 \binom{7}{a} r_{c,ij}^a \right\}^4$$

$$x \left\{ 1 - \sqrt{\frac{2}{2q_{d1}+2}} \sum_{k=0}^7 \binom{2k}{k} \left(\frac{\left(1 - \left(\sqrt{\frac{2}{2q_{d1}+2}}\right)^2\right)}{4} \right)^k \right\}$$

$$+ 4 \left\{ C^{-6} \sum_j \sum_{i,i\neq j} \frac{1}{(1+r_{c,ij})^7} \sum_a^3 \binom{7}{a} r_{c,ij}^a \right\}^3$$

$$x \left\{ 1 - \left\{ C^{-6} \sum_j \sum_{i,i\neq j} \frac{1}{(1+r_{c,ij})^7} \sum_a^3 \binom{7}{a} r_{c,ij}^a \right\} \right\}$$

$$x \left\{ 1 - \sqrt{\frac{2}{2q_{d2}+2}} \sum_{k=0}^7 \binom{2k}{k} \left(\frac{\left(1 - \left(\sqrt{\frac{2}{2q_{d2}+2}}\right)^2\right)}{4} \right)^k \right\}$$

$$+ 6 \left\{ C^{-6} \sum_j \sum_{i,i\neq j} \frac{1}{(1+r_{c,ij})^7} \sum_a^3 \binom{7}{a} r_{c,ij}^a \right\}^2$$

$$x \left\{ 1 - \left\{ C^{-6} \sum_j \sum_{i,i\neq j} \frac{1}{(1+r_{c,ij})^7} \sum_a^3 \binom{7}{a} r_{c,ij}^a \right\} \right\}^2$$

$$x \left\{ 1 - \sqrt{\frac{2}{2q_{d3}+2}} \sum_{k=0}^7 \binom{2k}{k} \left(\frac{\left(1 - \left(\sqrt{\frac{2}{2q_{d3}+2}}\right)^2\right)}{4} \right)^k \right\}$$

$$+ 4 \left\{ C^{-6} \sum_j \sum_{i,i\neq j} \frac{1}{(1+r_{c,ij})^7} \sum_a^3 \binom{7}{a} r_{c,ij}^a \right\}$$

$$x \left\{ 1 - \left\{ C^{-6} \sum_j \sum_{i,i\neq j} \frac{1}{(1+r_{c,ij})^7} \sum_a^3 \binom{7}{a} r_{c,ij}^a \right\} \right\}^3$$

$$x \left\{ 1 - \sqrt{\frac{2}{2q_{d4}+2}} \sum_{k=0}^7 \binom{2k}{k} \left(\frac{\left(1 - \left(\sqrt{\frac{2}{2q_{d4}+2}}\right)^2\right)}{4} \right)^k \right\}$$

$$+ \left\{ 1 - \left\{ C^{-6} \sum_j \sum_{i,i\neq j} \frac{1}{(1+r_{c,ij})^7} \sum_a^3 \binom{7}{a} r_{c,ij}^a \right\} \right\}^4$$

$$x \left\{ 1 - \sqrt{\frac{2}{2q_{d5}+2}} \sum_{k=0}^7 \binom{2k}{k} \left(\frac{\left(1 - \left(\sqrt{\frac{2}{2q_{d5}+2}}\right)^2\right)}{4} \right)^k \right\}$$
$$(22)$$

where $q_{dn} = \|\mathbf{H}'\|_F^2/\gamma_{dn}$, $n=\{1,2,3,4,5\}$. The average SER of SM users is already determined by (3), then it can be written as $P_{e,SM(2SM+1STBC\ HMRS)} = P_{ML_{N=3,M=4}}$.

In case of N is defined more than 3, the average SER can also be analyzed by calculating the number of occurrences of the event for each error propagation case, computing the effective SNR and writing

Fig.4:   2SM+1STBC HMRS system.
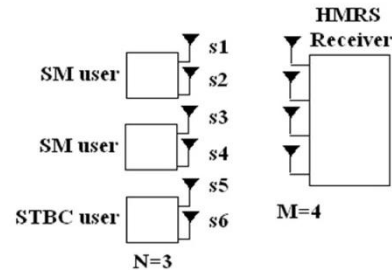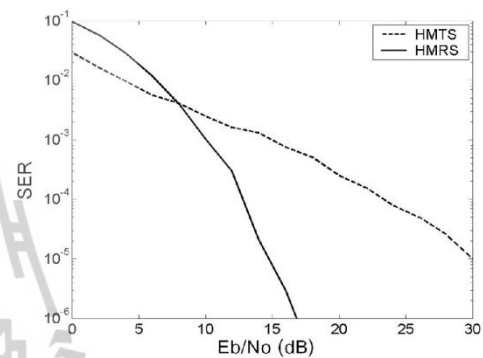

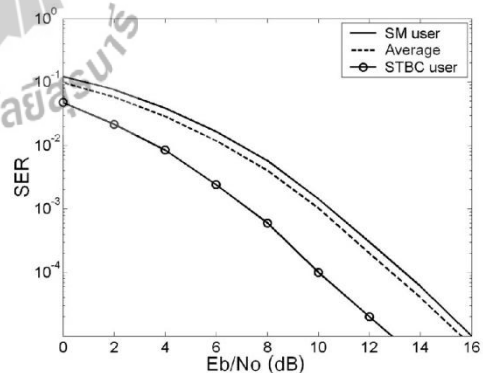Fig.5:   SER performance of HMRS and HMTS techniques.

Fig.6:   SER performance of 1SM+1STBC HMRS system.

all patterns of error propagation for $2^{2(N-1)}$ events. Then the analytical SER equation can be written by the method in (22).

5. NUMERICAL RESULTS AND DISCUSSION

In this section, the authors present numerical results for symbol error probability of HMRS systems
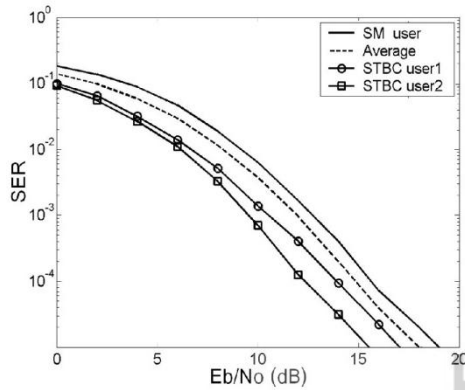
Fig.7: *SER performance of 1SM+2STBC HMRS system.*

Fig.8: *SER performance of 2SM+1STBC HMRS system.*

including SM and STBC users. The parameter N and M are varied to reveal the HMRS performances that support various types of user transmission modes. The performance comparisons between Monte-Carlo simulation and analysis are also presented to demonstrate the performance accuracy of this work.

5.1 Simulation Results of HMRS

The simulations of multi-user HMRS system in case of N users (N=2, 3 and 4) and M=4 are presented to reveal the effect of increasing the number of users at the transmitting side. The several transmitting configurations are assigned in the Monte-Carlo simulation model to investigate the trend of HMRS performance under the multi-user situation. Fig. 5 illustrates the SER performance comparison of HMRS and HMTS in case of two users. Both SM and STBC users apply BPSK modulation to form the transmitted signals. As the result, HMRS can offer higher performance than HMTS about 8 dB at 10^{-4} SER.

Fig.9: *SER performance of 1SM+3STBC HMRS system.*

Fig.6 presents the SER performance of the 1SM+1STBC HMRS system. The STBC user can achieve a higher performance than SM user because of applying the interference cancellation and the orthogonal structure of STBC code. The dash line shows the average performance of a whole system.

Fig.7 illustrates the SER performance of the 1SM+2STBC HMRS system, the STBC code is used by two users and the SM code is used by one user. The highest performance can be obtained by STBC user2 because the two steps of the interference cancellation are continuously used at the receiver to detect the symbols of STBC user2. The last layer has the minimum level of interference.

Fig.8 presents the SER performance of the 2SM+1STBC HMRS system, the STBC code is used by one user and the SM code is used by two users. The highest performance can be taken by STBC user because the SIC technique is employed before STBC layer is detected. The performances of two SM users are equivalence because the symbols of all SM users can be taken by MLD in one time. The HMRS in Fig. 7 has a higher performance than the HMRS in Fig. 8 because the two steps of the interference cancellation are continuously applied.

Fig.9 shows the SER performance of the 1SM+3STBC HMRS system. 1 SM and 3 STBC users are placed at the transmitting side. The highest performance can be achieved by STBC user3 because the three steps of the interference cancellation are continuously operated at the receiver to detect the symbols of STBC user3. The average performance of this mode has a higher performance than the HMRS in Fig. 10 and Fig. 11 because the interference level of this system can intensively be decreased by using many SIC modules and the orthogonal property of STBC users.

Fig.10 shows the SER performance of the 2SM+2STBC HMRS system. The STBC code is used
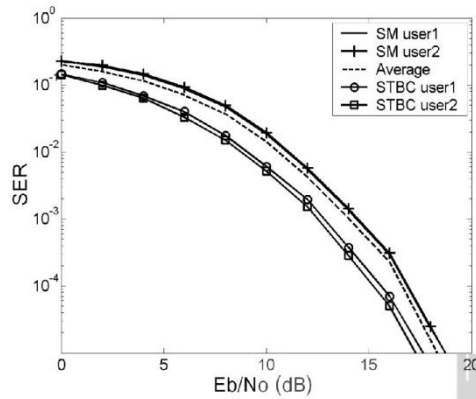
Fig.10: *SER performance of 2SM+2STBC system.*
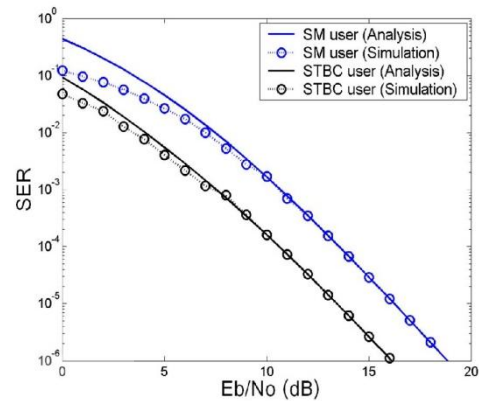
Fig.12: *Comparison between simulation results and analytical results for 1SM+1STBC HMRS system.*
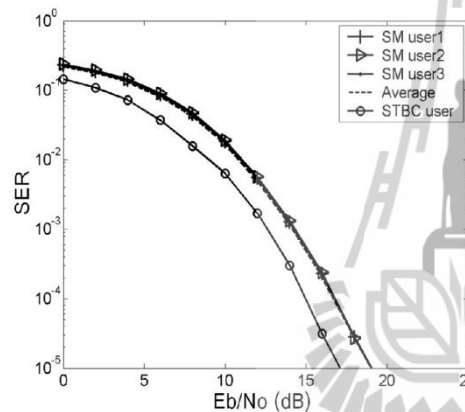
Fig.11: *SER performance of 3SM+1STBC HMRS system.*
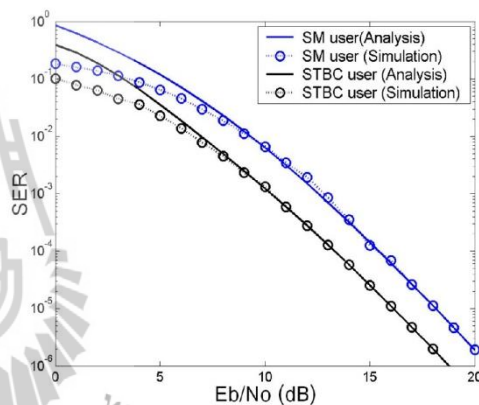
Fig.13: *Comparison between simulation results and analytical results for 2SM+1STBC HMRS system.*

by two users and the SM code is used by two users. The highest performance can be achieved by STBC user2 because the two steps of the interference cancellation are continuously applied at the receiver to detect the symbols of STBC user2. The performance of STBC users can also be enhanced by the orthogonal property of STBC code.

Fig.11 shows the SER performance of the 3SM+1STBC HMRS system. The STBC code is used by one user and the SM code is used by three users. The highest performance can be taken by STBC user. The performances of all SM users are equal because the symbols of all SM users can be taken by ML detection in one time.

5.2 Analytical Results of Error Rate Performance

Fig.12 presents the comparing results between analytical SER given by (21) and simulation results. The simulations employ BPSK modulation with one SM

user, one STBC user (1SM+1STBC HMRS system) and perfect CSI. The authors observe that, when the SER of simulation is below 0.01, the maximum relative error between simulation and analytical results is less than 5.3%.

Fig.13 shows the performance comparison between the analytical results given by (22) and simulation results for BPSK modulation with two SM users, one STBC user (2SM+1STBC HMRS system) and perfect CSI. The authors observe that, when the SER of simulation is below 0.01, the maximum relative error between simulation and analytical results is less than 3.6%.

From the results in Fig. 12 and Fig. 13, the relative error between simulation and analytical results is presented due to the approximation of the union bound on the SER in (3), (21) and (22). However, the performances in Fig. 12 and Fig. 13 can properly be used for general wireless systems because the rel-

ative error is not presented in the high SNR region, especially at 10^{-4}SER or better level.

6. CONCLUSIONS

In this paper, the investigation of MU-MIMO system with HMRS technique for N users (N=2, 3 and 4) are presented. The study of SER performance when increasing the number of users is reported. From the results, the average SER performance of the HMRS is degraded when the numbers of users is increased. The SER performances of HMRS can be improved when the number of STBC users is more than the number of SM users but the spectral efficiency is also degraded. The SER performances of SM users in any configurations of HMRS are corresponded when they have the same total number of users. When comparing between HMRS and HMTS performances, it can indicate that the HMRS offers a better advantage than HMTS, both in SER performance and the complexity of the detecting procedure under the same spectral efficiency scenario. In case of the 1SM+2STBC HMRS system, the simulation result can reveal that the performance of STBC user1 is close to SM user. The STBC user2 give a higher performance than STBC user1. Therefore, the system needs to detect the symbols of STBC user2 in the second step if the location of STBC user2 is placed far away from the base station more than STBC user1. In case of 2SM+2STBC HMRS system, the equivalent performances of both STBC users are presented. This transmission mode can appropriately be applied in MU-MIMO systems in the situation of the same distance between the location of both STBC users and the base station. In case of the multi-STBC user scenario, the symbol of STBC users can be detected in the end of process if the locations of the STBC users are positioned at the largest distance from the base station. Consequently, the signals of other cells are mildly interfered because this STBC layer can be transmitted by applying the lowest power. From above reasons, each transmission mode can offer the different benefits. Especially, the base station needs to detect the symbols in each STBC layer sequentially by considering the level of interference in each layer and the position of each user. Moreover, the limit of the Multi-user HMRS depends on the number of users. When many users are placed in the system, the complexity of ML detection is intensely increased. Therefore the system needs to choose the number of users carefully. The corresponding performances of analytical result and simulation result can indicate the accuracy of this work.

References

[1] T. Yucek, and H. Arslan, "A survey of spectrum sensing algorithms for CR applications first quarter," *University of South Florida*, USA, Tech. Rep., 2009.

[2] S. Alamouti, "A simple transmit diversity technique for wireless communication," *IEEE J. Selected Area Commun.*, vol. 16, no. 8, pp. 1451-1458, Oct. 1998.

[3] V. Tarokh, H. Jafarkhani, and A. R. Calderbank, "Space-time block codes from orthogonal designs," *IEEE Trans. Inform. Theory*, vol. 5, no.5, pp.1456-1467, Jul. 1999.

[4] G. J. Foschini, "Layered space-time architecture for wireless communications in a fading environment when using multiple antennas," *Bell Labs Tech. J.*, vol. 1, no. 2, pp. 41-59, Oct. 1996.

[5] Y. J. Song, S. W. Ko, H. J. Park, H. H. Lee, and H. K. Song, "A novel efficient detection scheme for hybrid STBC in MIMO-OFDM systems," *Proc. 12th IEEE Int. Conf. Commun. Technology*, pp. 701-704, 2010.

[6] L. Zhao, and V.K. Dubey, "Transmit diversity and combining scheme for spatial multiplexing over correlated channels," *Proc. Veh. Technology Conf. IEEE 59th*, pp. 380-383, 2004.

[7] J. Cortez, M. Bazdresch, D. Torres and R. Parra-Michel, "ABBA- VBLAST hybrid space-time code for MIMO wireless communications," *Proc. 5th IEEE Int. Conf. Elect. Eng., Computing Sci. Automat. Control*, pp. 257-262, 2008.

[8] Hien Q. Ngo, T.Q. Duong, and E.G. Larsson, "Uplink performance analysis of multicell MU-MIMO with zero-forcing receivers and perfect CSI," *IEEE Swedish Commun. Technologies Workshop*, pp. 40-45, 2011.

[9] C. W. Tan, and A. R. Calderbank, "Multiuser detection of Alamouti signals," *IEEE Trans. Commun.*, vol. 57, no. 7, pp. 2080-2089, Jul. 2009.

[10] L. L. Yang, "Receiver multiuser diversity aided multi-stage MMSE multiuser detection for DS-CDMA and SDMA systems employing I-Q modulation," *Proc. Veh. Technology Conf. Fall IEEE 72nd*, pp. 1-5, 2010.

[11] K. Liu, S. S. Xing, "Combined multi-stage MMSE and ML multiuser detection for under determined MIMO systems," *IET Int. Commun. Conf. on Wireless Mobile Computing*, pp. 10-14, 2011.

[12] M. A. Shah , B. Mennenga, and G. Fettweis, "Iterative Soft-In Soft-Out sphere detection for 3GPP LTE," *IEEE 71st Veh. Technology Conf.*, pp.1-5, 2010.

[13] Y. Sanada, and Q. Wang, "A co-channel interference cancellation technique using orthogonal convolutional codes on multipath Rayleigh fading channel," *IEEE Trans. Veh. Technology*, vol. 46, no. 1, pp. 114-128, Feb. 1997.

[14] W. da C. Freitas Jr., F. R. P. Cavalcanti, and R. R. Lopes, "Hybrid transceiver schemes for spatial multiplexing and diversity in MIMO systems," *J. Commun. Inform. Syst.*, vol. 20, no. 3, pp. 63-76, Mar. 2005.

[15] S. Reinhardt, T. Buzid and M. Huemer, "Successive interference cancellation for SC/FDE-MIMO system," *IEEE 17th Int. Symp. Personal, Indoor Mobile Radio Commun.*, pp. 1-5, 2006.

[16] T. Khomyat, P. Uthansakul, and M. Uthansakul, "Hybrid-MIMO receiver with both space-time coding and spatial multiplexing detections for cognitive radio networks," *IEEE 2011 Int. Symp. Intelligent Signal Process. Commun. Syst.*, pp. 1-4, 2011.

[17] X. Zhu and R. D. Murch, "Performance analysis of maximum likelihood detection in a MIMO antenna system," *IEEE Trans. Commun.*, vol. 50, no. 2, pp. 187-191, Feb. 2002.

[18] M. Kiessling, J. Speidel, N. Geng, and M. Reinhardt, "Performance analysis of MIMO maximum likelihood receivers with channel correlation, colored gaussian noise, and linear prefiltering," *IEEE Int. Conf. Commun.*, pp. 3026-3030, 2003.

[19] M. D. Renzo, and H. Haas, "Bit error probability of SM-MIMO over generalized fading channels," *IEEE Trans. Veh. Technology*, vol. 61, no. 3, pp. 1124-1144, Mar. 2012.

[20] R. V. Nee, A. V. Zelst, and G. Awater, "Maximum likelihood decoding in a space division multiplexing system," *Proc. IEEE 51th Veh. Technology Conf.*, pp. 6-10, 2000.

[21] A. I. Sulyman, Y. Al-Zahrani, S. Al-Dosari, A. Al-Sanie, and S. Al-Shebeili, "A two-stage constellation partition algorithm for reduced-complexity MIMO-MLD systems," *IEEE 35th Conf. Local Comput. Networks*, pp. 745-748, 2010.

[22] H. M. Carrascol, J. R. Fonollosa and J. A. Delgado-Penin, "Performance analysis of space-time block coding with adaptive modulation," *Proc. 15th IEEE Int. Symp. Personal, Indoor Mobile Radio Commun.*, pp. 493-497, 2004.

[23] W. Li, H. Zhang, and T. A. Gulliver, "Capacity and error probability analysis of orthogonal space-time block codes over correlated Nakagami fading channels," *IEEE Trans. Wireless Commun.*, vol. 5, no. 9, pp. 2408-2412, 2006.

[24] H. Zhang, and T. A. Gulliver, "Capacity and error probability analysis for orthogonal space-time block codes over fading channels," *IEEE Trans. Wireless Commun.*, vol. 4, no. 2, pp. 808-819, Mar. 2005.

[25] K. S. Ahn, R. W. Heath, and H. K. Baik, "Shannon capacity and symbol error rate of space-time block codes in MIMO Rayleigh channels with channel estimation error," *IEEE Trans. Wireless Commun.*, vol. 7, no. 1, pp. 324-333, Jan. 2008.

[26] G. Li, and C. Wang, "Performance analysis of space-time block codes with general rectangular QAM in MIMO fading channels with channel estimation error," *Proc. 11th IEEE Singapore Int. Conf. Commun. Syst.*, pp. 1405-1409, 2008.

[27] D. M. Shin, H. J. Lee, and K. Yang, "Closed-form expressions of the V-BLAST performance over quadrature-amplitude modulation," *Proc. 69th IEEE Veh. Technology Conf.*, pp. 1-5, 2009.

[28] C. Shen, Y. Zhu, S. Zhou, and J. Jiang, "On the performance of V-BLAST with zero-forcing successive interference cancellation receiver," *Proc. IEEE Global Telecommun. Conf.*, pp. 2818-2822, 2004.

Tanapong Khomyat received the B. Eng. and M. Eng degree in telecommunication engineering from Rajamangala University of Technology Thanyaburi, in 2000 and King Mongkut's Institute of Technology Ladkrabang, in 2006, respectively. At present, he is working towards his Ph.D. degree in telecommunication engineering at Suranaree University of Technology, Nakhon Ratchasima, Thailand. His current research interests concern the design, simulation, analysis, and testing of hybrid-MIMO systems.

Peerapong Uthansakul received the B.Eng and M.Eng of Electrical Engineering from Chulalongkorn University, Thailand, in 1996 and 1998 respectively, and Ph.D. degree (2007) in Information Technology and Electrical Engineering from The University of Queensland, Australia. From 1998 to 2001, he was employed as a telecommunication engineer at the Telephone Organization of Thailand. At present, he is working as Associate Professor in School of Telecommunication Engineering, Suranaree University of Technology, Thailand. His research interests include wave propagation modelling, MIMO, OFDM and advance wireless communications.

Monthippa Uthansakul received the B.Eng degree (1997) in Telecommunication Engineering from Suranaree University of Technology, Thailand, M.Eng degree (1999) in Electrical Engineering from Chulalongkorn University, Thailand, and Ph.D. degree (2007) in Information Technology and Electrical Engineering from The University of Queensland, Australia. She received 2nd prize Young Scientist Award from 16th International Conference on Microwaves, Radar and Wireless Communications, Poland, in 2006. At present, she is lecturer in School of Telecommunication Engineering, Suranaree University of Technology, Thailand. Her research interests include wideband/narrowband smart antennas, automatic switch beam antenna, DOA finder, microwave components, application of smart antenna on WLANs.

On the performance of the zero-forcing-space-time block coding multiple-input–multiple-output receiver with channel estimation error and error propagation

Tanapong Khomyat[1], Peerapong Uthansakul[1], Monthippa Uthansakul[1], Soong Boon Hee[2]

[1]Department of Telecommunication Engineering, Suranaree University of Technology, Thailand
[2]Division of Communication Engineering, Nanyang Technological University, Singapore
E-mail: k_tnp@hotmail.com

Abstract: Multi-user multiple-input–multiple-output (MU-MIMO) systems are a promising technology for increasing spectral efficiency and diversity gain in the up-link channel. Space-time block coding (STBC) or the spatial-multiplexing (SM) scheme may selectively be used by each user. The simple techniques, zero-forcing (ZF), STBC and successive interference cancellation are jointly applied to separate and detect all streams at the ZF-STBC MIMO receiver. Unfortunately the channel estimation error (CEE) and error propagation (EP) are usually presented in practical multi-layers detection. In this study, the author investigates the effect of CEE and EP on the bit error rate (BER) performance of the ZF-STBC MIMO receiver over Rayleigh flat fading channels. They derive a nearly exact closed-form BER for general phase shift keying/quadrature-amplitude modulation with CEE and EP for arbitrary number of users. Finally, simulation results demonstrate the validity of the author's analysis.

1 Introduction

For the up-link channel, multi-user multiple-input–multiple-output (MU-MIMO) systems becomes an interesting option for wireless networks because it can increase the spectral efficiency and maintain the diversity benefits [1–4]. With this technique, various users can transmit their signals simultaneously to the receiver by using different MIMO schemes. Generally, there are two such MIMO transmission schemes, namely, the space-time block coding (STBC) [5, 6] and the spatial-multiplexing (SM), that is an implementation of the Vertical Bell Labs Layered Space-Time (V-BLAST) algorithm or zero-forcing (ZF) receiver [7, 8]. For multi-mode MU-MIMO systems, either SM or STBC mode is may selectively be applied by each user. Mode selection approach between SM and STBC transmit diversity is discussed in [3, 4]. By considering the scenario in cellular network, any users usually move to the different locations and continue to face the different wireless channels. Thus mode selection in real time implementation should be continuously executed and decided by the receiver corresponding to the average speed of all users in the network. Generally, the existing works usually discuss either channel estimation error (CEE) or error propagation (EP). Unfortunately CEE and EP usually occurred in practical multi-layers detection. The CEE can cause error in the singular value of MIMO channel that the singular value is the important parameter for making mode selection at the receiver [4]. Therefore, the precision of mode selection is directly deducted by CEE. However, EP

only affects to the detection performance corresponding to the numerical results. The simple multi-mode MU-MIMO systems called ZF-STBC MIMO systems are presented in this work. Each transmitted stream can be detected by applying ZF detection, STBC decoding and successive interference cancellation (SIC) [9] at the receiver as shown in Fig. 1.

In this paper, we analyse the effects of CEE on the performance of ZF-STBC MIMO systems. During the detection process, the receiver needs to know the channel state information (CSI), however, accurate CSI will not be available in practice. Moreover, before the receiver detects the transmitted stream of the desired user, SIC is used to subtract the transmitted stream of the other users. However, this subtracted process cannot be done perfectly, because the probabilities of bit error of the other users is always presented. The error because of the SIC process is known as error propagation (EP), and the degree of EP for the desired user depends on total number of the other users. The performance of receiver is limited by EP [7, 10]. Therefore, the effect of CEE and EP need to be carefully considered in analysis and simulation in order to obtain the real performance. The work in [11] derived the closed-form bit error rate (BER) for ZF-MIMO receiver for a general phase shift keying/ quadrature-amplitude modulation (PSK/QAM) in MIMO Rayleigh channels with CEE. The nearly exact BER analysis of ZF-SIC vertical Bell laboratories layered space-time (ZF V-BLAST) for binary PSK (BPSK) modulation in MIMO Rayleigh channels with EP have been presented in [12]. The symbol error rate (SER) performances of the MIMO-minimum-mean-square-error-SIC (MIMO-MMSE-SIC)
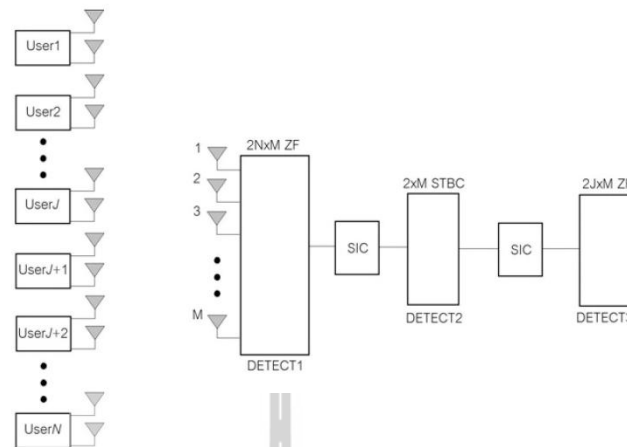
www.ietdl.org

Fig. 1 *ZF-STBC MIMO systems*

for a general PSK in flat Rayleigh-fading channels with EP have been derived in [13]. The exact closed-form SER of STBC system for general pulse-amplitude modulation (PAM)/PSK/QAM with CEE has been described in [14]. However, these techniques do not consider both CEE and EP on the general MIMO receiver as well as the multi-mode MU-MIMO receiver. Multi-mode MU-MIMO has been developed to apply in the next generation wireless network, thus the actual effects of CEE and EP are not clearly revealed from the real systems. However, the effect of CEE and EP decrease the system reliability obviously as presented in performance analysis and simulation results. Therefore, in practice, the problems of CEE and EP should be effectively solved by using an efficient channel estimation technique and applying appropriate channel coding or time diversity technique, respectively. From the above reasons, the problems of CEE and EP should be carefully considered otherwise we will miss the two important parameters for designing wireless network in practice.

In this work, we focus on the effect of CEE and EP on the effective signal-to-noise ratio (SNR) of ZF-STBC MIMO receiver in uncorrelated Rayleigh flat fading channels with N users and M receive antennas, where each user applies two antennas. The estimation error of MIMO channel is modelled as independent complex Gaussian random variables [11, 15, 16]. The average effective SNR for each data stream in ZF detection can be calculated by using a weighted chi-square distributed random variable with $2(M - 2N + 1)$ degrees of freedom. The effective SNR for STBC decoding can be derived from the combined signals at the receiver, where the average effective SNRs for ZF and STBC are evaluated in the presence of CEE and EP. Next, we apply the average effective SNRs to calculate tight closed-form approximations for BERs of SM and STBC user in ZF-STBC receiver for general PSK and QAM. In particular, the work in [13] uses an approach base on the total probability theorem to calculate the average SER that apply 2^{N_a} loops for computation, where N_a denotes the total number of transmitted streams of other users. Compared to this work, our analytical approach applies only $N_a + 1$ loops to calculate average SER or BER. An advantage of this work is that we present the simple analytical method to derive the average BER of multi-mode MU-MIMO systems in the

presence of CEE and EP. Simulation results are presented to demonstrate the validity of our analysis.

The remainder of this paper is structured as follows. In Section 2, we present the system model and explain the characteristic of error in imperfect channel estimation; then we investigate the EP of other users for BPSK, QPSK and QAM modulation signal. The performance analysis of ZF-STBC MIMO is derived with the CEE and EP in Section 3. Then the analysis and simulation results are described in Section 4. Section 5 concludes the work.

2 System model

In this section, we explain a description of the system model; discuss the characteristic and issue of EP because of the SIC process for C-PSK and C-QAM modulation signal. Next, we introduce the channel estimation model applied entirely this paper.

2.1 Signal and system overview

We consider the ZF-STBC MIMO system with N synchronous co-channel users (e.g. uplink cellular) in Fig. 1, where each user equipped with N_t-element antenna array ($N_t = 2$ for this work); we assume that J users are in SM mode and the remaining N–J users are in STBC mode. All $2N$ MIMO streams are simultaneously transmitted over the same frequency band without additional spreading to a common receiver equipped with M-element antenna array. All users are synchronous in the sense that each user transmits its symbol vector in the synchronisation with others. The transmitted signals are assumed to propagate through the $M \times 2N$ random channel matrix H in the uplink communication channel. The MIMO channel is assumed to be a rich-scattering and flat-fading, all sub-channels between all users and receiver are assumed to be independence. We assume that the mode of operation of each user is known at the receiver, which can be indicated in the packet header. The received signal is then given by

$$Y = \sum_{i=1}^{N} H_i s_i + w \qquad (1)$$

where the received signal Y is an $M \times 1$ vector, the signals of user i are sent through the $M \times N_t$ random channel matrix H_i, s_i represents $N_t \times 1$ transmit data symbol vector of user i consisting of N_t symbols each with a constellation size C and w denotes $M \times 1$ vector i.i.d. complex circular Gaussian random variable; each element distributed as $CN(0, N_0)$. The average energy of the transmitted symbol is assumed to be $E_s = E[|s_i|^2]$, where s_i denotes the element of s_i. The overall channel matrix is denoted by $H = \begin{bmatrix} H_z & H_s \end{bmatrix}$ that assumed to have unit variance such that $E[\|H\|_F^2] = N_t NM$, where the overall channel for all SM users and all STBC users are denoted by $H_z = \begin{bmatrix} H_1 & H_2 & \dots & H_J \end{bmatrix}$ and $H_s = \begin{bmatrix} H_{j+1} & H_{J+2} & \dots & H_N \end{bmatrix}$, respectively, $\|A\|_F$ denotes the Frobenius norm of $a \times b$ matrix A, it can be defined as $\|A\|_F \triangleq \sqrt{\sum_{i=1}^{a} \sum_{j=1}^{b} |A_{ij}|^2}$ and $E[\cdot]$ is the expectation operator.

2.2 Error propagation in SIC process

In MIMO uplink channel, we normally use SIC to cancel the early streams of the other users in order to detect the symbols for the desired user. The previous detected symbols $\hat{s}_m$ of other users in (2) are used to subtract with real symbols s_m in the received signal Y, where $m = 1, 2, 3, \dots, N$; then the received signal for user k (desired user) can be described as

$$Y_k = Y - \sum_{m=1}^{N} \hat{H}_m \hat{s}_m \qquad (2)$$

where $k \neq m$. However, the previously detected symbols always have the probability of symbol error during detection ($s_m \neq \hat{s}_m$); thus the cancellation of SIC cannot be completed without error. The error because of SIC process is known as error propagation (EP). In [17], the EP has been described in the form of distance between two symbols; the average distance can be represented by

different value depending on the type of modulation. The symbol distance d_{EP} for C-PSK case can be calculated [13] by $4\sin^2(\pi/C)$, where $d_{EP} = |s_m - \hat{s}_m|^2$. For C-QAM case, the symbol energy should be normalised by the average energy [7] $E_v = 2(C - 1)/3$. Thus the symbol distance d_{EP} for C-QAM case can be obtained by averaging the distance of all symbol pairs in constellation that, as $d_{EP} = (1/(C(C - 1))) \sum_i^C \sum_j^C |s_i - s_j|^2$, where s_i and s_j denote the symbol in constellation of C-QAM signal that are normalised by $\sqrt{E_v}$, and $i \neq j$. The pattern for the appearance of EP has 2^{N_a} possible patterns. However, the pattern for the appearance of EP can be reduced to be $N_a + 1$ possible patterns by using the coefficient vector β_{N_a} that is addressed in Section 3, because some patterns of 2^{N_a} possible patterns have the same value as others. One way to improve reliability in ZF receiver is to use STBC code, which increase the diversity gain and also mitigate the effect of EP in ZF receiver [18–20]. The detection process of ZF-STBC MIMO in Fig. 1 can be explained in Table 1.

2.3 CEE model

The receiver needs to estimate the channels for decoding the symbols from the transmitter, but the perfect channel estimation cannot be done in practice. Thus the model of CEE is described in this part. The good model to explain the characteristic of estimated channel $\hat{H}$ at the receiver is [11, 15, 16]

$$\hat{H} = H + \tau\varphi \qquad (3)$$

where all elements in φ are i.i.d zero-mean complex Gaussian having zero-mean and unit variance, and τ is used to measure an accuracy of channel estimation. The value $\tau = 0$ is presented in case of no estimation error. The normalised-mean-square-error (NMSE) between h_{ij} and $\hat{h}_{ij}$ can be

Table 1 Process of the ZF-STBC MIMO detection

Step	Process
1	**Begin:** The $2N$ transmitted streams are sent to the receiver at the same time. Y^{t_n} represents the received signal vector Y at time slot t_n, where $n = 1, 2$.
2	At DETECT1, all detected symbol $\hat{s}^{t_n} = \begin{bmatrix} \hat{s}_1^{t_n}, \hat{s}_2^{t_n}, \dots, \hat{s}_{2N}^{t_n} \end{bmatrix}$ are obtained by $2N \times M$ ZF detection. All detected symbols $\hat{s}^{t_n}$ are regenerated to be the estimated receive signal $Y_{SM}^{t_n}$ for all SM users and $Y_{STC}^{t_n}$ for all STBC users at time slot t_n, where
3	$Y_{STC}^{t_n} = \begin{bmatrix} Y_{STC,1}^{t_n} Y_{STC,2}^{t_n} \cdots Y_{STC,N-J}^{t_n} \end{bmatrix}$ At DETECT2, define $Y_{ST}^{t_n} = Y^{t_n} - Y_{SM}^{t_n}$. The detected symbols $\hat{s}_{STC,i}$ for all STBC users can be obtained by for $i = 1$ to $N-J$ $Y_{S,i}^{t_1} = Y_{ST}^{t_1} - \sum_{j=1}^{N-J} Y_{STC,j}^{t_1}$, where $j \neq i$ $Y_{S,i}^{t_2} = Y_{ST}^{t_2} - \sum_{j=1}^{N-J} Y_{STC,j}^{t_2}$ $\hat{s}_{STC,i} = \mathrm{dec}\left(Y_{S,i}^{t_1}, \ Y_{S,i}^{t_2} \right)$ $Y_{STC,i}^{t_1} = Y_{S,i}^{t_1}$ and $Y_{STC,i}^{t_2} = Y_{S,i}^{t_2}$ end where $\hat{s}_{STC,i}$ is 2×1 detected symbol vector for the ith STBC user and dec() denotes $N_t \times M$ STBC decoding operation. Define $\hat{s}_c = \begin{bmatrix} \hat{s}_{STC,1}^T \hat{s}_{STC,2}^T \hat{s}_{STC,3}^T \cdots \hat{s}_{STC,N-J}^T \end{bmatrix}$, where ^{T} denotes the matrix transpose operation.
4	At DETECT3, the new received signals $Y_z^{t_n}$ of SM users can be obtained by SIC that, as $Y_z^{t_n} = Y^{t_n} - \ddot{Y}_{STC}^{t_n}$, where $\ddot{Y}_{STC}^{t_n}$ denotes the regenerated receive signal for all STBC users that is generated by the elements of $\hat{s}_c$ according to the STBC structure. Then $Y_z^{t_n}$ is used to detect the transmitted symbols for all SM users by applying $JN_t \times M$ ZF detection. **End process.**

written as

$$\text{NMSE} = \frac{E\left[\left|h_{ij} - \hat{h}_{ij}\right|^2\right]}{E[|h_{ij}|^2]} = \tau^2 \qquad (4)$$

where h_{ij}, $\hat{h}_{ij}$ represent the (i, j)th element of $\boldsymbol{H}$ and $\hat{\boldsymbol{H}}$, respectively. The correlation coefficient between the true channel coefficients and their estimates can be defined as

$$\rho = \frac{E\left[h_{ij}\hat{h}_{ij}^*\right]}{\sqrt{E[|h_{ij}|^2] \cdot E[|\hat{h}_{ij}|^2]}} = \frac{1}{\sqrt{1 + \tau^2}} \qquad (5)$$

where * denotes the complex conjugate operation. The relation between NMSE and ρ in (4) and (5), can be shown as

$$\rho = 1/\sqrt{1 + \text{NMSE}} \qquad (6)$$

3 Performance analysis

The transmitted signals of ZF-STBC MIMO systems can be simultaneously sent by multi-user including SM users and STBC users. The transmitted symbols of each scheme can be continuously detected by using the different MIMO technique. Therefore, BER expression of each technique can be separately derived by applying the different methods. In this section, the BER analysis of both ZF and STBC techniques is separately derived; then the BER expression of both techniques are jointly applied to obtain the average BER expression for each user by considering the effects of CEE and EP.

3.1 Closed-form BER for ZF receiver

In this section, we derive the effective SNR and the closed-form BER with CEE and EP for ZF detection. At the fourth step in Table 1, the transmitted symbol with CEE [11] and EP can be written as

$$\hat{\boldsymbol{s}}_z = \hat{\boldsymbol{H}}_z^\dagger \boldsymbol{Y}_z = (\boldsymbol{H}_z + \tau\boldsymbol{\varphi})^\dagger (\boldsymbol{H}_z \boldsymbol{s}_z + \boldsymbol{w} + N_a \Delta \boldsymbol{H}_p) \qquad (7)$$

where $\boldsymbol{H}_z$ represents $M \times JN_t$ channel matrix for all SM users, $\boldsymbol{s}_z$ denotes the $JN_t \times 1$ symbol vector for the all SM users, † denotes the pseudo-inverse operation, $N_a\Delta\boldsymbol{H}_p$ term denotes the total EP because of SIC process, $\Delta = \sqrt{d_{EP}E_s}$, $\boldsymbol{H}_p$ represents $M \times 1$ channel vector for one other user and the $M \times 1$ received signal vector $\boldsymbol{Y}_z$ represents $\boldsymbol{Y}_z^{t_n}$ in Table 1, regardless of time slot. However, $\tau \ll 1$ in practice, then the pseudo-inverse of the estimated channel matrix can be approximated by the linear part of the Taylor expansion as

$$\hat{\boldsymbol{H}}_z^\dagger \cong \boldsymbol{H}_z^\dagger \left(\boldsymbol{I}_M - \tau\boldsymbol{\varphi}\boldsymbol{H}_z^\dagger\right) \qquad (8)$$

thus (7) can be reformed as

$$\begin{aligned}
\hat{\boldsymbol{Y}}_z &= \boldsymbol{H}_z^\dagger \left(\boldsymbol{I}_M - \tau\boldsymbol{\varphi}\boldsymbol{H}_z^\dagger\right)(\boldsymbol{H}_z \boldsymbol{s}_z + \boldsymbol{w} + N_a \Delta \boldsymbol{H}_p) \\
&= \boldsymbol{s}_z + \boldsymbol{H}_z^\dagger \boldsymbol{w} - \tau\boldsymbol{H}_z^\dagger \boldsymbol{\varphi}\boldsymbol{s}_z - \tau\boldsymbol{H}_z^\dagger \boldsymbol{\varphi}\boldsymbol{H}_z^\dagger \boldsymbol{w} \\
&\quad + N_a \Delta \boldsymbol{H}_z^\dagger \boldsymbol{H}_p - \tau N_a \Delta \boldsymbol{H}_z^\dagger \boldsymbol{\varphi}\boldsymbol{H}_z^\dagger \boldsymbol{H}_p
\end{aligned} \qquad (9)$$

From (9), the effective post-processing noise can be written as

$$\begin{aligned}
\hat{\boldsymbol{w}} &= \boldsymbol{H}_z^\dagger \boldsymbol{w} - \tau\boldsymbol{H}_z^\dagger \boldsymbol{\varphi}\boldsymbol{s}_z - \tau\boldsymbol{H}_z^\dagger \boldsymbol{\varphi}\boldsymbol{H}_z^\dagger \boldsymbol{w} \\
&\quad + N_a \Delta \boldsymbol{H}_z^\dagger \boldsymbol{H}_p - \tau N_a \Delta \boldsymbol{H}_z^\dagger \boldsymbol{\varphi}\boldsymbol{H}_z^\dagger \boldsymbol{H}_p
\end{aligned} \qquad (10)$$

In Appendix 1, we derive the covariance matrix of $\hat{\boldsymbol{w}}$ that can be described as (see (11))

where $\text{tr}(\cdot)$ is the matrix trace operation. In [11], the mean of $t_r\left(\left(\boldsymbol{H}_z^H \boldsymbol{H}_z\right)^{-1}\right)$ is quite small for practical number of transmit and receive antennas $(M > JN_t)$. Moreover, after $t_r\left(\left(\boldsymbol{H}_z^H \boldsymbol{H}_z\right)^{-1}\right)$ is scaled by τ^2 with $\tau \ll 1$, the term $\tau^2 t_r\left(\left(\boldsymbol{H}_z^H \boldsymbol{H}_z\right)^{-1}\right)$ in (11) can be ignored. Therefore, (11) can be besides presented as

$$E\left[\hat{\boldsymbol{w}}\hat{\boldsymbol{w}}^H\right] = \left(N_0 + \tau^2 N_t E_s + N_a^2 \Delta^2 M\right)\left(\boldsymbol{H}_z^H \boldsymbol{H}_z\right)^{-1} \qquad (12)$$

From (9) and (12), the effective SNR per symbol of the kth stream can be described as

$$\gamma_k = \frac{E_s/N_0}{\left(1 + \tau^2 N_t E_s/N_0 + N_a^2 \Delta^2 M/N_0\right)\left[\left(\boldsymbol{H}_z^H \boldsymbol{H}_z\right)^{-1}\right]_{kk}},$$
$$k = 1, 2, \ldots, N_t \qquad (13)$$

where $\left[\left(\boldsymbol{H}_z^H \boldsymbol{H}_z\right)^{-1}\right]_{kk}$ denotes the (k, k)th elements of $\left(\boldsymbol{H}_z^H \boldsymbol{H}_z\right)^{-1}$. From [21, 22], we know that $1/\left[\left(\boldsymbol{H}_z^H \boldsymbol{H}_z\right)^{-1}\right]_{kk}$ is a chi-square distributed random variable with $2(M - JN_t + 1)$ degrees of freedom. As the SNR distribution of each stream is the same, the subscript k in (13) can be dropped. Thus we denote the average SNR per symbol of each stream as $\gamma_z = \bar{\gamma}_s g$, where

$$\bar{\gamma}_s = \frac{E_s/N_0}{\left(1 + \tau^2 N_t E_s/N_0 + M d_{EP} N_a^2 E_s/N_0\right)} \qquad (14)$$

and g denotes a chi-square distributed random variable with $2(M - JN_t + 1)$ degrees of freedom. However, N_a in (14) can be defined by 0 for the first detection, because the EP is not presented before SIC process. From [11], we can write the approximate BER expression for ZF detection with CEE and EP as follows (see (15) at the bottom of the next page)

$$\begin{aligned}
E\left[\hat{\boldsymbol{w}}\hat{\boldsymbol{w}}^H\right] &= \left(N_0 + \tau^2 N_t E_s + \tau^2 N_0 t_r\left(\left(\boldsymbol{H}_z^H \boldsymbol{H}_z\right)^{-1}\right) + \tau^2 N_a \Delta s_z t_r\left(\left(\boldsymbol{H}_z^H \boldsymbol{H}_z\right)^{-1}\right)\boldsymbol{H}_p^H\left(\boldsymbol{H}_z^\dagger\right)^{-1} + N_a^2 \Delta^2 M \right. \\
&\quad \left. + \tau^2 N_a \Delta s_z^H t_r\left(\left(\boldsymbol{H}_z^H \boldsymbol{H}_z\right)^{-1}\right)\boldsymbol{H}_p\left(\left(\boldsymbol{H}_z^\dagger\right)^H\right)^{-1} + \tau^2 N_a^2 \Delta^2 M t_r\left(\left(\boldsymbol{H}_z^H \boldsymbol{H}_z\right)^{-1}\right)\right)\left(\boldsymbol{H}_z^H \boldsymbol{H}_z\right)^{-1}
\end{aligned} \qquad (11)$$

where $\quad \mu_i = \sqrt{\left(3(2i+1)^2 \bar{\gamma}_s\right)/\left(2(C-1)+3(2i+1)^2 \bar{\gamma}_s\right)}$, $G = M - JN_t$ and $\lfloor b \rfloor$ represents the largest integer that is no larger than b. (see (16) at the bottom of the page)

where

$$\mu_i = \sqrt{\bar{\gamma}_s \sin^2((2i-1)\pi/C)/(1 + \bar{\gamma}_s \sin^2((2i-1)\pi/C))},$$

$\lceil b \rceil$ represents the smallest integer that is no smaller than b. From [23], if we consider only the dominant terms ($i = 0, 1$) in (15), the equation can be reformed as (see (17) at the bottom of the page).

3.2 Closed-form BER for STBC systems

At the third step in Table 1, each STBC user applies $2 \times M$ STBC scheme. The code rate of STBC is 1, there are L symbols transmitted over T time slots, where L and T are defined to be 2 for this work. The received signal for the ith STBC user can be obtained by using SIC to cancel data streams of all SM users and other STBC users from the received signal, it can be described as

$$Y_{s,i} = H_{s,i} x_i + w' + w_{\mathrm{ep}} \tag{18}$$

where $Y_{s,i}$ represents the $M \times 2$ receive signal matrix $\left[Y_{s,i}^{t_1} \; Y_{s,i}^{t_2} \right]$ during two successive time slot for the ith STBC user addressed in Table 1, $H_{s,i}$ represents $M \times 2$ channel matrix, x_i is an 2×2 transmission matrix of STBC, w' denotes the $M \times 2$ noise matrix with i.i.d. complex circular Gaussian random variables, each element distributed as $CN(0, N_0)$ and w_{ep} denotes the $M \times 2$ error propagation matrix, each element of w_{ep} can be represented by $w_{\mathrm{ep}} = N_a h_{kl} \Delta$. Where h_{kl} denotes the channel gain describing the channel of the EP of $2(N-1)$ other users from the lth transmit antenna to the kth receive antenna, where h_{ij} denotes the sub-channel of $H_{s,i}$ describing the channel from the jth transmit antenna to the ith receive antenna. The channel matrix $H_{s,i}$ is normalised such that $E\left[\| H_{s,i} \|_F^2 \right] = 2M$.

The average energy of the transmitted symbols per each antenna are assumed to be $E_r/2$, thus the average power of the received signal for each receive antenna is E_r and the

average SNR per receive antenna is E_r/N_0. The total average energy of a symbol duration can be written as $E_T = TE_r = 2LE_s$. Thus the average energy of the constellation can be calculated as $E_s = TE_r/2L = E_r/2$. At the receiver, the received signals in the presence of EP are combined for decoding by maximum-likelihood (ML) decoder. The combined signal at the receiver can be expressed as

$$\tilde{r}_c = \| H_{s,i} \|_F^2 x + \hat{w}_p \tag{19}$$

where x denotes the element of matrix x_i, $\hat{w}_p$ is the noise plus EP term after combining that can be expressed as

$$\hat{w}_p = w' \sum_{j=1}^{2} \sum_{i=1}^{M} h_{ij} \tag{20}$$

where $w' = \sum_l^{N_a} h_{kl} |x - \hat{x}| + w = \sum_l^{N_a} h_{kl} \Delta + w$, $\hat{x}$ denotes the detected symbol from the previous detection and w is the element of vector w'. In Appendix 2, we derive the covariance of $\hat{w}_p$ that can be described as

$$E\left[\hat{w}_p \hat{w}_p^* \right] \cong \| H_{s,i} \|_F^2 (N_0 + N_a \Delta^2) \tag{21}$$

The transmitted symbol can be determined by $\hat{x}_c = \mathrm{argmin}_{\bar{x} \in C} \left| \tilde{r}_c - \| H_{s,i} \|_F^2 \bar{x} \right|^2$. Thus from (19) and (21), the effective SNR per symbol after STBC decoding [14] is derived in Appendix 3 that can be expressed as

$$\gamma_a = \frac{\| H_{s,i} \|_F^2}{2\left(1/\bar{\gamma} + N_a d_{\mathrm{EP}}/2\right)} \tag{22}$$

where $\bar{\gamma} = E_r/N_0 = 2E_s/N_0$. The probability density function (pdf) of the effective SNR (γ_a) under imperfect channel estimation and EP can be described as a function of the correlation coefficient. The similar pdf of the γ_a with CEE have been proposed in [14, 24, 25], the pdf of the

$$P_{b,C-\mathrm{QAM}}^{\mathrm{ZF}} \cong \frac{2}{\sqrt{C} \log_2 \sqrt{C}} \sum_{k=1}^{\log_2 \sqrt{C}} \sum_{i=0}^{(1-2^{-k})\sqrt{C}-1} \left\{ (-1)^{\left\lfloor \frac{i \cdot 2^{k-1}}{\sqrt{C}} \right\rfloor} \left(2^{k-1} - \left\lfloor \frac{i \cdot 2^{k-1}}{\sqrt{C}} + \frac{1}{2} \right\rfloor \right) \right.$$

$$\left. \times \left[\frac{1}{2}(1 - \mu_i) \right]^{G+1} \sum_{j=0}^{G} \binom{G+j}{j} \left[\frac{1}{2}(1 + \mu_i) \right]^j \right\} \tag{15}$$

$$P_{b,C-\mathrm{PSK}}^{\mathrm{ZF}} \cong \frac{2}{\max(\log_2 C, 2)} \sum_{i=1}^{\min\left(2, \left\lceil \frac{C}{4} \right\rceil\right)} \left\{ \left[\frac{1}{2}(1 - \mu_i) \right]^{G+1} \sum_{j=0}^{G} \binom{G+j}{j} \left[\frac{1}{2}(1 + \mu_i) \right]^j \right\} \tag{16}$$

$$P_{b,C-\mathrm{QAM}}^{\mathrm{ZF}} \cong \frac{2(\sqrt{C}-1)}{\sqrt{C} \log_2 \sqrt{C}} \left[\frac{1}{2}(1 - \mu_0) \right]^{G+1} \sum_{j=0}^{G} \binom{G+j}{j} \left[\frac{1}{2}(1 + \mu_0) \right]^j + \frac{2(\sqrt{C}-1)}{\sqrt{C} \log_2 \sqrt{C}} \left[\frac{1}{2}(1 - \mu_1) \right]^{G+1} \sum_{j=0}^{G} \binom{G+j}{j} \left[\frac{1}{2}(1 + \mu_1) \right]^j \tag{17}$$

www.ietdl.org

Table 2 Pattern vector for presenting error propagation

N_a	Coefficient vector $(\boldsymbol{\beta}_{N_a})$ $$\boldsymbol{\beta}_{N_a} = \left[\binom{N_a}{0}, \binom{N_a}{1}, \ldots, \binom{N_a}{N_a} \right]$$	The pattern vector for appearance of EP $\left(\boldsymbol{\psi}_{N_a} \right)$
1	[1, 1]	$[P_{b0}, (1 - P_{b0})]$
2	[1, 2, 1]	$\left[P_{b0}^2, P_{b0}(1 - P_{b0}), (1 - P_{b0})^2 \right]$
3	[1, 3, 3, 1]	$\left[P_{b0}^3, P_{b0}^2(1 - P_{b0}), P_{b0}(1 - P_{b0})^2, (1 - P_{b0})^3 \right]$
4	[1, 4, 6, 4, 1]	$\left[P_{b0}^4, P_{b0}^3(1 - P_{b0}), P_{b0}^2(1 - P_{b0})^2, P_{b0}(1 - P_{b0})^3, (1 - P_{b0})^4 \right]$
5	[1, 5, 10, 10, 5, 1]	$\left[P_{b0}^5, P_{b0}^4(1 - P_{b0}), P_{b0}^3(1 - P_{b0})^2, P_{b0}^2(1 - P_{b0})^3, P_{b0}(1 - P_{b0})^4, (1 - P_{b0})^5 \right]$
6	[1, 6, 15, 20, 15, 6, 1]	$\left[P_{b0}^6, P_{b0}^5(1 - P_{b0}), P_{b0}^4(1 - P_{b0})^2, P_{b0}^3(1 - P_{b0})^3, P_{b0}^2(1 - P_{b0})^4, P_{b0}(1 - P_{b0})^5, (1 - P_{b0})^6 \right]$
$\vdots$	$\vdots$	$\vdots$
n	$\left[\binom{n}{0}, \binom{n}{1}, \binom{n}{2}, \ldots, \binom{n}{n-1}, \binom{n}{n} \right]$	$\left[P_{b0}^n, P_{b0}^{n-1}(1 - P_{b0}), P_{b0}^{n-2}(1 - P_{b0})^2, P_{b0}^{n-3}(1 - P_{b0})^3, \ldots, P_{b0}(1 - P_{b0})^{n-1}, (1 - P_{b0})^n \right]$

received instantaneous SNR is described as

$$p_{\gamma_a}(\gamma_a) = \frac{e^{-q\gamma_a}}{(1 - \rho^2)^{1-D}} \cdot q \sum_{k=0}^{D-1} \left(\frac{1}{k!} \right) \binom{D-1}{k} \left(\frac{\rho^2 \gamma_a}{1 - \rho^2} \cdot q \right)^k \tag{23}$$

where $D = 2M$, $q = \|\boldsymbol{H}_{s,i}\|_F^2 / \gamma_a = 2(1/\bar{\gamma} + N_a d_{\text{EP}}/2)$, and $\binom{n}{k}$ denotes the binomial coefficient given by $\binom{n}{k} = n!/(n-k)!k!$. The Bernstein polynomials can be applied to regroup term [26, 27] in (23) as follows

$$p_{\gamma_a}(\gamma_a) = \sum_{k=1}^{D} \frac{B_{k-1}^{D-1}(\rho^2)}{(k)} q^k \gamma_a^{k-1} e^{-q\gamma_a} \tag{24}$$

where $\Gamma(\cdot)$ denotes the Gamma function and the Bernstein polynomials is defined as $B_i^n(t) \triangleq \binom{n}{i} t^i (1-t)^{n-i}$. The exact closed-form SER for STBC systems have been proposed in [14]. The instantaneous SER of C-PSK and rectangular C-QAM for the effective SNR γ_a over an AWGN channel are $P_{e,\text{PSK}}(\gamma_a) = a_p Q(\sqrt{G_{\text{PSK}} \gamma_a})$ and $P_{e,\text{QAM}}(\gamma_a) = \left[1 - a_q Q(\sqrt{G_{\text{QAM}} \gamma_a}) \right]^2$, respectively, where $a_p = 2$, $G_{\text{PSK}} = 2\sin^2(\pi/C)$, $a_q = 2(1 - 1/\sqrt{C})$ and $G_{\text{QAM}} = 3/(C-1)$ [17, 28]. The SER over fading channel can be often described by

$$\mathcal{V}(b, q, m) = \frac{q^m}{\Gamma(m)} \int_0^\infty Q(\sqrt{bn}) e^{-qn} n^{m-1} \, dn$$
$$= \frac{1}{2} \left[1 - \varepsilon \sum_{k=0}^{m-1} \binom{2k}{k} \left(\frac{1 - \varepsilon^2}{4} \right)^k \right] \tag{25}$$

where $\varepsilon = \sqrt{b/(b + 2q)}$, $b = G_{\text{PSK}}$ or G_{QAM} depending on modulation scheme. By applying (22), (24), (25) and the instantaneous SER over AWGN channel, the BERs for C-PSK and C-QAM signalling with CEE and EP can be

expressed as

$$P_{b,\text{CPSK}}^{\text{STBC}} = \frac{a_p}{\log_2 C} \sum_{i=1}^{D} B_{i-1}^{D-1}(\rho^2) \mathcal{V}(G_{\text{PSK}}, q, i) \tag{26}$$

$$P_{b,\text{CQAM}}^{\text{STBC}} = \frac{1}{\log_2 C} \left[1 - \left(1 - aq \sum_{i=1}^{D} B_{i-1}^{D-1}(\rho^2) \mathcal{V}(G_{\text{QAM}}, q, i) \right)^2 \right] \tag{27}$$

3.3 Average BER for STBC users

From Fig. 1, the ZF-STBC MIMO system is operated by STBC and SM users. The receiver detects the transmitted symbols successively by ZF detection and STBC decoding for each user. The BER performances of each user are different depending on the modulation scheme, number of antennas and number of users. In this part, we explain the procedure to evaluate the average BER for STBC user in ZF-STBC MIMO systems. By considering the presence of EP in multi-layers detection, the presence of EP can be appeared by $N_a + 1$ different patterns that represented by vector $\boldsymbol{\psi}_{N_a}$ in Table 2, each pattern has a different frequency for appearance that can be described by the elements of vector $\boldsymbol{\beta}_{N_a}$. The different pattern also gives the different bit error probability according to the element in vector $\boldsymbol{P}_{b,N_a}$ from Table 3. Finally, vector $\boldsymbol{\beta}_{N_a}$, $\boldsymbol{\psi}_{N_a}$ and $\boldsymbol{P}_{b,N_a}$ are jointly employed to calculate the average BER for the desired user corresponding to [12, 13]. From the first step in Table 1, all transmitted symbols are detected by applying $2N \times M$ ZF-detection; the bit error probability at this step named P_z can be evaluated by replacing (14) into (16) or (17) depending on modulation scheme, where N_a in (14) is defined by 0 because of no EP in the first detection. Then define $P_z = P_{b0}$ for vector $\boldsymbol{\psi}_{N_a}$ in Table 2, select the coefficient vector $\boldsymbol{\beta}_{N_a}$ by determining $N_a = 2(N-1)$ and compute BER vector $\boldsymbol{P}_{b,N_a}$ in Table 3, where each element in vector $\boldsymbol{P}_{b,N_a}$ can be calculated as follows

$$\breve{\gamma}_c(\chi) = \frac{\|\boldsymbol{H}_{s,i}\|_F^2}{2(1/\bar{\gamma} + \chi d_{\text{EP}}/2)} \tag{28}$$

Table 3 BER vector

N_a	BER vector $(\boldsymbol{P}_{b,N_a})$
1	$\boldsymbol{P}_{b,1} = [\breve{P}_b(\breve{\gamma}(1)), \breve{P}_b(\breve{\gamma}(0))]$
2	$\boldsymbol{P}_{b,2} = [\breve{P}_b(\breve{\gamma}(2)), \breve{P}_b(\breve{\gamma}(1)), \breve{P}_b(\breve{\gamma}(0))]$
3	$\boldsymbol{P}_{b,3} = [\breve{P}_b(\breve{\gamma}(3)), \breve{P}_b(\breve{\gamma}(2)), \breve{P}_b(\breve{\gamma}(1)), \breve{P}_b(\breve{\gamma}(0))]$
4	$\boldsymbol{P}_{b,4} = [\breve{P}_b(\breve{\gamma}(4)), \breve{P}_b(\breve{\gamma}(3)), \breve{P}_b(\breve{\gamma}(2)), \breve{P}_b(\breve{\gamma}(1)), \breve{P}_b(\breve{\gamma}(0))]$
5	$\boldsymbol{P}_{b,5} = [\breve{P}_b(\breve{\gamma}(5)), \breve{P}_b(\breve{\gamma}(4)), \breve{P}_b(\breve{\gamma}(3)), \breve{P}_b(\breve{\gamma}(2)), \breve{P}_b(\breve{\gamma}(1)), \breve{P}_b(\breve{\gamma}(0))]$
6	$\boldsymbol{P}_{b,6} = [\breve{P}_b(\breve{\gamma}(6)), \breve{P}_b(\breve{\gamma}(5)), \breve{P}_b(\breve{\gamma}(4)), \breve{P}_b(\breve{\gamma}(3)), \breve{P}_b(\breve{\gamma}(2)), \breve{P}_b(\breve{\gamma}(1)), \breve{P}_b(\breve{\gamma}(0))]$
$\vdots$	$\vdots$
n	$\boldsymbol{P}_{b,n} = [\breve{P}_b(\breve{\gamma}(n)), \breve{P}_b(\breve{\gamma}(n-1)), \breve{P}_b(\breve{\gamma}(n-2)), \breve{P}_b(\breve{\gamma}(n-3)), \ldots, \breve{P}_b(\breve{\gamma}(1)), \breve{P}_b(\breve{\gamma}(0))]$

$$\breve{P}_b\left(\breve{\gamma}_c(\chi)\right) = \frac{a_p}{\log_2 C} \sum_{i=1}^{D} B_{i-1}^{D-1}(\rho^2) \mathcal{V}\left(G_{\text{PSK}}, \frac{\|\boldsymbol{H}_{s,i}\|_F^2}{\breve{\gamma}_c(\chi)}, i\right) \tag{29}$$

or (see (30))

where $\breve{\gamma}_c(n) = \breve{\gamma}(n)$ in Table 3, (28)–(30) are modified from (22), (26) and (27), respectively. Equations (29) and (30) can be chosen for C-PSK and C-QAM modulation, respectively. All elements of $\boldsymbol{P}_{b,N_a}$ in Table 3 can be calculated by (28), (29) or (30). Here, we show a simple method to estimate the probability of bit error $\bar{P}_{b,k}$ of user k take into account the effects of EP. By using the total probability theorem, we can describe

$$\bar{P}_{b,k} \cong \sum_{n=1}^{N_a+1} \boldsymbol{\beta}_{N_a}(n) \Pr\{\text{EP}_n^{(k)}\} \Pr\{e_k | \text{EP}_n^{(k)}\} \tag{31}$$

where the $N_a + 1$ mutually exclusive events $EP_n^{(k)}$, with $\sum_{n=1}^{N_a+1} \boldsymbol{\beta}_{N_a}(n) \Pr\{EP_n^{(k)}\} = 1$, regarding the $(k-1)$ previous symbols decisions, $\Pr\{EP_n^{(k)}\}$ is the probability of event $EP_n^{(k)}$ and $\Pr\{e_k | EP_n^{(k)}\}$ is the probability of making an error in the detection of the symbols of kth user conditional on the event $EP_n^{(k)}$. For convenient calculation, we write the probability terms in (31) into vector form. All elements in $\boldsymbol{\beta}_{N_a}$, $\boldsymbol{\psi}_{N_a}$ and $\boldsymbol{P}_{b,N_a}$ are employed to calculate the average BER for STBC and SM user of ZF-STBC MIMO system by modifying (31) as follows

$$\bar{P}_b \cong \sum_{i=1}^{N_a+1} \boldsymbol{\beta}_{N_a}(i) \boldsymbol{\psi}_{N_a}(i) \boldsymbol{P}_{b,N_a}(i) \tag{32}$$

For calculating the average BER of STBC user $(\bar{P}_{b,\text{STBC}})$, the bit error probability P_z of the first detection is initially calculated by replacing (14) into (16), where $N_a = 0$ and $G = M - N_t N$. Next, we evaluate $\bar{P}_{b,\text{STBC}}$ by (32), where $N_a = 2$ $(N-1)$, $P_{b0} = P_z$ for vector $\boldsymbol{\psi}_{N_a}$ in Table 2 and the elements of $\boldsymbol{P}_{b,N_a}$ in Table 3 can be calculated by (28), and (29) or (30).

3.4 Average BER for SM users

To mitigate the effect of EP from other layers, the transmitted symbols for SM user are detected after STBC decoding and SIC process according to the fourth step in Table 1, thus the $\bar{P}_{b,\text{STBC}}$ in section C is applied for evaluating the average BER for SM user $(\bar{P}_{b,\text{SM}})$. $\bar{P}_{b,\text{SM}}$ can also be evaluated by (32), where $P_{b0} = \bar{P}_{b,\text{STBC}}$ for vector $\boldsymbol{\psi}_{N_a}$ in Table 2, $N_a = 2$ $(N-J)$, $G = M - JN_t$ and the elements of $\boldsymbol{P}_{b,N_a}$ in Table 3 can be calculated by (33), and (34) or (35) as follows

$$\breve{\gamma}_z(\alpha) = \frac{E_s/N_0}{(1 + \tau^2 N_t E_s/N_0 + M d_{\text{EP}} \alpha^2 E_s/N_0)} \tag{33}$$

(see (34))

where (see equation (35) at the bottom of the next page)

where

$$\mu'_i = \sqrt{\left(3(2i+1)^2 \breve{\gamma}_z(\alpha)\right) \Big/ \left(2(C-1) + 3(2i+1)^2 \breve{\gamma}_z(\alpha)\right)},$$

$\breve{\gamma}_z(n) = \breve{\gamma}(n)$ in Table 3, (33)–(35) are modified from (14), (16) and (17), respectively. Equations (34) and (35) can be selected for C-PSK and C-QAM modulation, respectively. Finally, all elements of $\boldsymbol{\beta}_{N_a}$, $\boldsymbol{\psi}_{N_a}$ and $\boldsymbol{P}_{b,N_a}$ in this section are

$$\breve{P}_b\left(\breve{\gamma}_c(\chi)\right) = \frac{\left[1 - \left(1 - aq \sum_{i=1}^{D} B_{i-1}^{D-1}(\rho^2) \mathcal{V}\left(G_{\text{QAM}}, \left(\|\boldsymbol{H}_{s,i}\|_F^2/\breve{\gamma}_c(\chi)\right), i\right)\right)^2\right]}{\log_2 C} \tag{30}$$

$$\mu'_i = \sqrt{\breve{\gamma}_z(\alpha)\sin^2((2i-1)\pi/C) \Big/ \left(1 + \breve{\gamma}_z(\alpha)\sin^2((2i-1)\pi/C)\right)}$$

$$\breve{P}_b\left(\breve{\gamma}_z(\alpha)\right) \cong \frac{2}{\max(\log_2 C, 2)} \sum_{i=1}^{\min(2, \lceil C/4 \rceil)} \left\{\left[\frac{1}{2}(1 - \mu'_i)\right]^{G+1} \sum_{j=0}^{G}\binom{G+j}{j}\left[\frac{1}{2}(1 + \mu'_i)\right]^j\right\} \tag{34}$$
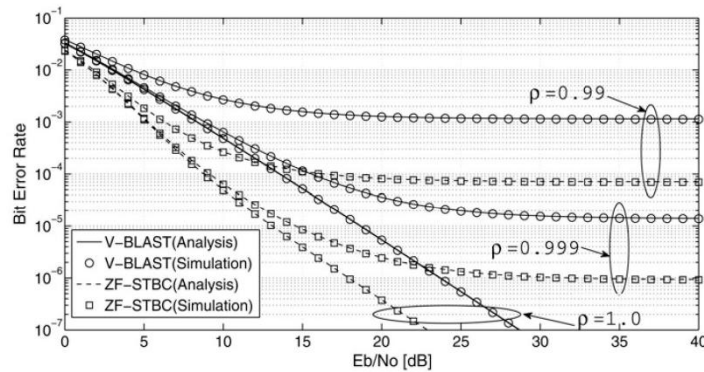
Fig. 2 *Performance comparison of V-BLAST systems and ZF-STBC systems with N = 2, M = 5*
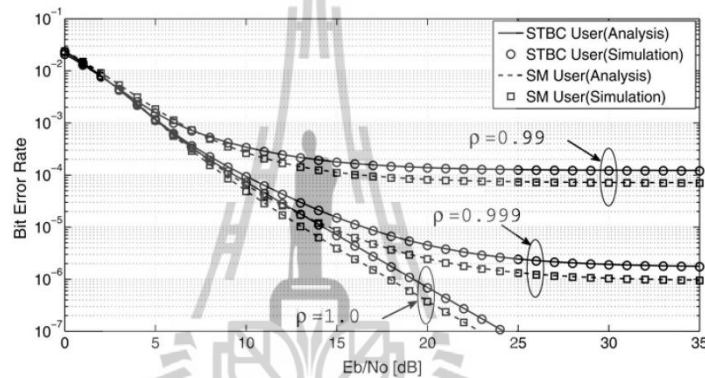

Fig. 3 *BER performance of QPSK ZF-STBC systems with N = 2, M = 5*

employed to calculate the average BER for SM user of the ZF-STBC MIMO system.

By averaging $\bar{P}_{b,\mathrm{STBC}}$ and $\bar{P}_{b,\mathrm{SM}}$, the average BER of the ZF-STBC MIMO receiver in the presence of CEE and EP can be obtained. For the general number for N, J and M, the BER of each user can easily be evaluated by assigning $N_a = 2(N-1)$ for STBC decoding and $N_a = 2(N-J)$ for SM detection. Moreover, (32), Tables 2 and 3 can be employed to evaluate the average BER for both STBC and SM users.

4 Numerical results

In this section, we present numerical results for BER with the effect of CEE and EP. Monte Carlo simulations are used to verify our analytical derivation. Fig. 2 shows the BER performance of the QPSK V-BLAST systems (the second layer) and the proposed systems (SM user of QPSK ZF-STBC systems) with CEE and EP when the accuracy of channel estimation is about 0.99, 0.999 and 1 (perfect case) for $N = 2$ users, $M = 5$ receive antennas. It should be noted that the performance of V-BLAST is worse than that of ZF-STBC for all cases of ρ. This means that the EP problem in V-BLAST or ZF-SIC receiver can be solved by STBC technique. According to our analysis in (32) and (34), these results agree very well with our simulation results shown in Fig. 2.

Fig. 3 shows the BER performance of QPSK ZF-STBC systems, where the BER expression of STBC user shown in (29) and (32), and BER expression of SM user given by (32) and (34) when the accuracy of channel estimation are

$$\mu_i' = \sqrt{3(2i+1)^2\breve{\gamma}_z(\alpha)/(2(C-1)+3(2i+1)^2\breve{\gamma}_z(\alpha))}$$

$$\breve{P}_b\left(\breve{\gamma}_z(\alpha)\right) \cong \frac{2\left(\sqrt{C}-1\right)}{\sqrt{C}\log_2\sqrt{C}}\left[\frac{1}{2}\left(1-\mu_0'\right)\right]^{G+1}\sum_{j=0}^{G}\binom{G+j}{j}\left[\frac{1}{2}\left(1+\mu_0'\right)\right]^j$$

$$+ \frac{2\left(\sqrt{C}-1\right)}{\sqrt{C}\log_2\sqrt{C}}\left[\frac{1}{2}\left(1-\mu_1'\right)\right]^{G+1}\sum_{j=0}^{G}\binom{G+j}{j}\left[\frac{1}{2}\left(1+\mu_1'\right)\right]^j \quad (35)$$

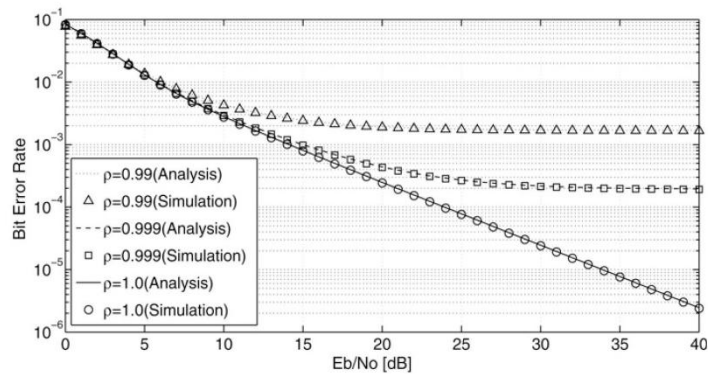**Fig. 4** *BER performance of BPSK ZF-STBC systems with N = 2, M = 4*

about 0.99, 0.999 and 1 for $N = 2$ users and $M = 5$ receive antennas. From Fig. 3, we can see that the average BERs of SM user offer higher reliability than average BERs of STBC user because the transmitted streams of SM user are detected after the previous STBC decoding that can mitigate the EP problem. The analytical results correspond closely to the simulation results.

Fig. 4 demonstrates the average BER performance of BPSK ZF-STBC systems, where the BER performance of both STBC user and SM user are averaged in the presence of CEE and EP when the accuracy of channel estimation are about 0.99, 0.999 and 1 (perfect case) for $N = 2$ users and $M = 4$ receive antennas. From Fig. 4, we found that the average BER performances are rapidly changed by varying
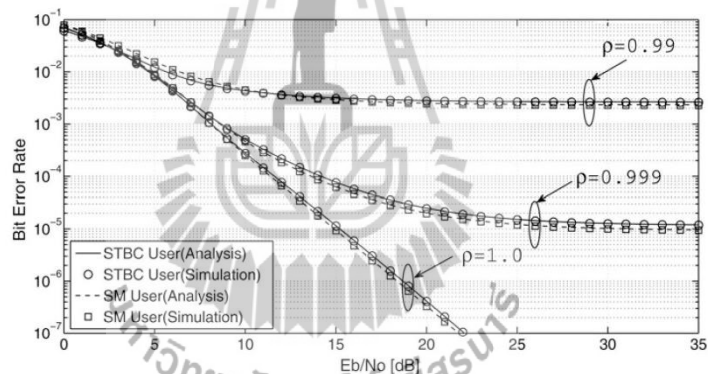

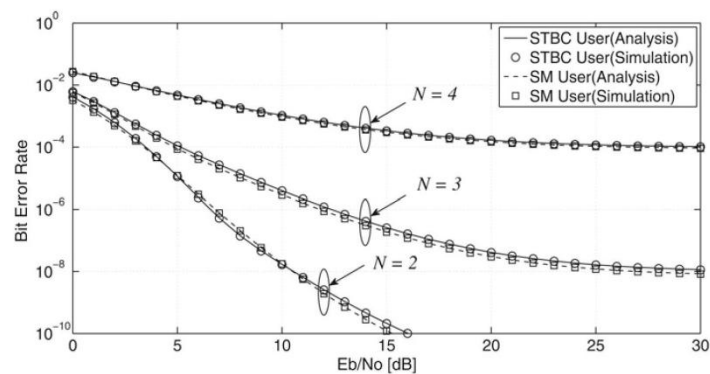**Fig. 5** *BER performance of 16QAM ZF-STBC systems with N = 2, M = 6*

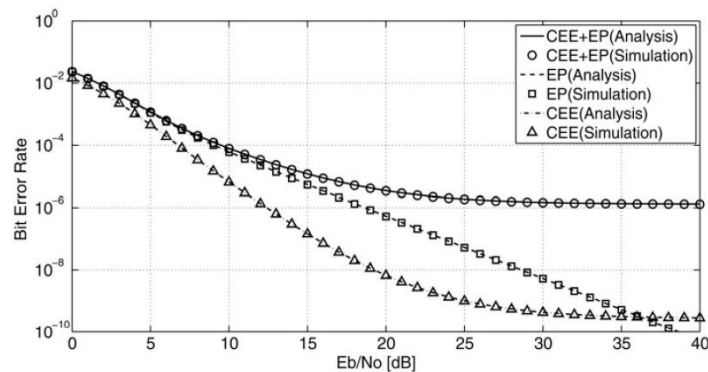**Fig. 6** *BER performance of QPSK ZF-STBC systems for different number of users, ρ = 0.999, M = 8*

Fig. 7 *BER performance of QPSK ZF-STBC systems for different case of error, ρ = 0.999, N = 2, M = 5*

the accuracy of channel estimation, and these agree with our simulation results.

Fig. 5 illustrates the BER performance of 16QAM ZF-STBC systems, where the BER of STBC user shown in (30) and (32), and BER of SM user given by (35) and (32) with EP when the accuracy of channel estimation are about 0.99, 0.999 and 1 (perfect case) for $N = 2$ users and $M = 6$ receive antennas. From Fig. 5, we can see that the average BERs of SM user correspond closely to the average BERs of STBC user. According to our analytical performances, these results agree very well with our simulation results.

Fig. 6 shows the BER performance of QPSK ZF-STBC systems with CEE and EP when the accuracy of channel estimation is about 0.999 for $N = 2$ ($J = 1$), $N = 3$ ($J = 1$) and $N = 4$ ($J = 2$) with $M = 8$ receive antennas. From Fig. 6, the simulation results agree with our analysis that, as the number of user increases, the sensitivity of the ZF-STBC system to the CEE and the EP increases.

Fig. 7 presents the BER performance comparison of QPSK ZF-STBC systems between only CEE case, only EP case, and both CEE and EP cases. From the first and second cases, it should be noted that EP degrades BER performance more than CEE. Significantly, the last case shows the most impact on the system performance and it is most similar to the real scenario. These mean that the problem of CEE and EP should be carefully considered for designing wireless network in practice.

5 Conclusion

In this paper, the performance of ZF-STBC MIMO receivers over uncorrelated Rayleigh flat fading channel in the presence of CEE and EP is investigated. The effective SNR and tight closed-form approximations for the BER expression of general PSK/QAM modulation are derived. It is found that the effect of EP on the BER performance of SM user in ZF-STBC systems is mitigated by the orthogonal property of previous detection of STBC user. Besides, the BER performance gets worse as N increases. By multi-detection of ZF-STBC systems, the BER performance is rapidly degraded by CEE and EP more than a single user MIMO case; because the error of estimated channel and error because of the SIC process are always present every time during detection.

6 References

1 Tan, C.W., Calderbank, A.R.: 'Multiuser detection of Alamouti signals', *IEEE Trans. Commun.*, 2009, **57**, (7), pp. 2080–2089
2 Muhammad, Z., Zhi, D.: 'Blind multiuser detection for synchronous high rate space-time block coded transmission', *IEEE Trans. Wirel. Commun.*, 2011, **10**, (7), pp. 2171–2185
3 Chun, Y.J., Kim, S.W.: 'Log-likelihood-ratio ordered successive interference cancellation in multi-user, multi-mode MIMO systems', *IEEE Commun. Lett.*, 2008, **12**, (11), pp. 837–839
4 Heath, R.W., Paulraj, A.J.: 'Switching between diversity and multiplexing in MIMO systems', *IEEE Trans. Commun.*, 2009, **53**, (6), pp. 962–968
5 Alamouti, S.M.: 'A simple transmit diversity technique for wireless communication', *IEEE J. Select. Areas Commun.*, 1998, **16**, (8), pp. 1451–1458
6 Tan, C.W., Calderbank, A.R.: 'Space-time block codes from orthogonal designs', *IEEE Trans. Inf. Theory*, 1999, **45**, (5), pp. 1456–1467
7 Foschini, G.J.: 'Layered space-time architecture for wireless communications in a fading environment when using multiple antennas', *Bell Labs. Tech. J.*, 1996, **1**, (2), pp. 41–59
8 Spencer, Q.H., Swindlehurst, A.L., Haardt, M.: 'Zero-forcing methods for downlink spatial multiplexing in multiuser MIMO channels', *IEEE Trans. Signal Process.*, 2004, **52**, (2), pp. 461–471
9 Wang, N., Blostein, S.D.: 'Approximate minimum BER power allocation for MIMO spatial multiplexing systems', *IEEE Trans. Commun.*, 2007, **55**, (1), pp. 180–187
10 Kailath, T., Vikalo, H., Hassibi, B.: 'From array processing to MIMO communications' (Cambridge University Press, 2005, 1st edn.)
11 Wang, C., Edward, K.S., Murch, R.D., Mow, W.H., Cheng, R.S., Lau, V.: 'On the performance of the MIMO zero-forcing receiver in the presence of channel estimation error', *IEEE Trans. Wirel. Commun.*, 2007, **6**, (3), pp. 805–810
12 Shen, C., Zhu, Y., Jiang, J.: 'On the performance of V-BLAST with zero-forcing successive interference cancellation receiver'. Proc. Int. Conf. IEEE Global Telecommunication, United States of America, November 2004, pp. 2818–2822
13 Zanella, A., Chiani, M., Win, M.Z.: 'MMSE reception and successive interference cancellation for MIMO systems with high spectral efficiency', *IEEE Trans. Wirel. Commun.*, 2005, **4**, (3), pp. 1244–1253
14 Ahn, K.S., HeathJr.R.W., Baik, H.K.: 'Shannon capacity and symbol error rate of space-time block codes in MIMO Rayleigh channels with channel estimation error', *IEEE Trans. Wirel. Commun.*, 2008, **7**, (1), pp. 324–333
15 Marzetta, T.L.: 'BLAST training: estimating channel characteristics for high-capacity space-time wireless'. Proc. Int. Conf. 37th Annual Allerton Conf. Communications, Control, and Computing, September 1999, pp. 958–966
16 Hassibi, B., Hochwald, B.M.: 'How much training is needed in multiple-antenna wireless links?', *IEEE Trans. Inf. Theory*, 2003, **49**, (4), pp. 951–963
17 Prasad, N., Varanasi, M.: 'Optimum efficiently decodable layered space-time block codes'. Proc. Int. Conf. 35th Asilomar Conf. on Signals, Systems and Computers, March 2001, pp. 227–231
18 Proakis, J.M.: 'Digital communications' (McGraw-Hill, New York, 2007, 5th edn.)

19 Biglieri, E., Taricco, G., Tulino, A.: 'Decoding space-time codes with BLAST architectures', *IEEE Trans. Signal Process.*, 2002, **50**, (10), pp. 2547–2552

20 Kazemitabar, J., Jafarkhani, H.: 'Multiuser interference cancellation and detection for users with more than two transmit antennas', *IEEE Trans. Commun.*, 2008, **56**, (4), pp. 574–583

21 Winters, J.H., Salz, J., Gitlin, R.D.: 'The capacity increase of wireless communication systems with antenna diversity'. Proc. Int. Conf. Conf. Information Sciences Systems, September 1992, pp. 1–5

22 Winters, J.H., Salz, J., Gitlin, R.D.: 'The impact of antenna diversity on the capacity of wireless communication systems', *IEEE Trans. Commun.*, 1994, **42**, (2/3/4), pp. 1740–1751

23 Cho, K., Yoon, D.: 'On the general BER expression of one- and two-dimensional amplitude modulations', *IEEE Trans. Commun.*, 2002, **50**, (7), pp. 1074–1080

24 Gans, M.J.: 'The effect of Gaussian error in maximal ratio combiners', *IEEE Trans. Commun. Technol.*, 1971, **19**, (4), pp. 492–500

25 Roy, S., Fortier, P.: 'Maximal-ratio combining architectures and performance with channel estimation based on a training sequence', *IEEE Trans. Wirel. Commun.*, 2004, **3**, (4), pp. 1154–1164

26 Maaref, A., Aïssa, S.: 'Capacity of space-time block codes in MIMO Rayleigh fading channels with adaptive transmission and estimation errors', *IEEE Trans. Wirel. Commun.*, 2005, 4, (5), pp. 2568–2578

27 Tomiuk, B.R., Beaulieu, N.C., Abu-Dayya, A.A.: 'General forms for maximal ratio diversity with weighting error', *IEEE Trans. Commun.*, 1999, **47**, (4), pp. 488–492

7 Appendix

7.1 Covariance and effective SNR derivation

In this appendix, we derive the covariance of the effective post-processing noise for ZF detection and STBC decoding

in the presence of CEE and EP, and derive the effective SNR per symbol after STBC decoding.

7.1.1 Appendix 1: Covariance of the effective post-processing noise for ZF detection: (see equation at the bottom of this page)

where we permute the matrixes by various relations as follows: $H_z^{\dagger}\left(H_z^{\dagger}\right)^H=\left(H_z^H H_z\right)^{-1}$, $E\left[s_z s_z^H\right]=E_s I_{N_t}$, $E\left[ww^H\right]=N_0 I_{N_r}$, $E\left[\varphi\varphi^H\right]=N_t I_{N_r}$ and $E\left[\varphi\left(H_z^H H_z\right)^{-1}\varphi^H\right]=t_r\left(\left(H_z^H H_z\right)^{-1}\right)I_{N_r}$.

7.1.2 Appendix 2: Covariance of the effective post-processing noise for STBC decoding: (see bottom of the equation)

$$
\begin{aligned}
E\left[\hat{w}\hat{w}^H\right] &= E\left[\left(H_z^{\dagger}w - \tau H_z^{\dagger}\varphi s_z - \tau H_z^{\dagger}\varphi H_z^{\dagger}w + N_a\Delta H_z^{\dagger}H_p - \tau N_a\Delta H_z^{\dagger}\varphi H_z^{\dagger}H_p\right)\right.\\
&\quad \left.\times\left(H_z^{\dagger}w - \tau H_z^{\dagger}\varphi s_z - \tau H_z^{\dagger}\varphi H_z^{\dagger}w + N_a\Delta H_z^{\dagger}H_p - \tau N_a\Delta H_z^{\dagger}\varphi H_z^{\dagger}H_p\right)^H\right]\\
&= E\left[N_0 H_z^{\dagger}\left(H_z^{\dagger}\right)^H + \tau^2 H_z^{\dagger}\left(H_z^{\dagger}\right)^H \varphi\varphi^H E_s + \tau^2 N_0 H_z^{\dagger}\left(H_z^{\dagger}\right)^H \varphi\varphi^H H_z^{\dagger}\left(H_z^{\dagger}\right)^H\right.\\
&\quad + \tau^2 N_a\Delta H_z^{\dagger}\left(H_z^{\dagger}\right)^H s_z\varphi\varphi^H\left(H_z^{\dagger}\right)^H H_p^H + N_a^2\Delta^2 H_z^{\dagger}\left(H_z^{\dagger}\right)^H H_p^H H_p\\
&\quad \left.+ \tau^2 N_a\Delta H_z^{\dagger}\left(H_z^{\dagger}\right)^H \varphi\varphi^H H_z^{\dagger}H_p s_z^H + \tau^2 N_a^2\Delta^2 H_z^{\dagger}\left(H_z^{\dagger}\right)^H \varphi\varphi^H H_z^{\dagger}\left(H_z^{\dagger}\right)^H H_p^H H_p\right]\\
&= \left(N_0 + \tau^2 N_t E_s + \tau^2 N_0 t_r\left(\left(H_z^H H_z\right)^{-1}\right)\right)\\
&\quad + \tau^2 N_a\Delta s_z t_r\left(\left(H_z^H H_z\right)^{-1}\right)H_p^H\left(H_z^{\dagger}\right)^{-1} + N_a^2\Delta^2 M\\
&\quad + \tau^2 N_a\Delta s_z^H t_r\left(\left(H_z^H H_z\right)^{-1}\right)H_p\left(\left(H_z^{\dagger}\right)^H\right)^{-1}\\
&\quad + \tau^2 N_a^2\Delta^2 M t_r\left(\left(H_z^H H_z\right)^{-1}\right)\right)\left(H_z^H H_z\right)^{-1}
\end{aligned}
$$

$$
\begin{aligned}
E\left[\hat{w}_p \hat{w}_p^*\right] &= E\left[\left(\sum_{j=1}^{2}\sum_{i=1}^{M}h_{ij}\right)\left(\sum_{j=1}^{2}\sum_{i=1}^{M}h_{ij}\right)^*\right]E\left[w'w'^*\right]\\
&\cong \|H_{s,i}\|_F^2 E\left[w'w'^*\right]\\
&\cong \|H_{s,i}\|_F^2 E\left[\left(\left(\sum_{l=1}^{N_a}h_{kl}|x-\hat{x}|\right)+w\right)\left(\left(\sum_{l=1}^{N_a}h_{kl}|x-\hat{x}|\right)+w\right)^*\right]\\
&\cong \|H_{s,i}\|_F^2\left\{E\left[|x-\hat{x}|^2\sum_{l=1}^{N_a}|h_{kl}|^2\right] + E[ww^*]\right\}\\
&\cong \|H_{s,i}\|_F^2(N_0 + N_a\Delta^2)
\end{aligned}
$$

www.ietdl.org

7.1.3 Appendix 3: Effective SNR per symbol after STBC decoding:

$$\gamma_a = \frac{E\left[\left(\|\boldsymbol{H}_{s,i}\|_F^2 x\right)\left(\|\boldsymbol{H}_{s,i}\|_F^2 x\right)^*\right]}{E\left[\hat{w}_p \hat{w}_p^*\right]}$$

$$= \frac{\|\boldsymbol{H}_{s,i}\|_F^4 E_s}{\|\boldsymbol{H}_{s,i}\|_F^2 (N_0 + N_a \Delta^2)}$$

$$= \frac{\|\boldsymbol{H}_{s,i}\|_F^2}{2\left(1/\bar{\gamma} + N_a d_{EP}/2\right)}$$

Hybrid-MIMO Receiver with Both Space-Time Coding and Spatial Multiplexing Detections for Cognitive Radio Networks

Tanapong Khomyat, Peerapong Uthansakul and Monthippa Uthansakul

School of Telecommunication Engineering
Suranaree University of Technology
Nakhonratchasima, Thailand
k_tnp@hotmail.com, uthansakul@sut.ac.th, mtp@sut.ac.th

Abstract—In Cognitive Radio (CR) network, the secondary users are required to sense the spectrum based on their environment and then they adapt the spectrum as well as the transmission scheme for CR services to the vacant channels. Multiple-Input Multiple-Output (MIMO) technique becomes an interesting option for CR networks because it can increase the spectrum efficiency and maintain the diversity benefits. In fact, there are two schemes of MIMO transmission including Spatial-Multiplexing (SM) and Space-time block coding (STBC) schemes. These schemes provide the different benefits according to the channel quality or user requirements. Therefore, base station or fusion center must have the capability of detecting both SM and STBC from each CR user at the same time. In this paper, the novel Hybrid-MIMO receiver has been proposed by merging the detection methods of both SM and STBC schemes. The simulation results confirm that the proposed system can improve the symbol error rate and still maintain the benefits of diversity.

Keywords-Cognitive Radio Network; Multiple-Input Multiple-Output(MIMO); Space-Time Block Code(STBC); Spatial Multiplexing(SM)

I. INTRODUCTION

Wireless communication technology is continuously developed and various techniques have been proposed to support the user requirements in the increase of channel capacity. MIMO technique seems to be the key technology to provide favors on many applications such as WLAN, WiMAX and LTE. This fame also gains the attention of new technology such as CR network. This is because the MIMO system consisting of both transmitting and receiving antennas can effectively combat the multi-path fading and greatly improve the diversity gain which supports the high speed wireless communications.

In November 2002, Federal Communications Commission (FCC) announce the spectrum utilization survey report in 6 state of USA that indicate 70% of the allocate spectrum are not consumed and many vacant frequency bands are quietly appeared [1]. Thus, the IEEE formed the 802.22 Working Group to develop a standard for wireless regional area networks (WRAN), which is an alternative broadband access

scheme operating in vacant VHF/UHF TV bands [2]. The smart systems are employed by CR users and fusion center that adapt transmission scheme according to their environment or user requirement [3]. MIMO technique is suitably applied on CR network to enhance both capacity gain and reliability of service. When difference MIMO schemes are used by CR users, SM and STBC hybrid-detection is employed by fusion center to enhance time and spectrum efficiency. Hybrid-MIMO techniques were proposed on many literatures. The switching of MIMO schemes was introduced in [4]. This switching process is operated by realizing the channel condition. The high performance is achieved but their structure of both transmitter and receiver are high complexity. The other hybrid technique is Multi-layer STBC code that has a very good performance but the system is so complicated and it is difficult to be implemented [5]. In [6], the hybrid technique was proposed by selecting one of many STBC patterns which offer the lowest bit error rate layer. This work provided the highest diversity gain but low capacity gain and the complex structure of the system was unattractive. From all literatures, both transmitter and receiver are necessary to be modified which are different from typical SM and STBC structures. These causes the real implementation is difficult in practice. In this paper, the novel Hybrid-MIMO technique merging both typical SM and STBC detections is proposed. The transmitter of CR users can independently transmit either SM or STBC schemes. In turn, the receiver of CR users is able to detect both SM and STBC schemes without known knowledge of transmitter. The Hybrid-MIMO detection is suitable for fusion center side that has a simple structure, high capacity gain and high diversity gain. In simulations, the various scenarios are undertaken in order to judge the advantages of the proposed system.

In this paper, the symbol error rate is used to indicate the figure of merit. The results of proposed Hybrid-MIMO scheme are compared to the conventional MIMO schemes with both SM and STBC. The remainder of this paper is organized as follows. The system overview is described in Section II. Then the novel concept of Hybrid-MIMO detection

is explained in Section III. Simulation results are presented in Section IV and followed by the conclusion in Section V.

II. SYSTEM OVERVIEW

The illustration of cognitive radio networks is presented in Figure 1. Transmit operation of both Primary User (PU) and Secondary User (SU) are actived simultaneously in the common area, which spectrum sensing or spectrum sharing is used to solve interfering problem. At CR transmitters, a modulation schemes, transmit power, carrier frequency and MIMO schemes are assigned suitably by each CR user. The MIMO schemes might be different depending on channel conditions or user requirements. Thus, it is better if the fusion centre can detect any MIMO schemes at the same time. For MIMO schemes, there are two main categories, STBC and SM.

A. STBC scheme

Space-Time block code (STBC) is a modify fashion of Alamouti code. Multiple antennas at both transmitter and receiver are utilized to increase diversity gain. All signals in symbol vector are orthogonal to each other then sink signal can be recovered by orthogonal channel matrix. The STBC structure for 2x2 MIMO system is given by

$$S_{STBC} = \begin{bmatrix} s1 & -s2* \\ s2 & s1* \end{bmatrix} \tag{1}$$

where $s1$ and $s2$ are the first and second transmitting symbols, ()* is a conjugate operation.

B. SM scheme

Spatial multiplexing (SM) scheme uses multiple antennas at both transmitter and receiver to carry independent signal vectors by same frequency band then data sink can be detected by many methods such as Zero-forcing (ZF), MMSE, Maximum likelihood detection (ML), Sphere detection etc. The capacity and diversity gain of SM scheme can be increased by the number of antennas used at transmitter and receiver respectively. In comparing with STBC scheme, SM scheme provides a higher data rate transmission while suffers from worse symbol error rate. Due to the different benefits from both schemes, there are various choices of users to use both of them. However, the detection methods of both schemes are different. As a result, the new design of receiver to have the capability of detecting both schemes at the same time is proposed here.

III. THE PROPOSED HYBRID-MIMO SCHEME

Figure 2 shows the proposed concept of hybrid-MIMO scheme which can detect both STBC and SM symbols at the same time. In Figure 2, two independent signal vectors are transmitted from CR-SM user and CR-STBC user through MIMO channel. Each user has two transmitting antennas. Then all signals are received by four receiving antennas. In the first step, SM sink vector and channel estimation matrix are achieved by SM-Detection block and channel estimation block

respectively. At this stage, the STBC symbols are treated as the unknown-independent symbols. For the second step, the estimated SM symbols are fed to generate SM receiving signals at R-SM GEN block. This SM receiving signals are used to subtract the input receiving signals at Signal subtraction block.
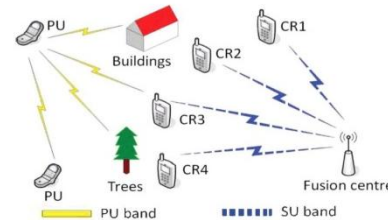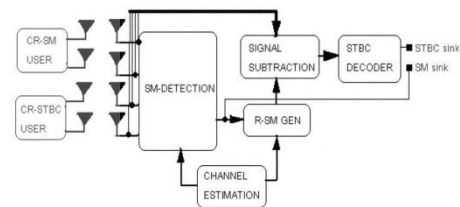

Figure 1. Cognitive radio network.

Figure 2. The proposed hybrid-MIMO receiver.

The purpose of this block is to eliminate all SM symbols from the input receiving signals. The output of this block remains only the information of STBC symbols. Then STBC sink vector can be recovered by STBC Decoder block. In the following subsections, the explanation on transmission process and detection process are detailed.

A. Transmission process

At transmitter, the transmission patterns of SM and STBC users are assigned as shown in (2) and (3), respectively. The column data in each matrix represents the transmit data in each symbol interval. S^{T1} and S^{T2} in equation (4) and (5) are the symbol vectors at the first and second period, respectively.

$$S_{SM} = \begin{bmatrix} s1 & s5 \\ s2 & s6 \end{bmatrix} \tag{2}$$

$$S_{STBC} = \begin{bmatrix} s3 & -s4* \\ s4 & s3* \end{bmatrix} \tag{3}$$

$$S^{T1} = \begin{bmatrix} s1 \\ s2 \\ s3 \\ s4 \end{bmatrix} \quad (4)$$

$$S^{T2} = \begin{bmatrix} s5 \\ s6 \\ -s4* \\ s3* \end{bmatrix} \quad (5)$$

All transmit symbols are sent through Rayleigh fading channel matrix (in equation 12) and then these signal qualities are degraded by Additive White Gaussian Noise (AWGN) channel at receiver. The receiving vector R_T is able to be expressed as

$$R_T = \begin{bmatrix} r_t^{T1} \\ r_t^{T2} \end{bmatrix} = \begin{bmatrix} HS^{T1} \\ HS^{T2} \end{bmatrix} + \begin{bmatrix} N^{T1} \\ N^{T2} \end{bmatrix} \quad (6)$$

where N^{T1} and N^{T2} are AWGN at receiver in the first and second period, respectively.

B. Detection process

The SM symbol vector is detected in the first step at the receiver. In this paper, ZF and ML detections are employed as given by

$$\widetilde{S}^{Tn} = H^{-1} r^{Tn} \quad (7)$$

$$\widetilde{S}^{Tn} = \arg\min_{s \in C^{N_T}} \left\| r^{Tn} - Hs \right\|^2 \quad (8)$$

Equation (7) and (8) express the estimated symbols from ZF and ML detections, respectively. Note that Tn denotes the symbol period index and C are all possible symbols in the specific modulation scheme. In this process, only sink symbols of SM user are available but the sink symbols of STBC user are rejected because they have a low benefit of diversity gain. Then R_{STBC} in (9) is employed to calculate receiving signal vector of STBC user and it can represent by $H_{STBC}S_{STBC}$ in (11). It is believed that the subtraction between R_T and R_{SM} in (9) will eliminate the signals of SM users. The SM symbols $\hat{S}_{SM}^{Tn}$ in (10) are the estimated receiving symbols of SM user. Where R_{SM} and $\widehat{H}_{SM}$ denote the estimated receiving signals and the estimated channel of SM user, respectively. After that, the STBC symbols can be achieved by decoding process shown in (11), where H_{STBC} denotes the channels of STBC users, N and N_S are a noise at receiver and a noise that appeared by SM signal decoding process, respectively.

$$R_{STBC} = R_T - R_{SM} \quad (9)$$

$$R_{SM} = \begin{bmatrix} \widehat{H}_{SM} \hat{S}_{SM}^{T1} \\ \widehat{H}_{SM} \hat{S}_{SM}^{T2} \end{bmatrix} \quad (10)$$

$$\hat{S}_{STBC} = H_{STBC} \widehat{H}_{STBC}^* S_{STBC} + \widehat{H}_{STBC}^* (N + N_S) \quad (11)$$

In this paper, the perfect channel estimation and perfect data synchronization are assumed in simulations. At the transmitting side, both CR-SM user and CR-STBC user completely send at the same time with the same power and the same distance to receiver. The proposed hybrid-detection is utilized on fusion center side to detect 6 symbols from both CR users within 2 symbol periods. The average throughput is 3 symbols per one period. To compare with only STBC users, the overall rate is 1 symbol per one period while the overall rate of only SM users is 4 symbols per one period. Roughly, the proposed concept improves the data throughput in comparing with only STBC users. However, it is interesting to see whether the proposed concept will provide a better symbol error rate than only SM users or not.

The N_Rx4 channel matrix H used in simulations is given by

$$H = \begin{bmatrix} h11 & h12 & h13 & h14 \\ h21 & \cdots & \cdots & \cdots \\ \cdots & \cdots & \cdots & \cdots \\ \cdots & \cdots & \cdots & hN_{R-1}4 \\ hN_R1 & hN_R2 & hN_R3 & hN_R4 \end{bmatrix} \quad (12)$$

Where h_{nm} is the complex channel coefficient of mth transmitting antenna to nth receiving antenna.

IV. SIMULATION RESULTS

In simulations, the symbol error rate is the parameter to indicate the system performance. The proposed Hybrid-MIMO system is simulated according to all process described in Section III. The ZF and ML detection are used to detect symbols for SM scheme. Only uplink communication is considered here. Simulation parameters are shown in Table I.

TABLE I. SIMULATION PARAMETERS

Modulation type	QPSK
Symbol length	1,000
Detection scheme	ZF, ML
No. of transmitting antennas for each user	2
No. of receiving antennas	1, 2, 3, 4
No. of STBC users	1
No. of STBC users	1

Figure 3 shows the SER performance of proposed hybrid-MIMO scheme in comparing with only SM users. For SM users, both first and second symbol periods are detected by ML detection. In turn, the proposed scheme uses ML detection to obtain SM symbols and then uses STBC detection to obtain STBC symbols. The results indicate that the proposed hybrid-MIMO scheme offers the best SER performance which means that it provides more diversity gain than system with only SM users.

In Figure 4, the SER performance of ZF and ML detections are presented for 4x4 MIMO configurations. The performance of ML detector is higher than ZF detector which is the well known conclusion as described in theoretical work. However, the interesting point of these results is that the SER performance of proposed hybrid scheme lies between SM and STBC schemes. The results confirm that the proposed scheme can merge the benefits of both SM and STBC scheme. The overall transmission rate is higher than STBC scheme and the SER performance is better than SM scheme.
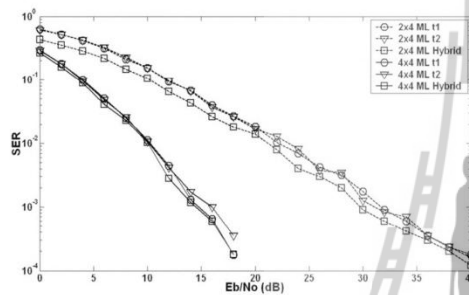

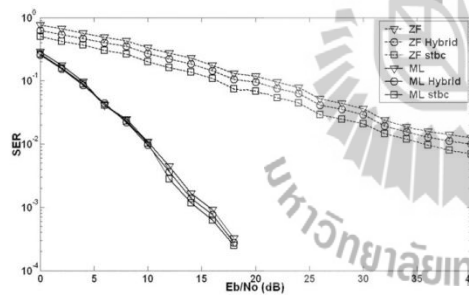Figure 3. SER performance of Hybrid-MIMO and Typical-MIMO.

Figure 4. SER performance of ML and ZF detection .
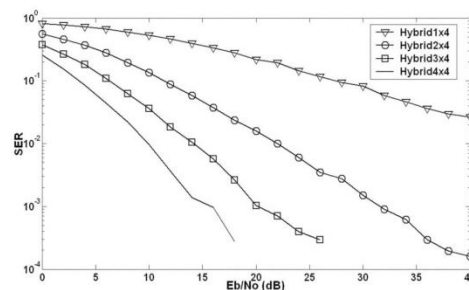

Figure 5. SER performance of Hybrid-MIMO on NR x 4 configuration.
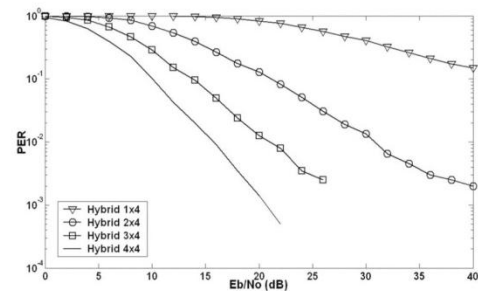

Figure 6. PER performance of Hybrid-MIMO on NRx4 configuration.

Figure 5 shows the SER performance of proposed hybrid-MIMO scheme when the N_R number is varied from 1 to 4. The results reveal that the more number of antennas are used, the better performance is obtained. In addition, the performances of packet error rate with the same scenario presented in Figure 5 is also investigated and shown in Figure 6. The same conclusion as Figure 5 can be also found in Figure 6.

V. CONCLUSION

This paper proposes the new hybrid-MIMO scheme that can detect both SM and STBC schemes at the same time. The simple structure is the distinctive point of the proposed technique. Especially, the CR-users on transmitting side are not required to modify any MIMO structure. The data rate and reliability of proposed MIMO system are easily enhanced by adapting antenna numbers and other parameters according to the simulation results. The proposed receiver is very useful for CR networks.

REFERENCES

[1] I.F. Akyildiz,W.-Y. Lee,M. C. Vuran, and S.Mohanty, " Next Generation /dynamic spectrum access/cognitive radio wireless networks: a survey," *Computer Networks*, vol. 50, no. 13, pp. 2127–2159, 2006.

[2] IEEE 802.22, URL: www.ieee802.org/22/.

[3] S. Haykin, D. Thomson, and J. Reed, "Spectrum sensing for cognitive radio," *Proceedings of the IEEE*, vol. 97, pp. 849 –877, May 2009.

[4] R.W. Heath Jr. and A. J. Paulraj, "Diversity versus multiplexing in narrow band MIMO channel: A tradeoff base on Euclidean distance", IEEE trans. On Communication, submitted 2002.

[5] Ming Lei, Ryuhei Funada, Hiroshi Harada, and Shuzo Kato. "High-Data-Rate DPC-OF/TDMA based on Multi-Layer STBC Coded MIMO OFDM", *publication in the WCNC 2007 proceedings*, pp. 938-942, 2007.

[6] H. Mohd, H. bin, C david, T. heng, "Adaptive MIMO-OFDM Combining Space-time Block codes and spatial multiplexinh", ISSSTA 2004, pp. 444-448, Sydney, Australia, 30 Aug. – 2 Sep. 2004

Performance of Hybrid-MIMO Receiver Scheme in Cognitive Radio Network

Tanapong Khomyat, Peerapong Uthansakul, and Monthippa Uthansakul

Abstract—In this paper, we evaluate the performance of the Hybrid-MIMO Receiver Scheme (HMRS) in Cognitive Radio network (CR-network). We investigate the efficiency of the proposed scheme which the energy level and user number of primary user are varied according to the characteristic of CR-network. HMRS can allow users to transmit either Space-Time Block Code (STBC) or Spatial-Multiplexing (SM) streams simultaneously by using Successive Interference Cancellation (SIC) and Maximum Likelihood Detection (MLD). From simulation, the results indicate that the interference level effects to the performance of HMRS. Moreover, the exact closed-form capacity of the proposed scheme is derived and compared with STBC scheme.

Keywords—Hybrid-MIMO, Cognitive radio network (CR-network), Symbol Error Rate (SER), Successive interference cancellation (SIC), Maximum likelihood detection (MLD).

I. INTRODUCTION

IN the present, the using of frequency band in wireless communication is continuously increased by the new applications such as WLAN, 3G and 4G. Consequently, the available spectrums are not enough used [1], the CR-network is established to solve this problem [2]. In CR-network, the spectrum sensing and the energy control are strictly operated by Fusion Center (FC) to eliminate the interference in Primary-network (PR-network) in common area. In Fig. 1, CR-network is a wireless communication that consumes the public frequency band commonly with PR-network during no PR-user is operated. CR-network can be simultaneously operated with PR-network in the common spectrum by adjusting the power under the enforcing threshold. Multiple-input multiple-output (MIMO) technique is an attracting choice for CR-networks because it can increase both capacity and diversity gain [3]-[6]. Normally, there are two schemes of MIMO technique including STBC [7], [8] and SM [9]. Hybrid-MIMO [10]-[12] is an efficient choice to apply in CR-network, because the receiver can detects both STBC and SM streams in the same time and the same frequency. Hence, it increases both the spectrum efficiency and the information rate. Generally, the Successive Interference Cancellation (SIC), Zero-Forcing (ZF), Minimum Mean Square Error

T. Khomyat is with the School of Telecommunication Engineering Suranaree University of Technology, Muang, Nakhon Ratchasima, Thailand 30000 (e-mail: k_tnp@hotmail.com).

P. Uthansakul is with the School of Telecommunication Engineering Suranaree University of Technology, Muang, Nakhon Ratchasima, Thailand 30000 (e-mail: uthansakul@sut.ac.th).

M. Uthansakul is with the School of Telecommunication Engineering Suranaree University of Technology, Muang, Nakhon Ratchasima, Thailand 30000 (e-mail: mtp@sut.ac.th).

(MMSE) detection and Maximum Likelihood Detection (MLD) are commonly used to separate each layer [13]. The closed-form capacity expression over MIMO fading channels has been presented in [14]. We proposed the HMRS technique in [15], the algorithm of detection and the performance are presented when the variety of both the antenna configuration and the detection techniques are applied to investigate the performance of HMRS technique.

In this article, we show the performance of HMRS when the system is effected by the interference of PR-user. When PR-user and FC are closely placed or the number of PR-user is increased, both the level of interference and the diversity gain are also changed. In addition, we show the varying of the CR-user energy and PR-user energy when CR-user moves directly to PR-network area under the limited threshold. The energy of CR-user can be adjusted to control the quality of information. Moreover, we derive an exact closed-form capacity expression over MIMO Rayleigh channels of HMRS by comparing with 2x2STBC technique.

This article is organized as follows. Section II discusses the CR-network environments that are modeled for simulation in section V. In section III, we present the construction of both 2x2STBC and HMRS. The exact closed-form capacity is derived in section IV. In section V, both SER under CR-network environment and capacity analysis are simulated. Finally, section VI summarizes the paper.
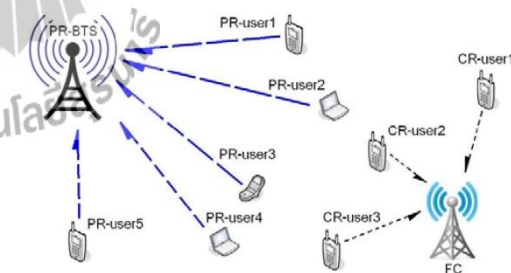

Fig. 1 Cognitive radio network

II. CR-NETWORK ENVIRONMENT

In this section, we introduce an environment of CR-network that operates with PR-network in common area. All CR-users transmit signal according to HMRS encoding, the detection of FC can be done corresponding to HMRS algorithm. The energy of CR-user and the number of PR-user are considered for studying the effective result in HMRS system. In this section, the models of CR-network are used to simulate in
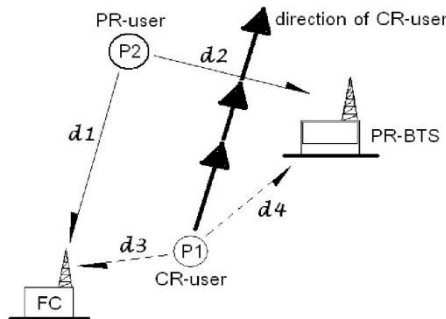
Fig. 2 The first model of CR-network in simulation

section V. In Fig. 2, the simulation model is assumed as follows. CR-user moves directly to PR-network (The biggest line represents the moving direction of CR-user), while other users do not move and all users operate simultaneously in the same spectrum band. Every time interval, CR-user moves closely into the center of PR-network, SNR and SER at FC are degraded. Therefore, the energy of CR-user is instantly increased for keeping the diversity order at FC. Presently, signal to noise ratio (SNR) at PR-base station (PR-BTS) is also decreased when CR-user moves closely. Therefore, the PR-BTS commands CR-network urgently to change the operating frequency or decrease the transmitted power. The received energy at FC can be described as

$$E_{FC} = d_3 E_1 + d_1 E_2 + \sigma_\omega^2 \qquad (1)$$

where d_n denote a scaling constant of path loss for P1 and P2, E_1 denotes the transmitted symbol energy of CR-user, E_2 denotes the transmitted symbol energy of PR-user (we assigned $E_2 = 1.3E_1$) and another denotes the noise energy. SNR at FC can be expressed as

$$SNR = \gamma = \frac{d_3 E_1}{d_1 E_2 + \sigma_\omega^2} = \frac{d_3}{2d_1 + 1/\overline{\gamma}} \qquad (2)$$

where $d_1 = 0.01$, $d_3 = [1, 0.9, 0.8, \ldots, 0.3]$ in each time interval and $\overline{\gamma}$ denotes the average SNR per received antenna.
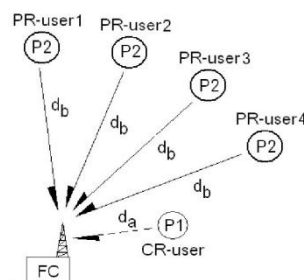

Fig. 3 The second model of CR-network in simulation

In Fig. 3, the simulation model is assumed as follows. All members in two networks operate on fixed position in common area. The interference powers of all PR-users are equally assigned as $d_b P_2$ by using the power control technique, where $d_b = 0.01$, $d_a = 1$ and P_1 denotes the power of CR-user. Therefore, the SNR at FC can be considered as

$$SNR = \gamma = \frac{E_1}{d_b N E_2 + \sigma_\omega^2} = \frac{1}{1.3 d_b N + 1/\overline{\gamma}}. \qquad (3)$$

When the number of PR-user (N) increases, the interference level at FC is also changed. We will discuss this effect in section V.

III. SYSTEM MODEL

In this section, we present the structure and signals in 2x2STBC and HMRS. The effective SNR of both schemes are explained.

A. Space-Time Block Code scheme

The received signal of 2x2STBC can be described as

$$\mathbf{Y} = \mathbf{H}_{2x2}\mathbf{G} + \mathbf{W}$$
$$= \begin{bmatrix} h_{11} & h_{21} \\ h_{12} & h_{22} \end{bmatrix} \begin{bmatrix} s_1 & -s_2^* \\ s_2 & s_1^* \end{bmatrix} + \begin{bmatrix} w_1 \\ w_2 \end{bmatrix} \qquad (4)$$

where $\mathbf{Y}$ denotes the vector of received signal, $\mathbf{H}_{2x2}$ is an 2x2 MIMO channel matrix, $\mathbf{G}$ is an 2x2 space-time block code matrix and W is an 2x1 vector i.i.d. complex circular Gaussian random variable. The received signal of each receiving antenna in each time interval can be written as

$$r_{t1}^1 = h_{11}s_1 + h_{21}s_2 + w_1$$
$$r_{t1}^2 = h_{12}s_1 + h_{22}s_2 + w_2$$
$$r_{t2}^1 = -h_{11}s_2^* + h_{21}s_1^* + w_1 \qquad (5)$$
$$r_{t2}^2 = -h_{12}s_2^* + h_{22}s_1^* + w_2$$

where r_{tb}^a denotes the received signal of the ath antenna in the bth time interval in block. The combining signal can be expressed as

$$\tilde{s}_n = r_{t1}^1 h_{11}^* + r_{t1}^2 h_{12}^* + r_{t2}^{1*} h_{21} + r_{t2}^{2*} h_{22}$$
$$= \left(|h_{11}|^2 + |h_{12}|^2 + |h_{21}|^2 + |h_{22}|^2 \right) s_1 + n_1 h_{11}^* + n_2 h_{12}^* + n_1^* h_{21} + n_2^* h_{22} \qquad (6)$$

Hence, the transmitted symbol can be determined as $\hat{s}_n = \arg \min_{s \in A} \left| \tilde{s}_n - \|\mathbf{H}_{2x2}\|_F^2 s \right|^2$, where A denote the signal constellation. Therefore, the effective SNR per symbol after combining can be written as [14]

$$\gamma_{STBC} = \frac{\|\mathbf{H}_{2x2}\|_F^4 E_0}{\|\mathbf{H}_{2x2}\|_F^2 \sigma_w^2} = \frac{\overline{\gamma}\|\mathbf{H}_{2x2}\|_F^2}{2} \qquad (7)$$

where $\|\mathbf{B}\|_F$ denotes the Frobenius norm of matrix $\mathbf{B}$. it can be defined as $\|\mathbf{B}\|_F \triangleq \sqrt{\sum_{i=1}^{m}\sum_{j=1}^{n}|B_{ij}|^2}$.

B. Hybrid-MIMO receiver scheme (HMRS)

In this paper, we provide two CR-users that use STBC and SM technique for transmitting signal to FC. In Fig. 4, each layer can be separated by using SIC and MLD at FC. The received signal at FC can be expressed as

$$\mathbf{Y} = \begin{bmatrix} h_{11} & h_{21} & h_{31} & h_{41} \\ h_{12} & h_{22} & h_{32} & h_{42} \\ h_{13} & h_{23} & h_{33} & h_{43} \\ h_{14} & h_{24} & h_{34} & h_{44} \end{bmatrix} \begin{bmatrix} s_1 & s_5 \\ s_2 & s_6 \\ s_3 & -s_4^* \\ s_4 & s_3^* \end{bmatrix} + \begin{bmatrix} w_1 \\ w_2 \\ w_3 \\ w_4 \end{bmatrix} \tag{8}$$

$$\overline{\mathbf{Y}}_{SM} = \begin{bmatrix} h_{11} & h_{21} \\ h_{12} & h_{22} \\ h_{13} & h_{23} \\ h_{14} & h_{24} \end{bmatrix} \begin{bmatrix} \hat{s}_1 & \hat{s}_5 \\ \hat{s}_2 & \hat{s}_6 \end{bmatrix} \tag{9}$$

where $\hat{s}_n$ denotes the transmitted symbol of SM user that is detected by MLD in the first step at FC, the received signal of SM layer can be regenerated as (9). Then the received signal of STBC user can be approximated as

$$\overline{\mathbf{Y}}_{STBC} = \mathbf{Y} - \overline{\mathbf{Y}}_{SM} = \begin{bmatrix} r_{t1}^1 & r_{t2}^1 \\ r_{t1}^2 & r_{t2}^2 \\ r_{t1}^3 & r_{t2}^3 \\ r_{t1}^4 & r_{t2}^4 \end{bmatrix} \tag{10}$$

therefore, the combining signal can be expressed as

$$\tilde{s}_3 = r_{t1}^1 h_{31}^* + r_{t1}^2 h_{32}^* + r_{t1}^3 h_{33}^* + r_{t1}^4 h_{34}^* + r_{t2}^{1*} h_{41} + r_{t2}^{2*} h_{42} + r_{t2}^{3*} h_{43} + r_{t2}^{4*} h_{44}$$

$$\tilde{\mathbf{s}}_n = \|\mathbf{H}_{STBC}\|_F^2 s_n + \Delta s \mathbf{L} + \|\mathbf{H}_{STBC}\| w_n \tag{11}$$

where $\mathbf{H}_{STBC}$ is all elements in the 3rd and the 4th column of MIMO channels during two consecutive time in (8), $\Delta s = s_n - \hat{s}_n$ and L denotes the product of $|h|_{ij}$ in STBC combining process. From (11), the transmitted symbol of STBC user can be determined as $\hat{s}_n = \arg\min_{s \in A} |\tilde{s}_n - \|\mathbf{H}_{STBC}\|_F^2 s|^2$. Hence, the effective SNR per symbol after combining of HMRS STBC-user can be written as

$$\gamma_{HMRS}^{STBC} = \frac{\overline{\gamma}\|\mathbf{H}_{STBC}\|_F^2}{2\left(\dfrac{|\Delta s L|^2}{\sigma_\omega^2\|\mathbf{H}_{STBC}\|_F^2}+1\right)} \tag{12}$$
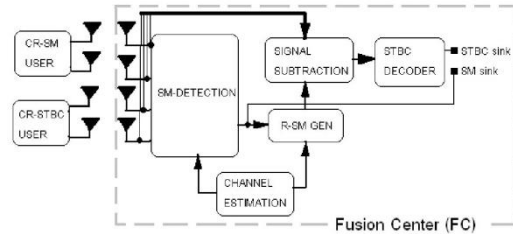

Fig. 4 Hybrid-MIMO receiver scheme (HMRS)

IV. EXACT CLOSED-FORM CAPACITY

In CR-network, CR-user and FC communicate to each other over fading channels. The channel capacity can be represented as the maximum data rate that can be supported by channel without error. It can be used to indicate the merit of the communication system. In this section, we derive the exact closed-form ergodic capacity of both HMRS (STBC-user) and 2x2STBC (single user). The probability density function (pdf) of the effective SNR can be expressed as

$$p_{\gamma_n}(\gamma_n) = \frac{\gamma_n^{(n_T n_R)-1}}{\Gamma(n_T n_R)\overline{\gamma}_s^{(n_T n_R)}} e^{-\gamma_n/\overline{\gamma}_s} \tag{13}$$

where $\Gamma(\cdot)$ is the Gamma function that can be defined as $\Gamma(a) = \int_0^\infty x^{a-1}e^{-a}da$, the average SNR per channel can be expressed as $\overline{\gamma}_s = \gamma_n / \|H_n\|_F^2$, n_T and n_R denote the number of transmitted antenna and the number of received antenna, respectively. The ergodic capacity can be written as

$$C = R\int_0^\infty \log_2(1+\gamma_n)p_{\gamma_n}(\gamma_n)d\gamma_n \tag{14}$$

we can reduce the complexity of (14) by using the formula

$$I(m,n) = \frac{n^m}{\Gamma(m)}\int_0^\infty ln(1+x)x^{m-1}e^{-nx}dx \tag{15}$$

or

$$I(m,n) = P_m(-n)E_1(n) + \sum_{k=1}^{m-1}\frac{P_k(n)P_{m-k}(-n)}{k} \tag{16}$$

where $P_m(\cdot)$ denotes the Poisson distribution, which can be defined as

$$P_m(x) \triangleq \sum_{k=0}^{m-1}\frac{x_k}{k!}e^{-x} \tag{17}$$

and $E_1(\cdot)$ is the exponential integral function of the first order, which can be described as

$$E_1(x) \triangleq \int_x^\infty \frac{e^{-t}}{t}dt, \qquad x > 0. \tag{18}$$

Under perfect CSI, the Shannon capacity of (14) can be

easily calculated [14] as following using (13) and (16)

$$C = \frac{R}{\ln(2)} \mathcal{I}(n_T n_R, q_n) \qquad (19)$$

or

$$C = \frac{R}{\ln(2)}\left[\mathrm{P}_{n_T n_R}(-q_n)\mathrm{E}_1(q_n) + \sum_{k=1}^{(n_T n_R)-1} \frac{\mathrm{P}_k(q_n)\mathrm{P}_{(n_T n_R)-k}(-q_n)}{k} \right] \quad (20)$$

where R denotes the STBC code rate, $q_n = 1/\overline{\gamma}_s$, q_n of 2x2STBC and HMRS scheme can be obtained by using (7) and (12), respectively. Therefore, the ergodic capacity of 2x2STBC scheme and HMRS technique can be calculated by (21) and (22), respectively.

$$C_{STBC} = \frac{1}{\ln(2)}\left[P_4\left(-\frac{\left\|\mathbf{H}_{2x2}\right\|_F^2}{\gamma_{STBC}} \right)E_1\left(\frac{\left\|\mathbf{H}_{2x2}\right\|_F^2}{\gamma_{STBC}} \right) + \ldots \right.$$
$$\left. \ldots \sum_{k=1}^{3} \frac{P_k\left(\frac{\left\|\mathbf{H}_{2x2}\right\|_F^2}{\gamma_{STBC}} \right)P_{4-k}\left(-\frac{\left\|\mathbf{H}_{2x2}\right\|_F^2}{\gamma_{STBC}} \right)}{k} \right] \qquad (21)$$

$$C_{HMRS} = \frac{1}{\ln(2)}\left[P_8\left(-\frac{\left\|\mathbf{H}_{STBC}\right\|_F^2}{\gamma_{HMRS}^{STBC}} \right)E_1\left(\frac{\left\|\mathbf{H}_{STBC}\right\|_F^2}{\gamma_{HMRS}^{STBC}} \right) + \ldots \right.$$
$$\left. \ldots \sum_{k=1}^{7} \frac{P_k\left(\frac{\left\|\mathbf{H}_{STBC}\right\|_F^2}{\gamma_{HMRS}^{STBC}} \right)P_{8-k}\left(-\frac{\left\|\mathbf{H}_{STBC}\right\|_F^2}{\gamma_{HMRS}^{STBC}} \right)}{k} \right]. \qquad (22)$$

The exact closed-form ergodic capacities of two schemes are simulated in the next section.

V. SYSTEM PERFORMANCE

In this section, the SER of HMRS under the adjusting power of CR-user and the number of PR-user are presented by using Monte Carlo simulation method. QPSK modulation is applied to simulate SER. We consider the N number of PR-user that degrades the SER performance. In addition, the ergodic capacities of both HMRS and 2x2STBC are analyzed by applying (7), (12) and (20).

Fig. 5 presents the SER performance of each HMRS-user when PR-network is not operated, the SER performance of STBC-user is higher than SM-user about 2 dB at 10^{-4}. The average SER of both users are also presented.
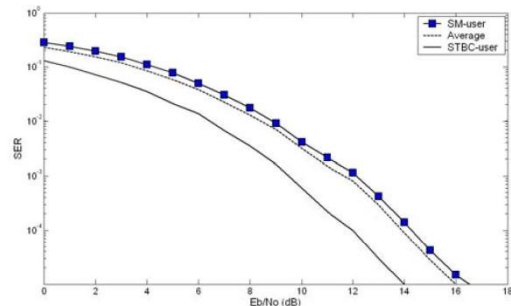

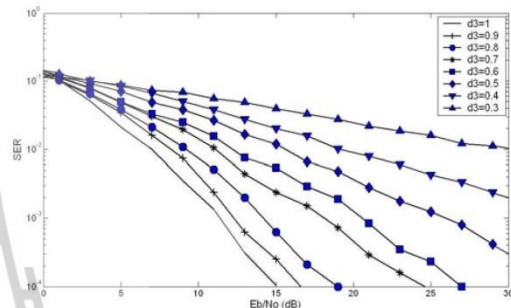Fig. 5 Symbol error rate for HMRS technique

Fig. 6 Symbol error rate of FC when CR-user moves directly to PR-network area
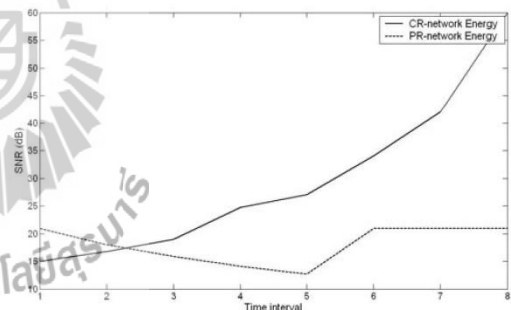

Fig. 7 The varying powers of the CR-network and the PR-network versus the time interval

Fig. 6 shows the SER performance under the situation of the first model in Fig. 2. The power of CR-user is increased for keeping the SER level, because the SNR at FC and the interference from PR-user are changed when CR-user moves directly to PR-network area. Every time interval, d_3 in (2) is increased about 0.1 times of the CR-user power. If FC wants to keep SER as 10^{-4}, the CR-user needs to increase the power continuously in every time interval. Initially, CR-user applies power at SNR=12dB for keeping SER=10^{-4}. Then in the 1st time interval, CR-user increases power until SNR=15dB. After that in the 2nd time interval, CR-user increases power until SNR=16.8dB. The power of CR-user is continuously increased until the CR-user stops his motion.
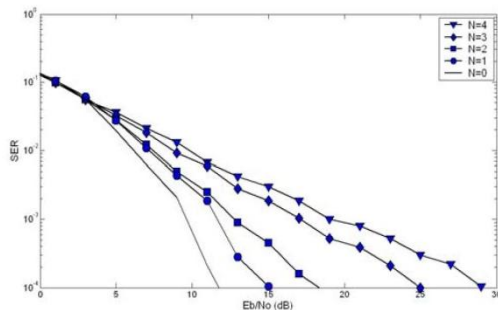
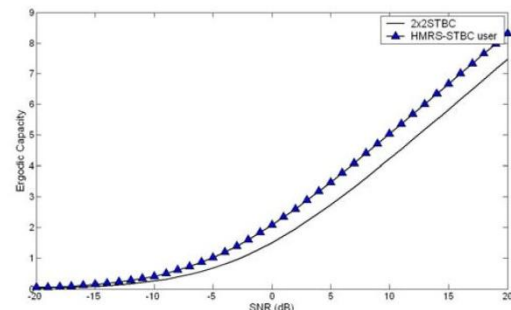Fig. 8 Symbol error rate of FC when the number of PR-user (N) is increased

Fig. 10 Exact closed-form ergodic capacity of HMRS (STBC user) and 2x2STBC

second model in Fig. 3. The interference level in PR-network is changed according to the number of PR-user. The power of CR-user is needs increased for keeping the quality of information at SER=10^{-4}. Therefore, N number is an important factor for designing the CR-network.

Fig. 10 illustrates the exact closed-form ergodic capacity of 2x2STBC and HMRS by using (21) and (22), respectively. As the results, the maximum data rate that can be supported by channel without error of HMRS technique exceeds the data rate of 2x2STBC scheme. Therefore, the higher modulation order can be applied by HMRS technique.
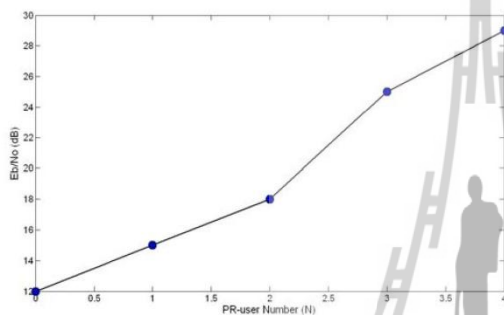

Fig. 9 The varying power of CR-user versus the number of PR-user

Fig. 7 illustrates the changing of both CR-user power and SNR at the PR-BTS versus time interval under the situation of the first model in Fig. 2. When CR-user moves continuously to the center of PR-network, the SNR at PR-BTS is also decreased because the interference in PR-network is increased versus the distance between CR-user and PR-BTS. At time interval=5, the SNR at PR-BTS is closely decreased to the threshold level (we assume threshold level=12dB). Hence, the PR-network commands CR-network urgently to change the operating frequency. Finally, the SNR at PR-BTS can be returned to the initial level (21dB) after CR-network changes the spectrum band.

Fig. 8 illustrates the varying of SER of HMRS when N number is increased. We assign d_b=0.01 in (3), the power from each PR-user is assigned by E_2=1.3E_1 in simulation. The distances between FC and each PR-user are assumed as the equal distance under the situation of the second model in Fig. 3. If CR-network wants to keep the quality of signal, CR-user needs to increase power according to the N number. The interfering level increases according to the number of PR-user. As the results, if the number of PR-user (N) is 1 then CR-user needs to increase power until SNR at FC is 15dB that differ from the case of no PR-user about 3dB at SER=10^{-4}. Similarly, if the number of PR-user (N) is 4 then CR-user needs to increase power until SNR at FC is 29dB that differ from the case of no PR-user about 17dB at SER=10^{-4}.

Fig. 9 presents the varying power of CR-user when the number of PR-user is increased under the situation of the

VI. CONCLUSION

In this paper, we evaluate SER of HMRS in the model of cognitive radio network under the varying of both power and the number of PR-user. We apply HMRS technique for CR-network to investigate its performance in the environment of CR-network. As the results, the SER performance of HMRS is degraded by increasing the PR-user number corresponding to a far distance between FC and CR-user. In Fig. 7, the correlation between the power of CR-user and PR-user may be represented as a key for the energy handling in CR-network in future work. In addition, we derive an exact closed-form expression of the ergodic capacity of the HMRS technique compare with 2x2STBC scheme. We will investigate the HMRS performance in case of channel estimation error which can be written as a topic of future research.

REFERENCES

[1] T. Yucek and H. Arslan, "A Survey of Spectrum Sensing Algorithms for CR Applications first quarter 2009," University of South Florida, USA, Tech. Rep., 2009.
[2] S. Haykin, "Cognitive radio: Brain-empowered wireless communications", *IEEE Journal on Selected Areas in Communications*, vol. 23, no. 2, pp. 201–219, Feb 2005.
[3] Akin. S and Gursoy M.C.,"On the performance limits of cognitive radio MIMO channels", *WCNC. 2011 IEEE*, pp. 1640-1645, 2011.
[4] Xiaoming Chen, Zhaoyang Zhang and Chao Wang, "Dual QoS Driven Power Allocation in MIMO Cognitive Network with Limited Feedback", *WCNC. 2011 IEEE*, pp. 1829-1833, 2011.
[5] Sha Hua, Hang Liu, Mingquan Wu and Panwar, S.S., "Exploiting MIMO Antennas in Cooperative Cognitive Radio Network", *INFOCOM, 2011 Proceeding IEEE*, pp. 2714-2722, 2011.
[6] Jorswieck, E.A. and Jing Lv, "Spatial shaping in cognitive MIMO MAC with coded Legacy transmission", *SPAWC, 2011 IEEE 12th*, pp. 451-455, 2011.

[7] S. Alamouti, "A simple transmit diversity technique for wireless communication", IEEE Journal of Selected Area in Communications, vol. 16, pp. 1451-1458, Oct 1998.

[8] V. Tarokh, H. Jafarkhani, and A. R. Calderbank, "Space-time block codes from orthogonal designs," *IEEE Transactions on Information Theory, vol.5,* pp.1456–1467, Jul 1999.

[9] G. J. Foschini, "Layered space-time architecture for wireless communications in a fading environment when using multiple antennas", *Bell Labs Tech. J.*, v.1, n.2, pp.41–59, 1996.

[10] Chee Wei Tan and A. Robert Calderbank, "Multiuser Detection of Alamouti Signals", *IEEE Transactions on Communications, Vol. 57, No. 7, 2009,* pp. 2080-2089, 2009.

[11] Walter da C. Freitas Jr., Francisco R. P. Cavalcanti and Renato R. Lopes, "Hybrid Transceiver Schemes for Spatial Multiplexing and Diversity in MIMO Systems", *Journal of Communication and Information systems, vol. 20, No. 3, 2005,* pp. 63-76, 2005.

[12] R.W. Heath Jr. and A. J. Paulraj, "Diversity versus multiplexing in narrow band MIMO channel: A tradeoff base on Euclidean distance", *IEEE trans. On Communication* submitted 2002.

[13] Yong Soo Cho, Jaekwan Kim, *MIMO-OFDM Wireless Communication with MATLAB*, John Wiley&Sons (Asia) Pte Ltd, 2010.

[14] Kyung Seung Ahn, Robert W. Heath Jr. and Heung Ki Baik, "Shannon Capacity and Symbol Error Rate of Space-Time Block Codes in MIMO Rayleigh Channels with Channel Estimation Error", IEEE Transactions on Wireless Communications, Vol. 7, No. 1, pp. 324-333, 2008.

[15] Tanapong Khomyat, Peerapong Uthansakul and Monthippa Uthansakul, "Hybrid-MIMO Receiver with Both Space-Time Coding and Spatial Multiplexing Detections for Cognitive Radio Networks", *ISPACS 2011 IEEE*, pp. 2011.

Performance of MU-MIMO Systems Using HMRS Technique for Various Transmission Modes

Tanapong Khomyat, Peerapong Uthansakul, Monthippa Uthansakul

School of Telecommunication Engineering
Suranaree University of Technology
Nakhonratchasima, Thailand
k_tnp@hotmail.com, uthansakul@sut.ac.th, mtp@sut.ac.th

Abstract— **It is the fact that the bandwidth of wireless communication system is such a limited resource that several techniques are selectively applied to increase the bandwidth efficiency. The highest bandwidth efficiency can be taken by applying MU-MIMO technique. For this technique, the complexity of detection at receiving side is rapidly increased by increasing the number of users at transmitting side. Therefore the lower complex detection is necessarily required for MU-MIMO system. Recently, the simple detection technique called hybrid-MIMO receiver scheme (HMRS) has been proposed by the authors. However, that study neglected the demands of multiple users for transmitting MIMO modes (STBC or SM) which are crucially unpredictable in practice. In this paper, the performance of MU-MIMO system using HMRS technique to support various types of user transmission modes is presented. The results indicate that the HMRS technique can significantly improve the error rate for any modes of transmission.**

Keywords— **SIC,MMSE, ML detection, Hybrid-MIMO**

I. INTRODUCTION

Wireless communications are widely used around the world. The new applications have been frequently established such as WLAN, 3GB, LTE, etc. Many customers need to access the limited spectrum in the same time. Therefore the available bandwidth cannot be enough used for every user [1]. The saving bandwidth techniques for wireless communication have been researched and already applied such as TDMA, CDMA, MIMO [2]-[4], hybrid-MIMO [5]-[7], MU-MIMO [8], etc. Fig. 1 illustrates MU-MIMO system. The transmitted signals from N users are sent through MIMO channel and reached to the receiver in the same time and frequency to take a high bandwidth efficiency, capacity gain and diversity gain. The receiver must have capability to suppress interference and detect all symbols from all users by using multi-users detection such as QR decomposition [9], ZF detection, MMSE detection [10], ML detection [11], Sphere detection [12], IC [13], etc. In 2005, the simple hybrid-MIMO technique called Hybrid-MIMO Transceiver Scheme (HMTS) [14] has been proposed. The two users at transmitting side apply Space-Time Block Code (STBC) or Spatial Multiplexing (SM) to encode the transmitted signals. It has a simple structure when a few users are operated in the system because MMSE detection and Successive Interference Cancellation (SIC) [15] are jointly applied. However, the complexity of detection at

receiver is increased when a lot of users are operated because the MMSE detection and SIC are operated every time of detecting SM layer. Recently, we proposed the novel hybrid-MIMO technique called Hybrid-MIMO Receiver Scheme (HMRS) [16] that the system applies ML detection and SIC jointly to detect all symbols in entire layers. The ML detection is operated only one time for every case of N users, thus this scheme has the number of detecting procedures less than HMTS.The comparison of SER performance between HMRS and HMTS is presented in Section IV. However, the work in [16] did not study on the various types of user demand on MIMO transmission modes.

In this paper, we investigate the SER performances of HMRS in case of N users, where N can be assigned as 2,3 and 4, in order to study the effect of the various transmission modes. Because the several users may be randomly operated in practice, thus the evaluation of SER performance under this situation is an important task. From the aboveanalyzing results, we can use it to assign the transmittingparameterskeenly including the transmitting power, antenna gain, modulation scheme, channel coding scheme and the number of antennas. Moreover, the transmitted signal, the received signal and the structure of N users HMRS are presented in this work in order to reveal the procedure of the HMRS system clearly.

The remainder of this paper is structured as follows. In Section II, we present the system overview. Then the concept of HMRS is depicted in section III. The system performances are shown in section IV and followed by the conclusion in section V.
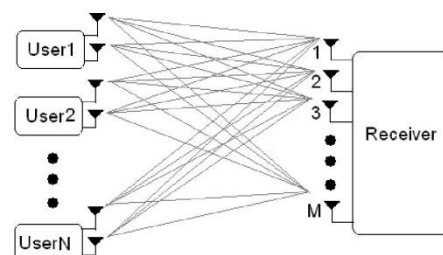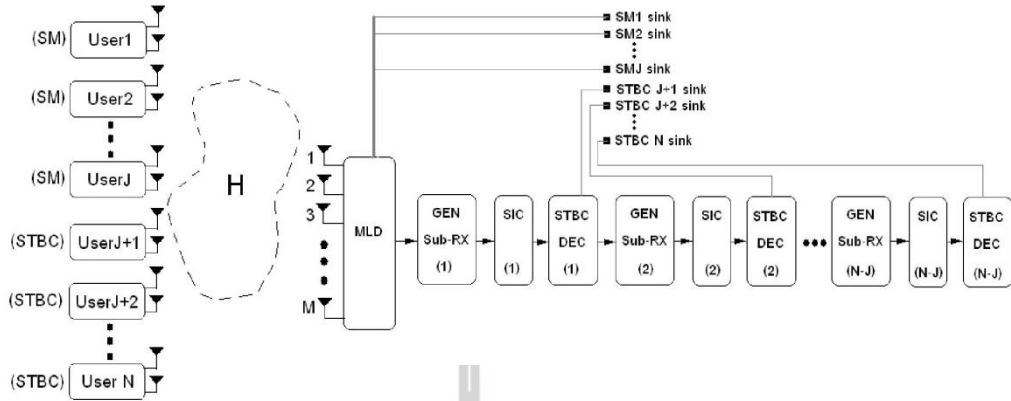

Fig. 1 MU-MIMO system

Fig. 2 MU-MIMO system with HMRS technique

II. SYSTEM OVERVIEW

The structure of MU-MIMO system is shown in Fig. 1. All MIMO streams are simultaneously transmitted by N users at transmitter. Each user equipped with a 2-element antenna array and applies the 2xM STBC or 2xM SM system. The receiver equipped with an M-element array. The transmitted signals are sent through a random channels matrix **H** in uplink channel. Flat and slow Rayleigh fading is assumed to evaluate the SER performance. The receiver can detect all symbols from all users by using MU detection. We can express the received signal as

$$\mathbf{y} = \mathbf{Hs} + \mathbf{w} \qquad (1)$$

where **y** is the received signal, **H** is Mx2N MIMO channel matrix, **s** represents the 2Nx1 transmitted signal vector and **w** denotes Mx1 AWGN vector. The channel matrix **H** is assumed to have unit variance that can be described as

$$E\left[\|\mathbf{H}\|_F^2\right] = 2NM \qquad (2)$$

where $\|\mathbf{A}\|_F$ denotes the Frobenius norm of axb matrix **A**, it can be expressed as $\|\mathbf{A}\|_F \triangleq \sqrt{\sum_{i=1}^{a}\sum_{j=1}^{b}|A_{ij}|^2}$ and $E[\cdot]$ represents the expectation operator.

III. MU-MIMO SYSTEM USING HMRS

The hybrid-MIMO system applies both SM and STBC to encode the transmitted signals for each user at the transmitting side. The structure of Multi-user HMRS is illustrated in Fig. 2. The N users at transmitting side are encoded by using SM and STBC code where J users and N-J users are applied by encoding SM and STBC code, respectively. The transmitted signals are sent through the MIMO channel. At the receiver, the ML detection is used to get all symbols of SM users. All

symbols of STBC users can be successively taken by operating the N-J modules ofthe sub-received signals generator (GEN Sub-RX), SIC and STBC decoding. In this section, the signals and detecting procedure of the HMRS are demonstrated (where N=3, J=2 and M=4). The equivalent Space-Time Coding matrix for three users HMRS can be given by

$$\mathbf{s} = \begin{bmatrix} s_1 & s_2 & s_3 & s_4 & s_5 & s_6 \\ s_7 & s_8 & s_9 & s_{10} & -s_6^* & s_5^* \end{bmatrix}^T \qquad (3)$$

the 2x2N MIMO channel can be described as

$$\mathbf{H} = \begin{bmatrix} h_{11} & h_{21} & h_{31} & h_{41} & h_{51} & h_{61} \\ h_{12} & h_{22} & h_{32} & h_{42} & h_{52} & h_{62} \\ h_{13} & h_{23} & h_{33} & h_{43} & h_{53} & h_{62} \\ h_{14} & h_{24} & h_{34} & h_{44} & h_{54} & h_{64} \end{bmatrix} \qquad (4)$$

where h_{mn} is the complex channel coefficient of the mth transmit antenna to the nth receive antenna.The corresponding received signals can be expressed as

$$\mathbf{y} = \mathbf{Hs} + \mathbf{w} = \begin{bmatrix} y_1 & y_5 \\ y_2 & y_6 \\ y_3 & y_7 \\ y_4 & y_8 \end{bmatrix} \qquad (5)$$

all symbols of SM user can be calculated by

$$\hat{\mathbf{s}} = \arg\min_{\tilde{\mathbf{s}} \in C^{2N}} \|\mathbf{y} - \mathbf{H}\tilde{\mathbf{s}}\|^2 \qquad (6)$$

$$\hat{\mathbf{s}}_{SM} = \begin{bmatrix} \hat{s}_1 & \hat{s}_2 & \hat{s}_3 & \hat{s}_4 \\ \hat{s}_7 & \hat{s}_8 & \hat{s}_9 & \hat{s}_{10} \end{bmatrix}^T \qquad (7)$$

where $\hat{\mathbf{s}}_{SM}$ denotes the 1st row to the 4th row in (6). The equivalent received signals of SM users can be generated as

$$\hat{\mathbf{y}}_{SM} = \mathbf{H}_{SM}\hat{\mathbf{s}}_{SM} \qquad (8)$$

where $\mathbf{H}_{SM}$ is the 1st column to the 4th column of MIMO channel $\mathbf{H}$. The equivalent received signals of STBC users can be calculated as

$$\hat{\mathbf{y}}_{STBC} = \mathbf{y} - \hat{\mathbf{y}}_{SM} = \begin{bmatrix} y_a & y_b \\ y_c & y_d \\ y_e & y_f \\ y_g & y_h \end{bmatrix} \qquad (9)$$

$$\mathbf{y}_{STBC}^{\nabla} = \begin{bmatrix} y_a & y_b^* & y_c & y_d^* & y_e & y_f^* & y_g & y_h^* \end{bmatrix}^T \qquad (10)$$

$$\mathbf{H}_{STBC}^{\nabla} = \begin{bmatrix} h_{51} & h_{61}^* & h_{52} & h_{62}^* & h_{53} & h_{63}^* & h_{54} & h_{64}^* \\ h_{61} & -h_{51}^* & h_{62} & -h_{52}^* & h_{63} & -h_{53}^* & h_{64} & -h_{54}^* \end{bmatrix}^T \qquad (11)$$

$$\hat{\mathbf{s}}_{STBC} = \mathbf{H}_{STBC}^{\nabla}\mathbf{y}_{STBC}^{\nabla} = \begin{bmatrix} \hat{s}_5 \\ \hat{s}_6 \end{bmatrix}. \qquad (12)$$

Finally, the decoding symbols of SM and STBC users can be taken from (7) and (12), respectively. As indicated in the HMRS procedure, all symbols of SM users can easily be obtained by using ML detection in only one times but HMTS technique in [14] applies MMSE filter many times to take all symbols of SM users. Hence it can be indicated that the HMRS can offer the benefit of simplification more than the HMTS.

IV. Performance Evaluations

In this section, the simulations of MU-MIMO with HMRS performances in case of N users (N=2, 3 and 4) are presented to reveal the effect of increasing the number of user at the transmitting side. The several transmitting configuration are assigned in the Monte-Carlo simulation model to investigate the trend of HMRS performance under the multi-users situation. Fig. 3 illustrates the SER performance comparison of HMRS and HMTS in case of two users. Both SM and STBC user apply BPSK modulation to form the transmitted signals. As the result, HMRS can offer higher performance than HMTS about 10dB at 10^{-4} SER.

Fig. 4 presents the SER performance of the two users HMRS. STBC user can take higher performance than SM user because of applying the interference cancellation and the orthogonal structure of STBC code. The dash line is represented the average performance of the system.

Fig. 5 illustrates the SER performance of the three users HMRS, the STBC code is used by two users and the SM code is used by one user. The highest performance can be taken by STBC user2 because the two steps of the interference cancellation are continuously applied at the receiver to detect
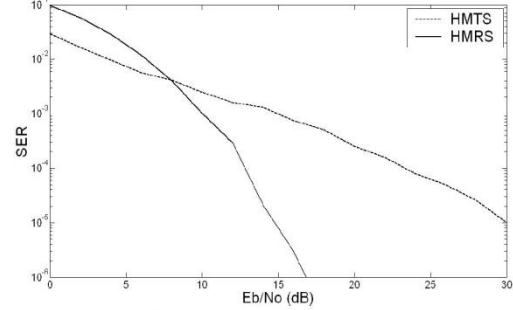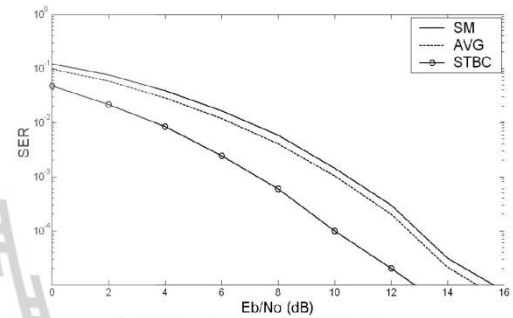

Fig. 3 SER performance of HMRS and HMTS.

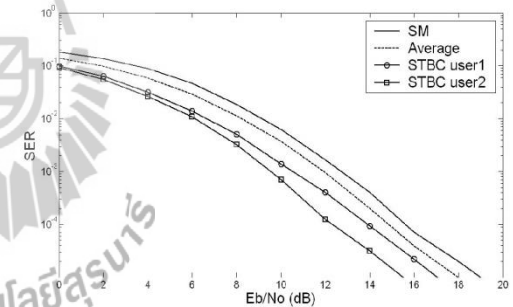Fig. 4 SER performance of HMRS for 2 users.

Fig. 5 SER performance of HMRSfor 3 users (1SM, 2STBC).

the symbols of STBC user2. Hence the last layer has the level of interference less than other layers.

Fig. 6 illustrates the SER performance of the three users HMRS, the STBC code is used by one user and the SM code is used by two users. The highest performance can be taken by STBC user because the SIC technique is employed before this layer is detected. The performance of SM user1 and SM user2 are equivalence because the symbols of all SM users can be taken by ML detection in one times. The HMRS in Fig. 5 has a higher performance than the HMRS in Fig. 6 because the two steps of the interference cancellation are continuously applied at the receiver.

Fig. 7 shows the SER performance of the four users HMRS. The STBC code is used by one user and the SM code is used
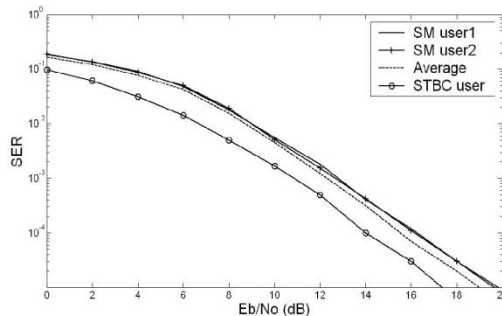
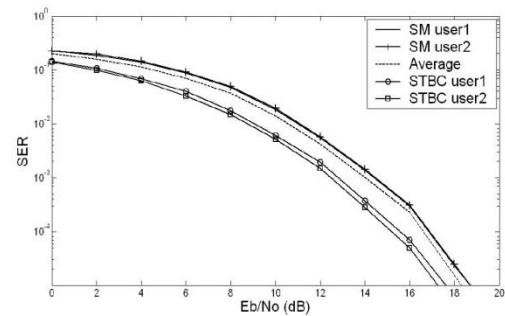Fig. 6 SER performance of HMRS for 3 users (2SM, 1STBC)

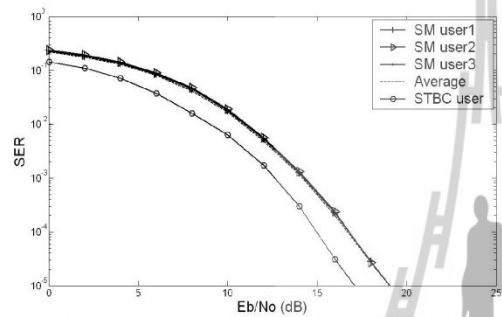Fig. 8 SER performance of HMRS for 4 users (2SM, 2STBC)

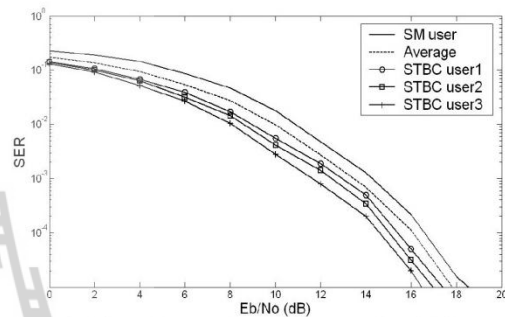Fig. 7 SER performance of HMRS for 4 users (3SM, 1STBC)

Fig. 9 SER performance of HMRS for 4 users (1SM, 3STBC)

by three users. The highest performance can be taken by STBC user. The performance of all SM users are equivalence because the symbols of all SM users can be taken by ML detection in one times.

Fig. 8 shows the SER performance of the four users HMRS. The STBC code is used by two users and the SM code is used by two users. The highest performance can be achieved by STBC user2 because the two steps of the interference cancellation are continuously applied at the receiver to detect the symbols of STBC user2. The performance of STBC users can also be enhanced by the orthogonal property of STBC code.

Fig. 9 shows the SER performance of the four users HMRS. The STBC code is used by three users and the SM code is used by one user. The highest performance can be achieved by STBC user3 because the three steps of the interference cancellation are continuously operated at the receiver to detect the symbols of STBC user3. The performance of HMRS in this figure has a higher performance than the HMRS in Fig. 7 and Fig. 8 (four users HMRS) because the interference level of this system can intensely be decreased by using many SIC modules and the orthogonal property of STBC users.

V. CONCLUSIONS

In this paper, the investigation of MU-MIMO system with HMRS technique for N users (N=2, 3 and 4) are presented. The study of SER performance when increasing the number of

users is reported. From the results, the average SER performance of the HMRS is degraded when the number of users are increased. The SER performances of HMRS can be improved when the number of STBC users more than the number of SM users but the spectral efficiency is also degraded. The SER performances of SM users in any configuration of HMRS are corresponded when they have the same total number of users. When the comparison between HMRS and HMTS is presented, it can indicate that the HMRS offers higher advantages than HMTS, both in SER performance and the complexity of the detecting procedure under the same spectral efficiency scenario. In case of the three users HMRS (1SM user, 2STBC users), the simulation result can reveal that the performance of STBC user1 is close to SM user. The STBC user2 give higher performance than STBC user1. Therefore, the system needs to detect the symbols of STBC user2 in the second step if the location of STBC user2 is placed far away from the base station more than STBC user1. In case of four users HMRS (2SM users, 2STBC users), the equivalent performances of both STBC users are presented. This transmission mode can appropriately be applied in MU-MIMO systems in the situation of the same distance between the location of both STBC users and the base station. In case of the multi-STBC users scenario, the sysmbol of STBC users can be detected in the end of process if the locations of the STBC users are positioned at the largest distance from the base station. Consequently, the signals of other cells are mildly interfered because this STBC layer can

be transmitted by applying the lowest power. From above reasons, each transmission mode can offer the different benefits. Especially, the base station needs to detect the symbols in each STBC layer sequentially by considering the level of interference in each layer and the position of each user. Moreover, the limit of the Multi-user HMRS depends on the number of users. When many users are placed in the system, the complexity of ML detection is intensely increased. Therefore the system needs to choose the number of users carefully.

REFERENCES

[1] T. Yucek and H. Arslan, "A Survey of Spectrum Sensing Algorithms forCR Applications first quarter 2009," University of South Florida, USA,Tech. Rep., 2009.

[2] S. Alamouti, "A simple transmit diversity technique for wireless communication", IEEE Journal of Selected Area in Communications, vol.16, pp. 1451-1458, Oct 1998.

[3] V. Tarokh, H. Jafarkhani, and A. R. Calderbank, "Space-time block codes from orthogonal designs," *IEEE Transactions on Information Theory, vol.5*, pp.1456–1467, Jul 1999.

[4] G. J. Foschini, "Layered space-time architecture for wireless communications in a fading environment when using multiple antennas", *Bell Labs Tech. J.*, v.1, n.2, pp.41–59, 1996.

[5] Yu-Jin Song, Seong-WeonKo, Hyun-Jin Park, Hun-Hee Lee and Hyoung-Kyu Song, "AnovelefficientdetectionschemeforhybridSTBCinMIMO-OFDMsystems", *ICCT 2010 12th IEEE*, pp. 701-704, 2010.

[6] L. Zhao and V.K. Dubey. Transmit diversity and combining scheme for spatial multiplexing over correlated channels. *Vehicular Technology Conference, 2004. VTC 2004-Spring. 2004 IEEE 59th*, 1:380–383, 2004.

[7] J. Cortez, M. Bazdresch, D. Torres and R. Parra-Michel, "ABBA-VBLAST hybrid space-time code for MIMO wireless communications",*CCE 2008 5th IEEE*, pp. 257-262, 2008.*FLEXChip Signal Processor (MC68175/D)*, Motorola, 1996.

[8] HienQuoc Ngo, Duong, T.Q. and Larsson, E.G., "Uplinkperformance analysis of multicellMU-MIMO with zero-forcing receivers and perfect CSI", *Swe-CTW, 2011 IEEE*, pp. 40-45, 2011.

[9] Chee Wei Tan and A. Robert Calderbank, "Multiuser Detection of Alamouti Signals", *IEEE Transactions on Communications, Vol. 57, No. 7, 2009*, pp. 2080-2089, 2009.

[10] Lie-Liang Yang, "Receiver Multiuser Diversity Aided Multi-Stage MMSE Multiuser Detection for DS-CDMA and SDMA Systems Employing I-Q Modulation", Vhhicular Technology Conference Fall, 2010, IEEE 72nd.

[11] Kai Liu, Xing, S. S., "Combined Multi-stage MMSE and ML multiuser detection for underdetermined MIMO systems", CCWMC 2011. pp. 10-14, 2011.

[12] Ali Shah M., Mennenga B. and Fettweis G., "Iterative Soft-In Soft-Out Sphere Detection for 3GPP LTE", VTC 2010-Spring, IEEE 71st, pp.1-5, 2010

[13] Sanada, Y. and Qiang Wang, "A co-channel interference cancellation technique using orthogonal convolutional codes on multipath Rayleigh fading channel", *Vehicular Technology, IEEE Transactions on Volume: 46 , Issue: 1*, pp. 114-128, 1997

[14] Walter da C. Freitas Jr., Francisco R. P. Cavalcantiand Renato R. Lopes, "Hybrid Transceiver Schemes for SpatialMultiplexing and Diversity in MIMO Systems", *Journal of Communication and Information systems, vol. 20, No. 3, 2005*, pp. 63-76, 2005.

[15] Steffen Reinhardt, TufikBuzid and Mario Huemer, "Successive interference cancellation for SC/FDE-MIMO system", *PIMR C2006 IEEE*, pp. 1-5, 2006.

[16] TanapongKhomyat, Peerapong Uthansakul and MonthippaUthansakul,"Hybrid-MIMO Receiver with Both Space-Time Coding and Spatial Multiplexing Detections for Cognitive Radio Networks", *ISPACS 2011 IEEE*, 2011.

Switching Transmission Mode in Multiuser-MIMO systems

Tanapong Khomyat[1,2], Peerapong Uthansakul[2], Monthippa Uthansakul[2] and Soong Boon Hee[3]
[1]Department of Electrical Engineering
Rajamangala University of Technology Lanna Tak, Tak, Thailand
[2]School of Telecommunication Engineering
Suranaree University of Technology
Nakhonratchasima, Thailand
[3]Division of Communication Engineering
Nanyang Technological University, Singapore
Email: k_tnp@hotmail.com

Abstract—**The developing fifth generation (5G) wireless networks are prepared to support the fundamental challenges, for example, very high data rate application, power control and high spectrum efficiency. To achieve these requirements, Multiuser Multiple-Input Multiple-Output (MU-MIMO) systems is the attractive option to increase both data rate and spectrum efficiency in uplink channel. In this paper, switching between spatial multiplexing (SM) and transmit diversity (TD) is proposed to increase the diversity performance in MU-MIMO systems. In this technique, the different transmission modes can be chosen for each user based on the instantaneous channel state at the receiver. Monte Carlo simulations validate advantage of the proposed technique over either spatial multiplexing or hybrid-MIMO technique in term of symbol error rate.**

Index Terms—**Multiuser Multiple-Input Multiple-Output (MU-MIMO), space-time coding, spatial multiplexing.**

I. INTRODUCTION

In the next generation, the available wireless channel is continuously decreased by the various wireless applications that support the increasing demand for worldwide communication [1]-[3]. Many techniques have been applied to increase the spectral efficiency such as Orthogonal Frequency Division Multiplexing (OFDM), Multiple-Input Multiple-Output (MIMO) systems [4] and spreading code that have a limit to expand the available channel and increase data rate. One optional technique to increase the spectral efficiency is Multi-modes MIMO systems [5], because it can increase the spectral efficiency and maintain the diversity benefits in the uplink channel. To improve performance of MU-MIMO in practice, among users can apply different transmission mode independently by decision of receiver because the channel states in MIMO systems are continuously changed. Two general modes in MIMO channel are spatial multiplexing (SM) [6] and transmit diversity (TD) [7] can improve capacity gain and diversity advantage, respectively. However the switching transmission mode in MU-MIMO has not been proposed in literatures.

In this paper, we consider the problem of mode selection between SM and TD mode in MU-MIMO systems based on the instantaneous channel at the receiver [5]. Low-rate feedback channel from the receiver to each user is required.

The receiver utilizes switching criterion by considering minimum Euclidean distance of the receive signal. Flat-fading channel is known perfectly to the receiver but not to each user. Transmitted data of two users are mapped by 4QAM signal and send simultaneously to the receiver. We consider Alamouti scheme and BLAST system (Maximum likelihood detection: MLD) for TD and SM mode, respectively. To succeed the mode selection, we calculate Euclidean distance of both TD and SM mode for comparing the channel quality between two modes for each user at the receiver. Simulations show advantage of the proposed technique over static SM and static hybrid MIMO [8] (the fixed number of SM and TD user are assigned at the transmitter).

The remainder of this paper is structured as follows. In Section II, we present the system model. The Euclidean distances of SM and TD mode and the switching criterion are presented in Section III. In Section IV, the simulation results are discussed. Finally, Section V concludes the work.
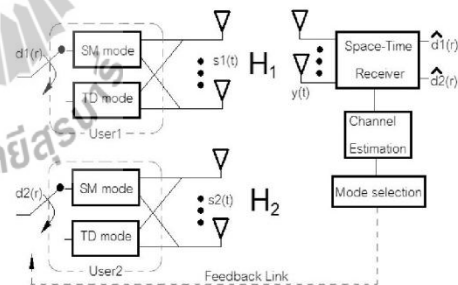

Fig. 1. MU-MIMO system where each user switches between SM and TD mode based on feedback from the receiver.

II. SYSTEM MODEL

We consider the MU-MIMO system with K users, K=2 (e.g. uplink cellular) in Fig. 1, where each user equipped with N_t antennas, N_t = 2. All streams are simultaneously transmitted to a receiver equipped with N_r antennas, N_r=4. All users are synchronous in the sense that each user transmits its symbol

vector in the synchronization with others. To succeed the mode selection, the MIMO channel matrix of each user is independently utilized to compute the minimum Euclidean distance of both SM and TD mode. The decisions at the receiver are sent back to each user at transmitting side. The signals of user k are sent through the $N_r \times N_t$ random channel matrix $\mathbf{H}_k$, and the overall channel matrix is denoted by $\mathbf{H}=[\mathbf{H}_1, \mathbf{H}_2, \ldots, \mathbf{H}_K]$. The MIMO channel is assumed to be a flat-fading, all sub-channels between all users and receiver are assumed to be independence. The received signal is then given by

$$\mathbf{Y} = \sum_{k=1}^{K} \mathbf{H}_k \mathbf{s}_k + \mathbf{w},$$

(1)

where $\mathbf{Y}$ denotes the $N_r \times 1$ vector of received signal, $\mathbf{s}_k$ represents $N_t \times 1$ transmit data symbol vector consisting of N_t symbols each with a constellation size M, $\mathbf{w}$ denotes $N_r \times 1$ vector i.i.d. complex circular Gaussian random variable; each element distributed as $CN(0, N_0)$. The average energy of the transmitted symbol from each antenna is assumed to be E_s. The entries of channel matrix $\mathbf{H}$ is assumed to have unit variance that can be expressed as

$$E[\|\mathbf{H}\|_F^2] = N_t K N_r.$$

(2)

The transmitted power is constrained by

$$E[\mathbf{s}_k \mathbf{s}_k^H] = E_s \mathbf{I}_{N_t},$$

(3)

where $\mathbf{I}_B$ is the identity matrix of size $B \times B$, ^{H} denotes the complex conjugate transpose, $\|\mathbf{A}\|_F$ denotes the Frobenius norm of $a \times b$ matrix $\mathbf{A}$, it can be defined as $\|\mathbf{A}\|_F \triangleq \sqrt{\sum_{i=1}^{a} \sum_{j=1}^{b} |A_{ij}|^2}$ and $E[\cdot]$ is the expectation operator. In the MU-MIMO receiver, the previous decoding symbols usually have the probability of error during detection; thus the cancellation of Successive Interference Cancellation (SIC) cannot be completed without error propagation (Ep). For detecting symbol of user k, all streams of other users are cancelled to get the received signal for user k as follows:

$$\mathbf{Y}_k = \mathbf{Y} - \sum_{m=1}^{K} \hat{\mathbf{H}}_m \hat{\mathbf{s}}_m,$$

(4)

where $\hat{\mathbf{H}}_m$ denotes the estimated channel for user m, $m \neq k$ and $\hat{\mathbf{s}}_m$ denotes detected signal vector for user m. From (4), $\hat{\mathbf{s}}_m$ can be detected by spatial multiplexing (SM). The receiver solves the ML detection problem

$$\hat{\mathbf{s}}_m = \frac{\arg\min}{\mathbf{s} \in M^{N_t}} \|\mathbf{Y} - \mathbf{H}\mathbf{s}\|^2,$$

(5)

The detected symbols of user k in (4) can be detected by applying MLD or Alamouti decoding. Repeat all process until the detected symbols of all K users are received.

III. TRANSMISSION MODE

In this section, we present the method to compute the squared minimum Euclidean distance [5] for the two utilized modes and the switching criterion at the transmitting side.

A. Spatial multiplexing mode

SM technique can send independent streams of transmitted symbols from each antenna. All streams are simultaneously transmitted to the receiver by the same spectrum without spreading code. MLD technique is applied for all users. The squared minimum Euclidean distance of SM mode can be computed by search the minimum distance as follows:

$$d_{\min,\mathrm{SM}}^2(\mathbf{H}_k) := \min_{\mathbf{m},\mathbf{n} \in M, \mathbf{m} \neq \mathbf{n}} \|\mathbf{H}_k(\mathbf{m} - \mathbf{n})\|^2,$$

(6)

$$\min_{\mathbf{m},\mathbf{n} \in M, \mathbf{m} \neq \mathbf{n}} \|\mathbf{m} - \mathbf{n}\|^2 = \frac{d_{\min,\mathrm{sm}}^2}{N_t},$$

(7)

$$\sigma_{\min}^2(\mathbf{H}_k) \frac{d_{\min,\mathrm{sm}}^2}{N_t} \leq d_{\min,\mathrm{SM}}^2(\mathbf{H}_k)$$

(8)

where $\mathbf{m}$ and $\mathbf{n}$ denote the transmitted code words, $d_{\min,\mathrm{sm}}^2$ denotes the minimum Euclidean distance of the transmit constellation, $\sigma_{\min}^2(\mathbf{H}_k)$ denotes the minimum singular value of $\mathbf{H}_k$ and $\|\mathbf{A}\|^2$ is the matrix norm of matrix $\mathbf{A}$. From (8), singular value of channel matrix indicates the quality of MIMO channel for each user.

B. Transmit diversity mode

TD mode is the second mode for all users. The improvement of diversity gain can be archived by the orthogonal property of Alamouti code. The orthogonal code words are sent to multiple antennas during 2 time slot of Alamouti code.

$$d_{\min,\mathrm{TD}}^2(\mathbf{H}_k) \leq \frac{1}{N_t} \|\mathbf{H}_k\|_F^2 d_{\min,\mathrm{td}}^2$$

(9)

$$d_{\min,\mathrm{TD}}^2(\mathbf{H}_k) \leq \frac{1}{N_t} d_{\min,\mathrm{td}}^2 \sum_{j=1}^{G} \sigma_j^2(\mathbf{H}_k)$$

(10)

where $G = \min(N_t, N_r)$ and σ_j is the jth singular value of $\mathbf{H}_k$. From (10), the quality of MIMO channel can also be indicated by the singular value of channel matrix.

C. Switching criterion for each user

In MU-MIMO systems, the quality of MIMO channel for each user is always changed. Thus the static MIMO schemes cannot always offer the best performance. Either SM or TD mode may take more advantage than other at any instantaneous time. Therefore the switching transmission mode is the attractive option to improve the performance of
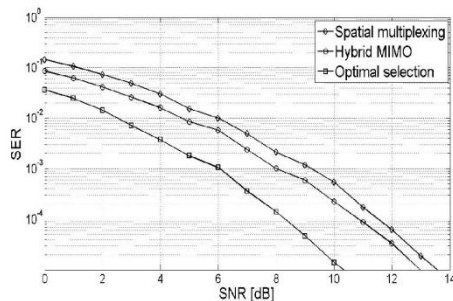
Fig. 2. Symbol error rate versus SNR for $K=2$, $N_t=2$,$N_r=4$ MU-MIMO system with 4-QAM signal and optimal selection of SM or TD mode based on minimum Euclidean distance.

Fig. 3. Symbol error rate versus SNR for each user when $K=2$, $N_t=2$,$N_r=4$ with 4-QAM signal and optimal selection of SM or TD mode based on minimum Euclidean distance.

MU-MIMO systems. The selection criterion for obtaining the best transmission mode can be done by calculating the minimum Euclidean distance of both SM and TD mode for each user. In order to get the switching criterion, compute $d_{\min,\text{TD}}^2(\mathbf{H}_k)$ from (9) and $d_{\min,\text{SM}}^2(\mathbf{H}_k)$ from (6). The best mode can be chosen from the largest minimum Euclidean distance. Therefore the SM mode is preferred when

$$\|\mathbf{H}_k\|_F^2 d_{\min,\text{td}}^2 \leq \sigma_{min}^2(\mathbf{H}_k) d_{\min,\text{sm}}^2. \qquad (11)$$

IV. SIMULATION RESULTS

In this section, Monte Carlo simulation is used to reveal the advantage of the switching transmission mode in MU-MIMO system over the general SM-MIMO and hybrid-MIMO system. The bit streams of all users are mapped with 4-QAM signal and encode symbol streams by either SM or Alamouti code. In simulation, the mode selection in (11) of each user in the proposed technique is always made every two symbols periods by computing the minimum Euclidean distance of both SM and TD mode. To present the advantage of the proposed technique, the general SM-MIMO and hybrid-MIMO technique are utilized in MU-MIMO system to compare with the switching transmission mode technique. Where hybrid-MIMO system also applies MLD, SIC and Alamouti coding like the proposed technique, but the transmission mode of each user in hybrid-MIMO are not changed (SM and Alamouti scheme are always applied by User1 and User2, respectively). In contrast, both users of SM-MIMO system apply only SM mode.

Fig. 2 shows the SER performance of the optimal selection technique (proposed scheme) with $K=2$, $N_t=2$, $N_r=4$. It shows that power gain of the proposed scheme against the SM-MIMO and hybrid-MIMO are 3 dB and 3.5 dB, respectively. The performance of hybrid-MIMO is better than SM-MIMO because the orthogonal structure of Alamouti code at User2. However the proposed technique offers the highest diversity advantage because the qualities of MIMO channels are always changed by the traveling of users and any object in
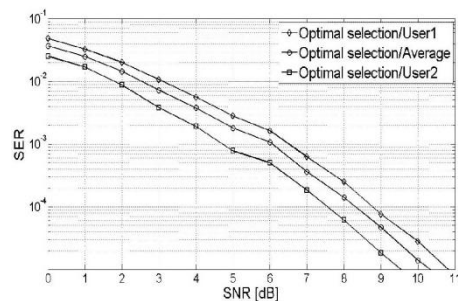
real practical network. Mode of each user is always selected according to the quality of MIMO channels by utilizing (6), (9) and (11). Moreover the diversity advantage of SM and TD mode are differently given by varying SNR in the networks.

Fig. 3 illustrates the SER performance of each user in the optimal selection technique (proposed scheme) with $K=2$, $N_t=2$, $N_r=4$. It shows that performance of User2 is higher than User1, because the second detection experiences lower interference level than the first detection. Thus the detected sequence of each user should be carefully considered by decision of the base station.

V. CONCLUSIONS

In this paper we propose the switching criterion to apply in MU-MIMO system that switches between spatial multiplexing (SM modes) and transmit diversity (TD mode) based on instantaneous channel state information. The receive signal of both SM and TD mode are utilized to calculated the minimum Euclidean distance for making decision at the receiver. The proposed technique offers the highest diversity advantage when compare with SM-MIMO and hybrid-MIMO system because the qualities of MIMO channels are always changed by the traveling of users and any object in real practical scenario. Moreover the second detection experiences lower interference level than the first detection. Thus the detected sequence of each user should be carefully considered by decision of the base station and the requirements of each user.

REFERENCES

[1] E. Hossain, M. Rasti, H. Tabassum and A. Abdelnasser, "Evolution toward 5G multi-tier cellular wireless networks: An interference management perspective," *IEEE Trans. Wireless. Commun.*, vol. 21, no. 3, pp. 118-127, June. 2014.

[2] W. H. Chin, Z. Fan and R. Haines, "Emerging technologies and research challenges for 5G wireless networks," *IEEE Trans. Wireless Commun.*, vol. 21, no. 2, pp. 106-112, April. 2014.

[3] S. Y. Lien, K. C. Chen, Y. C. Liang and Y. Lin, "Cognitive radio resource management for future cellular networks," *IEEE Trans. Wireless. Commun.*, vol. 21, no. 1, pp. 70-79, Feb. 2014.

[4] C. W. Tan and A. R. Calderbank, "Multiuser Detection of Alamouti Signals", *IEEE Trans. Commun.*, vol. 57, No. 7, pp. 2080-2089, July 2009.

[5] R. W. Heath and A. J. Paulraj, "Switching between diversity and multiplexing in MIMO systems," *IEEE Trans. Commun.*, vol. 53, no. 6, pp. 962-968, June. 2005.

[6] G. J. Foschini, "Layered space-time architecture for wireless communications in a fading environment when using multiple antennas", *Bell Labs Tech. J.*, vol.1, no.2, pp.41–59, Oct 1996.

[7] S. Alamouti, "A simple transmit diversity technique for wireless communication", *IEEE J. Select. Areas Commun.*, vol. 16, no. 8, pp. 1451-1458, Oct 1998.

[8] L. Zhao and V.K. Dubey. "Transmit diversity and combining scheme for spatial multiplexing over correlated channels," in *Proc. VTC*, May 2004, pp. 380–383.

ผลกระทบจากการเคลื่อนที่ของผู้ใช้งานระบบแบบแผน
เครื่องรับไฮบริดไมโมและจำนวนผู้ใช้งานที่มีต่อเครือข่ายรับรู้ทางวิทยุ

ธนพงศ์ คุ้มญาติ

สาขาวิศวกรรมโทรคมนาคม

มหาวิทยาลัยเทคโนโลยีสุรนารี

k_tnp@hotmail.com

พีระพงษ์ อุฬารสกุล

สาขาวิศวกรรมโทรคมนาคม

มหาวิทยาลัยเทคโนโลยีสุรนารี

uthansakul@sut.ac.th

มนต์ทิพย์ภา อุฬารสกุล

สาขาวิศวกรรมโทรคมนาคม

มหาวิทยาลัยเทคโนโลยีสุรนารี

mtp@sut.ac.th

บทคัดย่อ

ในบทความนี้ เสนอผลการจำลองและวิเคราะห์สมรรถนะของระบบแบบแผนเครื่องรับไฮบริดไมโม (HMRS) ที่ใช้งานบนเครือข่ายรับรู้ทางวิทยุ (Cognitive Radio Network: CR network) มีการหาผลกระทบทางด้านพลังงานในเครือข่ายเมื่อมีการปรับระดับพลังงานของลูกข่าย (CR user) ในเครือข่าย และในกรณีที่มีการเพิ่มจำนวนของผู้ใช้งานของเครือข่ายหลัก (Primary user) ภาคส่งของระบบแบบแผนเครื่องรับไฮบริดไมโม สามารถส่งสัญญาณที่ใช้การเข้ารหัสไมโมได้ทั้งแบบบล็อกเชิงตำแหน่งเวลา (STBC) และแบบมัลติเพล็กซ์เชิงตำแหน่ง (SM) บนความถี่และเวลาเดียวกันไปยังเครื่องรับที่ใช้เทคนิคการตัดสัญญาณแทรกสอดแบบต่อเนื่อง (SIC) ร่วมกับการตรวจวัดสัญญาณแบบความน่าจะเป็นจริงสูงสุด (MLD) จากผลการจำลองพบว่าการเคลื่อนที่ของลูกข่ายและจำนวนผู้ใช้งานของเครือข่ายหลักมีผลอย่างมากต่อการควบคุมพลังงานในเครือข่ายรับรู้ทางวิทยุ นอกจากนี้ในบทความได้วิเคราะห์สมการความจุช่องสัญญาณของระบบแบบแผนเครื่องรับไฮบริดไมโมเปรียบเทียบกับระบบที่เข้ารหัสไมโมแบบบล็อกเชิงตำแหน่งเวลา

Abstract

In this paper, we evaluate the performance of the Hybrid-MIMO Receiver Scheme (HMRS) in Cognitive Radio network (CR-network). We investigate the efficiency of the proposed scheme which the energy level and the total number of primary user are varied according to the characteristic of CR-network. HMRS can allow users to transmit either Space-Time Block Code (STBC) or Spatial-Multiplexing (SM) streams simultaneously by using Successive Interference Cancellation (SIC) and Maximum Likelihood Detection (MLD). From simulation, the results indicate that the interference level and the number of primary user can effect to the performance of HMRS intensely. Moreover, the exact closed-form capacity of the proposed scheme is derived and compared with STBC scheme.

คำสำคัญ

ไฮบริดไมโม, เครือข่ายรับรู้ทางวิทยุ, การตัดสัญญาณแทรกสอดแบบต่อเนื่อง, การตรวจวัดแบบความน่าจะเป็นจริงสูงสุด

1. บทนำ

การใช้แบนด์วิดท์ในเครือข่ายการสื่อสารไร้สายมีอัตราการใช้งานเพิ่มขึ้นอย่างต่อเนื่อง จากระบบให้บริการการสื่อสารใหม่ๆในปัจจุบัน เช่น การสื่อสารยุคที่สาม และยุคที่สี่ แบนด์วิดท์ที่มีอยู่อย่างจำกัดจะไม่เพียงพอในอนาคตอันใกล้ [1] จึงมีการสร้างมาตรฐานเครือข่ายรับรู้ทางวิทยุ (Cognitive Radio Network) [2] ขึ้นมา เครือข่ายรับรู้ทางวิทยุจะทำงานบนพื้นที่ร่วมกับเครือข่ายหลัก ใช้การตรวจจับแถบความถี่ตรวจหาแถบความถี่ที่สนใจ แล้ววิเคราะห์ว่าช่องความถี่ใดที่ใช้งานอยู่ และเข้าไปใช้ช่องสัญญาณที่ว่าง มีการควบคุมพลังงานไม่ให้รบกวนเครือข่ายหลักเกินกว่าระดับที่ยอมรับได้ รูปที่ 1 อธิบายการทำงานของเครือข่ายรับรู้ทางวิทยุที่ทำงานบนพื้นที่เดียวกันกับเครือข่ายหลัก สามารถใช้ช่องสัญญาณร่วมกับเครือข่ายหลักได้โดยควบคุมพลังงานในระดับที่กำหนด เทคนิคไมโมเป็นเทคนิคที่น่าสนใจที่ใช้ในเครือข่ายรับรู้ทางวิทยุ เนื่องจากใช้งานแบนด์วิดท์ได้มีประสิทธิภาพ เพิ่มทั้งระดับไดเวอร์ซิตี้และความจุได้ดี [3]-[6] ไมโมมีสองแบบคือแบบบล็อกเชิงตำแหน่งเวลา (STBC) [7], [8] และแบบมัลติเพล็กซ์เชิงตำแหน่ง (SM) [9] แต่ในทางปฏิบัติเครือข่ายรับรู้ทางวิทยุจะมีผู้ใช้งานหลายคน และอาจเข้ารหัสไมโมต่างกัน ดังนั้นระบบไฮบริดไมโม [10]-[12] ที่ผู้ใช้งานแต่ละคนสามารถเข้ารหัสไมโมต่างกันได้

จึงจำเป็นต่อเครือข่ายรับรู้ทางวิทยุ โดยใช้การตัดสัญญาณ แทรกสอด (SIC) ร่วมกับการตรวจวัดสัญญาณแบบความ น่าจะเป็นจริงสูงสุด (MLD) [13] เพื่อแยกสัญญาณและ ตรวจวัดเพื่อหาสัญลักษณ์ที่ส่งมาจากเครื่องส่ง ผู้เขียน บทความได้เสนอเทคนิคไฮบริดไมโมที่เรียกว่าแบบแผน เครื่องรับไฮบริดไมโม (HMRS) [14] ที่เหมาะสมสำหรับ เครือข่ายรับรู้ทางวิทยุ มีโครงสร้างของระบบที่ง่ายในทาง ปฏิบัติ บทความนี้เสนอการหาสมรรถนะของระบบแบบแผน เครื่องรับไฮบริดไมโมที่ใช้ในเครือข่ายรับรู้ทางวิทยุ เมื่อได้รับ ผลกระทบจากการเคลื่อนที่ของผู้ใช้งานในเครือข่ายที่เข้าใกล้ เครือข่ายหลักส่งผลให้ผู้ใช้งานต้องปรับเพิ่มพลังงานเพื่อ ควบคุมคุณภาพสัญญาณ และเมื่อปรับเพิ่มจำนวนผู้ใช้งาน ของเครือข่ายหลัก จะกระทบต่อพลังงานโดยรวมของเครือข่าย

เนื้อหาบทความแบ่งเป็นหัวข้อต่างๆ ดังนี้ หัวข้อที่ 2 กล่าวถึงสภาพแวดล้อมของเครือข่ายรับรู้ทางวิทยุ หัวข้อที่ 3 อธิบายโครงสร้างและสัญญาณของระบบแบบแผน เครื่องรับไฮบริดไมโม การวิเคราะห์ความจุของระบบแบบแผน เครื่องรับไฮบริดไมโม เพื่อเทียบกันในหัวข้อที่ 4 การจำลอง แบบถูกแสดงผลในหัวข้อที่ 5 และสรุปผลในหัวข้อที่ 6
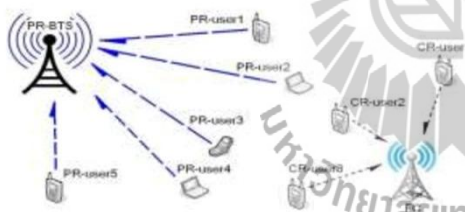
รูปที่ 1 เครือข่ายรับรู้ทางวิทยุ

2. สภาพแวดล้อมของเครือข่ายรับรู้ทางวิทยุ

การทำงานของเครือข่ายรับรู้ทางวิทยุที่ใช้พื้นที่ร่วมกัน ผู้ใช้งานและเครื่องรับจะเข้ารหัสและถอดรหัสตามแบบของ ระบบแบบแผนเครื่องรับไฮบริดไมโม การจำลองแบบจะ พิจารณาระดับพลังงานของผู้ใช้งานที่เปลี่ยนตามตำแหน่ง มี การปรับจำนวนผู้ใช้งานของเครือข่ายหลัก เพื่อศึกษา ผลกระทบ ในรูปที่ 2 เป็นแบบจำลองที่1 ที่จะใช้ในการจำลอง แบบ โดยสมมุติให้ผู้ใช้งานที่1 เคลื่อนที่เข้าใกล้เครือข่ายหลัก (ตามทิศทางของลูกศรเส้นหนา) ผู้ใช้งานคนอื่นอยู่กับที่ และส่ง สัญญาณความถี่เดียวกันออกมาพร้อมกัน
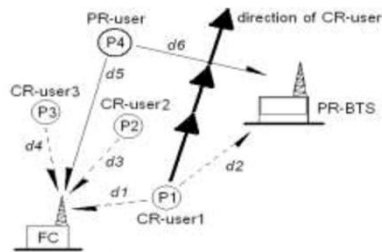
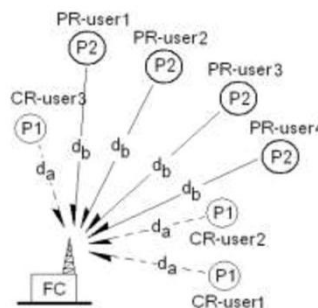รูปที่ 2 แบบจำลองที่1ของเครือข่ายรับรู้ทางวิทยุในการจำลองแบบ

ทุกช่วงเวลาที่ผู้ใช้งานที่1เคลื่อนที่จะห่างสถานีฐาน FC มาก ขึ้น ทำให้อัตราสัญญาณต่อสัญญาณรบกวนและอัตรา ผิดพลาดบิตมีค่าแย่ลงทุกช่วง ดังนั้นผู้ใช้งานที่1ต้องปรับเพิ่ม กำลังส่งทุกช่วง เพื่อรักษาคุณภาพสัญญาณให้ได้มาตราฐาน อัตราสัญญาณต่อสัญญาณรบกวนของเครือข่ายหลักก็มีค่าลด ลงจนใกล้ระดับที่ยอมรับได้ สถานีฐานของเครือข่ายหลักจะสั่ง ให้เครือข่ายรับรู้ทางวิทยุลดกำลังส่งลง หรือเปลี่ยนความถี่ เพื่อให้สัญญาณของเครือข่ายหลักมีคุณภาพตามมาตรฐาน พลังงานที่สถานีฐาน FC สามารถเขียนเป็นสมการได้ดังนี้

$$E_{FC} = d_1 E_1 + d_3 E_2 + d_4 E_3 + d_5 E_4 + \sigma_\omega^2 \qquad (1)$$

เมื่อ d_n คือค่าคงที่สเกลพลังงานจากการสูญเสียวิถี (Path loss), E_n คือพลังงานผู้ใช้งาน และ σ_ω^2 คือพลังงานสัญญาณ รบกวน (กำหนดให้ $E_1=E_2=E_3$ และ $E_4=1.3E_1$) อัตราสัญญาณ ต่อสัญญาณรบกวนเขียนเป็นสมการได้ดังนี้

$$SNR = \gamma = \frac{d_1 E_1 + d_3 E_2 + d_4 E_3}{d_5 E_4 + \sigma_\omega^2} = \frac{d_1 + d_3 + d_4}{1.3 d_5 + 1/\overline{\gamma}} \qquad (2)$$

กำหนดให้ d3=d4=1, d5=0.01, d1=[1, 0.9, 0.8,...,0.3] แต่ ละช่วงเวลาที่ผู้ใช้งานที่1เคลื่อนที่ และ $\overline{\gamma}$ เป็นค่าอัตรา สัญญาณต่อสัญญาณรบกวนเฉลี่ยต่อสายอากาศรับ

รูปที่ 3 แบบจำลองที่ 2 ของเครือข่ายรับรู้ทางวิทยุในการจำลองแบบ

ในรูปที่ 3 เป็นแบบจำลองที่ 2 เมื่อผู้ใช้งานทุกคนอยู่นิ่ง และกำลังงานของผู้ใช้งานเครือข่ายหลักมีค่า d_bP_2 เท่ากัน และให้ d_b =0.01, d_a =1 และ P_1 เป็นกำลังงานของผู้ใช้งานของเครือข่ายรับรู้ทางวิทยุ อัตราสัญญาณต่อสัญญาณรบกวนของสถานีฐาน FC เขียนได้ดังนี้

$$SNR = \gamma = \frac{3E_1}{d_b NE_2 + \sigma_\omega^2} = \frac{3}{1.3d_b N + 1/\overline{\gamma}} \qquad (3)$$

เมื่อจำนวนผู้ใช้งานของเครือข่ายหลักเพิ่ม (ค่า N) ทำให้ระดับสัญญาณแทรกสอดเพิ่มขึ้น จะอธิบายในหัวข้อผลการจำลอง

3. สัญญาณและระบบ

ในหัวข้อนี้จะแสดงโครงสร้างและสัญญาณของระบบ 2x2 STBC และ HMRS รวมถึงอัตราสัญญาณต่อสัญญาณรบกวนประสิทธิผลของทั้งสองระบบ

3.1 ระบบ 2x2STBC

สัญญาณรับเขียนดังสมการ

$$\mathbf{y=H}_{2x2}\mathbf{G+w}$$
$$= \begin{bmatrix} h_{11} & h_{21} \\ h_{12} & h_{22} \end{bmatrix} \begin{bmatrix} s_1 & -s_2^* \\ s_2 & s_1^* \end{bmatrix} + \begin{bmatrix} w_1 \\ w_2 \end{bmatrix} \qquad (4)$$

เมื่อ H_{2x2} คือช่องสัญญาณไมโมขนาด 2x2, G คือสัญลักษณ์ส่งที่เข้ารหัส STBC และ w คือเวกเตอร์สัญญาณรบกวน เมื่อสัญญาณที่สายอากาศรับในสองช่วงเวลาเขียนได้ดังนี้

$$r_{t1}^1 = h_{11}s_1 + h_{21}s_2 + w_1$$
$$r_{t1}^2 = h_{12}s_1 + h_{22}s_2 + w_2$$
$$r_{t2}^1 = -h_{11}s_2^* + h_{21}s_1^* + w_1 \qquad (5)$$
$$r_{t2}^2 = -h_{12}s_2^* + h_{22}s_1^* + w_2$$

เมื่อ r_{tb}^a คือสัญญาณรับที่สายอากาศ a ที่เวลา b และหลังจากรวมสัญญาณแล้ว (combining) จะได้สัญญาณดังนี้

$$\tilde{s}_n = r_{t1}^1 h_{11}^* + r_{t1}^2 h_{12}^* + r_{t2}^{1*} h_{21} + r_{t2}^{2*} h_{22}$$
$$= \left(|h_{11}|^2 + |h_{12}|^2 + |h_{21}|^2 + |h_{22}|^2 \right) s_1 \qquad (6)$$
$$+ n_1 h_{11}^* + n_2 h_{12}^* + n_1^* h_{21} + n_2^* h_{22}$$

เมื่อสัญลักษณ์จากเครื่องส่งที่ถอดรหัสได้คือ

$\hat{s}_n = \arg \min_{s \in A} \left| \tilde{s}_n - \|\mathbf{H}_{2x2}\|_F^2 s \right|^2$ เมื่อ A คือสัญลักษณ์ที่เป็นไปได้ในการมอดูเลต ดังนั้นอัตราสัญญาณต่อสัญญาณรบกวนประสิทธิผลหลังการรวมสัญญาณคือ [15]

$$\gamma_{STBC} = \frac{\|\mathbf{H}_{2x2}\|_F^4 E_0}{\|\mathbf{H}_{2x2}\|_F^2 \sigma_w^2} = \frac{\overline{\gamma}\|\mathbf{H}_{2x2}\|_F^2}{2} \qquad (7)$$

เมื่อ $\|\mathbf{B}\|_F$ คือ Frobenius norm ของเมตริก B ซึ่งมีค่าเท่ากับ $\|\mathbf{B}\|_F \triangleq \sqrt{\sum_{i=1}^m \sum_{j=1}^n |B_{ij}|^2}$

3.2 ระบบแบบแผนเครื่องรับไฮบริดไมโม (HMRS)

กำหนดให้ระบบ HMRS มีผู้ใช้งานสองคน โดยเขียนสัญญาณรับได้ตามสมการ

$$\mathbf{y} = \begin{bmatrix} h_{11} & h_{21} & h_{31} & h_{41} \\ h_{12} & h_{22} & h_{32} & h_{42} \\ h_{13} & h_{23} & h_{33} & h_{43} \\ h_{14} & h_{24} & h_{34} & h_{44} \end{bmatrix} \begin{bmatrix} s_1 & s_5 \\ s_2 & s_6 \\ s_3 & -s_4^* \\ s_4 & s_3^* \end{bmatrix} + \begin{bmatrix} w_1 \\ w_2 \\ w_3 \\ w_4 \end{bmatrix} \qquad (8)$$

$$\mathbf{y}_{SM} = \begin{bmatrix} h_{11} & h_{21} \\ h_{12} & h_{22} \\ h_{13} & h_{23} \\ h_{14} & h_{24} \end{bmatrix} \begin{bmatrix} \hat{s}_1 & \hat{s}_5 \\ \hat{s}_2 & \hat{s}_6 \end{bmatrix} \qquad (9)$$

เมื่อ $\hat{s}_n$ คือสัญลักษณ์ที่เข้ารหัส SM ที่ถอดรหัสจากการตรวจวัดแบบความน่าจะเป็นจริงสูงสุด (MLD) และ (9) คือสัญญาณรับของผู้ใช้งานที่เข้ารหัส SM และสัญญาณรับของผู้ที่เข้ารหัส STBC สามารถคำนวณได้ดังสมการ

$$\mathbf{Y}_{STBC} = \mathbf{Y} - \mathbf{Y}_{SM} = \begin{bmatrix} r_{t1}^1 & r_{t2}^1 \\ r_{t1}^2 & r_{t2}^2 \\ r_{t1}^3 & r_{t2}^3 \\ r_{t1}^4 & r_{t2}^4 \end{bmatrix} \qquad (10)$$

จากนั้นนำสัญญาณใน (10) ไปรวมสัญญาณได้เป็น

$$\tilde{s}_3 = r_{t1}^1 h_{31}^* + r_{t1}^2 h_{32}^* + r_{t1}^3 h_{33}^* + r_{t1}^4 h_{34}^* + r_{t1}^{1*} h_{41}$$
$$+ r_{t2}^{2*} h_{42} + r_{t2}^{3*} h_{43} + r_{t2}^{4*} h_{44} \qquad (11)$$

$$\tilde{s}_n = \|\mathbf{H}_{STBC}\|_F^2 s_n + \Delta sL + \|\mathbf{H}_{STBC}\| w_n$$

เมื่อ H_{STBC} คือสมาชิกของ H หลักที่สามถึงสี่ $\Delta s = s_n - \hat{s}_n$ และ L คือผลลัพธ์ของ $|h|_{ij}$ จากการรวมสัญญาณของรหัส STBC จาก (11) สามารถถอดรหัส STBC ได้จาก $\hat{s}_n = \arg \min_{s \in A} \left| \tilde{s}_n - \|\mathbf{H}_{STBC}\|_F^2 s \right|^2$ ดังนั้นอัตราสัญญาณต่อสัญญาณรบกวนประสิทธิผล หลังการรวมสัญญาณคือ

$$\gamma_{HMRS}^{STBC} = \frac{\overline{\gamma}\|\mathbf{H}_{STBC}\|_F^2}{2\left(\frac{|\Delta sL|^2}{\sigma_\omega^2 \|\mathbf{H}_{STBC}\|_F^2} + 1 \right)} \qquad (12)$$
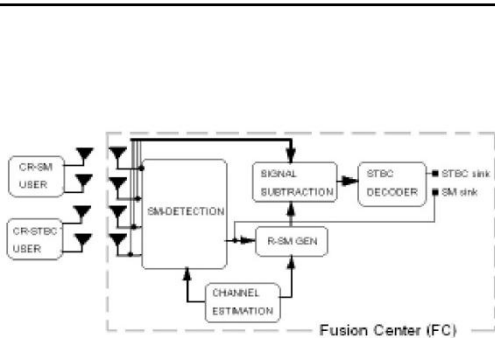
รูปที่ 4 แบบแผนเครื่องรับไฮบริดไมโมแบบสองผู้ใช้งาน

4. การวิเคราะห์ความจุช่องสัญญาณ

มีการส่งสัญญาณผ่านช่องสัญญาณเฟดดิง มีผลกระทบ
ต่อความจุช่องสัญญาณ ในหัวข้อนี้จะวิเคราะห์ความจุ
ช่องสัญญาณ สมการฟังก์ชันความหนาแน่นความน่าจะเป็น
(pdf) ของอัตราสัญญาณต่อสัญญาณรบกวนประสิทธิผลคือ

$$p_{\gamma_n}(\gamma_n) = \frac{\gamma_n^{(n_T n_R)-1}}{\Gamma(n_T n_R)\bar{\gamma}_s^{-(n_T n_R)}}e^{-\gamma_n/\bar{\gamma}_s} \tag{13}$$

เมื่อ $\Gamma(\bullet)$ คือฟังก์ชันแกมม่าเขียนได้เป็น $\Gamma(a) = \int_0^\infty x^{a-1}e^{-a}da$,

ค่าเฉลี่ยของ SNR คือ $\bar{\gamma}_s = \gamma_n / \|H_n\|_F^2$, n_T และ n_R คือจำนวน
สายอากาศส่งและรับตามลำดับ สมการความจุคือ [15]

$$C = R\int_0^\infty \log_2(1+\gamma_n)p_{\gamma_n}(\gamma_n)d\gamma_n \tag{14}$$

สามารถลดความซับซ้อนของ (14) จากสูตร

$$I(m,n) = \frac{n^m}{\Gamma(m)}\int_0^\infty \ln(1+x)x^{m-1}e^{-nx}dx \tag{15}$$

หรือ

$$I(m,n) = P_m(-n)E_1(n) + \sum_{k=1}^{m-1}\frac{P_k(n)P_{m-k}(-n)}{k} \tag{16}$$

เมื่อ $P_m(\bullet)$ เป็นฟังก์ชันการกระจายปัวซอง และ $E_1(\bullet)$ เป็น
ฟังก์ชันอินทิกรัลเอ็กโพเนนเชียล ซึ่งมีค่าเป็น

$$P_m(x) \triangleq \sum_{k=0}^{m-1}\frac{x_k}{k!}e^{-x} \tag{17}$$

$$E_1(x) \triangleq \int_x^\infty \frac{e^{-t}}{t}dt, \quad x > 0. \tag{18}$$

ถ้า CSI สมบูรณ์ ความจุใน (14) คำนวณโดย (13) และ (16)
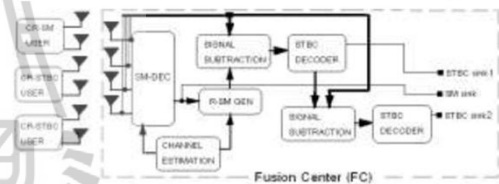
$$C = \frac{R}{\ln(2)}I(n_T n_R, q_n) \tag{19}$$

หรือ

$$C = \frac{R}{\ln(2)}\left[P_{n_T n_R}(-q_n)E_1(q_n) + \sum_{k=1}^{(n_T n_R)-1}\frac{P_k(q_n)P_{(n_T n_R)-k}(-q_n)}{k}\right] \tag{20}$$

เมื่อ R เป็นอัตรารหัส STBC, $q_n = 1/\bar{\gamma}_s$, q_n ของระบบ STBC
และ HMRS ได้จาก (7) และ (12) ตามลำดับ ผลการวิเคราะห์
ค่าความจุของ HMRS และ STBC เขียนได้ดัง (21) และ (22)

$$C_{STBC} = \frac{1}{\ln(2)}\left[P_4\left(-\frac{\|H_{2\times2}\|_F^2}{\gamma_{STBC}}\right)E_1\left(\frac{\|H_{2\times2}\|_F^2}{\gamma_{STBC}}\right)\right. \tag{21}$$

$$\left. + \sum_{k=1}^{3}\left(P_k\left(\frac{\|H_{2\times2}\|_F^2}{\gamma_{STBC}}\right)P_{4-k}\left(-\frac{\|H_{2\times2}\|_F^2}{\gamma_{STBC}}\right)\right)/k\right]$$

$$C_{HMRS} = \frac{1}{\ln(2)}\left[P_8\left(-\frac{\|H_{STBC}\|_F^2}{\gamma_{HMRS}^{STBC}}\right)E_1\left(\frac{\|H_{STBC}\|_F^2}{\gamma_{HMRS}^{STBC}}\right)\right. \tag{22}$$

$$\left. + \sum_{k=1}^{7}\left(P_k\left(\frac{\|H_{STBC}\|_F^2}{\gamma_{HMRS}^{STBC}}\right)P_{8-k}\left(-\frac{\|H_{STBC}\|_F^2}{\gamma_{HMRS}^{STBC}}\right)\right)/k\right].$$

รูปที่ 5 แบบแผนเครื่องรับไฮบริดไมโมแบบสามผู้ใช้งาน

5. การจำลองสมรรถนะ

หัวข้อนี้ทำการจำลองแบบระบบ HMRS แบบสามผู้ใช้งาน
ดังรูปที่ 5 เมื่อจำลองแบบตามแบบจำลองในรูปที่ 2 และ 3
โดยใช้การจำลองแบบมอนติคาร์โล ใช้การมอดูเลต BPSK

รูปที่ 6 แสดงสมรรถนะอัตราผิดพลาดบิตของระบบ
HMRS แบบสามผู้ใช้งานเมื่อเครือข่ายหลักไม่ได้ทำงาน จะ
เห็นได้ว่าผู้ใช้งานที่เข้ารหัส STBC มี BER ดีกว่า 3dB ที่ 10^{-4}
และเส้นปะแสดงค่าเฉลี่ยของ BER

รูปที่ 7 แสดงสมรรถนะอัตราผิดพลาดบิตของระบบ
HMRS แบบสามผู้ใช้งาน เมื่อมีผู้ใช้งาน 1 คนเคลื่อนที่เข้าใกล้
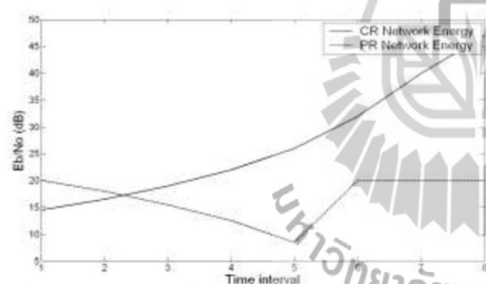เครือข่ายหลักทำให้มีค่า SNR ลดลงและส่งผลต่อค่า BER

รูปที่ 8 แสดงพลังงานของทั้งสองเครือข่าย เมื่อผู้ใช้งาน
ของเครือข่ายเคลื่อนเข้าใกล้เครือข่ายหลัก ค่า SNR ของ FC
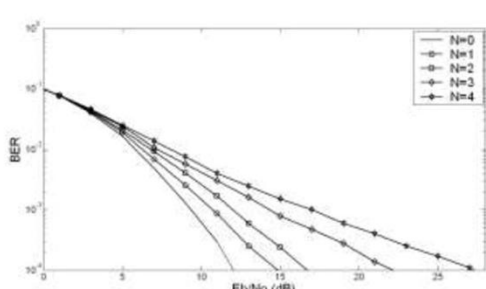จะลดลง ผู้ใช้งานต้องเพิ่มกำลังส่ง ค่า SNR ของเครือข่ายหลัก
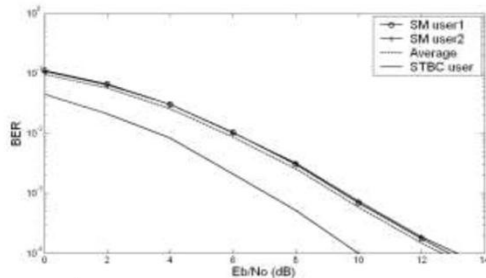
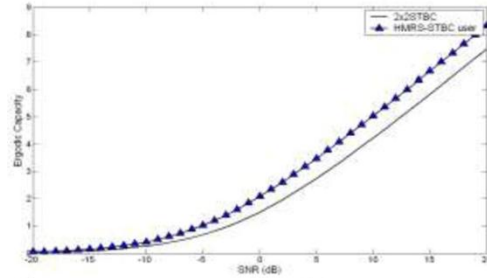รูปที่ 6 สมรรถนะ BER ของระบบ HMRS แบบสามผู้ใช้งาน
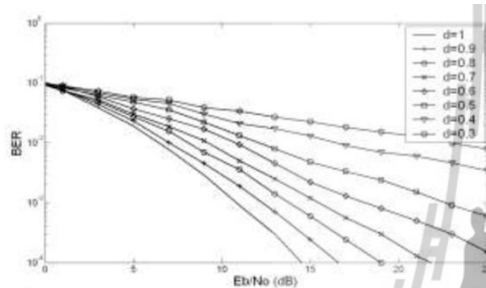
รูปที่ 7 สมรรถนะ BER ของระบบ HMRS แบบสามผู้ใช้งาน เมื่อมีผู้ใช้งาน 1 คนเคลื่อนที่เข้าใกล้เครือข่ายหลัก

รูปที่ 8 ระดับพลังงานของทั้งสองเครือข่าย เมื่อผู้ใช้งาน CR เคลื่อนเข้าใกล้เครือข่ายหลัก

รูปที่ 9 แสดงสมรรถนะ BER ของระบบ HMRS แบบสามผู้ใช้งานเมื่อมีการเพิ่มจำนวนผู้ใช้งานของเครือข่ายหลัก

รูปที่ 10 ความจุช่องสัญญาณของผู้ใช้งานที่เข้ารหัส STBC ของระบบ HMRS และ ระบบ2x2STBC

จึงลดลง จนช่วงที่ 5 ค่า SNR ของเครือข่ายหลักลดลงจนเข้าใกล้ระดับที่ยอมรับได้ เครือข่ายหลักจะสั่งให้เครือข่าย CR เปลี่ยนความถี่ เพื่อรักษาคุณภาพสัญญาณที่ 20dB

รูปที่ 9 แสดงสมรรถนะอัตราผิดพลาดบิตของระบบ HMRS แบบสามผู้ใช้งานเมื่อมีการเพิ่มจำนวนผู้ใช้งานของเครือข่ายหลัก จะเห็นได้ว่าสมรรถนะ BER ของระบบ HMRS จะลดลงตามจำนวน N

รูปที่ 10 คือสมรรถนะของความจุช่องสัญญาณของผู้ใช้งานที่เข้ารหัส STBC ของระบบHMRS และ ระบบ 2x2STBC ที่วิเคราะห์ได้จากสมการที่ (21) และ (22) ซึ่งจะเห็นได้ว่าระบบ HMRS มีความจุสูงกว่าและสามารถใช้การมอดูเลตระดับสูงกว่าได้

6. สรุปผล

บทความนี้มีการหาสมรรถนะอัตราผิดพลาดบิตของระบบแบบแผนเครื่องรับไฮบริดไมโมเพื่อหาผลกระทบทางด้านพลังงานในเครือข่ายเมื่อมีการปรับระดับพลังงานของลูกข่าย (CR user) เมื่อมีการเคลื่อนที่เข้าใกล้เครือข่ายหลัก และในกรณีที่มีการเพิ่มจำนวนของผู้ใช้งานของเครือข่ายหลัก จากผลการจำลองพบว่ามีการส่งผลกระทบอย่างมากต่อสมรรถนะ BER และการใช้พลังงานในเครือข่าย และจากผลการวิเคราะห์ความจุช่องสัญญาณพบว่าความจุของระบบ HMRS มีค่าสูงกว่าระบบ 2x2STBC

7. เอกสารอ้างอิง

[1] T. Yucek and H. Arslan, "A Survey of Spectrum Sensing Algorithms for CR Applications first quarter 2009," University of South Florida, USA, Tech. Rep.

[2] S. Haykin, "Cognitive radio: Brain-empowered wireless communications", *IEEE Journal on Selected Areas in Communications,* vol. 23, no. 2, pp. 201–219, Feb 2005.

[3] Akin. S and Gursoy M.C.,"On the performance limits of cognitive radio MIMO channels", *WCNC. 2011 IEEE*, pp. 1640-1645, 2011.

[4] Xiaoming Chen, Zhaoyang Zhang and Chao Wang, "Dual QoS Driven Power Allocation in MIMO Cognitive Network with Limited Feedback", *WCNC. 2011 IEEE,* pp. 1829-1833, 2011.

[5] Sha Hua, Hang Liu, Mingquan Wu and Panwar, S.S., "Exploiting MIMO Antennas in Cooperative Cognitive Radio Network", *INFOCOM, 2011 Proceeding IEEE,* pp. 2714-2722, 2011.

[6] Jorswieck, E.A. and Jing Lv, "Spatial shaping in cognitive MIMO MAC with coded Legacy transmission", *SPAWC, 2011 IEEE 12th,* pp. 451-455, 2011.

[7] S. Alamouti, "A simple transmit diversity technique for wireless communication", IEEE Journal of Selected Area in Communications, vol. 16, pp. 1451-1458, Oct 1998.

[8] V. Tarokh, H. Jafarkhani, and A. R. Calderbank, "Space-time block codes from orthogonal designs," *IEEE Transactions on Information Theory, vol.5,* pp.1456–1467, Jul 1999.

[9] G. J. Foschini, "Layered space-time architecture for wireless communications in a fading environment when using multiple antennas", *Bell Labs Tech. J.,* v.1, n.2, pp.41–59, 1996.

[10] Chee Wei Tan and A. Robert Calderbank, "Multiuser Detection of Alamouti Signals", *IEEE Transactions on Communications, Vol. 57, No. 7, 2009,* pp. 2080-2089, 2009.

[11] Walter da C. Freitas Jr., Francisco R. P. Cavalcanti and Renato R. Lopes, "Hybrid Transceiver Schemes for Spatial Multiplexing and Diversity in MIMO Systems", *Journal of Communication and Information systems, vol. 20, No. 3, 2005,* pp. 63-76, 2005.

[12] R.W. Heath Jr. and A. J. Paulraj, "Diversity versus multiplexing in narrow band MIMO channel: A tradeoff base on Euclidean distance", *IEEE trans. On Communication*, submitted 2002.

[13] Yong Soo Cho, Jaekwan Kim, *MIMO-OFDM Wireless Communication with MATLAB*, John Wiley&Sons (Asia) Pte Ltd, 2010.

[14] Tanapong Khomyat, Peerapong Uthansakul and Monthippa Uthansakul, "Hybrid-MIMO Receiver with Both Space-Time Coding and Spatial Multiplexing Detections for Cognitive Radio Networks", *ISPACS 2011 IEEE*, pp. 2011.

[15] Kyung Seung Ahn, Robert W. Heath Jr. and Heung Ki Baik, "Shannon Capacity and Symbol Error Rate of Space-Time Block Codes in MIMO Rayleigh Channels with Channel Estimation Error", IEEE Transactions on Wireless Communications, Vol. 7, No. 1, pp. 324-333, 2008.

BIOGRAPHY

Mr. TanapongKhomyat was born in September 30, 1978 in Tak province, Thailand. He received the Bachelor's Degree and Master's Degree in Telecommunication Engineering from Rajamangala University of Technology Thanyaburi, in 2000 and King Mongkut's Institute of Technology Ladkrabang, in 2006, respectively. He served in position of lecturer at Division of Electronics Engineering, Rajamangala University of Technology Lanna since 2006. At present, he is working towards his Ph.D. degree in telecommunication engineering at Suranaree University of Technology.